NASA Contractor Report 171984

National Aeronautics and Space Administration (NASA)/ American Society for Engineering Education (ASEE) Summer Faculty Fellowship Program--1986

Volume 2

Bayliss McInnis, Editor
University of Houston--University Park
Houston, Texas

Stanley Goldstein, Editor
University Programs Office
Lyndon B. Johnson Space Center
Houston, Texas

Grant NGT-44-005-803

June 1987

National Aeronautics and Space Administration

Lyndon B. Johnson Space Center
Houston, Texas

PREFACE

The 1986 Johnson Space Center (JSC) National Aeronautics and Space Administration (NASA)/American Society for Engineering Education (ASEE) Summer Faculty Fellowship Program was conducted by the University of Houston and JSC. The ten week program was operated under the auspices of the ASEE. The program at JSC, as well as the programs at other NASA Centers, was funded by the Office of University Affairs, NASA Headquarters, Washington, D.C. The objectives of the programs, which began in 1965 at JSC and in 1964 nationally, are

a. to further the professional knowledge of qualified engineering and science faculty members;

b. to stimulate an exchange of ideas between participants and NASA;

c. to enrich and refresh the research and teaching activities of participants' institutions; and

d. to contribute to the research objectives of the NASA Centers.

Each faculty fellow spent ten weeks at JSC engaged in a research project commensurate with his interests and background and worked in collaboration with a NASA/JSC colleague. This document is a compilation of the final reports on the research projects done by the faculty fellows during the summer of 1986. Volume 1 contains sections 1 through 14, and volume 2 contains sections 15 through 30.

CONTENTS

1986

NASA/ASEE SUMMER FACULTY RESEARCH FELLOWSHIP PROGRAM

Johnson Space Center

University of Houston-University Park

Solar Prediction and Intelligent Machines

Prepared by: Gordon G. Johnson

Academic Rank: Professor

University & Department:

University of Houston-University Park

Department of Mathematics

NASA/JSC

Directorate: Mission Support

Division: Mission Planning and Development

Branch: Technical Development and Applications

JSC Colleague: Robert T. Savely

Date: August 11, 1986

Contract #: NGT 44-005-803

N87-25885

SOLAR PREDICTION AND INTELLIGENT MACHINES

Gordon G. Johnson
Professor
Department of Mathematics
University of Houston-University Park
Houston, Texas 77004

There are two projects running concurrently, one dealing with solar prediction and the second is developing an intelligent machine.

The solar prediction program is aimed at reducing or eliminating the need to throughly understand the process previously developed and to still be able to produce a prediction. Substantial progress has been made in identifying the procedures to be coded as well as testing some of the presently coded work.

The second project involves work on developing ideas and software that should result in a machine capable of learning as well as carrying on an intelligent conversation over a wide range of topics. The underlying idea is to use primitive ideas and construct higher order ideas from these, which can then be easily related to one to another.

NASA Colleague: Robert T. Savely FM7 X4751

SOLAR PREDICTION AND INTELLIGENT MACHINES

Gordon G. Johnson
Professor
Department of Mathematics
University of Houston-University Park
Houston, Texas 77004

There are two projects being developed concurrently, the first deals with the prediction of solar activety as measured by sunspot numbers and the second project pertains to the development of an intelligent machine.

The method developed in 1978-79 for predicting monthly mean sunspot numbers[1] has been refined in order to reduce the amount of time and expertise required to produce an eight to ten year prediction of monthly mean sunspot numbers. The availability of such predictions are clearly useful for well known technical reasons such as communications and orbit determination.

The refined method was developed with the aid of the work of J. Parker and M. Boarnet that provided an environment in which to ferret out the step by step procedure that a person generating a prediction actually does, and to then capture this procedure in code, thus removing the requirement that a person throughly understand the process before attempting to generate a prediction.

Mr. J. Parker created LISP code to perform the extensive calculations required. His work adds several enhancements to the original FORTRAN code in that it allows maximun use of the available data at each step in the computations.

Mr. M. Boarnet then built an interface that provides an easily operated interactive interface as well as graphics displays, both of which were essential in the development work leading to the present procedure. The interface allows the operator to control all essential parameters that guide the calculations needed to generate the prediction.

It was found that the implementation on the SYMBOLICS machine required excessive machine time, on the order of fifty hours. To reduce this time by a substantial amount, the calculations will be done on the FLEX to gain from the advantages of parallel processing. The code is being written in **C** by K. Fields for the FLEX, who has added enhancements to the previously written code, which should result in shorter execution time on the order of four to five hours. The results of the computations will then be transferred to the SYMBOLICS for display.

When the process is fully operational on the FLEX, then the daily sunspot prediction will be tried. This would involve a thirty fold increase in data to be processed. However, it is planned that the long term monthly mean prediction would have been generated, and fine grain daily prediction will then be made, and should require only a small amount of additional time on the order of four hours.

The underlying support for this method is the anharmonic technique of A. K. Paul[2] which provides us with a tool to search for and

extract particular sine functions from the solar data.

The search is restricted to sine functions i.e., frequencies, amplitudes and phases, that have periods between six months and forty years and amplitudes greater than some preset minimum. There is no attempt to completely decompose the data set into a sum of sine functions, but rather to find approximately thirty sine functions such that the sum of those found, when subtracted from the original data set, results in a "smooth" curve that can be extrapolated. After the extrapolation is completed the subtracted sine functions are added back, resulting in the original data set as well as the predicted values.

The second project concerns the work of developing ideas and code that should result in a machine capable of learning as well as carrying on an intelligent conversation[3]. The code is being written in COMMON LISP by L. Wang on the SYMBOLICS.

Preliminary coding to find first and second level relationships has been written . The underlying notion that drives this development is that of primitive ideas. Ideas contained in the words such as toward , hold, place, time, are examples of primitive ideas. The number of words in the list of primitves is about thirty five, and it is from this short list that all the ideas are formed. The ideas form patterns that are then compared and related.

The next part to be encoded deals with analogies that should produce "new" ideas. The machine will not store results given in response to statements but each time will reconstruct anew the proper response.

If the machine does not understand a statement given to it it will inquire as to the meaning of the word or words that it does not recognize. The response to a machines inquiry will be stored and internally related to previously understood ideas. The new ideas given will then be used to resopd to the initial statement. In addition, when a statement is given to the machine the machine will then, unbeknowst to the person communicating with the machine, form a view of all the ideas that relate to the subjects in in the first statement, so that if additional statements that deal with ideas similiar to those initially given to the machine are presented to the machine it will be able to respond quickly.

There are many levels within the machine, the first consists of the ideas closely and directly related to a statement given the machine, the second level consists of all ideas directly related to content of the statement, the third level consists of all ideas related to the ideas in the second level. The higher levels are formed in a similiar fashion. The forming of the first two levels is automatic. The machines response to the initial statement is usually formed from the ideas found in the first two levels. If there is insufficient information to respond, then the machine proceeds to higher levels in its search for a response. The various ideas in the various levels are retained in preparation for expected statements related to the first statement. If a second statement that is related to the first statement is given to the machine it may cause the machine to enlarge the pool of ideas in all levels. However, if the second statement is on an entirely different topic, then the machine will form new first, and second levels.

This report is a brief description of the development, and is only the start of a much more complex involvement with machines that should result in a machine that will converse in a "natural" manner with any person.

REFERENCES

1. G. G. Johnson and S. R. Newman, "Solar Activity Prediction of Sunspot Numbers", NASA, JSC-16390 1980.

2. A. K. Paul, "Anharmonic Analysis", Mathematics of Compution, Vol.26, No. 118, April 1972.

3. T. Winograd, "Language as a Cognitive Process", Vol. 1: Syntax, Addison-Wesley Pub. Co. Reading, Mass., 1983.

NASA/ASEE SUMMER FACULTY RESEARCH FELLOWSHIP PROGRAM

Johnson Space Center

University of Houston

NON-EQUILIBRIUM EFFECTS IN HIGH TEMPERATURE CHEMICAL REACTIONS

Prepared by:	Richard E. Johnson, Ph.D.
Academic Rank:	Professor
University & Department:	LeTourneau College, Longview, TX Natural Science Department
NASA/JSC	
Directorate:	Engineering
Division:	Advanced Programs Office
Branch:	Aeroscience
JSC Colleague:	Carl D. Scott, Ph.D.
Date:	August 8, 1986
Contract #:	NGT-44-005-803 (University of Houston)

NON-EQUILIBRIUM EFFECTS IN HIGH TEMPERATURE CHEMICAL REACTIONS

Richard E. Johnson, Ph.D.
Professor of Chemistry
LeTourneau College
Longview, Texas

ABSTRACT

Reaction rate data have been collected for chemical reactions occuring at high temperatures during reentry of space vehicles. Large differences in reaction rate data are reported by various authors in the literature.

The principle of detailed balancing is used in modeling kinetics of chemical reactions at high temperatures. Although this principle does not hold for certain transient or incubation times in the initial phase of the reaction, it does seem to be valid for the rates of internal energy transitions that occur within molecules and atoms. That is, for every rate of transition within the internal energy states of atoms or molecules, there is an inverse rate that is related through an equilibrium expression involving the energy difference of the transition.

Future goals include theoretical modeling to include internal energy transitions into overall rate expressions that can then be used to predict radiation heating effects for reentry vehicles under non-equilibrium conditions.

NASA Colleague: Carl D. Scott, Ph.D., ED3, X4306

TABLE OF CONTENTS

INTRODUCTION

Data from Space Shuttle flights and experimental work indicate that non-equilibrium radiation due to chemical non-equilibrium in the shock layer of rentry vehicles may result in a significant added heat load.(1,2,3) For OTV and AOTV with higher reentry velocities, these non-equilibrium effects may be even more significant.(4)

This work is a continuation of work from last summer which will focus in on reaction rate data reported in the literature and also consider furthur the principle of detailed balancing as applied to transitions within the internal energy states of molecules.

CHEMICAL REACTION RATES

At an altitude of 80-100 kilometers, the reactant substances in the atmosphere include N_2, O_2, N, O, NO, various positive ions and electrons. However, with these few reactants, a multitude of reactions with various interdependent relationships could possibly occur upon the initiation of a shock wave by a reentry vehicle. The low pressure at these altitudes and the high energy input due to the shock wave from Mach 20-35 results in a region of chemical non-equilibrium between the reentry vehicle's surface and the shock front. This chemical non-

equilibrium is not just due to the progress of reactions from reactants to products in the ordinary sense of chemical reactions. A more significant and complicating factor is that internal energies of atoms and molecules also take a finite time to change with the rapid input of energy. During this time of internal energy equilibration, the ordinary rate constant of a chemical reaction is not definable. This time of internal energy equilibration has been referred to in the literature as an incubation time or a pre-quasistationary time.(5,6,7)

The chemical reactions that could occur are many and some of the representative ones are given on the next page.

Carlson and Rieper(8) considered only the first twelve reactions given on the next page in their investigations on medium shock waves(5-7 km/sec). Their numerical predictions agreed with their experimental data on the electron temperature variation in these shock waves.

$$O_2 + O \rightleftarrows 2O + O$$

$$O_2 + O_2 \rightleftarrows 2O + O_2$$

$$O_2 + M \rightleftarrows 2O + M$$

$$N_2 + O \rightleftarrows NO + N$$

$$O_2 + N \rightleftarrows NO + O$$

$$N + O \rightleftarrows NO^+ + e$$

$$NO + M \rightleftarrows N + O + M$$

$$N + N \rightleftarrows N_2^+ + e$$

$$O + O \rightleftarrows O_2^+ + e$$

$$N_2 + N_2 \rightleftarrows 2N + N_2$$

$$N_2 + N \rightleftarrows 2N + N$$

$$N_2 + M \rightleftarrows 2N + M$$

$$NO + O \rightleftarrows N + O_2$$

$$O + O_2^+ \rightleftarrows O_2 + O^+$$

$$N_2 + N^+ \rightleftarrows N + N_2^+$$

$$O + NO^+ \rightleftarrows NO + O^+$$

$$N_2 + O^+ \rightleftarrows O + N_2^+$$

$$N + NO^+ \rightleftarrows NO + N^+$$

$$O_2 + NO^+ \rightleftarrows NO + O_2^+$$

$$O + NO^+ \rightleftarrows O_2 + N^+$$

$$NO^+ + N \rightleftarrows O + N_2^+$$

$$O + e \rightleftarrows O^+ + e + e$$

$$N + e \rightleftarrows N^+ + e + e$$

Chul Park(9,10) has used all of the above reactions in a computer program(NEQAIR) to calculate the extent of reactions and radiation in the non-equilibrium zone for a shock wave speed of 10km/sec. At this higher shock speed, calculated results did not fit the limited experimental data from shock tube experiments.

There are still discrepancies in the literature for reaction rate data as reported by various authors. Some of these are given in Table 1 below.

Some of these differences in reaction rate data are small in magnitude and would not affect the results of computations drastically. However, many of the reactions have orders of magnitude differences in the rate contants and also differences in the temperature dependency of the reactions. These include the nitrogen, oxygen and nitric oxide dissociations as well as the impact ionization reactions.

Further work on the effect of varying the rate constants upon the output of computer programs would seem to be a worthwhile effort. Better agreement with experimental data may be obtained by adjusting rate parameters within the computer program itself.

Table 1. Reaction Rate Data

Rate Constant, $k = AT^{-s} e^{-B/T}$ (cc/mole-sec)

Reaction	A	s	B	Ref.
$N_2 + N_2 \rightleftarrows N + N + N_2$	3.7(21)	1.6	113,200	10
	4.7(17)	0.5	113,200	11
	2.3(29)	3.5	113,200	12
$N_2 + N \rightleftarrows N + N + N$	1.1(22)	1.6	113,200	10
	4.1(22)	1.5	113,200	11
	8.5(25)	2.5	113,200	12
$O_2 + O_2 \rightleftarrows O + O + O_2$	2.8(19)	1.0	59,500	10
	3.2(19)	1.0	59,500	11
	6.2(24)	2.5	59,500	13
$O_2 + O \rightleftarrows O + O + O$	8.3(19)	1.0	59,500	10
	2.0(19)	1.0	59,500	11
	4.0(18)	1.0	59,500	13
$N_2 + O \rightleftarrows NO + N$	3.2(13)	0.1	37,700	10
	7.3(13)	0.0	38,000	11
	1.8(14)	0.0	38,300	13
$NO + M \rightleftarrows N + O + M$ (M = O or N)	2.3(17)	0.5	75,500	10
	3.9(20)	1.5	75,500	11
	1.4(14)	0.0	74,600	14
	5.2(15)	0.0	75,800	15
$NO + M \rightleftarrows N + O + M$ (M = O,N or NO)	4.6(17)	0.5	75,500	10
	7.8(20)	1.5	75,500	11
	3.0(14)	0.0	76,400	14
	5.2(15)	0.0	75,800	15
$N + O \rightleftarrows NO^+ + e$	1.5(10)	-.37	32,000	10
	1.4(6)	-1.5	31,900	11
	3.0(13)	0.5	32,500	16
$N + N \rightleftarrows N_2^+ + e$	1.8(10)	-.77	67,500	10
	1.4(13)	0.0	67,800	11
$5.4\times10^{13} T^{-\frac{1}{2}} (1 + 1.3\times10^{-4} T + 3.3\times10^{-8} T^2 - 10^{-12} T^3)\, e^{-67,300/T}$				17
$O + O \rightleftarrows O_2^+ + e$	3.9(10)	-.49	80,600	10
	1.6(17)	.96	80,800	11
$1.9\times10^{13} T^{-\frac{1}{2}} (1 + 7.5\times10^{-5} T + 2.2\times10^{-8} T^2)\, e^{-80,100/T}$				17

DETAILED BALANCING PRINCIPLE

For ordinary, one-step chemical reactions, the principle of detailed balancing can be shown to follow from equilibrium relationships. Consider the reaction

$$AB + M \underset{k_r}{\overset{k_d}{\rightleftharpoons}} A + B + M$$

at equilibrium, $k_d (AB)(M) = k_r (A)(B)(M)$

and therefore $k_d / k_r = (A)(B)/(AB) = K$, the equilibrium constant.

Even away from equilibrium, $k_d / k_r = K$ because the k's do not depend upon concentrations.

Usually k_d and k_r are not both available from experimental data. Especially at high temperatures, k_r is expressed as k_d / K in computer programs and calculations involving these rates of reactions.

Work last summer led to the conclusion that this relationship, $k_d / k_r = K$, also called the principle of detailed balancing, does not hold under certain conditions. If a large, sudden change in temperature occurs in a system, such as that generated by a high energy shock wave, then the equilibration of energy into the internal states will take a finite time and this time may become comparable to the reaction time of the system. When this occurs, the ordinary chemical rate constant is not well defined since

it usually represents an average rate of reaction over many individual rates from internal energy states. There is then an incubation time before the reaction rate reaches a steady-state or defined value. During this incubation time, the principle of detailed balancing does not hold for overall chemical reaction rates.(7)

During the incubation time, internal energy transitions become important and the approach to considering all of these transitions is summarized in the " Master Equation Approach" which is shown diagramatically below.

MASTER EQUATION APPROACH

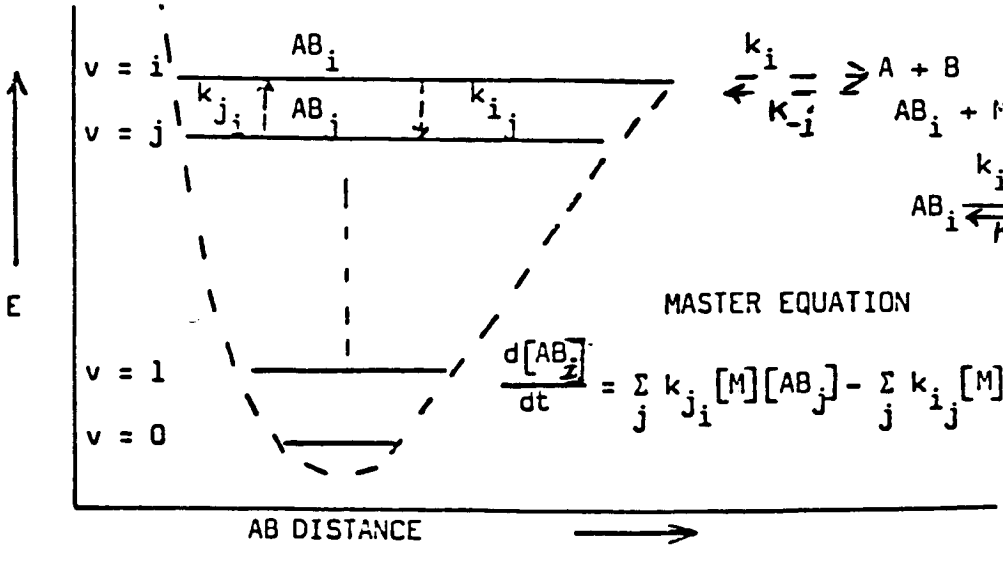

$$AB_i \underset{k_{-i}}{\overset{k_i}{\rightleftharpoons}} A + B \qquad AB_i + M \underset{k_{j_i}}{\overset{k_{i_j}}{\rightleftharpoons}} AB_j + M$$

MASTER EQUATION

$$\frac{d[AB_i]}{dt} = \sum_j k_{j_i}[M][AB_j] - \sum_j k_{i_j}[M][AB_i] - k_i[AB_i] + K_{-i}[A][B]$$

This equation could be solved if all k_{ij} , k_{ji} , k_i and k_{-i} are known. Approximations to this equation have been tried using detailed balancing for the internal energy transitions (k_{ij} and k_{ji}), and also assuming a harmonic oscillator. This development is shown in several references such as "Introduction to Physical Gas Dynamics" by Vincenti and Kruger.(18) This particular development is for vibration levels only and is breifly summarized below.

$$k_{ji}\,[AB_j] = k_{ij}\,[AB_i]$$

$$\frac{k_{ji}}{k_{ij}} = \frac{[AB_i]}{[AB_j]} = K = e^{-\frac{(E_i - E_j)}{KT}} = e^{-\frac{h\nu}{KT}}$$

$$\therefore \quad \frac{k_{ji}}{k_{ij}} = e^{-\frac{h\nu}{KT}}$$

$$k_{ij} = i\,k_{1,0} \quad , \quad i - j = 1$$

$$k_{1,0} = \frac{1 - e^{-h\nu/KT}}{\tau}$$

τ = RELAXATION TIME

$$\frac{d[AB_i]}{dt} = k_{1,0}\left[-i[AB_i] + (i+1)[AB_{i+1}] + e^{\frac{-h\nu}{KT}}\left(-(i+1)[AB_i] + i[AB_{i-1}]\right)\right]$$

IN TERMS OF ENERGY

$$\frac{d\,E_v}{dt} = k_{1,0}\left(1 - e^{-\frac{h\nu}{KT}}\right)\left[\frac{[AB]\,h\nu}{e^{-h\nu/KT} - 1} - E_v\right] = \frac{E_v^* - E_v}{\tau}$$

$[AB] = \Sigma\,[AB_i]$ $\qquad$ E_v^* = EQUILIBRIUM ENERGY

Probably the best assumption in this development is the principle of detailed balancing for the internal energy states. At the molecular level, where elementary collisions cause internal energy transitions, the exchange from translational to vibrational energy or vice-versa in a collisional process should be reversible in time by energy conservation principles. Thus there is no reason to suspect the failing of the principle of detailed balancing at this elementary level unless some other energy equilibration procedure is occuring that is not known. Rotational energies are lower than vibrational energies, but those transitions are assumed to occur very quickly even at low pressures so that rotational energies and translational energies are very quickly equilibrated. The effect of anharmonicity of the vibrational mode within the molecule is an effect that should be considered. This effect becomes more pronounced at higher energies and it is these higher energies that are important for dissociation.

Thus the development of the Master Equation using detailed balancing and harmonic oscillator assumptions is a valid first approximation to calculation of rates of reaction in high energy shock waves. However, other approaches are also presently being worked on and these are summarized below.

OTHER APPROACHES TO NON-EQUILIBRIUM REACTION RATES

Dove, et al have calculated the effects of coupling for the internal modes upon the relaxation of internal energies for hydrogen.(19) They concluded that at high rotational energies (J 10), coupling between translational, vibrational and rotational becomes almost as significant as translational-roatational coupling and is greater than translational-vibrational coupling. Thus at high rotaional energies, equilibration in the internal energies occurs through combined rotational-vibrational energy level changes.

Koshi has calculated the effect of vibrational-dissociation and dissociation-vibrational coupling(CVDV effect) and compared it with experimental data on NO dissociation.(15) His agreement is very good and indicates that as the translational temperature increases, the vibrational temperature lags behind and seems to approach a limit in the range of 5000K even though the translational temperature is above 7500K. The CVDV effect is due to the reduction of the dissociation rate due to the lack of vibrational equilibration within the molecule and also the coupled effect of a slower vibrational equilibration time due to dissociation removing energy from the upper vibrational levels and thus depleting them too rapidly.

This could result in a "bottle-neck" effect. That is, with a very rapid and high energy input, such as that from a high energy shock wave, the dissociation rate is limited by internal energy transitions within vibrational levels and not by the dissociation of the molecule from highly excited vibrational energies into two atoms.

Carlson compared experimental results with calculations on nitrogen in moderate shock waves studies and included the CVDV efeect as well as electronic-vibrational coupling. His claculated electronic temperature and the measured values agreed well within experimental error for this series of experiments.(8)

Finally, Chul Park has worked extensively on this problem and has written a computer program for predicting the non-equilibrium radiation in a shock front using available rate data.(9,10) His approach utilizes a two or three temperature model assuming different temperatures for different internal modes of energy and also a translational temperature. For some reactions, he uses the translational temperature, for some, the vibrational temperature and for others, the electronic temperature. Although this is an interesting approach, the calculated distances in the shock wave for peak and equilibrium temperatues, do not agree with experimental data.

SUMMARY

The most significant finding this summer was that there are large differences in important reaction rates as reported in the literature by various authors. These large differences could have significant effects on any computer programs or calculations of chemically reacting systems utilized in shock wave heat load predictions. It would be worthwhile to try some of these other rates in present computer programs and check the resulsts with known data.

The principle of detailed balancing is used widely in calculations of reaction rates. It is not valid during short incubation times in high energy shock waves in terms of the overall dissociation or recombination rate expressions. It does appear to be valid at the micro energy level concerning transitions within molecules. These transitions occur when translational energy is exchanged for vibrational energy in a collision for example. However, another significant find this summer is that in collisional processes, multi-jump transitions in vibrational levels can and do occur. This does not violate the law of detailed balancing, but makes it more complicated to take this into account.

Further refinements in calulation on these high energy reactions would benefit from the use of coupling effects

such as some of those mentioned in this paper. These include translation-vibration-rotational coupling, electronic-vibrational coupling and vibration-dissociation, dissociation-vibration coupling.

Future investigations should include models with limiting expressions such as the vibrational temperature reaching a limit and thus simplify the overall rate expressions. This may or may not occur within a time period that is insignificant in high energy shock waves. Approaches utilizing partition functions and activated complex theory also should be investigated. One final approach for future work would include the information theory approach by such authors as Levine to predict products of chemical reactions on the basis of excess entropy.(20)

ACKNOWLEDGEMENTS

I would like to thank my NASA Colleague, Dr. Carl Scott for the opportunity to work with him these past two summers on this interesting and challenging problem. It has increased my interest in the field of chemistry and in NASA.

I would also like to thank NASA and ASEE for these summer program opportunities for faculty such as myself to enrich our teaching and allow us to carry back some of this enthusiasm to our students who will become the engineers and scientists of tomorrow.

BIBLIOGRAPHY

1. Scott, C. D.: "Catalytic Recombination of Nitrogen and Oxygen oh High Temperature Reusable Surface Insulation," in Aerothermodynamics and Planetary Entry, ed. by L. Crosbie, Vol. 77 of Progress in Astronautics and Aeronautics, 1981, pp 192-212.

2. Scott, C. D.: "Effects of Nonequilibrium and Catalysis on Shuttle Heat Transfer," AIAA 18th Thermophysics Conference 1983.

3. Blackwell, H. E., Scott, C. D., Hoffman, J. A., Mende, S. B. and Swenson, G. P., "Spectral Measurements of the Space Shuttle Leeside Shock Layer and Wake", AIAA/ASME 4th Joint Thermophysics and Heat Transfer Conference, June 2-4, 1986, Boston MA.

4. Scott, C. D., Ried, R. C., Maraia, R. J., Li, C. P. and Derry, S. M.: "An AOTV Aeroheating and Thermal Protection Study", in Thermal Design of Aeroassisted Orbital Transfer Vehicles, ed. by H. F. Nelson,Vol 96, Progress in Astronautics and Aeronautics, 1985, pp. 309-337.

5. Greene and Toennies, Chemical Reactions in Shock Waves, Academic Press, NY, 1964, pp. 72-85.

6. Luther, K. and Troe, J.: "Influence of Temperature on Unimolecular and Termolecular Reactions", in Reactions of Small Transient Species, ed. by Fontijin and Clyne, Academic Press, NY, 1983, pp. 65-76.

7. Troe, J. and Wagner, H. G.: "Unimolecular Dissociation of Small Molecules", in Physical Chemistry of Fast Reactions-Vol. 1 Gas Phase Reactions of Small Molecules, ed. by B. P. Levitt, Plenum Press, NY, 1973, pp. 1-80.

8. Carlson, L. A. and Rieper, R. G.: "Electron Temperature and Relaxation Phenomena Behind Shock Waves", J. Chem. Phys. 57, 760-766, 1972.

9. Park, Chul: "Calculation of Nonequilibrium Radiation in the Flight Regimes of Aeroassisted Orbital Transfer Vehicles", Paper 84-0306 at AIAA 22nd Aerospace Sciences Meeting, Reno, Nevada, Jan. 9-12, 1984.

10. Park, Chul: "Problems of Rate Chemistry in the Flight Regimes of Aeroassisted Orbital Transfer Vehicles", Paper 84-1730 at AIAA 19th Thermophysics Conference, Snowmass, Colorado, June 25-28, 1984.

11. Kang, S. W. and Dunn, M. G.: "Theoretical and Measured Electron Density Distributions for the RAM Vehicle at High Altitudes", Paper 72-689, AIAA 5th Fluid and Plasma Dynamics Conference, Boston, MA, June, 1972.

12. Kewley, D. J. and Hornung, H. G.: "Free-Piston Shock-Tube Study of Nitrogen Dissociation", Chem. Phys. Letters 25, 531-536, 1974.

13. Oertel, H. Jr.: "Regular Shock Reflection Used for Study in Oxygen Dissociation", Modern Developments in Shock Tube Research-Proceedings of International Shock Tube Symposium(10th), ed. Kamimoto, 605-612, 1975.

14. Myerson, A. L.: "Shock-Tube Atom Kinetics of Nitric Oxide Decomposition", Symposium(International) on Combustion 14, 219-228, 1973.

15. Koshi, M. et al: "Dissociation of Nitric Oxide in Shock Waves", Symposium(International) on Combustion 17, 553-562, 1978.

16. Lin, S. C. and Teare, J. D.: Physics of Fluids 6, 355, 1963.

17. Wilson, J.: "Ionization Rate of Air Behind High-Speed Shock Waves", Physics of Fluids 9, 1913-1921, 1966.

18. Vincenti, W. G. and Kruger, C. H. Jr.: Introduction to Physical Gas Dynamics, John Wiley and Sons, pp. 198-202, 1965, New York.

19. Dove, J. E. et al: "The Mechanism of Vibrational Relaxation of Molecular Hydrogen", J. Phys. Chem. 81, 2564-2572, 1977.

20. Levine, R. D.: "Information Theory Approach to Molecular Reaction Dynamics", in Annual Review of Physical Chemistry, ed. B. S. Rabinovitch, Vol 29, pp. 59-92, Annual Reviews Inc., Palo Alto, CA., 1978.

1986

NASA/ASEE SUMMER FACULTY RESEARCH FELLOWSHIP PROGRAM

Johnson Space Center

Lamar University

Rare Gas Analysis of Size Fractions from the Fayetteville Meteorite

Prepared by:	Jim L. Jordan
Academic Rank:	Assistant Professor
University & Department:	Lamar University Beaumont, TX Department of Geology
NASA/JSC	
Directorate:	Space and Life Sciences
Division:	Solar System Exploration
Branch:	Experimental Planetology
JSC Colleague:	D.D. Bogard
Date:	August 11, 1986

RARE GAS ANALYSIS OF SIZE FRACTIONS FROM THE FAYETTEVILLE METEORITE

Jim L. Jordan
Assistant Professor
Department of Geology
Lamar University
Beaumont,TX 77710

Abstract

Eight size separates of grains from the Fayetteville meteorite ranging from less than 20 microns to greater than .1 millimeter are being analyzed for their rare gas elemental and isotopic composition.At this time measurements on five of the samples have been performed. All five reveal a mixture of solar, planetary, cosmic ray produced and radiogenic gases.The solar component is of particular interest since it suggest that the meteorite may represent a fragment of an ancient protoplanetary regolith which was exposed to the solar wind.Solar wind elements are implanted in the outer few hundred Angstroms of exposed grains and are therefore expected to be surface correlated.At present the data do not suggest that such a correlation exists,but the final conclusion must await further analyses and data reduction.

1. Introduction

Elemental and isotopic studies of meteoritic and lunar material have been extensively used to characterize the physical and chemical environment in which these materials formed and currently exist. Rare gases are particularly attractive for this purpose because their low abundance allows for the effects of processes such as cosmic ray induced nuclear reactions and radioactive decay to be detected easily above the trapped primordial gas background. The inert character and wide mass range of these gases make them particularly useful monitors of the thermal history of planetary materials. The ages and duration of these events may be determined from those rare gases that are products of nuclear reactions and radioactive decay as well.

Before the Apollo program meteorites provided the most important source of information on the nature of solids in the extraterrestrial environment, both past and present.Unlike the Earth , most meteorites show little evidence for having experienced severe thermal metamorphism and therefore become useful objects of study for the earliest events in the solar system , including the formation itself. The Apollo missions added abundant information about lunar materials to the realm of our knowledge regarding extraterrestrial matter.Since the moon has at present no magnetic field it is a passive object to solar wind,solar flares,and galactic cosmic rays and thus is a good target for recording these radiations in the grains at its surface.A very large database for this record now exists from laboratory measurements made on lunar soil samples.Lunar soils have proven to be particularly useful in providing well defined compositions for solar wind implanted particles.Since solar wind elements have typical energies of 1 keV/nucleon they are implanted in the outer few hundred Angstroms of exposed grains and are therefore

expected to be surface correlated. Analyses of size fractions of lunar soils show such a correlation exist for solar wind implants and these surface correlated elements have been used to define the solar wind composition albeit fractionated by a large number of regolith processes (see for example [1]).

One of the goals of lunar soil studies has been to determine the composition of the ancient solar wind. Indeed such information would not only aid in the understanding of the behavior of the sun at the time of solar system formation 4.5 billion years ago, but it would enhance our knowlege of stellar processes in general. The soil studies have failed to provide the answer to this question since the history of the regolith of the moon is extremely complex. Down to a depth of greater than a meter evidence exist for grains having been exposed to the solar wind, indicating that they had resided at the very surface at one time [2]. There has not been any satisfactory means found thus far, however, for determining when and

how long an individual grain was at the very surface.

To address the problem of the ancient solar wind interest has turned once again to meteorites.Some meteorites may represent the surface of their parent body which apparently broke up very early in the history of the solar system .These "regolith" meteorites have probably recorded an earlier solar wind.Rare gas analyses of these meteorites have revealed that they are "gas-rich" compared to others and that the composition is both elementally and isotopically distinct from other meteorites as well [3]. Lunar samples confirmed the long standing suspicion that a large portion of the gas in these objects is from the solar wind.

For the aforementioned reasons we have undertaken the study of the Fayetteville meteorite, the most gas rich of this class of meteorites.Our goal was to carry out rare gas analyses of several size separates of a disaggregated portion of this meteorite to determine if a surface correlation exists and better define the composition of this gas. A large number of rare gas analyses have been

performed on Fayetteville, but none were done on size fractions from a disaggregated sample [4,5,6,7,8,9, 10,11,].It is indeed a challenging task to disaggregate a compacted meteorite into its constituent grains and the meaningfulness of the rare gas data depends in part on the success of that experiment.It represents an important first step for expanding our understanding of parent body regoliths and their record of the ancient solar wind.

2.Experimental

Prior to rare gas analyses 561 mg of the Fayetteville meteorite was disrupted by D.McKay and co-workers with a freeze-thaw technique using alternating cycles of liquid nitrogen and hot water baths.A total of 24,440 cycles taking 64.5 days were performed before stopping the procedure because of Fe oxidation.Disaggregation was not complete. Following this procedure the disrupted portion was sieved into seven size fractions ranging from less than 20 microns to 1 mm in diameter.

Small masses of each size fraction were wrapped

in aluminum foil "boats" and loaded in the ultrahigh vacuum system (<10E-8 mmHg) gas extraction system.Gas extraction was performed by heating the sample at 1550 C in an RF induction furnace.The evolved gas cleaned with a hot Ti-getter and two Zr-getters. Separation of lighter from heavier gases was accomplished through "freezing" gases on a charcoal finger with liquid nitrogen (Ar,Kr,Xe bound;He and Ne measured),liquid nitrogen+isobutonal (Ar freed,some Kr),and liquid nitrogen+hexonal (Kr freed,some Xe). Xe was released from the charcoal finger with hot water.

The separated gases are admitted through a gas inlet valve to a static mode rare gas mass spectrometer.The sensitivities for He,Ne,Ar are of the order of magnitude 10E-10 cc/mv and 10E-13 cc/mv for Kr and Xe when the accelerating voltage , ionization potential,electron current,magnetic field, and electrometer resistance are appropriately set. The sensitivities are accurately determined using air pipettes (1/10th cc) as standards.Sample gas isotopes were measured by computer driven magnetic field

changes (peak jumping) 10 - 15 times and extrapolation of peak values and isotopic ratios to the time of gas inlet was done by fitting the data to a fourth order polynomial.

3.Results and Discussion

The rare gas concentrations of five of a total eight samples (including 1 undisrupted sample) measured thus far are listed in Table 1.Elemental ratios of the same are given in Table 2 and isotopic ratios may be found in Tables 3 - 5.It is clear from all of these data that there is no correlated variation with the diameter of the grains obtained through the freeze - thaw technique.Our results agree well with previous measurements of bulk samples of Fayetteville suggesting that the failing correlation was not the result of an experimental mishap.

The failure to obtain a correlation of rare gas contents with grain size may be due to the disruption technique.It is not absolutely certain that any grain size fraction is made up of completely disaggregated

material.Grains may have broken across their boundaries as well.This technique must be compared with others before one can relate these results to grains as they were in the regolith.

4.Conclusions

It should not be concluded at this stage that the solar wind surface correlation never existed in the regolith of the Fayetteville parent body.One should first appeal to other methods of extracting this information such as disruption by sonification or stepwise heating.The former method will call for additional rare gas measurements of grain size separates.The latter method allows for measurement of bulk sample but requires many temperature steps.In this procedure advantage is taken of the different activation energies of rare gas components in meteoritic minerals.Both of these methods will be investigated in the future.

Table 1

FAYETTEVILLE RARE GAS DATA FOR GRAIN SIZE SEPARATES
ccSTP/g

SIZE (MICRONS)		3 HE E-6	4 HE E-3	22 NE E-6
<20		8.351	8.282	1.993
20-45		1.362	3.18	1.771
45-90	*			
90-150		4.069	12.072	3.0235
150-250	*			
250-500	*			
500-1000		2.99	8.13	2.0397
>1000		2.465	6.971	2.137

		36 AR E-6	86 KR E-10	136 XE E-10
<20		1.207	82.86	90.78
20-45		0.801	4.921	2.631
45-90	*			
90-150		1.666	8.585	5.942
150-250	*			
250-500	*			
500-1000		0.442	12.14	8.832
>1000		1.105	4.802	1.735

*) Not measured at this time

Table 2 ELEMENTAL RATIOS

SIZE (MICRONS)	4/20	20/36	36/84	84/132
<20	363.5	18.9	44.7	0.998
20-45	168.9	23.5		
45-90				
90-150	353.6	20.5	596.4	1.537
150-250				
250-500				
500-1000	352.4	52.2	111.8	1.485
>1000	289.6	21.8	700.6	2.942

Table 3 ISOTOPIC RATIOS - LIGHT GASES

	4/3	20/22	21/22
<20	991.6	11.43	0.0547
20-45	2334.2	10.63	0.0876
45-90			
90-150	2967.1	11.29	0.059
150-250			
250-500			
500-1000	2719.1	11.31	0.0621
>1000	2827.8	11.26	0.0517

	36/38	40/36
<20	5.207	36.61
20-45	5.018	43.14
45-90		
90-150	5.189	29.47
150-250		
250-500		
500-1000	5.011	35.05
>1000	5.08	30.02

Table 4 VALUES OF ^{i}KR / ^{86}KR

ISOTOPE	<20	90-150	500-1000	>1000
78	0.0623	0.194	0.0803	0.1422
80	0.134	0.1651	0.1439	0.1624
82	0.6609	0.6862	0.6677	0.6855
83	0.6574	0.6723	0.6588	0.6756
84	3.257	3.253	3.256	3.284

Table 5 VALUES OF ^{i}XE / ^{136}XE

ISOTOPE	<20	20-45	90-150	500-1000	>1000
124	0.01183	0.04835	0.02133	0.01372	0.0214
126	0.01146	0.04639	0.0216	0.01332	0.02158
128	0.2159	0.3294	0.2616	0.2288	0.2702
129	2.885	3.167	3.302	3.24	3.355
130	0.4502	0.5096	0.485	0.4636	0.4983
131	2.344	2.42	2.448	2.386	2.493
132	2.979	3.044	3.058	3.014	3.089
134	1.169	1.221	1.198	1.177	1.201

References

1.P.Eberhardt,J.Geiss,H.Graf,N.Groegler,U.Kraehenbuehl H.Schwaller,J.Schwarzmueller,A.Stettler,Science 167, 558 (1970).

2.D.D.Bogard and W.C.Hirsch,Proc.Lunar Sci. Conf.6th, 2057 (1975).

3.R.O.Pepin and P.Signer,Science 149,253 (1965).

4.D.C. Black,Geochem.Cosmochem.Acta 36,347 (1972).

5.H.Hintenberger,H.Koenig,L.Schultz,and H.Waenke, Z. Naturf. 19A,327 (1964).

6.O.K.Manuel and P.K.Kuroda,J.Geophys.Res.69,1413 (1967).

7.O.K.Manuel,Geochem.Cosmochem.Acta 31,2413 (1967).

8.G.H.Megrue,Science 157,1555 (1967).

9.G.H.Megrue,Meteorite Research (Ed. P.M.Millman), 922 Reidel,Dordrecht (1969).

10.O.Mueller and J.Zaehringer,Earth Planet Sci.Lett. 1,25 (1966).

11.J.Zaehringer,Meteortika 27,25 (1966).

1986

NASA/ASEE SUMMER FACULTY RESEARCH FELLOWSHIP PROGRAM

Johnson Space Center

University of Houston

An Analysis of Bipropellant Neutralization for Spacecraft Refueling Operations

Prepared by:	David Kauffman, P.E., Ph.D.
Academic Rank:	Associate Professor
University & Department:	University of New Mexico
	Chemical & Nuclear Engineering
NASA/JSC	
Directorate:	Engineering
Division:	Propulsion and Power
Branch:	Propulsion
JSC Colleague:	Ralph J. Taeuber
Date:	August 15, 1986
Contract #:	NGT-44-005-803 (University of Houston)

AN ANALYSIS OF BIPROPELLANT NEUTRALIZATION FOR SPACECRAFT REFUELING OPERATIONS

Abridged Version

David Kauffman, Ph.D.

Chemical and Nuclear Engineering Department
The University of New Mexico
Albuquerque, New Mexico

National Aeronautics and Space Administration
Lyndon B. Johnson Space Center
Propulsion and Power Division
Houston, Texas

August 15, 1986

ABSTRACT

Refueling of satellites on orbit with storable propellants will involve venting part or all of the pressurant gas from the propellant tanks. This gas will be saturated with propellant vapor, and it may also have significant amounts of entrained fine droplets of propellant. The two most commonly used bipropellants, monomethyl hydrazine (MMH) and nitrogen tetroxide (N204), are highly reactive and toxic. This study examines various possible ways of neutralizing the vented propellants.

The amount of propellant vented in a typical refueling operation is shown to be in the range of 0.2 to 5 percent of the tank capacity. Four potential neutralization schemes are examined: chemical decomposition, chemical reaction, condensation and adsorption. Chemical decomposition to essentially inert materials is thermodynamically feasible for both MMH and N204. It would be the simplest and easiest neutralization method to implement. Chemical decomposition would require more complex control. Condensation would require a refrigeration system and a very efficient phase separator. Adsorption is likely to be much heavier.

A preliminary assessment of the four neutralization schemes is presented, along with suggested research and development plans for more detailed investigation of the problem.

Note: A more extensive report on this project has been written and will be published as a NASA JSC Internal Note.

CONTENTS

Sections 2 through 8 are contained in the full report only, not in this abridged version.

SUMMARY

Venting of propellants on orbiting spacecraft is an area that has not received a great deal of attention in the past. As refueling and other servicing operations become more common, however, propellant venting will be required more often. The commonly used bipropellants, monomethyl hydrazine (MMH) and nitrogen tetroxide (N2O4) are both toxic, highly reactive chemicals. If they must be vented, it would be far better to neutralize them to more innocuous species first.

The amounts of bipropellants vented during various on-orbit servicing operations are not well established. Preliminary estimates indicate that the amount of propellant vented during a typical refueling operation is likely to be about 0.2 to 5 percent of the total fuel tank capacity. Depending on the operational mode, the fuel may or may not be highly diluted with pressurant gas, helium or nitrogen. Tank leakage or deliberate propellant dumping could vent considerably more propellant.

Four potential propellant neutralization methods have been identified in the course of this study: catalytic chemical decomposition, chemical reaction, condensation and adsorption.

Catalytic decomposition is thermodynamically feasible for both MMH and N2O4. Previous experience with catalytic decomposition of hydrazine indicates a high probability of finding a suitable catalyst for MMH decomposition. With MMH, the desired reaction products (methane, nitrogen and hydrogen) are thermodynamically favored at temperatures below about 300 C. Above that temperature, however, catalytic decomposition of MMH will most likely lead to deposition of solid carbon on the catalyst, thus making it inactive. With N2O4, the desired products (nitrogen and oxygen) are thermodynamically favored from ambient temperature up to about 500 C. Previous work in development of catalysts for air pollution control, however, has never been successful in finding a decompose N2O4 to nitrogen and oxygen.

A laboratory investigation of propellant decomposition was started at JSC. Laboratory equipment was assembled to examine the products obtained when dilute streams of MMH and N2O4 are passed over catalysts. Only very limited data have been collected to date due to the limited time available during the author's summer visit.

Chemical reaction systems for neutralization of MMH and N2O4 should be feasible. It is easy to get MMH to react with an oxidizer and to get N2O4 to react with a reducing agent. The most practical system is likely to use small amounts of N2O4 to neutralize MMH and small amounts of MMH to neutralize N2O4. At the present time, however, there is very little information available on feasible mixture ratios and the effects of diluent helium or nitrogen for such systems. Operation and control of a reaction system will be considerably more complex than for simple catalytic decomposition.

Condensation and adsorption systems trap vented propellant vapors for return to earth or for later disposal in space. Condensation systems cool the vapors to low enough temperatures to condense them, then collect the droplets. Such a system would require an extremely efficient liquid-vapor phase separator, something which does not now exist. The vapor-pressure curve and very low freezing point of MMH make it a suitable candidate for a condensation system. N204, however, freezes at 11.2 C, at which point it still has a fairly high vapor pressure. It would be a poor candidate for a condensing system. Both MMH and N204 should be suitable candidates for adsorption systems, in which the propellants are adsorbed on the surface of highly porous solids. The major disadvantage to these systems is their relatively high intrinsic weight. A system capable of collecting ten pounds of propellant is likely to weigh fifty pounds.

Suggested research and development programs are outlined for each of the four potential propellant neutralization processes.

A preliminary system comparison indicates that chemical decomposition would be the simplest system to operate and control. Chemical reaction systems represent a lower development risk. Adsorption systems also have a very low development risk, but they are likely to be much heavier. Condensing systems appear to be impractical.

Conclusions and recommendations presented in this report must be considered very preliminary. The single most significant conclusion is that hard data are lacking on the feasibility of many of the candidate processes.

Note: Sections 2 through 8 are contained in the full report only, not in this abridged version.

SECTION 1

INTRODUCTION

Venting of excess liquid propellants and vapors during on-orbit refueling operations is an area that has not been studied a great deal in the past. On-orbit servicing of satellites is becoming more common, however, and on-orbit refueling is expected to become a fairly routine operation in the near future. NASA's Orbital Spacecraft Consumables Resupply Systems (OSCRS) is being developed for just this purpose.

When propellants are supplied to a satellite, the vapors present in the satellite tank must be displaced, either by venting them to space or by collecting them. In many refueling operations, there will also be pressurant gas, helium or nitrogen, present as well as propellant vapors. In addition, any venting of vapors and gases is likely to entrain significant amounts of liquid droplets or mist as well.

The most commonly used bipropellants are monomethyl hydrazine (MMH) and nitrogen tetroxide (N2O4). These are highly reactive, toxic chemicals. It is imperative that they not be spilled or vented toward astronauts or toward sensitive materials, such as optical surfaces and solar cells, on spacecraft. To accomplish refueling, then, the vented propellants must either be dispersed far from the satellite or must be treated in some manner to make them more innocuous.

1.1 ORBITAL REFUELING OPERATIONS

In a typical refueling operation, a satellite will be secured to the Shuttle Orbiter. Fuel lines will be connected by astronauts. The satellite tanks will be depressured, and possibly completely emptied, by venting to space or by venting to a catch tank on the Orbiter. Propellants will then be loaded into the satellite by pressurization or pumping from the Orbiter. If this is done with the receiving tanks kept at constant pressure, additional venting will be required as the liquids enter the tanks. If the receiving tanks are pressured by the refilling, additional venting may not be necessary.

The amount of propellant that will be vented during a refueling operation depends on many factors, some of which are very poorly defined at this time. Clearly, the size and type of tank involved will have an influence, as will the physical properties of the propellant, particularly the vapor pressure and liquid density. The

amount vented will also depend on the amount and type of pressurant gas vented in the operation. To the extent possible in this limited study, these factors are addressed in Section 2.

To place the venting problem in perspective, however, it is useful to have some idea of the possible ranges of vent flows. The studies in Section 2 generally indicate propellant venting on the order of one percent of the propellant tank capacity, with various factors pushing this from near zero to 5 percent or more. Typical refueling operations are likely to involve several thousand pounds of propellant at a time. The total to be vented, then, will be on the order of several tens of pounds of propellants along with an equal or lesser amount of pressurant.

1.2 PROPELLANT NEUTRALIZATION METHODS

There are four candidate neutralization methods considered in this study: chemical decomposition, chemical reaction, condensation and adsorption. This section describes each one briefly. More details are given in Sections 3, 4, 6, 7 and 8.

1.2.1 Decomposition

A chemical may decompose to other smaller molecules provided the overall free energy of the decompositon is negative. This criteria establishes that the process is thermodynamically feasible. Whether or not the chemical will actual decompose, assuming the decompositon is thermodynamically feasible, depends on the kinetics of the decomposition reaction. Some chemicals will decompose spontaneously at ambient temperatures; others will decompose only at higher temperatures or in the presence of an appropriate catalyst. Still others are virtually inert.

MMH can decompose in at least six ways, all of which are thermodynamically possible:

$$CH_3NHNH_2 \rightarrow CH_4 + N_2 + H_2 \qquad (1\text{-}1)$$

$$\Delta F^\circ = -56.8 \text{ kcal/g.mole}$$

$$CH_3NHNH_2 \rightarrow C(s) + 2NH_3 \qquad (1\text{-}3)$$

$$\Delta F^\circ = -52.4 \text{ kcal/g.mole}$$

$$CH_3NHNH_2 \rightarrow CH_3NH_2 + \tfrac{1}{2}N_2 + \tfrac{1}{2}H_2 \qquad (1\text{-}2)$$

$$\Delta F^\circ = -37.0 \text{ kcal/g.mole}$$

$$CH_3NHNH_2 \longrightarrow C(s) + N_2 + 3H_2 \qquad (1\text{-}4)$$

$$\Delta F^\circ = -44.7 \text{ kcal/g.mole}$$

$$CH_3NHNH_2 \longrightarrow HCN + NH_3 + H_2 \qquad (1\text{-}5)$$

$$\Delta F^\circ = -18.7 \text{ kcal/g.mole}$$

$$CH_3NHNH_2 \longrightarrow CH_3NH_2 + \tfrac{1}{3}NH_3 + \tfrac{1}{3}N_2 \qquad (1\text{-}6)$$

$$\Delta F^\circ = -10.8 \text{ kcal/g.mole}$$

The free energies listed above are for standard conditions, one atmosphere pressure at 25 C. The free energies vary considerably with temperature; so the most thermodynamically stable products vary with temperature. Thermodynamics also favors reactions creating the largest number of product moles at lower pressures and reactions creating the fewest number of product moles at higher pressures.

N204 can decompose by two paths which are thermodynamically possible:

$$N_2O_4 \longrightarrow N_2 + 2O_2 \qquad (1\text{-}7)$$

$$\Delta F^\circ = -23.4 \text{ kcal/g.mole}$$

$$N_2O_4 \longrightarrow 2NO_2 \qquad (1\text{-}8)$$

$$\Delta F^\circ = +1.1 \text{ kcal/g.mole}$$

Even though its free energy of reaction is slightly positive, the second of these reactions takes place spontaneously, but it does not go to completion. An equilibrium mixture of N204 and N02 is always present; by convention it is usually referred to simply as N204.

Decomposition of MMH by Equation 1-1 and N204 by Equation 1-7 would be the most desirable in terms of propellant neutralization. Ideally, a simple catalytic packed-bed reactor could be placed in vent lines to promote these reactions. Decompositon is examined in more detail in Sections 3 and 4.

1.2.2 Chemical Reaction

If simple chemical decomposition is not feasible, an alternative

would be chemical reaction. In this mode of operation, each propellant would be reacted with another chemical to yield innocuous products. The reactions might take place over a catalyst, or they might be simple spontaneous homogeneous reactions. MMH, a strong reducing agent, would be reacted with an oxidizing agent. N2O4, a strong oxidizer, would be reacted with a reducing agent. One obvious set of choices would be to use N2O4 in substoichiometric amounts to react with MMH, and to use MMH to react with N2O4. There are, however, other choices which should also be considered.

A chemical reaction neutralization process would obviously be more complex and require more equipment than would a simple decomposition process. In addition to the reactors themselves, there would have to be supplies of reactants and a control system to provide the right amounts when needed. Chemical reaction systems are discussed in more detail in Section 6.

1.2.3 Condensation

In a condensation system, the vent gases would be cooled to a temperature low enough to cause virtually all of the propellent to condense out of the pressurant gas. Propellant droplets, or solid particles if the temperature were low enough, would be collected by impingement devices. Collected propellants would be returned to their tanks or held in separate containers for later use or later release.

A condensation system would have the advantage of avoiding chemical reactions entirely. It would require a refrigeration system and a very efficient collection system. Condensation systems are discussed in more detail in Section 7.

1.2.4 Adsorption

An adsorption system would be similar to a condensation system in that the propellants would be trapped for later use or controlled venting. An adsorption system, however, would operate at ambient temperature. Propellant vapors and mist droplets would be adsorbed and held by suitable high-surface-area materials, such as activated carbon or silica gel. The system is simpler than a condensation system, but it may be somewhat larger since the net mass of propellant adsorbed per unit volume of sorbent is considerably less than the density of liquid or solid propellant. Adsorption systems are discussed in more detail in Section 8.

1.3 SCOPE OF THIS STUDY

The purpose of this study is to examine the bipropellant venting problem, with emphasis on methods of neutralizing MMH and N2O4. Section 2 of this report addresses the problem of estimating the amounts of propellants likely to be vented during typical operations. Sections 3 and 4 go into some detail on chemical decomposition

processes for MMH and N2O4, respectively. Section 5 discusses the laboratory program started at JSC in 1986 to assess the feasibility of propellant decomposition. Sections 6, 7 and 8 look at the other three possible neutralization processes: chemical reaction, condensation and adsorption. Section 9 presents some preliminary comparisons among the four processes.

Conclusions and recommendations presented in this report must be considered very preliminary. The single most significant conclusion is that hard data are lacking on the feasibility of many of the candidate processes. Outlines of suggested research and development programs to provide the necessary data are presented.

SECTION 9

PRELIMINARY NEUTRALIZATION SYSTEM COMPARISON

The various possible bipropellant neutralization systems can best be compared at this time by a simple summary of the pros and cons associated with each system. Neither venting system requirements nor neutralization system designs are well enough established for a quantitative comparison at this time.

9.1 DECOMPOSITION SYSTEMS

MMH and N204 must be considered separately in terms of chemical decomposition processes. First consider MMH:

Pro:

In terms of chemical thermodynamics, the most stable decomposition products of MMH at temperatures up to 300 to 400 C are methane, nitrogen and hydrogen, all quite harmless. Previous experience with hydrazine decomposition leads to the expectation that suitable decomposition catalysts can be developed relatively easily. Operation and control would be quite simple; the MMH and accompanying pressurant gas, if any, would simply be vented through a packed catalyst bed. The system would be fairly light weight and compact.

Con:

Carbon deposition on the catalyst surface, resulting in catalyst poisoning, can be expected at high temperatures. Either a temperature control system on the catalyst bed or a highly selective catalyst may be required. Considerable effort may be required to obtain a catalyst which will work successfully for an extended period of time.

For N204:

Pro:

In terms of chemical thermodynamics, the most stable decomposition products of N204 at temperatures up to 1800 C are nitrogen and oxygen, both quite harmless. Operation and control would be quite simple; the MMH and accompanying pressurant gas, if any, would simply be vented through a packed catalyst bed. The system would be fairly light weight and compact.

Con:

A great deal of effort has been spent in the past searching for catalysts to decompose nitrogen oxides to nitrogen and oxygen for use in air pollution control systems. To date, no such catalyst has been found.

9.2 CHEMICAL REACTION SYSTEMS

Pro:

Both MMH and N2O4 are highly reactive. They can be reacted with each other, or with other suitable chemicals. If reacted with each other, no additional chemical supply systems would have to be carried, only the extra amounts of propellant needed for reaction. System development and design should be fairly simple. The total amount of hardware needed for the system would be quite small.

Con:

A moderately complex sensing and control system would have to be developed to feed the right amounts of reactants to the venting gases at the right times. The reaction products which would be obtained from non-stoichiometric combustion, especially ion the presence of large amounts of diluent gases, are not fully established. Ignition and stable operation over a wide range of non-stoichiometric mixtures must be established.

9.3 CONDENSATION SYSTEMS

Pro:

Chemical reactions are avoided. The propellants are trapped for return to earth or for venting at a later, safer time.

Con:

A complex system is required, including a refrigeration system and an extremely efficient phase separation device. The latter is not available at this time. In the case of N2O4, freezing takes place under conditions where the vapor pressure is still fairly high. An effective condensation system for N2O4 would have to operate in the vapor-solid region, not in the vapor-liquid region.

9.4 ADSORPTION SYSTEMS

Pro:

Solid adsorption systems have been developed for many different vapors in the past. It should be fairly easy to develop systems for MMH and N2O4. Such systems are inherently simple to design, build and operate. Propellants would be captured for return to earth or for release to space at more convenient, safer times.

Con:

Adsorption systems are likely to be quite heavy compared with other alternatives. Sorbent capacities of a few tenths of a pound of propellant per pound of sorbent can be expected. The systems have fixed capacities. Once their sorption capacities are reached, any additional propellent will simply pass on through them.

SECTION 10

CONCLUSIONS

The following principal conclusions have been reached as a result of this study:

1. There has been little systematic study of the problem of on-orbit venting of storable bipropellants, either in terms of requirements for various servicing operations or in terms of methods for dealing with the propellants.

2. Preliminary estimates indicate that propellant venting during refueling operations may amount to 0.2 to 5 percent of the capacity of a propellant tank. Amounts on the order of tens of pounds of propellants may be expected.

3. Four potential processes for treating vented storable bipropellants have been identified: chemical decomposition, chemical reaction, condensation and adsorption.

4. Catalytic chemical decomposition of MMH is probably feasible. The major uncertainty in the process is carbon deposition and poisoning of the catalyst surface. This problem may be avoided by operation at relatively low temperatures (below about 300 C) or by developing a catalyst that is highly selective.

5. Catalytic decomposition of N2O4 to less innocuous materials is probably not feasible.

6. Chemical reaction systems (reacting MMH with a small amount of an oxidizer and reacting N2O4 with a small amount of a reducing agent) represent a low-risk development alternative. On-orbit operation and control, however, will be considerably more complex than for chemical decomposition.

7. Condensing systems appear to be of limited practical value. Any such system would have to incorporate an extremely efficient vapor-liquid phase separation device. A system for N2O4 is further complicated by the relatively high vapor pressure of N2O4 at its freezing point (about 2.7 psia at 11. 8 F).

8. Adsorption systems represent a low development risk alternative, but are likely to be much heavier than other systems for comparable performance.

SECTION 11

RECOMMENDATIONS

The following recommendations are made based on the conclusions reached in this study:

1. System requirement studies should be carried out to define the needs and operational limitations associated with on-orbit venting of bipropellants, both during satellite servicing and other operations.

2. Catalytic decomposition of MMH should be explored as a prime treatment method. Initial emphasis should be on catalyst screening and development to obtain a catalyst that will work effectively without becoming poisoned due to carbon deposition.

3. Catalytic decomposition of N2O4 should be explored to a limited extent only, with emphasis on determining whether the process is at all feasible.

4. Chemical reaction systems should be examined as a low-risk alternative to decomposition systems. Initial work should be aimed at determining non-stoichiometric reaction behavior of MMH and N2O4 diluted with pressurant gases.

5. If the amounts of vented propellants are expected to be very small, or if the weight penalty is tolerable, adsorption systems should be examined as a low-risk alternative to chemical treatment methods. Initial work should be aimed at identifying the best sorbents for MMH and N2O4 and determining their capacities under a variety of conditions.

1986

NASA/ASEE SUMMER FACULTY FELLOWSHIP PROGRAM

Johnson Space Center

University of Houston

Geometric Description and Grid Generation for Space Vehicles

Prepared by:	Madakasira G. Krishna
Academic Rank:	Professor
University & Department:	South Carolina State College Department of Mathematics and Computer Science
NASA/JSC	
Directorate:	Engineering
Division:	Advanced Programs Office
Branch:	Aeroscience
JSC Colleague:	Dr. Chien-Peng Li
Date:	August 15, 1986
Contract #:	NGT-44-005-803 (University of Houston)

GEOMETRIC DESCRIPTION AND GRID GENERATION FOR SPACE VEHICLES

Madakasira G. Krishna
Professor
Department of Mathematics and Computer Science
South Carolina State College
Orangeburg, SC 29117

ABSTRACT

The understanding and analysis of Three-dimensional fluid behavior around reentry vehicles, like the Space Shuttle Orbiter, is of considerable importance for flight applications. Vehicle designers need pressure, heat transfer, and shear distributions to support design activities. Traditionally these have been obtained by experimental data. Significant reduction in design costs can be obtained if the calculated results based on finite difference procedures are used to verify and supplement experimental results.

Computing the flowfield over Space Shuttle Orbiter, which has complex cross-sectional geometries is a major problem. A first step in this direction is development of body definition and grid generation procedure. In this project a digitized body definition and grid generation procedure, developed earlier at JSC, is modified and applied to the Shuttle Orbiter X24C-10D. Two-dimensional grid and body defintion for varous sections of the space vehicle is obtained using the differential equation method.

This study demonstrates that this geometry and grid generation rpocedure can be applied to other aerospace vehicles such as aerospaceplane.

1. INTRODUCTION

Analysis of three-dimensional fluid behavior around reentry vehicle such as X-24C-10D is of considerable importance for flight applications. A vehicle like this can produce very complex flow fields. The flow field changes radically with leeside of vehicle becoming dominated by large regions of cross flow separation, when angle of attack is increased. Calculated results are useful to verify and supplement the experimental results. For the chosen aircraft a detailed experimental data base exists in the form of a flow field pitot survey, surface pressures, heat transfer, force and moment measurements.[1, 2, 3]

A first step in calculating the flow parameters using finite difference methods is to generate a satisfactory grid. The grid generation process must achieve the following:

1. Develop accurate surface definition
2. Distribute grid points on the body surface
3. Generate a clustred smoothly varying interior mesh.

Algebraic or differentiated equation techniques[4] can be used to generate grid on complicated three-dimensional problems. In this study a digitized body definition and grid generation procedure developed earlier at Johnson Space Center is modified and applied to the Shuttle Orbiter X-24C-10D in order to test the procedure. This hypersonic research aircraft is selected in this investigation for its rather blunt leading edges, canopy, strake fin and wing formations, which are typical

of those encountered in a modern aerospace vehicle. The object of this testing is to apply this procedure to other aerospace vehicles such as the aerospaceplane at a later date. A differential equation method developed by Thompson et al.[5] and windslow[6] is used to generate two-dimensional elliptic grid in each cross section plane between two control surfaces.

2. PROCEDURE

The block diagram of the digitized procedure used to generate the body and the two-dimensional grid for various sections of the Shuttle Orbiter X-25C-10D is shown in figure 2. X-axis is chosen along the body axis. The X=constant plane in which Y and Z vary is chosen as a plane normal to the body axis. Coordinates of points on various segments of sections of the body are obtained from a blue print supplied by Martin Marietta Corporation, Denver, Colorado. The coordinate system is constructed by a series of coaxial cross sections. In each cross section plane a two-dimensional grid system is established between the body contour and an ellipse.

The grid is generated by using the differential equation method, which is one of the highly developed techniques for generating acceptable grids. The procedure transforms the physical plane in to computational plane where the mapping is controlled by a poission

equation. Elliptic partial differential equations are used to generate the grids.

The mapping is constructed by specifying the desired grid points (Y,Z) on the boundary of the physical domain. The distribution of points on the interior is then determined by solving:

$$\xi_{yy} + \xi_{zz} = P(\xi,\eta)$$
$$\eta_{yy} + \eta_{zz} = Q(\xi,\eta) \quad \ldots\ldots (1)$$

Where (,) represent the coordinates in the computational domain and P and Q are terms which control point spacing on the interior of physical domain. Equations (1) are then transformed to computational space by interchanging the roles of the independent and dependent variables. This yields a system of two elliptic equations of the form

$$\alpha Y_{\xi\xi} - 2\beta Y_{\xi\eta} + \gamma Y_{\eta\eta} = -J^2 (P \cdot Y_\xi + Q \cdot Y_\eta)$$

$$\alpha Z_{\xi\xi} - 2\beta Z_{\xi\eta} + \gamma Z_{\eta\eta} = -J^2 (P \cdot Z_\xi + Q \cdot Z_\eta)$$

Where

$$\alpha = Y_\eta^2 + Z_\eta^2$$
$$\beta = Y_\xi Y_\eta + Z_\xi Z_\eta$$
$$\gamma = Y_\xi^2 + Z_\xi^2$$

$$J = \frac{\partial(Y,Z)}{\partial(\xi,\eta)} = Y_\xi Z_\eta - Y_\eta Z_\xi$$

. . . . . (2)

This system of equations is solved on a uniformly spaced grid in the computational plane. This provides the (Y,Z) coordinates of each point in the physical space. The advantage of using this method is that the grid is smooth, the transformation is one to one and complex boundaries are easily treated. All of this is accomplished by the main program GRID. The functions of the subroutines used in the program are given below briefly.

INPUT- Specifies number of points in normal and circumferential direction of grid, number of segments in a section of body and number of points supplied in each segment.

GEOM- Interpolates body points (obtained from a blue print) between two given meridionals.

PNTIB- Distributes points on the body at equal space.

PNT2B- Helps to distribute and cluster the points on the body.

KEYPT- Defines points on a section of the body

COEFF- Patches the end points of each segment of a section of the body.

CUBSPL- Fits cubic splines inbetween points.

TRID- Solves a tridiagonal system of equations.

PLOT- Calls various plotting routines.

3. CONCLUDING REMARKS and RECOMMENDATIONS

A digitized procedure is used to obtain body definition and two-dimensional grid perpendicular to the body axis. A few sections of the body defined by this procedure along with elliptic grid at several axial stations is presented in figures 4 to 8. The body definition obtained by the method for each section is remarkably close to the ones obtained by the author[7] analytically for the same reentry vehicle. In figure 3 a section of the body at axial station X=430 before the elliptic grid is generated is shown. The advantage of this method is that it is very easy to obtain any body section and two-dimensional grid by supplying a few points on segments of the Shuttle Orbiter. It is highy recommended that this procedure be used for other aerospace vehicles such as aerospaceplane to obtain body definition and grid.

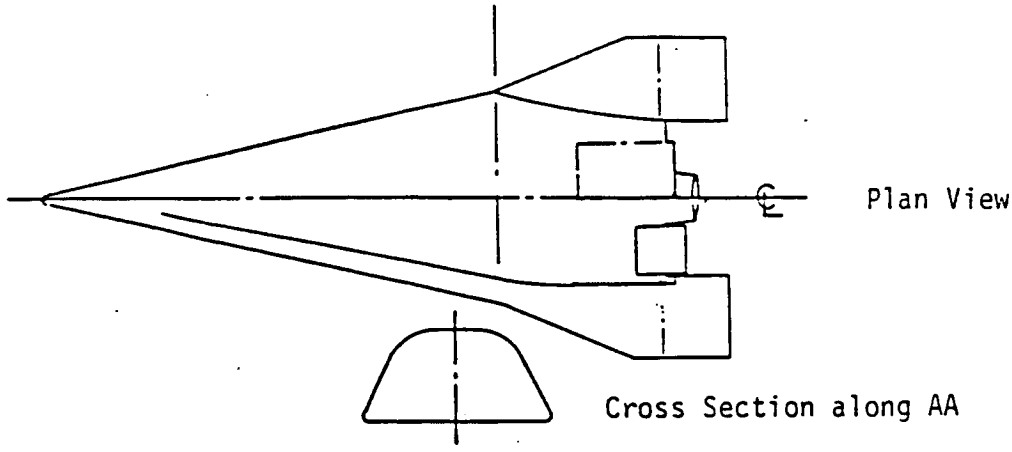

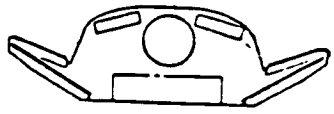

End View

X-24C-10D BODY

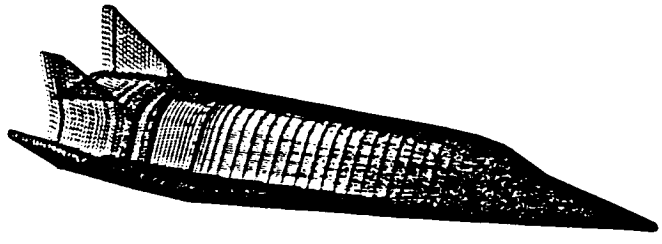

Figure 1 X24C-10D Configuration

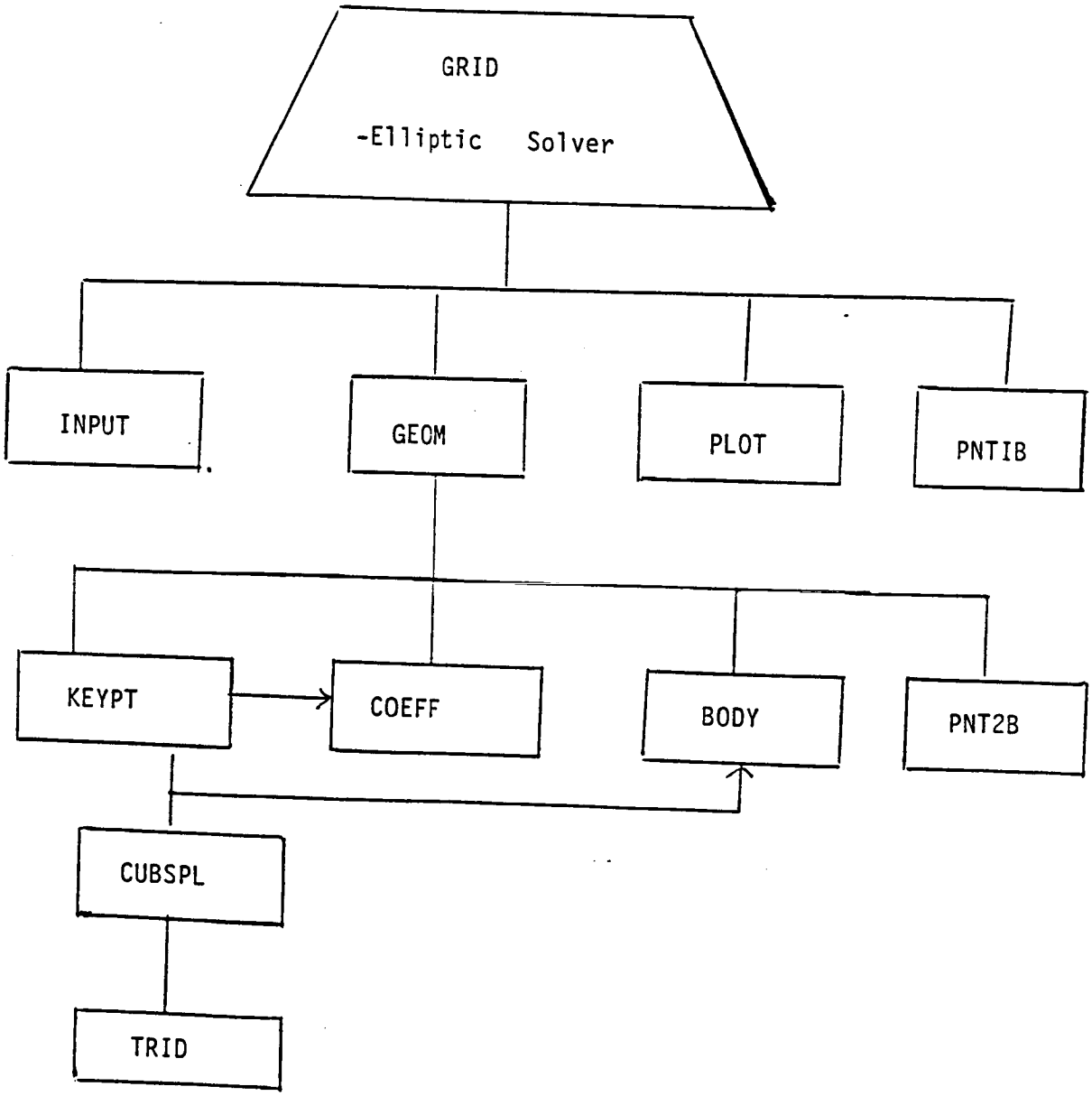

Figure 2: Digitized Body Definition and Grid Generation Procedure - Block Diagram

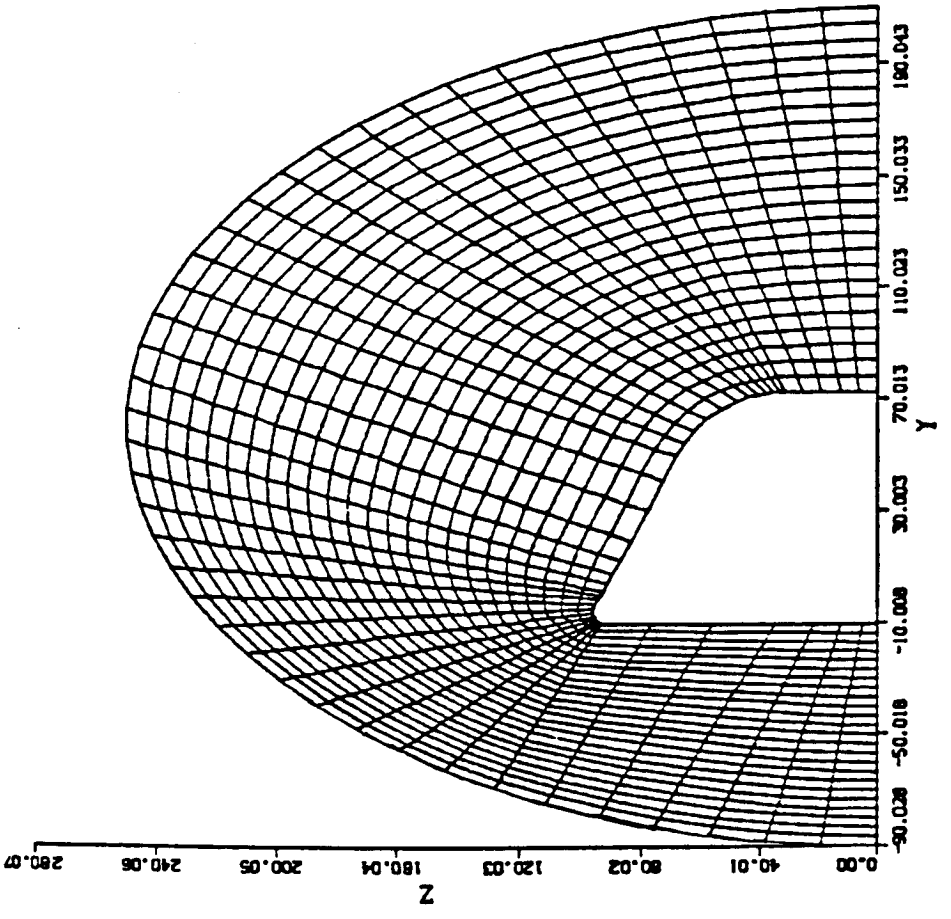

Figure 3: Body Profile for Shuttle Orbiter X - 24C - 10D at Axial Station X = 430 before the Elliptic Grid is Generated.

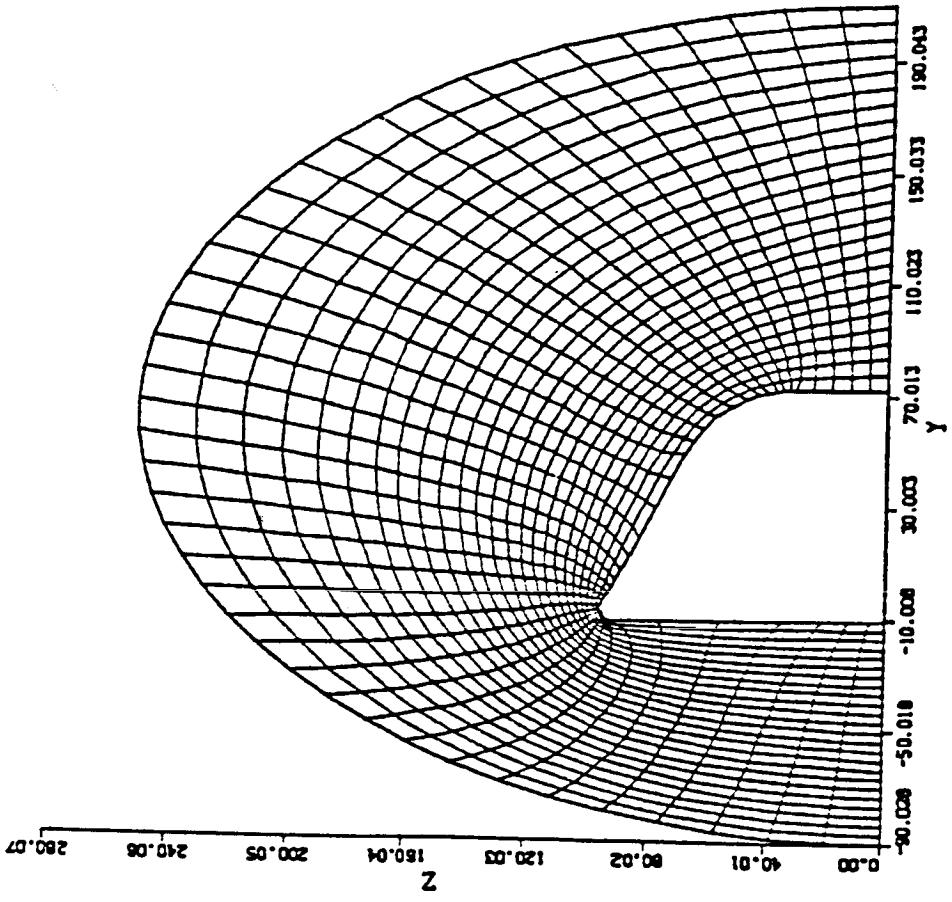

Figure 4: Body Profile and Elliptic Grid for Shuttle Orbiter X-24C-10D at Axial Station X=430.

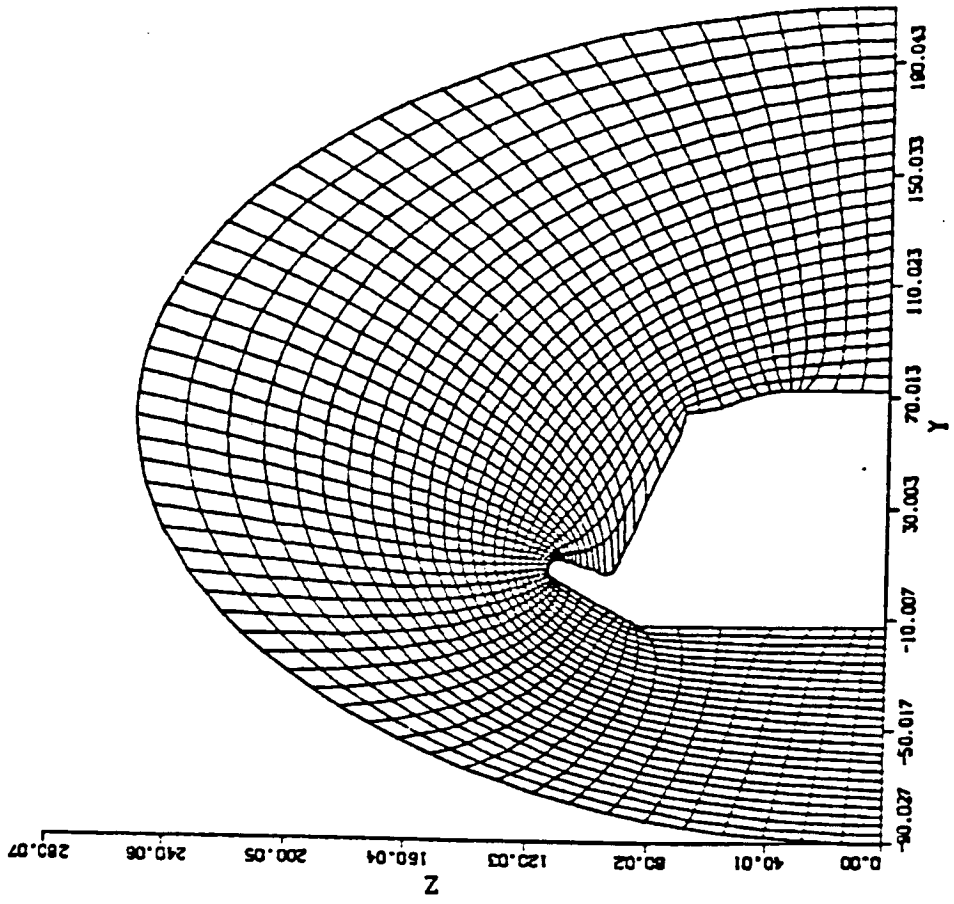

Figure 5: Body Profile and Elliptic Grid at Axial Station X=475.

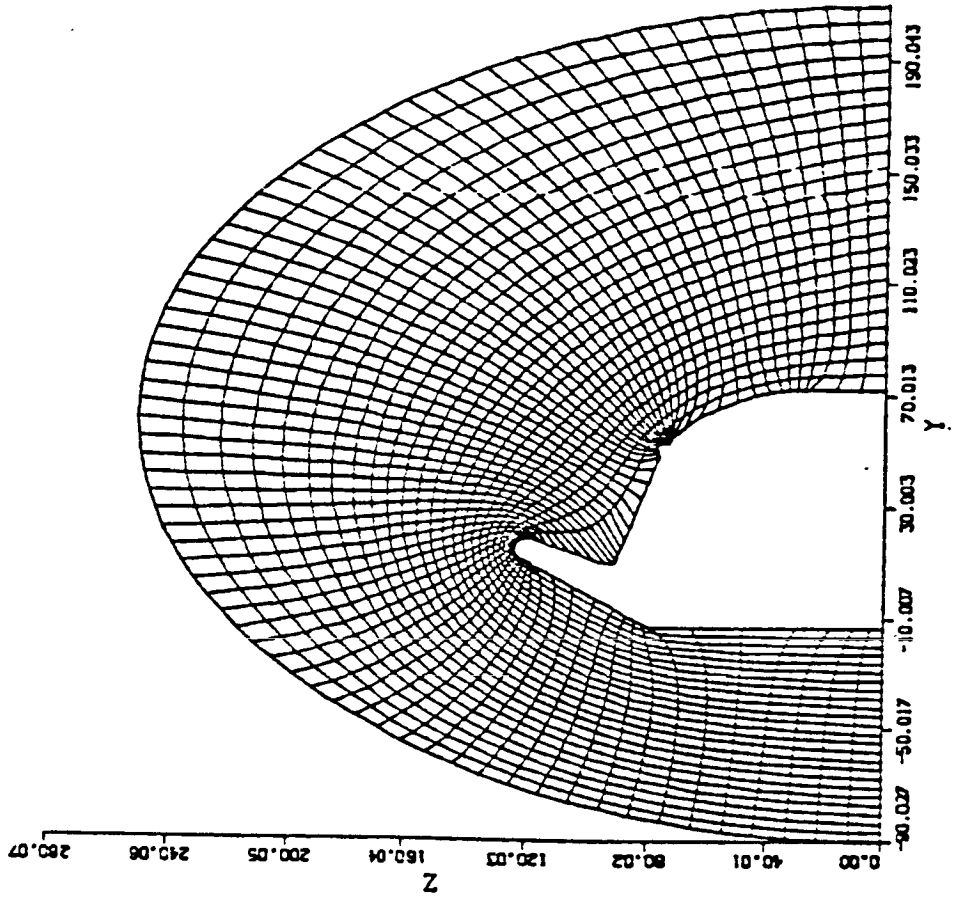

Figure 6: Body Profile and Elliptic Grid at Axial Station X=500.

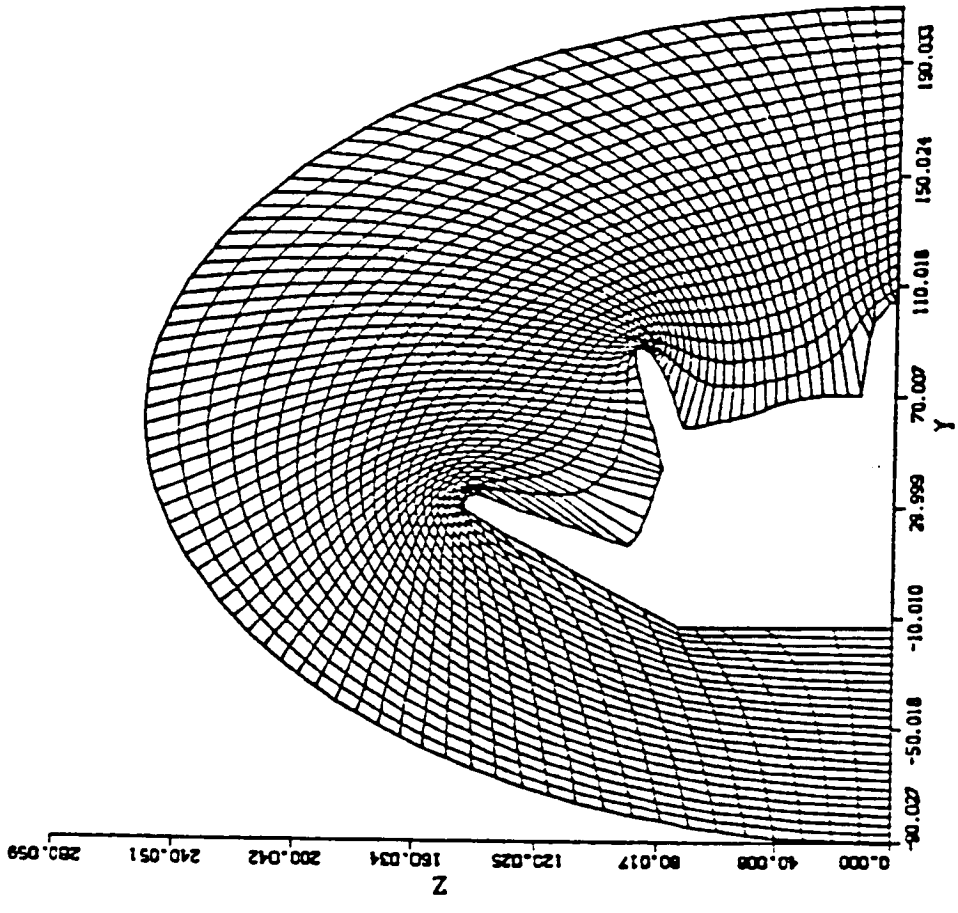

Figure 7: Body Profile and Elliptic Grid at Axial Station X=550.

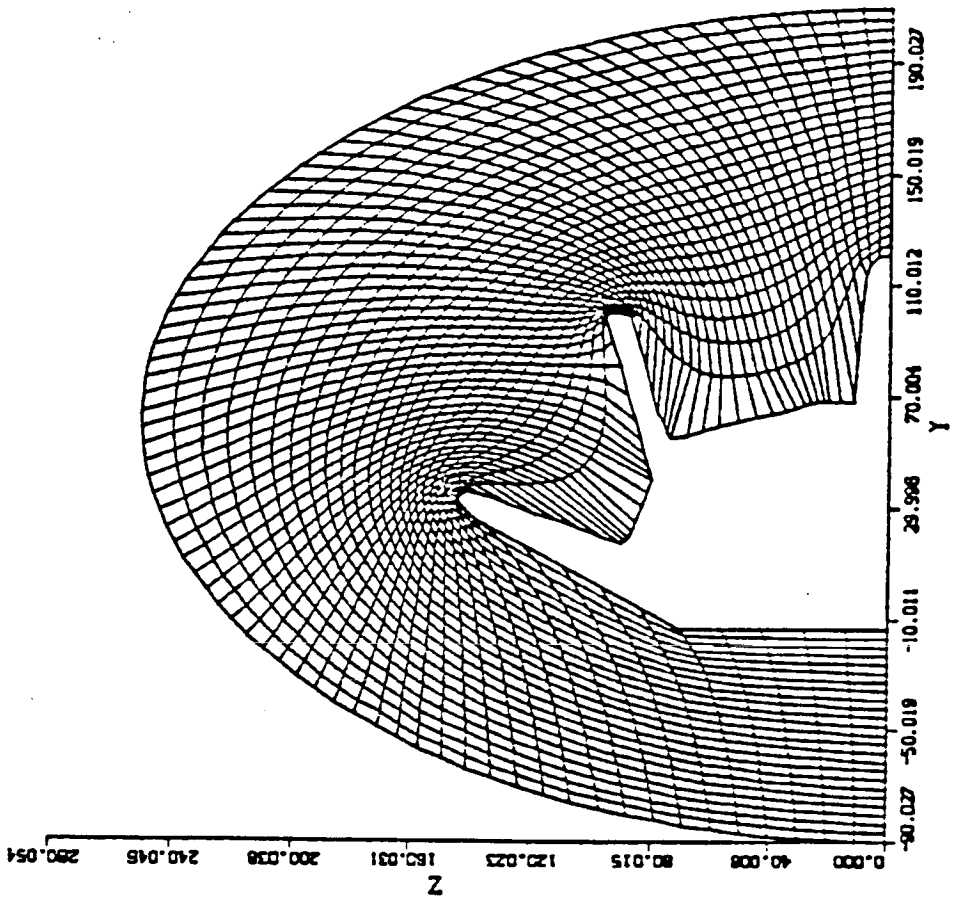

Figure 8: Body Profile and Elliptic Grid at Axial Station X=575.

REFERENCES

1. Carver, D. B., "Mach Number/Flow Angle Surveys Within Bow Shock of X24C Model at Mach Number 6," AEDC-TSR-79-V47.
2. Wannenwetsch, G. D. "Pressure Tests of the AFFDL X24C-10D Model at Mach Number of 1.5, 3.0, 5.0, and 6.0," AEDC-DR-76-V92.
3. Gord, P. R., Brigalli, A. J., "X-24C-10D Force and Moment Test Results at Mach Numbers from 0.4 to 8.0," AFFDL-TM-78-3-FXG, January 1976.
4. Anderson, D. H., Tannenhill, J. C., Pletcher, R. H., "Computational Fluid Mechanics and Heat Transfer," Hemisphere Publishing Corp., Washington, 1984.
5. Thompson, J. F., Thames, F. C., and Mastin, C. W. "Automatic Numerical Generation of Body-Fitted Containing Any Number of Arbitrary Two-dimensional Bodies," J. Comp. Phys., Vol. 15, pp. 299-319, 1974.
6. Winslow, A. "Equipotential Zoning of Two-dimensional Meshes," J. Comp. Phys., Vol. 149, pp. 153-172, 1966.
7. Krishna, M. V. G., "Analytical Representation of Afterbody Surface of X-24C-10D Reentry Vehicle," SCEEE-SFRP, Contractor Report, 1983.

ACKNOWLEDGEMENT

The author would like to thank NASA, American Society for Engineering Education, and University of Houston for providing him with the opportunity to spend a very worthwhile and interesting summer at the

Johnson Space Center, Houston, Texas. He would like to acknowledge the center, in particular, the Aeroscience Branch of Advanced Programs Office, for its hospitality and excellent working conditions.

Finally, he would like to thank Dr. Chen-Peng Li for suggesting this area of research.

1986

NASA/ASEE SUMMER FACULTY RESEARCH FELLOWSHIP PROGRAM

Johnson Space Center

University of Houston

Integration of Communications and Tracking Data Processing Simulation for Space Station

Prepared by:	Robert C. Lacovara
Academic Rank:	Affiliate Instructor
University	Stevens Institute of Technology
and Department:	Department of Electrical Engineering
NASA/JSC	
Directorate:	Engineering
Division:	Tracking and Communications
Branch:	Communications Performance and Integration
JSC Colleague:	Oron L. Schmidt
Date:	August 15, 1986
Contract #:	NGT44-005-803

INTEGRATION OF COMMUNICATIONS AND TRACKING DATA PROCESSING SIMULATION FOR SPACE STATION

Robert C. Lacovara, E. E.
Affiliate Instructor
Department of Electrical Engineering and Computer Science
Stevens Institute of Technology
Hoboken, New Jersey

A simplified model of the communications network for the Communications and Tracking Data Processing System (CTDP) is developed. It is simulated by use of programs running on several on-site computers. These programs communicate with one another by means of both local area networks and direct serial connections. The domain of the model and its simulation is from Orbital Replaceable Unit (ORU) interface to Data Management Systems (DMS).

The simulation was designed to allow status queries from remote entities across the DMS networks to be propagated through the model to several simulated ORU's. The ORU response is then propagated back to the remote entity which originated the request. Response times at the various levels were investigated in a multi-tasking, multi-user operating system environment.

Results indicate that the effective bandwidth of the system may be too low to support expected data volume requirements under conventional operating systems. Instead, some form of embedded process control program may be required on the node computers.

NASA Colleague: Oron L. Schmidt EE7 X6301

Introduction

Whatever the form of flight hardware which eventually comprises Space Station, distributed processors linked by local area networks are certainly to be incorporated. This study addresses one such distribution which supports the Communications and Tracking Data Processor (CTDP). This system is complex and incorporates many functions, but may be considered a data portal to other satellites and earth stations. Consequently, CTDP accepts and encodes on-board data for transmission, receives data from external sources, and points antennas as required. Additionally, various housekeeping tasks are performed. Some of these are computationally intensive. As it progresses in orbit, for example, Station presents parts of itself as obstacles to antenna patterns. A real time obscuration map must be maintained so that transmit antennas do not illuminate Station structure, experimental apparatus, or extra-vehicular crew.

Baseline concepts of the CTDP computer network have been proposed, and work on the implementation has started. This study examines a simplified version of the network, reduced in number of nodes and branches. This is not a graph-theoretic study. Instead, a network of processors have been linked in an approximation of expected requirements and simple programs have been installed at the computational nodes.

The objectives of the study are straightforward. The ability of the network to handle data loads by measuring data throughputs is of interest. So is the ability of off-shelf multi-tasking systems to operate in an environment of mixed local area networks (LANs) and dedicated point to point links. Lastly, some judgements are made concerning the applicability of different operating systems and programming languages.

The approach of the study is direct. The linked computers executed simple communication programs. Data loads of the magnitude estimated for some Space Station equipment were applied to the system. The coding was performed in C and Pascal under the Ultrix and VMS operating systems running on a Digital Micro-Vax and a Digital 11/780. Conclusions are drawn from the outcome.

Hardware Environment

The simplified model of the CTDP network consists of a tree whose nodes are computers and whoses branches are either dedicated RS-232 links or a common LAN, TCP-IP. The overall system which was modeled consisted of 3 layers in this tree.

The root of the tree is the main CTDP processor. It communicates via LAN with some number of subordinate processors called comtrollers (short for communication controllers).

The comtrollers in turn communicate via point to point links such as RS-232 with hardware modules such as signal processors, antenna gimbal systems, and so on. These hardware modules are termed orbital replaceable units (ORU) and are considered physically proximate to the associated comtroller.

At the time of this study the CTDP main computer (a VAX 11/750), a single comtroller (Micro-VAX), and a software simulation of three ORU's on a VAX 11/780 are available.

The study utilized the comtroller and the ORU simulation under simulated loads. The CTDP main computer was not included in this study at the time of writing. Therefore the hardware under consideration is a Micro-VAX connected via three dedicated RS-232 lines to three simulations of ORU's on a VAX 11/780.

The structure of parent (comtroller) with three children (ORU's) may be further elaborated. Specifically, the RS-232 line characteristics become important. These three lines are connected at each computer to a multiplexer, such as a Digital DZ. The salient characteristic of the multiplexer is that the four to eight lines which it supports are handled by a single processor local to the multiplexer. As a result, the multiplexer throughput is significantly less than the individual line rates supported by the device.

In this case, the three lines are operated asynchronously at 19,200 baud, with 8 bit data and single stop bit. After accounting for parity and so on, each line could support 1,920 characters per second. The effect of having a multiplexer for the three lines is that a total throughput of about 775 characters per second is attained in aggregate, as opposed to an ideal aggregate rate of 3 times 1,920 or about 6,000 characters per second. This will be seen to be a major limitation of the simulation.

Software Environment

The comtroller is a Micro-VAX operating under Ultrix-32m. This is a port of a Berkeley Unix operating system and supports a range of languages and utilities. Of chief interest are the following features: the operating system detached process utilities, the interprocess communication support, and the programming language used for the simulations.

Unix provides a simple mechanism to start processes detached from the user's terminal. Almost as convenient is an interprocess communication facility called a socket mechanism. The combination of these abilities makes it possible to create some number of detached processes which may still communicate with each other via sockets.

Since it was determined early in the study that these features would be required, the C language was chosen to code the programs which would process data. Other languages were available, but an unfortunate characteristic of Unix systems is an apparent disinterest in providing "equal access" from all supported languages to the operating system features. Although another language such as Pascal might have been used, the differences between C and Pascal did not justify any effort to make the Berkeley Pascal implementation compatible with all the operating system features readily accessed from C.

The comtroller software consists of a controlling process called CMTR, and three subordinate processes called RX7, RX6, and RX5. The socket mechanism provides communication between CMTR and each of the RX programs.

The three RX programs act as interfaces to the three ORU simulations. The processes are run detached, and thereby provide some degree of parallelism in the multitasking system. Unfortunately, the three processes each use the same serial line multiplexer, which essentially destroys any efficiency gained by using detached processes.

CMTR periodically querys RX7, RX6 and RX5. Each of these three programs in turn interrogates the software ORU simulations on the 11/780. Normally, the ORU simulations will return between 100 and 1000 characters as a response, and once these are received by the RX programs they are passed on to CMTR. CMTR then indicates to the user the total number of characters transferred, the time required to transfer, and calculates the rate of transfer. The number of transfers and size of data transferred may be varied.

As has been indicated, the serial communication lines pass only 775 characters per second. This is the rate limiting path in the system. The socket mechanism in comparison is far faster, and easily exceeds 50000 characters per second. As a result, of the two mechanisms used to transfer data between processes, only degradation in response due to the effective throughput rate of the serial communication lines need be considered.

On receipt of a status query, the RSP programs open an associated text file containing data representing ORU status, and write this data to an associated RS-232 port. The RSP programs do little else but housekeeping, and each program is only 30 lines of code. In practice, the programs exist as blocked tasks waiting to read a status query.

The ORU simulation programs running on the 11/780 are quite simple. There are three called RSP7, RSP6, and RSP5. These programs are like their counterparts RX7, RX6, and RX5 in that they are identical to each other except for the I/O ports to which they are attached. However, these programs run detached under the VMS operating system, and are coded in Pascal.

Simulation Behaviour

The simulation was operated for several hours of CPU time. Data rate from CMTR query through the return of the data from the three ORU's was calulated under various conditions of system loading, data block size, and program priority.

The result may be summarized easily. Using standard DZ style multiplexers and standard Digital terminal drivers allows data rates of the three lines to be less than 775 characters per second under any conditions. Data rates may be as low as 100 characters per second if task priorities are low while the system is heavily loaded. Estimates made by experienced NASA staff indicated that the traffic to be expected from three ORU's is likely to range from 1000 to 8000 characters per second. In short, the commonly available hardware and software, even with informed tuning, is unacceptable in terms of realistic data requirements.

The immediate conclusion is that specialized drivers for communication need to be developed to support block data transfer under multitasking operating systems.

Several other conclusions may be drawn from observations made during the development of the system.

Neither C nor Pascal are particularly appropriate languages in the application. Neither language inherently supports concurrency or interprocess communication. These are very desirable attributes of languages for this application. One advantage of C is that it is probably a good choice of a language in which to write a customized driver for the serial communication lines. The two languages are otherwise equally ill-suited to the task of networking support.

During the course of the study, some attention was paid to the use of ADA as a programming environment. Although availability precluded use of ADA for this study, it appears that ADA incorporates concurrency and communication features which make it a reasonable choice for an embedded control application such as the present study.

Note that since concurrency and interprocess communication in the present study are provided by the operating system, the code and techniques are non-portable. It is in fact unlikely that the C code or the Pascal code could be ported to any other operating systems and still be made to work. This unhappy result is due to the fact that the socket mechanism provided under Ultrix is not part of the C language, but of Ultrix itself. Similar comments may be made about features of the Pascal code.

Summary

The CTDP network may be simulated in non-real time by use of typical operating systems and typical driver packages. Real time simulation, and simulation of extended systems will require customized software.

Traditional modular programming languages such as C and Pascal are unsuitable when compared to ADA. Although ADA code was not written, examination of ADA features indicate that ADA is a potentially superior language in the application.

1986

NASA/ASEE SUMMER FACULTY FELLOWSHIP PROGRAM

Johnson Space Center

University of Houston

General Purpose Algorithms for Characterization of Slow and Fast Phase Nystagmus

Prepared by:	Charles S. Lessard, Ph.D., P.E.
Academic Rank:	Associate Professor
University & Department:	Texas A&M University Bioengineering Program Dept. of Industrial Engineering
NASA/JSC	
Directorate:	Space and Life Sciences Div.
Division:	Space Biomedical Research Inst.
Branch:	
JSC Colleague:	Millard Reschke, Ph.D.
Date:	15 August 1986
Contract #:	NGT-44-005-803 (U. of Houston)

GENERAL PURPOSE ALGORITHMS FOR CHARACTERIZATION OF SLOW AND FAST PHASE NYSTAGMUS

Charles S. Lessard, Ph.D., P.E.
Associate Professor
Department of Industrial Engineering
Texas A&M University
College Station, TX 77840

In the overall aim for a better understanding of the vestibular and optokinetic systems and their roles in space motion sickness, the eye movement responses to various dynamic stimuli are measured. The vestibulo-ocular reflex (VOR) and the optokinetic response, as the eye movement responses are known, consist of slow phase and fast phase nystagmus.

The specific objective of this study is to develop software programs necessary to characterize the vestibulo-ocular and optokinetic responses by distinguishing between the two phases of nystagmus. The overall program is to handle large volumes of highly variable data (nystagmus waveforms) with minimum operator interaction. The programs include digital filters, differentiation, identification of fast phases, and reconstruction of the slow phase with a least squares fit such that sinusoidal or psuedorandom data may be processed with accurate results. The resultant waveform, slow phase velocity eye movements, serves as input data to the spectral analysis programs previously developed for NASA, Johnson Space Center, Neurophysiology Laboratory to analyze nystagmus responses to psuedorandom angular velocity inputs.

NASA Colleague: Millard Reschke, Ph.D., SB X2381

Introduction

Stimulation of the vestibular system by angular acceleration during head movements results in a reflexive eye movement called nystagmus. The resulting response (nystagmus) resembles a sawtooth waveform of which slow rotation of the eyes to maintain gaze on an object are related to the simulus (slow phase) while rapid resets of the eye position are related to some centering mechanism (fast phase). Quantitative properties of nystagmus are important in the characterization of the vestibular and ocular systems. Thus, the specific objective of this study is to develop the necessary software programs to characterize the vestibular and optokinetic responses to sinusoidal stimuli by distinguishing between the two components of nystagmus.

Background

The methods used to analyze nystagmus vary from manual, to real-time automated processing in the time domain. Massoumnia presented models of the slow and fast phase velocities to establish that the slow and fast phase velocity spectra were superimposed. Thereby, he concluded that it was not possible to distinguish between the slow phase velocity and the fast phase velocity by analysis in the frequency domain (7).

In general, there are two time domain methods for identification of a fast phase event. One method is based on the analytical geometric property that points at which the first derivative waveform equals zero correspond to point at which the position waveform is an extremum (maximum or minimum). This method involves digital filtering and differentiating the ocular position signal prior to detecting the fast event with some velocity criterium. The second method is based on identification of the position waveform extrema by a search algorithm. Then a psuedo position waveform is obtained by connecting straight line segments between maxima and minima. The psuedo position waveform is used to calculate slopes (velocities), position changes, and time durations which in turn, are used to identify the fast phase events (8). An assumption of the method is that the information of value which is contained in the nystagmus can be obtained by replacing the detailed time-varying path of the EOG with straight-line approximations between points of maxima and minima. Seven parameter can be extracted by the method as is shown in figure 1. To date, one major vestibular research laboratory in the United States, out of the seven major laboratories which were selected for this study, uses the psuedo waveform method.

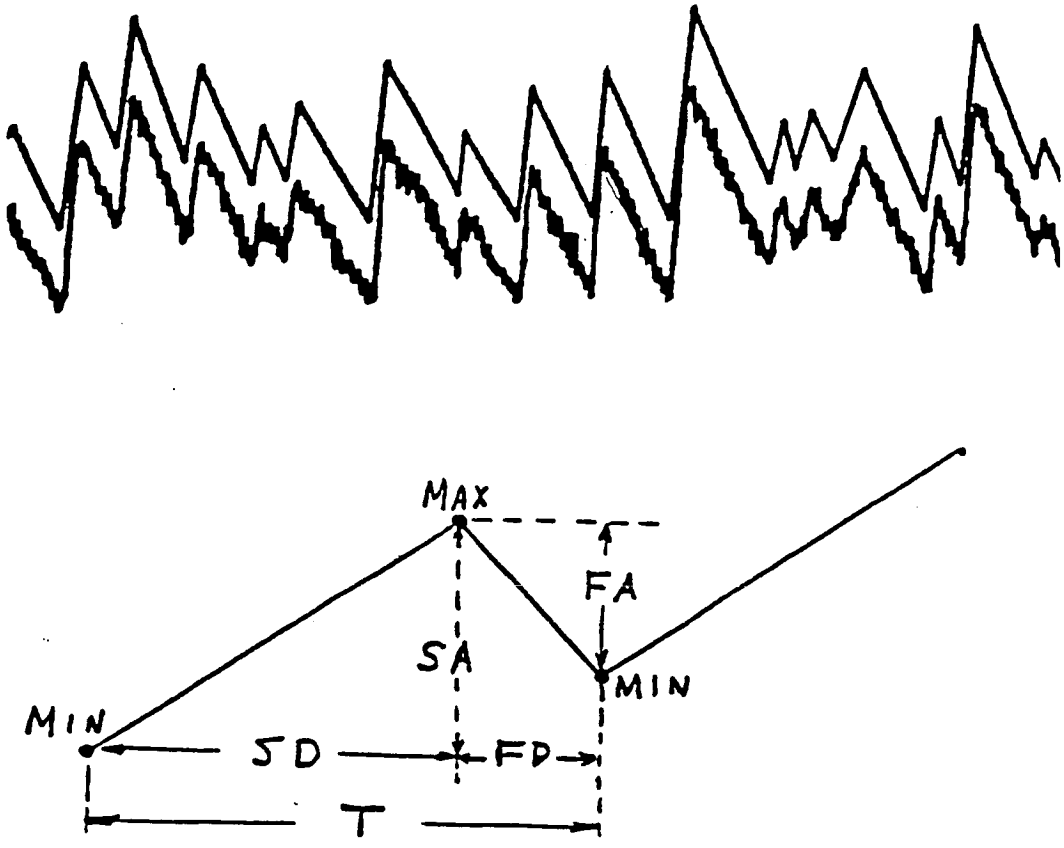

Fig. 1. Upper trace shows the psuedo position EOG waveform superimposed on the raw data. Lower drawing is an expanded version of the straight line approximation between points of extrema (MAX and MIN). SA denotes slow phase amplitude, FA is fast phase amplitude, SV is slow phase velocity, FV is fast phase velocity, SD is the slow phase duration, FD is the fast phase duration and T is the period; where frequency is 1/T.

Characteristic Parameters

In characterizing the slow phase velocity component vestibular researchers have used the engineer's approach to the analysis of a system, i.e., observe the response to a predetermined excitation in order to determine the system's transfer function. Knowledge of the system's transfer function permits prediction of the system response to other deterministic excitations. The most commonly used excitation signals in signal analysis are single frequency sinusoid, step, and impulse functions. The most popular analytical method is the use of a single frequency sinusoidal stimulus which applies only to linear systems analysis. The only parameters that can vary are the magnitude and phase of the resulting sinusoid. The frequency of the input and output are unchanged unless the system is nonlinear. Thus, gain (the ratio of output magnitude to input magnitude) and phase (the delay of signal transmission through the system) at a constant frequency are the only two parameters necessary to characterize the slow phase velocity systems.

Characterization of the fast phase velocity components of nystagmus (saccades) is not obtained by the frequency response method but rather by identifying true saccades, then measuring the maximum velocity of the fast phase segment (saccade), the total change of amplitude from the

start to the end of the fast phase segment, and the duration of the saccade. A least square exponential curve fit to the saccade maximum velocity versus total change of the saccade amplitude data results in two best fit coefficients. In addition saccade velocity, accuracy, and reaction time were used test the oculomotor system (2,3,4 and 5).

Current Processing

A general review of the analog and digitizing processes used by the laboratory reveals no agreement on filtering or digitizing as seen in Table I. Most laboratories used DEC LSI-11 computers with 12 bit analog-to-digital converters. The sampling rate at which the EOG data is digitized depends upon the objective of the analysis. If the principle goal is to identify and quantify the characteristics of the fast phase velocity components of nystagmus (saccades) as a means of diagnosing vestibulo-ocular disorders (3), then the data is sampled at 200 samples per second. Whereas, if the primary interest is solely on removal of the fast phases as a means of obtaining a more accurate estimate of the slow phase velocity parameters, then lower sampling rates are used.

The algorithms for processing the eye movements vary in structure primarily because of the ultimate aim of the analysis. Laboratories interested in retaining fast phase

TABLE I

Comparison of Analog Antialiasing Filtering and Digitizing in Vestibular Laboratories

	LAB A	B	C	D	E	F	G
ANALOG							
PREAMPS	IH	IH	IH	IH	IH	IH	IH
FILTER TYPE	Bu	6-pt Bessel	2-pt Bu	none	Bu	Bu	
CUTOFF (Hz)	35	41.6	80	--	35	35	
GAIN	--	--	--	--	--	--	--
DIGITAL							
COMPUTER	PDP 11/34	LSI 11	LSI 11	LSI 11/73	LSI 11/73	LSI 11/73	LSI 11
A/D (Bits)	12	12	12	12	12	12	12
SAMPLING RATE (S/S)	122.8	200	200	200	200	100	120

IH Fabricated in-house

Bu Butterworth filter

S/S Samples per second

information use higher bandwidth digital filters in order to maintain waveform and timing accuracy.

Two laboratories use optimal band limited derivatives (BLD) in lieu of some smoothing routine followed by a two-point central difference equation (CDE). The two-point central difference is popular as a first order differentiator because of its speed, simplicity, accuracy and low pass filtering (1). The laboratories using optimal filtering techniques convolve a finite impulse response (FIR) filter with an finite impulse differentiator to obtain velocity or acceleration filters. TABLE II compares the digital processes for eye movement analysis used by the seven vestibular laboratories.

It is interesting to note that three laboratories identify three classes of fast phase events but only one laboratory uses the saccade velocity information. In the evaluation of the slow phase velocity, most laboratories have algorithms which remove the fast phase events and fill-in the removed points with a linear extrapolation across either the position or velocity waveform. Two laboratories use a least squares sinusoidal fit to the velocity curve without filling the gap between slow velocity segments. Three laboratories have equally spaces intervals after the waveform reconstruction and only two of those laboratories

TABLE II

Comparison of Digital Processes

For Eye Movement Analysis

Laboratory

	A	B	C	D	E	F	G
FILTER TYPE	BLD	None	7-pt LP	LP ReF	BLD	None	15-pt LP FIR
CUTOFF (Hz)	--	--	20	35	--	--	25
DERIVATIVES							
1st		2-pt CDE	2-pt CDE	3-pt CDE		2-pt FWD	4-pt CDE
2nd	--	--	--	--	3-pt CDE	--	--
VEL. FILTER CUTOFF	31-pt 25	--	--	--	9-pt FIR	--	--
ACCEL. FILTER CUTOFF	61-pt 30 Hz	-- --	-- --	-- --	-- --	-- --	-- --
EXTRAPOLATION	Lin	Lin	None	None	Lin	Lin	Lin
SLOW PHASE WAVE RECONSTRUCTION	Vel	Vel	None	None	Vel	Pos	Pos
FAST PHASE CLASSIFICATION		3	--	3	3	--	--
LEAST SQUARES TRANSFORM	--	--	Sin	Avg SPV	--	Sin	--
DIRECT FOURIER TRANSFORM	--	yes	--	--	--	--	--
FFT	yes	--	--	--	--	--	yes

CDE Central difference equation

FWD Forward difference equation

FFT Fast Fourier Transform

Vel Velocity

Sin Sinusoidal

Pos Position

Lin Linear

ReF Recursive Filter

use a fast fourier transform to obtain the frequency response parameters.

NASA FPID Program

Development of the fast phase identification (FPID) program began prior to evaluation of the seven U.S. laboratories. The engineering approach dictated the analytical geometric method. Horizontal eye movements (VOR) response to a sinusoidal stimulation of the vestibular system is digitized at 120 samples per second (Fig 2) and filtered with a digital 15-point, low-pass, finite-impulse-response (FIR) filter. The FIR filter cutoff is set at 25 Hz. The signal at 36 Hz is -40.1 db. Several FIR filters and smoothing routines were evaluated before selection of the final 15-point, FIR filter. The filtered EOG (position) signal is shown in figure 3.

The filtered signal is then differentiated with a central difference equation. The program permits the operator to select the polynomial order of the differentiator up to a sixth order central difference equation with error of order (h^6), where h is the sampling interval of 0.00833 seconds (8.33 msec.). Higher order equations result in better accuracy, but increase computation time. Hence, the fourth order (4-point) central difference equation with error of order (h^4) is used to obtain the first derivative of the EOG since it gives

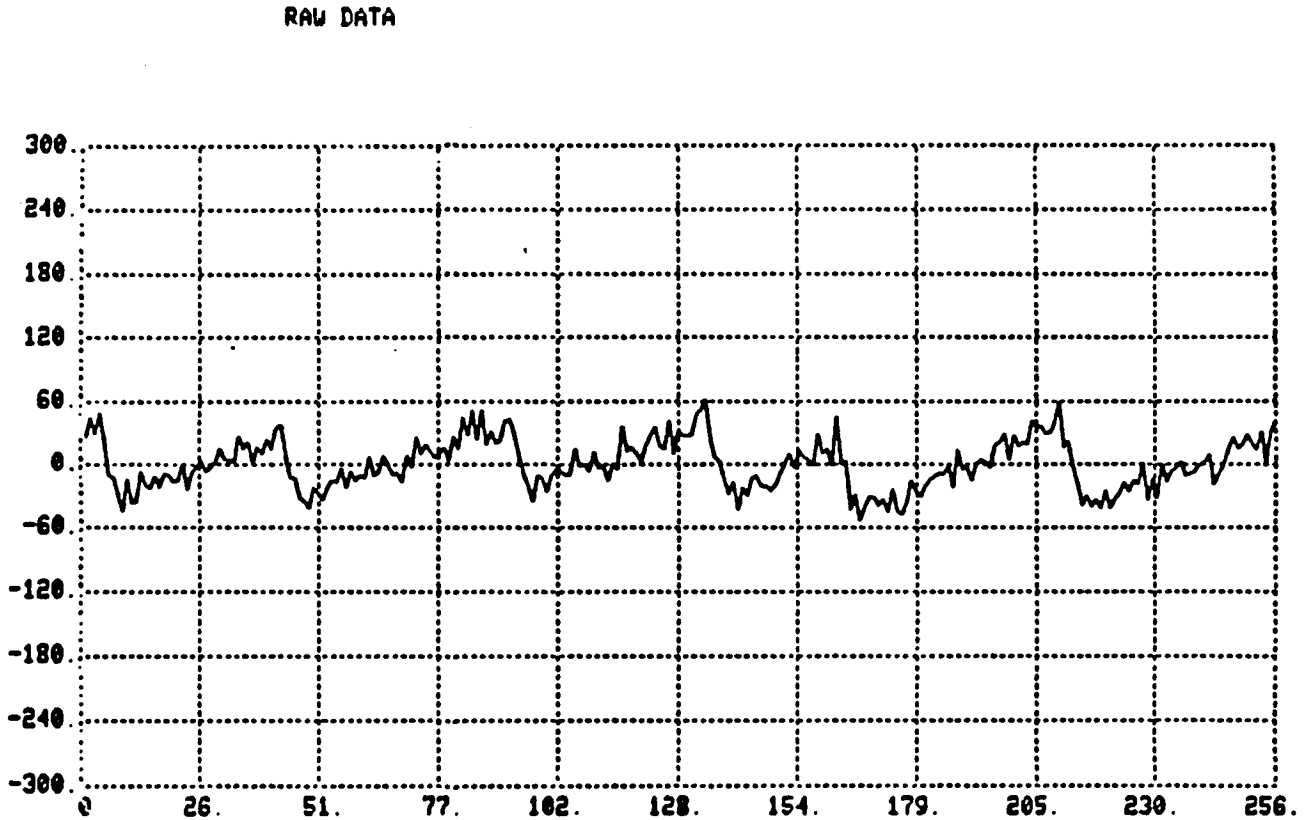

Fig. 2. Raw horizontal eye movements are shown after removal of the D.C. offset.

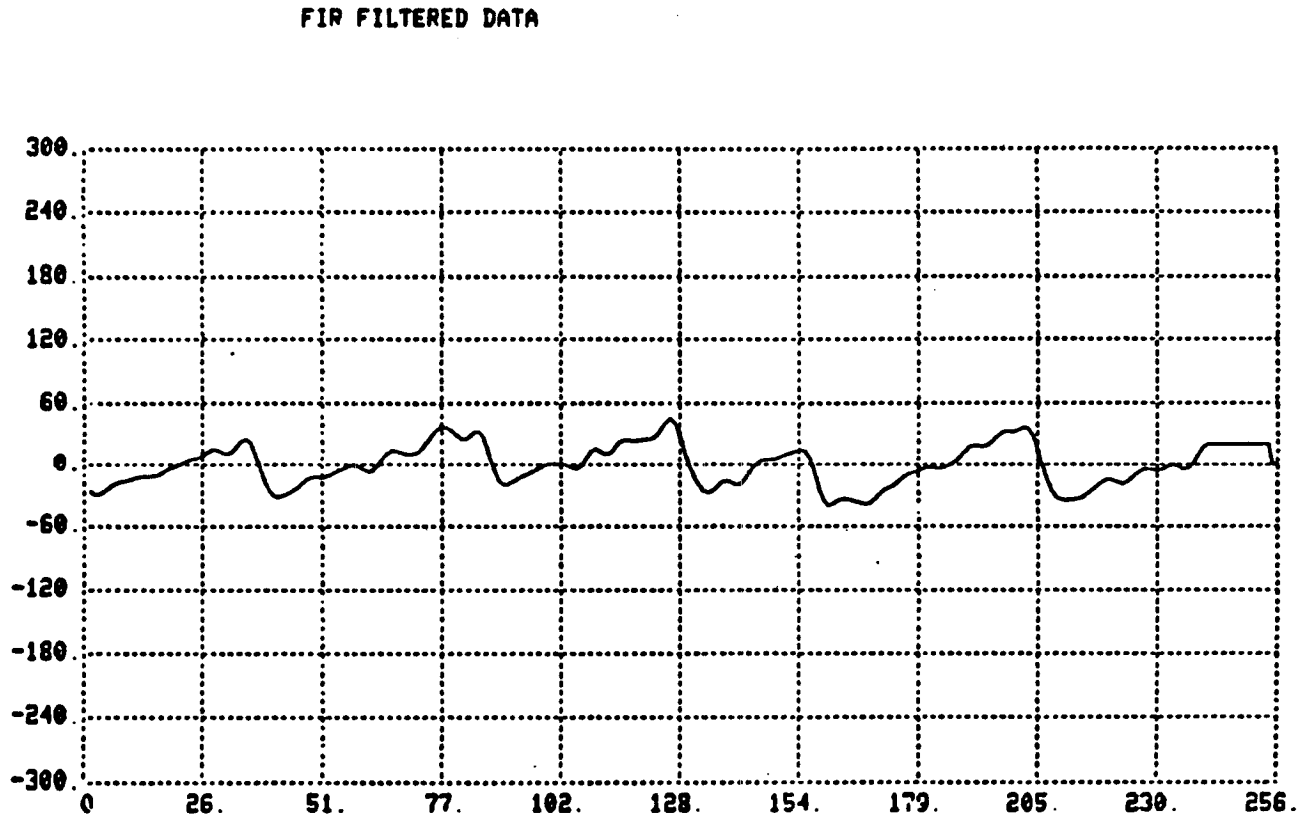

Fig. 3. Horizontal eye movements after FIR filtering.

accurate results with only two points on either side of center (fig. 4).

The second derivative is obtained by differentiating the filtered EOG position signal with a 5-point, second derivative central difference equation of error order (h^4). The second derivative is shown in figure 5. The third derivative of the EOG position signal was also obtained with a 7-point central difference equation (6). The third derivative waveform was noisier than the lower derivative filters so it was removed from the program.

Following differentiation, the program computes the root-mean-square (RMS) value of the various derivatives waveforms in order to set a threshold value above the noise level so as to reduce false detection errors. From RMS values and approximate signal-to-noise ratios of each derivative waveform, detection of a fast velocity event is based on exceeding the first derivative threshold value rather than the second derivative as used by Massoumnia (7). The first derivative offersd the least amount of noise and the best signal-to-noise ratio for threshold detection.

Once the threshold of the EOG velocity signal is exceeded the search point is move backward to find where the derivative zero crossing occurrs. This point is flagged as the beginning of the fast phase event and the search is

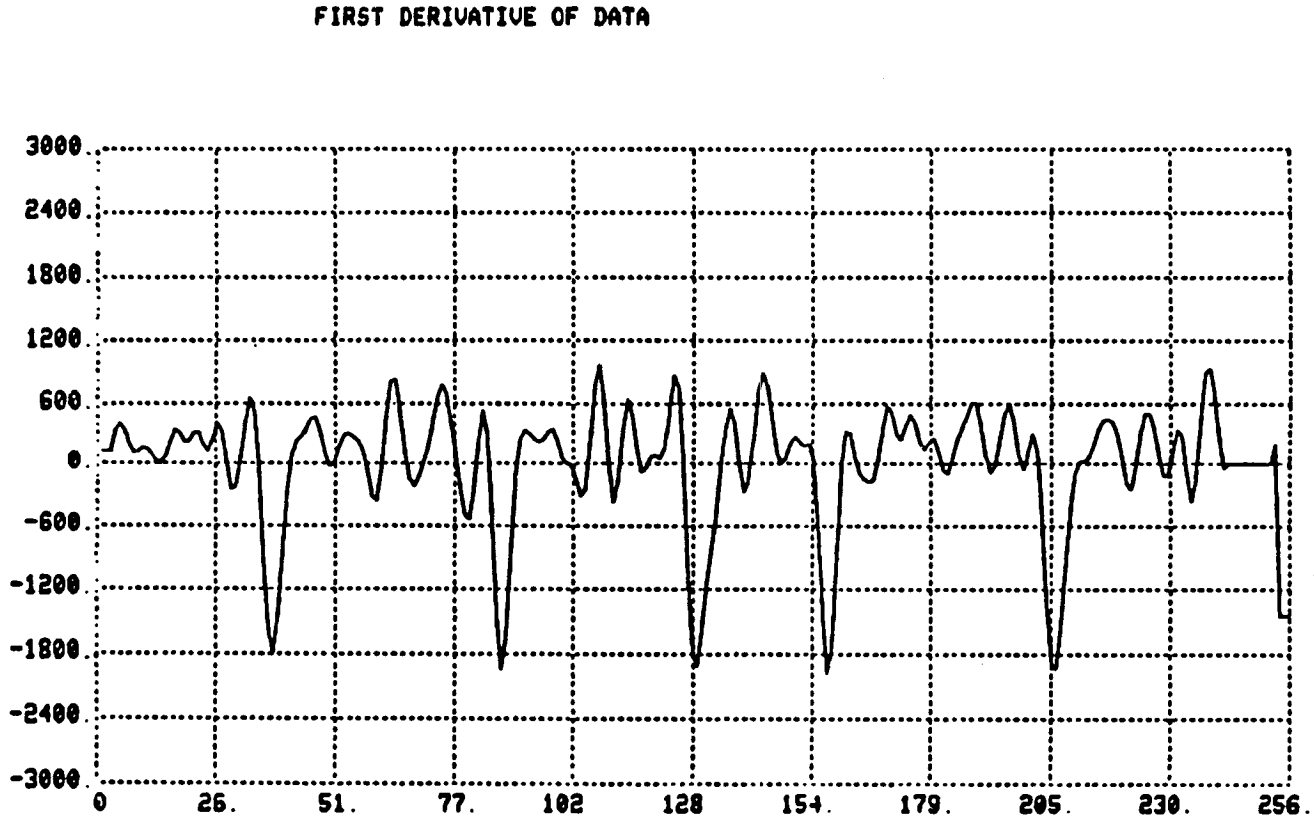

Fig. 4. First derivative of the filtered eye movements. The RMS value is 585 A/D counts for 2.08 seconds of data. The signal-to-noise ratio is 3.3:1.

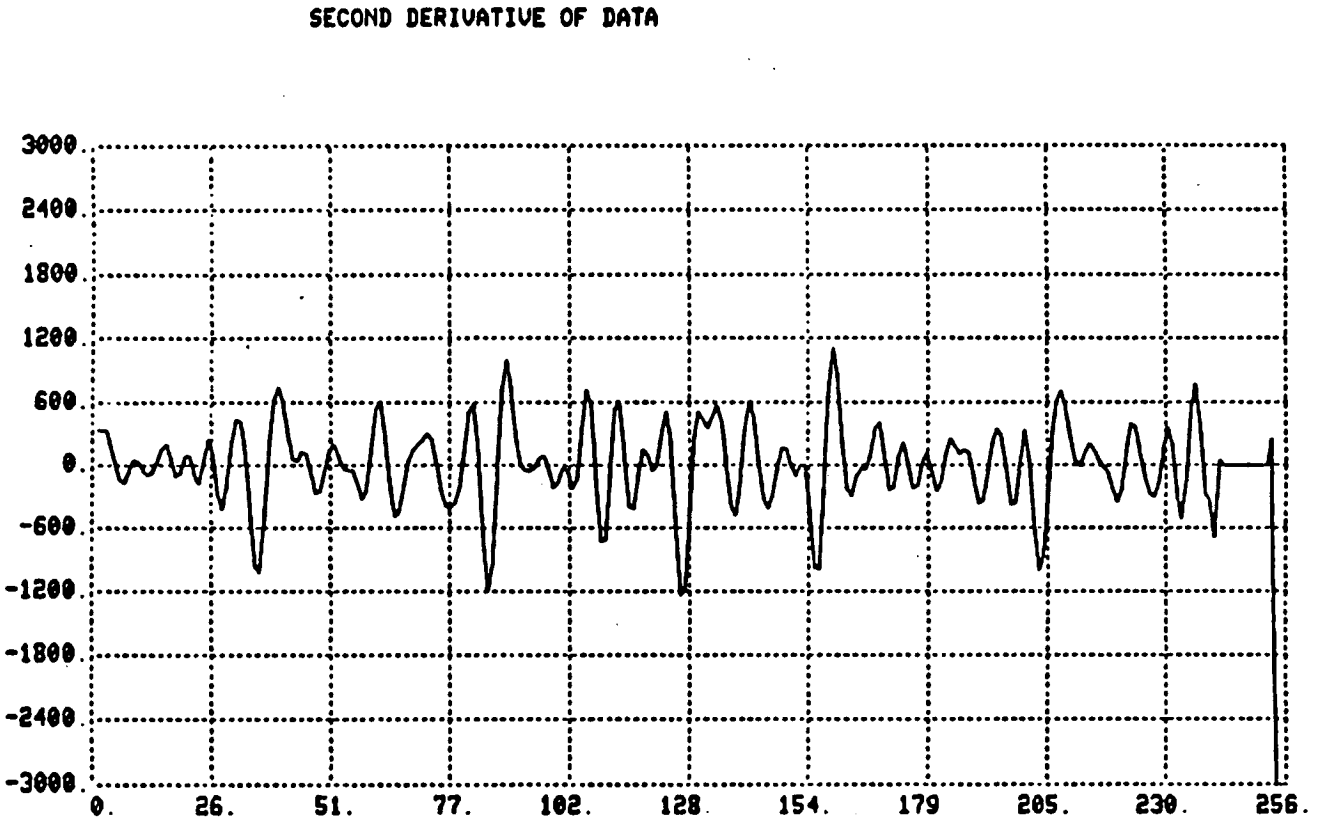

Fig. 5. The second derivative of the filtered eye movements. The RMS value was 485 x 10^2 A/D counts for 2.08 seconds of data. The signal-to-noise ratio is 2.3:1.

reversed (forward direction) until a zero crossing occurrs. This point was flagged as the end of the fast phase event.

In the next steps, the program uses the filtered eye position (EOG) waveform to perform a least squares linear regression on the slow phase velocity segment preceding the starting index of the current fast phase event. Then the points between start and end of the fast phase event are extrapotated and added to the position waveform.

Prior to output of the reconstructed slow phase EOG signal, a correction of slow segment height is necessary. This is accomplished by obtaining the change of position (height) from the last point of the extrapolated EOG position (end of fast phase index) and the start of the following slow phase segment (end point + 1). Height corrections are cummulative and must carry the proper sign. The reconstructed slow phase EOG position waveform is shown in figure 6. The FPID program listing is given in the appendix.

Conclusion and Recommendations

Although the fast phase identification (FPID) and slow phase reconstruction appear to work, the program needs to be evaluated with various types of VOR and OKN data. At the present time only short segments of data can be analyzed. The program needs a circular buffer, so that long data records can be analyzed. Additionally, the reconstructed

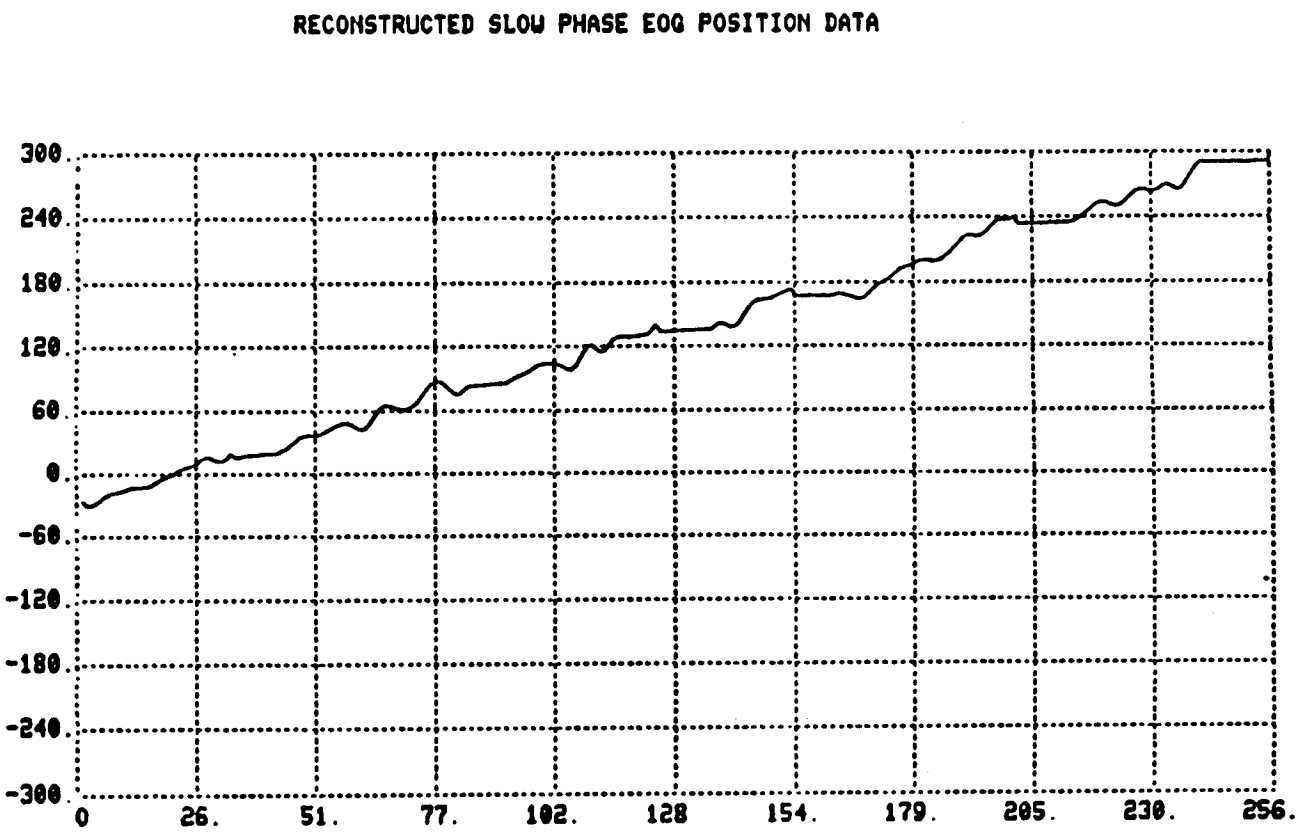

Fig. 6. The reconstructed slow phase horizontal eye movements.

wave must be written to a new data file prior to being used by the spectral programs written for NASA last summer.

REFERENCES

1. Bahill, A.T., et al., "Frequency Limitations of the Two-point Central Difference Differentiation Algorithm", Biol. Cybern. 45:1-4, 1982.

2. Baloh, R.W., et al., "Quantitative Measurement of Saccade Amplitude, Duration and Velocity", Neurology, 25(11):1065-1070, Nov. 1975.

3. Baloh, R.W., et al., "The Saccade Velocity Test", Neurology, 25(11):1071-1076, Nov. 1975.

4. Baloh, R.W., Et al., "Algorithm for Analysis of Saccadic Eye Movements Using a Digital Computer," Aviat., Space, and Environ. Med., 47(5):523-527, May 1976.

5. Baloh, R.W., et al., "Microcomputer Analysis of Eye Movements", Diagnosis 2(4):52-57, July 1984.

6. Hornbeck, R.W., Numberical Methods, QPI Series, Prentice-Hall, Inc. New Jersy, 1975.

7. Massoumnia, M.A., Detection of Fast Phase of Nystagmus Using Digital Filtering, Unpublished Master's Thesis, MIT, May 1983.

8. Wall, C. III, and Black, F.O., "Algorithms for the Clinical Analysis of Nystagmus Eye Movements", IEEE/BME Trans. Biomed. Eng., 28(9):638-646, Sept. 1981.

APPENDIX

FAST PHASE IDENTIFICATION

(FPID)

PROGRAM LISTING

```
FORTRAN IV      V02.6      Wed 06-Aug-86 17:01:54                PAGE 001

0001            PROGRAM FFID
      C
0002            INTEGER Z(512),DSKINC,NBLK,IPOSN(16),MAX(16),ICHNUM(16),LENGTH
0003            REAL AMPL, PERIOD, INTRAT, HEOG(512), XT(512), COEF(15),
               1 YHEOG(512), SDEOG(512), SPEOG(512), SPYHEOG(512), FDEOG(512)
      C
0004            EQUIVALENCE (AMPL,Z(150)),(PERIOD,Z(152)),(INTRAT,Z(159)),
               1 (DSKINC,Z(167)),(NBLK,Z(172)),(ICHNUM,Z(177)),
               2 (IPOSN,Z(225)),(MAX,Z(241))
      C
0005            COEF(1) = .0037165603
0006            COEF(2) = .020235427
0007            COEF(3) = .013399956
0008            COEF(4) = -.040643737
0009            COEF(5) = -.066073574
0010            COEF(6) = .061152663
0011            COEF(7) = .30294424
0012            COEF(8) = .43047285
0013            NEH = 8
0014            DO 5 N = 1, 7
0015            COEF(16-N) = COEF(N)
0016      5     CONTINUE
      C
0017            HHT = 0.
0018            THT = 0.
0019            ISLG = 0
      C
0020            INTEGER BUFR2(1024), IERR
0021            BYTE FILNAM(12)
0022      10    DO 20 K=1,12
0023      20    FILNAM(K)=0
0024            TYPE 30
0025      30    FORMAT (' ENTER COMPLETE FILENAME'/'  FILENAME ?',$)
0026            ACCEPT 40,FILNAM
0027      40    FORMAT (12A1)
      C
0028            CALL DISKIO(FILNAM,-3,Z,256,0,NDUMMY,IERR)
0029            IF (IERR .NE. 0) TYPE *,' ERROR CODE',IERR,' DURING READING'
      C
0031      42    TYPE *,' CHAN NO.'
0032            ACCEPT *,K
0033      45    TYPE *,' ENTER THE NUMBER OF DATA POINTS FOR EOG'
0034            ACCEPT *,LENGTH
      C       TYPE *,'   DO YOU WANT FILES LEFT OPEN? (1=YES)'
      C       ACCEPT *,LOPEN
0035            LOPEN = 1
0036            TYPE *,' ENTER STARTING BLOCK NUMBER'
0037            ACCEPT *,IBLK
      C       TYPE *,' DO YOU WANT TO PLOT EVERY POINT? ENTER STEP SIZE!'
      C       ACCEPT *,ISTEP
0038            ISTEP = 1
      C
0039            NWRDS = DSKINC* 256
0040            ITEMP = 0
```

```
0041  48    TYPE 50, NBLK, NWRDS, IBLK,DSKINC
0042  50    FORMAT (' NBLK=',I5,' NWRDS=',I5,' IBLK=',I5,'DSKINC=',I5)
0043        TYPE 51,MAX(K),IPOSN(K)
0044  51    FORMAT (' MAX(K) = ',I5,' IPOSN(K) = ',I5)
      C
0045        IRMODE=3
0046        IF (LOPEN .EQ. 1) IRMODE = -3
0048        TYPE *,'   NOW READING FROM DISK'
      C
0049  52    CALL DISKIO(FILNAM,IRMODE,BUFR2,NWRDS,IBLK,NDUMMY,IERR)
0050        IF (IERR .NE. 0) TYPE *,' ERROR CODE',IERR,' DURING READ'
      C
0052        NPTS = (MAX(K)-IPOSN(K)+1)/ISTEP
0053        DO 57 L = 1,NPTS
0054        HEOG(L+ITEMP) = BUFR2(IPOSN(K) + L*ISTEP)
0055  57    CONTINUE
      C
0056        DO 950 I = 1, 26
0057        TYPE 951, I, HEOG(I)
0058  951   FORMAT (' I = ',I4,' HEOG = ',F12.5)
0059  950   CONTINUE
0060        DO 960 I = LENGTH-26, LENGTH
0061        TYPE 961, I, HEOG(I)
0062  961   FORMAT (' I = ',I4,' HEOG = ',F12.5)
0063  960   CONTINUE
0064        TYPE 962, NPTS, ITEMP
0065  962   FORMAT (' NPTS = ',I8,' ITEMP = ',I8)
0066        TYPE *,' WAITING TYPE 1'
0067        ACCEPT*,ISN
      C
0068        IBLK = IBLK + DSKINC
0069        ITEMP = ITEMP + NPTS
      C
0070        IF (ITEMP .LT. LENGTH) GO TO 52
0072        XLGT = FLOAT(LENGTH)
0073        TYPE 50,NBLK,NWRDS,IBLK,DSKINC
      C
0074        DO 60 J = 1,LENGTH
0075        XT(J) = FLOAT(J)
0076  60    CONTINUE
0077        TYPE *,' SET YMIN!'
0078        ACCEPT *,YMIN
0079        TYPE *,' SET YMAX!'
0080        ACCEPT *,YMAX
      C
0081        ILFT = 600
0082        IRIT = 3500
0083        IBOT = 1000
0084        ITOP = 2500
0085        XMIN = 0.
0086        XMAX = XLGT
      C
0087        TYPE *,' DO YOU WANT TO REMOVE D.C.? (YES=1)'
0088        ACCEPT *, IYES
```

```
0089          IF (IYES .NE. 1) GO TO 162
      C
      C       COMPUTE THE MEAN OF THE DATA
0091          XSUM = 0.0
0092          DO 58 I = 1, LENGTH
0093          XSUM = XSUM + HEOG(I)
0094    58    CONTINUE
0095          XMEAN =XSUM/XLGT
0096          DO 59 I = 1, LENGTH
0097          HEOG(I) = HEOG(I) - XMEAN
0098    59    CONTINUE
      C
      C
0099          CALL TSXCHK
0100          CALL GRINIT(4014,4631,1)
0101          CALL CHRSIZ(2)
0102          CALL ERASE
0103          CALL GRID(10,10,ILFT,IRIT,IBOT,ITOP,97)
0104          CALL ANOTAT(10,10,ILFT,IRIT,IBOT,ITOP,XMIN,XMAX,YMIN,YMAX)
0105          CALL XYPLOT(XT,HEOG,LENGTH,ILFT,IRIT,IBOT,ITOP,XMIN,XMAX,
             1 YMIN,YMAX,1,0)
      C
0106          CALL MPLOT(ILFT+500,ITOP+300,-1)
0107          TYPE 61
0108    61    FORMAT('+RAW DATA ')
      C
0109          TYPE *,' DO YOU WANT A HARD COPY? (YES=1)'
0110          ACCEPT *,IS
0111          IF (IS .NE. 1) GO TO 62
      C
0113          CALL COPY(0)
      C
0114    62    DO 500 I = 3, LENGTH-2
0115          YHEOG(I) = .11*(HEOG(I-2)+HEOG(I+2))+.22*(HEOG(I-1)+HEOG(I+1))
             1 + .33*HEOG(I)
0116    500   CONTINUE
0117          YHEOG(1) = YHEOG(3)
0118          YHEOG(2) = YHEOG(3)
0119          YHEOG(LENGTH) = YHEOG(LENGTH-2)
0120          YHEOG(LENGTH-1) = YHEOG(LENGTH)
      C
0121          DO 510 I = 1, LENGTH
0122          HEOG(I) = YHEOG(I)
0123    510   CONTINUE
      C
0124    162   NCO = 15
0125          TYPE *,' FILTERING DATA WITH 15-POINT FIR FILTER!'
      C
0126          DO 80 I = 2, LENGTH+NCO
0127          SUM =0.0
0128          DO 70 J = 1,NCO
0129          L = J
0130          IF (J .GE. I) GO TO 70
0132          IF (I-J .GT. LENGTH) GO TO 70
```

```
0134          H = COEF(J) * HEOG(I-J)
0135          SUM = SUM + H
0136    70    CONTINUE
0137          YHEOG(I-1) = SUM
0138    80    CONTINUE
      C
0139          J2 = 14
0140          DO 81 J = 15, LENGTH+J2
0141          YHEOG(J-J2) = YHEOG(J)
0142    81    CONTINUE
      C
0143          DO 630 I = 1, 14
0144          YHEOG(LENGTH-I-1)=YHEOG(LENGTH-14)
0145    630   CONTINUE
      C
0146          CALL TSXCHK
0147          CALL GRINIT(4014,4631,1)
0148          CALL CHRSIZ(3)
0149          CALL ERASE
0150          CALL GRID(10,10,ILFT,IRIT,IBOT,ITOP,97)
0151          CALL ANOTAT(10,10,ILFT,IRIT,IBOT,ITOP,XMIN,XMAX,YMIN,YMAX)
0152          CALL XYPLOT(XT,YHEOG,LENGTH,ILFT,IRIT,IBOT,ITOP,XMIN,XMAX,
             1 YMIN,YMAX,1,0)
      C
0153          CALL MPLOT(ILFT+500,ITOP+300,-1)
0154          TYPE 261
0155    261   FORMAT('+ FIR FILTERED DATA ')
      C
0156          TYPE *,' DO YOU WANT A HARD COPY? (YES=1)'
0157          ACCEPT *,IS
0158          IF (IS .NE. 1) GO TO 83
      C
0160          CALL COPY(0)
      C
0161    83    H = FLOAT(ISTEP)/120.
0162          L = LENGTH
0163          TYPE *,' SET DESIRED HALF ORDER OF DIFFERENTIATOR:'
0164          ACCEPT *,NDIF
0165          GO TO (84,86,88),NDIF
      C
0166    84    DO 85 I = 2, LENGTH
0167          FDEOG(I) = (YHEOG(I+1) - YHEOG(I-1))/(H * 2.)
0168    85    CONTINUE
0169          FDEOG(1) = FDEOG(2)
0170          FDEOG(L) = FDEOG(L-1)
0171          GO TO 1000
      C
0172    86    DO 87 I = 3, L-2
0173          FDEOG(I) = ((YHEOG(I-2) - YHEOG(I+2)) + (8.*(YHEOG(I+1) -
             1 YHEOG(I-1))))/(H*12.)
0174    87    CONTINUE
0175          FDEOG(1) = FDEOG(3)
0176          FDEOG(2) = FDEOG(3)
0177          FDEOG(L) = FDEOG(L-2)
```

```
0178          FDEOG(L-1) = FDEOG(L-2)
      C
0179    1000  DO 200 I = 3, L-2
0180          SDEOG(I) = ((-1.)*(YHEOG(I-2) + YHEOG(I+2)) + (16.*(YHEOG(I+1) +
             1 YHEOG(I-1))) - 30.*YHEOG(I))/(12.*H**2.)
0181    200   CONTINUE
0182          SDEOG(1) = SDEOG(3)
0183          SDEOG(2) = SDEOG(3)
0184          SDEOG(L) = SDEOG(L-2)
0185          SDEOG(L-1) = SDEOG(L-2)
      C
0186          REAL XMFSD
0187          TYPE *,' SETTING MULTIPLYING FACTOR FOR  2ND DERIVATIVE'
      C       ACCEPT *,XMFSD
0188          XMFSD = .01
      C
0189          DO 400 I = 1, L
0190          SDEOG(I) = XMFSD*SDEOG(I)
0191    400   CONTINUE
      C
0192          FDRMS = 0.
0193          SSFD = 0.
0194          DO 700 I = 1, LENGTH-20
0195          SSFD = SSFD + FDEOG(I)**2.
0196    700   CONTINUE
0197          SSMFD = SSFD/FLOAT(LENGTH-20)
0198          FDRMS = SQRT(SSMFD)
0199          TYPE 725,FDRMS
0200    725   FORMAT (' RMS OF 1ST DERV. =',F8.3)
      C
0201          SDRMS = 0.
0202          SSSD = 0.
0203          DO 750 I = 1, LENGTH-20
0204          SSSD = SSSD + SDEOG(I)**2.
0205    750   CONTINUE
0206          SSMSD = SSSD/FLOAT(LENGTH-20)
0207          SDRMS = SQRT(SSMSD)
0208          TYPE 775,SDRMS
0209    775   FORMAT (' RMS OF 2ND DERV. =',F8.3)
      C
0210          TYPE *,' WAITING! TYPE 1 TO CONTINUE.'
0211          ACCEPT*, JES
0212          GO TO 90
      C
0213    88    DO 89 I = 4, L-3
0214          FDEOG(I) = ((YHEOG(I+3) - YHEOG(I-3)) + (9.*(YHEOG(I-2) -
             1 YHEOG(I+2))) + (45.*(YHEOG(I+1) - YHEOG(I-1))))/(H*60.)
0215    89    CONTINUE
0216          FDEOG(1) = FDEOG(4)
0217          FDEOG(2) = FDEOG(4)
0218          FDEOG(3) = FDEOG(4)
0219          FDEOG(L) = FDEOG(L-3)
0220          FDEOG(L-1) = FDEOG(L-3)
0221          FDEOG(L-2) = FDEOG(L-3)
```

```
0222          GO TO 1000
      C
0223   90     YMIN = YMIN*10.
0224          YMAX = YMAX*10.
0225          CALL TSXCHK
0226          CALL GRINIT(4014,4631,1)
0227          CALL CHRSIZ(3)
0228          CALL ERASE
0229          CALL GRID(10,10,ILFT,IRIT,IBOT,ITOP,97)
0230          CALL ANOTAT(10,10,ILFT,IRIT,IBOT,ITOP,XMIN,XMAX,YMIN,YMAX)
0231          CALL XYPLOT(XT,FDEOG,LENGTH,ILFT,IRIT,IBOT,ITOP,XMIN,XMAX,
             1 YMIN,YMAX,1,0)
      C
0232          CALL MPLOT(ILFT+500,ITOP+300,-1)
0233          TYPE 282
0234   282    FORMAT ('+ FIRST DERIVATIVE OF DATA')
0235          TYPE *,' DO YOU WANT A HARD COPY? (YES=1)'
0236          ACCEPT *,IS
0237          IF (IS .NE. 1) GO TO 283
      C
0239          CALL COPY(0)
      C
0240   283    TYPE *,' DO YOU WANT A SINGLE CURVE PLOT? (YES=1)'
0241          ACCEPT *, IYES
0242          IF (IYES .NE. 1) GO TO 210
0244          CALL TSXCHK
0245          CALL GRINIT(4014,4631,1)
0246          CALL CHRSIZ(3)
0247          CALL ERASE
0248          CALL GRID(10,10,ILFT,IRIT,IBOT,ITOP,97)
0249          CALL ANOTAT(10,10,ILFT,IRIT,IBOT,ITOP,XMIN,XMAX,YMIN,YMAX)
0250          GO TO 250
0251   210    IBOT = 1250
0252          ITOP = 2750
0253   250    CALL XYPLOT(XT,SDEOG,LENGTH,ILFT,IRIT,IBOT,ITOP,XMIN,XMAX,
             1 YMIN,YMAX,1,0)
      C
0254          CALL MPLOT(ILFT+500,ITOP+300,-1)
0255          TYPE 382
0256   382    FORMAT ('+ SECOND DERIVATIVE OF DATA')
0257          TYPE *,' DO YOU WANT A HARD COPY? (YES=1)'
0258          ACCEPT *,IS
0259          IF (IS .NE. 1) GO TO 92
      C
0261          CALL COPY(0)
      C
0262   92     TYPE *,' ANOTHER DIFFERENTIATOR? (YES=1)'
0263          ACCEPT *,IS
0264          IF (IS .EQ. 1) GO TO 83
      C
0266          CALL ERASE
0267          TYPE *,' IDENTIFICATION OF FAST PHASES'
0268          FDRMSTH = FDRMS*2.
0269          TYPE 410, FDRMSTH
```

```
0270  410   FORMAT (' 1ST DERV. RMS THRESHHOLD =',F9.3)
      C
0271  110   LTERM = LENGTH - ISLG
0272        DO 112 J = 1, LTERM
0273        IF (ABS(FDEOG(ISLG+J)) .GT. ABS(FDRmSTH)) GO TO 115
0275  112   CONTINUE
      C
0276  115   ITLST = J + ISLG
0277        TYPE 411,ITLST
0278  411   FORMAT (' INDEX TSH EXCD AT I =',I5)
      C
0279        IF (FDEOG(ITLST) .GE. 0.) GO TO 120
0281        TYPE *,' NEGATIVE VALUES START'
0282        DO 117 L = 1, 10
0283        IF (FDEOG(ITLST - L) .GE. 0.) GO TO 124
0285  117   CONTINUE
0286        TYPE *,' POSITIVE VALUES START'
0287  120   DO 122 L = 1, 10
0288        IF (FDEOG(ITLST - L) .LT. 0.) GO TO 128
0290  122   CONTINUE
0291        TYPE *,' NEGATIVE VALUES END'
0292  124   ISTRT = ITLST - L
0293        TYPE 412,ISTRT
0294  412   FORMAT (' STRT NEG INDEX AT I = ',I4)
      C
0295        DO 126 K = 1, 30
0296        IF (FDEOG(ITLST + K) .GE. 0.) GO TO 135
0298  126   CONTINUE
0299        TYPE *,' POSITIVE VALUES END'
0300  128   ISTRT = ITLST - L
0301        TYPE 414, ISTRT
0302  414   FORMAT (' STRT POS INDEX AT I = ',I4)
      C
0303        DO 130 LN = 1, 30
0304        IF (FDEOG(ITLST + LN) .LT. 0) GO TO 134
0306  130   CONTINUE
0307  134   ISTP = ITLST + LN
0308        TYPE 415, ISTP
0309  415   FORMAT (' END POS INDEX AT I = ',I4)
0310        GO TO 136
      C
0311  135   ISTP = ITLST + K
0312        TYPE 416, ISTP
0313  416   FORMAT (' END NEG INDEX AT I = ',I4)
      C
      C     LEAST SQUARES FIT
0314  136   XN = 10.
0315        DXSUM =  0.
0316        DXSSUM = 0.
0317        DYSUM = 0.
0318        DXYSUM = 0.
0319        DO 140 ISL = ISTRT-10, ISTRT
0320        FI2 = FLOAT(ISL)
0321        DXSUM = DXSUM + FI2
```

```
0322          DXSSUM = DXSSUM + FI2*FI2
0323          DYSUM = DYSUM + YHEOG(ISL)
0324          DXYSUM = DXYSUM + FI2*YHEOG(ISL)
0325    140   CONTINUE
      C
0326          DENOM = (XN*DXSSUM - DXSUM*DXSUM)
0327          SLOPE = (XN*DXYSUM - DXSUM*DYSUM)/DENOM
0328          YINT = (DYSUM*DXSSUM - DXSUM*DXYSUM)/DENOM
0329          TYPE 417, SLOPE, YINT
0330    417   FORMAT (' SLOPE =',F12.5,' YINT =',F12.5)
      C
0331          DO 142 ILF = ISTRT, ISTP
0332          XILF = FLOAT(ILF)
0333          YHEOG(ILF) = SLOPE*XILF + YINT
0334          TYPE *, ILF, YHEOG(ILF)
0335    142   CONTINUE
      C
0336          TYPE *,' TO CONTINUE TYPE: 1 '
0337          ACCEPT*,IX
0338          CALL ERASE
      C
0339          TYPE *,' RECONSTRUCT SLOW PHASE'
      C
0340          HHT = HHT + YHEOG(ISTP) -YHEOG(ISTP+1)
0341          TYPE 420, HHT
0342    420   FORMAT(' HEIGHT CORRECTION =',F12.5)
      C
0343          TYPE 421, ISLG, ISTP
0344    421   FORMAT (' STRT SP INDX = ,'I4,'STP SP INDX = ',I4)
      C
0345          DO 145 I = ISLG+1, ISTP
0346          SPEOG(I) = YHEOG(I) + THT
0347          TYPE *, I, SPEOG(I)
0348    145   CONTINUE
      C
0349          THT = HHT
0350          ISLG = ISTP
0351          TYPE 425,ISLG
0352    425   FORMAT(' NEW SEARCH STARTS AT I = ',I4)
0353          TYPE *,' TO CONTINUE TYPE: 1'
0354          ACCEPT *, IXS
      C
0355          IF (ISLG .LT. LENGTH) GO TO 110
      C
0357          TYPE *,' PLOT RECONSTRUCTED SLOW WAVE? (YES = 1)'
0358          ACCEPT *, IYES
0359          IF (IYES .NE. 1) GO TO 149
      C
0361          YMIN = YMIN*.1
0362          YMAX = YMAX*.1
      C
0363    900   CALL TSXCHK
0364          CALL GRINIT(4014,4631,1)
0365          CALL CHRSIZ(3)
```

```
0366          CALL ERASE
0367          CALL GRID(10,10,ILFT,IRIT,IBOT,ITOP,97)
0368          CALL ANOTAT(10,10,ILFT,IRIT,IBOT,ITOP,XMIN,XMAX,YMIN,YMAX)
0369          CALL XYPLOT(XT,SPEOG,LENGTH,ILFT,IRIT,IBOT,ITOP,XMIN,XMAX,
             1 YMIN,YMAX,1,0)
      C
0370          CALL MPLOT(ILFT+500,ITOP+300,-1)
0371          TYPE 882
0372    882   FORMAT ('+ RECONSTRUCTED SLOW PHASE EOG POSITION DATA')
0373          TYPE *,' DO YOU WANT A HARD COPY? (YES=1)'
0374          ACCEPT *,IS
0375          IF (IS .NE. 1) GO TO 149
      C
0377          CALL COPY(0)
      C
      C
      C262    TYPE *,' DO YOU WANT 5-POINT SMOOTHING? (YES=1)'
      C       ACCEPT *,IYES
      C       IF (IYES .NE. 1) GO TO 149
      C
      C       DO 600 I = 3, LENGTH-2
      C       SPYHEOG(I) = .11*(SPEOG(I-2)+SPEOG(I+2))+.22*(SPEOG(I-1)
      C       1 +SPEOG(I+1)) + .33*SPEOG(I)
      C600    CONTINUE
      C       SPYHEOG(1) = SPYHEOG(3)
      C       SPYHEOG(2) = SPYHEOG(3)
      C       SPYHEOG(LENGTH) = SPYHEOG(LENGTH-2)
      C       SPYHEOG(LENGTH-1) = SPYHEOG(LENGTH)
      C
      C375    CALL TSXCHK
      C       CALL GRINIT(4014,4631,1)
      C       CALL CHRSIZ(2)
      C       CALL ERASE
      C       CALL GRID(10,10,ILFT,IRIT,IBOT,ITOP,97)
      C       CALL ANOTAT(10,10,ILFT,IRIT,IBOT,ITOP,XMIN,XMAX,YMIN,YMAX)
      C       CALL XYPLOT(XT,SPYHEOG,LENGTH,ILFT,IRIT,IBOT,ITOP,XMIN,XMAX,
      C       1 YMIN,YMAX,1,0)
      C
      C       CALL MPLOT(ILFT+500,ITOP+300,-1)
      C       TYPE 82
      C82     FORMAT ('+ FIR FILTERED AND 5-PT. SMOOTHED DATA')
      C       TYPE *,' DO YOU WANT A HARD COPY? (YES=1)'
      C       ACCEPT *,IS
      C       IF (IS .NE. 1) GO TO 149
      C
      C       CALL COPY(0)
      C
0378    149   TYPE *,' DO YOU WANT A 15-PT FIR FILTER? (YES=1)'
0379          ACCEPT *,IYES
0380          IF (IYES .NE. 1) GO TO 150
      C
0382          DO 100 I = 2, LENGTH+NCO
0383          DSUM =0.0
0384          DO 95 J = 1, NCO
```

```
0385          IF (J .GE. I) GO TO 95
0387          IF (I-J .GT. LENGTH) GO TO 95
0389          DH = COEF(J) * SPEOG(I-J)
0390          DSUM = DSUM + DH
0391    95    CONTINUE
0392          SPYHEOG(I-1) = DSUM
0393    100   CONTINUE
      C
0394          DO 101 M = 15, LENGTH+J2
0395          SPYHEOG(M-J2) = SPYHEOG(M)
0396    101   CONTINUE
      C
0397          DO 102 I = 1, 14
0398          SPYHEOG(LENGTH-I-1) = SPYHEOG(LENGTH-14)
0399    102   CONTINUE
      C
0400          CALL TSXCHK
0401          CALL GRINIT(4014,4631,1)
0402          CALL CHRSIZ(3)
0403          CALL ERASE
0404          CALL GRID(10,10,ILFT,IRIT,IBOT,ITOP,97)
0405          CALL ANOTAT(10,10,ILFT,IRIT,IBOT,ITOP,XMIN,XMAX,YMIN,YMAX)
0406          CALL XYPLOT(XT,SPYHEOG,LENGTH,ILFT,IRIT,IBOT,ITOP,XMIN,XMAX,
             1 YMIN,YMAX,1,0)
      C
0407          CALL MPLOT(ILFT+500,ITOP+300,-1)
0408          TYPE 104
0409    104   FORMAT ('+ 15-PT FILTERED SLOW PHASE EOG DATA')
0410          CALL COPY(0)
      C
0411    150   IBLK = IBLK - 3
0412          IF( IBLK .LT. NBLK) GO TO 48
      C
0414          TYPE *,' ANOTHER CHANNEL OF DATA? (YES=1)'
0415          ACCEPT *,JES
0416          IF (JES .EQ. 1) GO TO 42
      C
0418          TYPE *,' TRY ANOTHER FILE? (1=YES) ? '
0419          ACCEPT *, MORE
0420          IF (MORE .EQ. 1) GO TO 10
      C
0422          STOP
0423          END
```

```
FORTRAN IV      Storage map for Program Unit FFID

Local Variables, .PSECT $DATA, Size = 042652 ( 8917. words)

Name    Type  Offset      Name    Type  Offset      Name    Type  Offset
AMPL    R*4   000454 Eqv  DENOM   R*4   042516      DH      R*4   042550
DSKINC  I*2   000516 Eqv  DSUM    R*4   042544      DXSSUM  R*4   042474
DXSUM   R*4   042470      DXYSUM  R*4   042504      DYSUM   R*4   042500
FDRMS   R*4   042414      FDRMST  R*4   042446      FI2     R*4   042512
H       R*4   042404      HHT     R*4   042262      I       I*2   042320
IBLK    I*2   042302      IBOT    I*2   042346      IERR    I*2   042250
ILF     I*2   042532      ILFT    I*2   042342      INTRAT  R*4   000476 Eqv
IRIT    I*2   042344      IRMODE  I*2   042312      IS      I*2   042374
ISL     I*2   042510      ISLG    I*2   042272      ISN     I*2   042322
ISTEP   I*2   042304      ISTP    I*2   042462      ISTRT   I*2   042456
ITEMP   I*2   042310      ITLST   I*2   042454      ITOP    I*2   042350
IX      I*2   042540      IXS     I*2   042542      IYES    I*2   042362
J       I*2   042330      JES     I*2   042444      J2      I*2   042410
K       I*2   042274      L       I*2   042316      LENGTH  I*2   042246
LN      I*2   042460      LOPEN   I*2   042300      LTERM   I*2   042452
M       I*2   042554      MORE    I*2   042556      N       I*2   042260
NBLK    I*2   000530 Eqv  NCO     I*2   042376      NDIF    I*2   042412
NDUMMY  I*2   042276      NEH     I*2   042256      NPTS    I*2   042314
NWRDS   I*2   042306      PERIOD  R*4   000460 Eqv  SDRMS   R*4   042430
SLOPE   R*4   042522      SSFD    R*4   042420      SSMFD   R*4   042424
SSMSD   R*4   042440      SSSD    R*4   042434      SUM     R*4   042400
THT     R*4   042266      XILF    R*4   042534      XLGT    R*4   042324
XMAX    R*4   042356      XMEAN   R*4   042370      XMFSD   R*4   042252
XMIN    R*4   042352      XN      R*4   042464      XSUM    R*4   042364
YINT    R*4   042526      YMAX    R*4   042336      YMIN    R*4   042332

Local and COMMON Arrays:

Name      Type    Section Offset  ------Size-----  Dimensions
BUFR2     I*2     $DATA   036076  004000 ( 1024.)  (1024)
COEF      R*4     $DATA   012002  000074 (   30.)  (15)
FDEOG     R*4     $DATA   032076  004000 ( 1024.)  (512)
FILNAM    L*1     $DATA   042076  000014 (    6.)  (12)
HEOG      R*4     $DATA   002002  004000 ( 1024.)  (512)
ICHNUM    I*2     $DATA   000542  000040 (   16.)  (16)
IPOSN     I*2     $DATA   000702  000040 (   16.)  (16)
MAX       I*2     $DATA   000742  000040 (   16.)  (16)
SDEOG     R*4     $DATA   016076  004000 ( 1024.)  (512)
SPEOG     R*4     $DATA   022076  004000 ( 1024.)  (512)
SPYHEO    R*4     $DATA   026076  004000 ( 1024.)  (512)
XT        R*4     $DATA   006002  004000 ( 1024.)  (512)
YHEOG     R*4     $DATA   012076  004000 ( 1024.)  (512)
Z         I*2     $DATA   000002  002000 (  512.)  (512)

Subroutines, Functions, Statement and Processor-Defined Functions:

Name    Type  Name    Type  Name    Type  Name    Type  Name    Type
ABS     R*4   ANOTAT  R*4   CHRSIZ  R*4   COPY    R*4   DISKIO  R*4
ERASE   R*4   FLOAT   R*4   GRID    R*4   GRINIT  R*4   MPLOT   I*2
SQRT    R*4   TSXCHK  R*4   XYPLOT  R*4
```

1986

NASA/ASEE SUMMER FACULTY RESEARCH FELLOWSHIP PROGRAM

JOHNSON SPACE CENTER

UNIVERSITY OF HOUSTON

LUNAR COMPOSITE PRODUCTION: INTERIM REPORT

Prepared by:	William C. Lewis, Ph.D.
Academic Rank:	
University & Department:	Clemson University ECE Department
NASA/JSC	
Directorate:	Space and Life Sciences
Division:	Solar System Exploration
Branch:	
JSC Colleague:	Michael B. Duke
Date:	August 8, 1986
Contract #:	NGT 44-005-803

Lunar Composite Production: Interim Report

William Lewis, ECE Dept.
Theodore Taylor, Ceramic Engr. Dept.
Clemson University, Clemson, SC 29634

This work was performed in cooperation with Mike Duke, Head, Solar System Exploration Division, NASA, Johnson Space Center.

Summary

A minimally processed composite material derived from lunar soil and possessing tensile strength is described. Laboratory work conducted during June and July of 1986 and the direction of future work are discussed.

Introduction

The National Commission on Space suggests "Research to pioneer the use, in construction and manufacturing, of space materials that do not require chemical separation, for example, lunar glasses and metallic iron concentrated in the lunar fines."[1]

Lunar glasses can be produced simply by melting certain kinds of regolith (lunar soil).[a] Like terrestrial glasses, they have considerable strength in tension and compression,[b] but are too brittle to be safely used in construction. Under moderate tensile loads, cracks of less than a millimeter depth propagate spontaneously at the speed of sound.[2] That is why a dropped dish cracks. While glass with an unflawed surface exhibits considerable tensile strength, there is no inspection method which can tell whether any given surface is, in fact, flawed. Therefore, bulk glass (like bulk rock) is an inherently unsafe structural material if subject to tensile stresses.

A material which cannot tolerate tensile stresses cannot be used for beams.[c]

Architecturally, its applications are restricted to thick walls, columns, domes, and arches (although flying buttresses can alleviate the severity of these restrictions to some extent). Structures employing only these forms are typically massive and require considerable labor to erect; in part for this reason stone architecture has been largely restricted to public buildings on Earth. There is no reason to believe that costs would be less on the lunar surface.

Two methods of avoiding the crack propagation failure mode[d] are of interest. One is pre-stressing. A glass plate, for example, can be solidified rapidly by air blast. If the solidification is only partial, an outside shell forms around a molten center. When the center cools, it contracts, putting itself in tension and the shell in compression. The center part, in tension, has to all intents and purposes an unflawed surface. The outer part, in compression and thus insensitive to cracks, protects the inner part. This pre-stressed system is quite strong and tough, but will release its stress energy suddenly if a crack does manage to penetrate the compressed region. The energy release is often enough to reduce the system to glass chips.

A second method of avoiding crack propagation is to make the unit glass structure smaller than the critical crack length. This is done by forming glass into long strands of ten to twenty microns thickness and several centimeters length. The glass fibers are held together by a matrix, and thus are one component of a composite material. The most commonly encountered material of this sort is fiberglass, which typically uses epoxy resin for the matrix.

The glass fiber composite appeared most suitable for initial investigation, primarily on grounds of safety. A glass matrix composite is not subject to catastrophic failure when its design stresses are exceeded, whereas a pre-stressed system (including, interestingly enough, pre-stressed concrete in compression) is.[e]

Microstructure

A lunar derived glass fiber composite cannot very well use epoxy as a matrix; neither epoxy nor its component element carbon can be readily found on the lunar surface. We intend to produce, not fiberglass, but rather an analog to fiberglass. We are not the only group doing this; Goldsworthy's group at the Space Studies Institute is pursuing development of a similar material.[3]

Strictly speaking, the proposed composite is three phase: glass, metal, and vacuum. The microstructure should look like a mass of sticky cotton. The threads will be glass, the glue will be metal, and the spaces between threads vacuum. The metals will be sticky because they will have free surfaces, created and maintained in high vacuum.[f] The threads will stick together where they touch; they will be unsupported between intersections.

The incentive for studying a three phase material is potential reduction of matrix volume fraction. To obtain Lunar metal requires more processing than to obtain lunar regolith; the less metal required, the less labor and capital required to make the composite. Should it be necessary, a more conventional matrix could be obtained by increasing the metal fraction. At the limit, the glass fibers would no longer touch each other significantly often, and would act as an extender for lunar derived metal (at some cost in energy: the metal would have to be vaporized, or at least melted, before mixing with the glass).

The tensile strength of this material should depend on the cross-sectional area fraction which is glass (and the resistance to delamination). The compressive strength should depend on the force required to initiate bending in fibers between junctions (which must therefore be rather tightly spaced). The ultimate compressive stress may be fairly low (5E3psi),[g] but this does not preclude its use in beams. The corresponding stress for commercial pine beams is much lower (250 psi).[h]

A long shot, but an interesting one, is a glass / vacuum composite. It is possible that

newly drawn glass fibers will vacuum weld without metal coating. If so, the strength of the glass / glass bonds could be increased by heat treatment. While this composite would probably not be as strong as a glass / metal / vacuum composite, it may be comparable to wood in strength. If so, it would still be useful for light duty applications.

It would have the immense advantage of being fabricable entirely from Apollo 16 regolith,[i] with no preprocessing whatsoever. Glass / metal / vacuum composite production costs appear likely to be dominated by metal mining and extraction. While metal related costs could be greatly reduced by using byproducts of a lunar oxygen process as composite feedstock,[j] these byproducts may at times be unavailable. If composite production is run as a solo process, costs might be significantly reduced by electing to produce a glass / vacuum composite.

Previous Work

As part of a Universities Space Research Association (USRA) supported course on Advanced Mission Design, a group at Clemson specified a method of converting Apollo 16 bulk regolith into glass fibers. The method is based on the commercial Tel disk process, and is shown in Figure 1. It relies on introducing molten regolith into a rapidly rotating shallow bowl (called a disk) with perforated sides. Centrifugal force extrudes glass through the perforations as fibers, which break free from the disk upon reaching a length of several centimeters. The fibers are thinly metal coated by vapor deposition before landing on collection surfaces. Glass mat accumulating on the collection surfaces should form a glass / metal / vacuum composite of the kind discussed above.

Predictions of the composite's properties must be experimentally tested before they can be accepted. The Clemson group has, during June and July of 1986, done preliminary work required to fabricate and test composites of this kind.

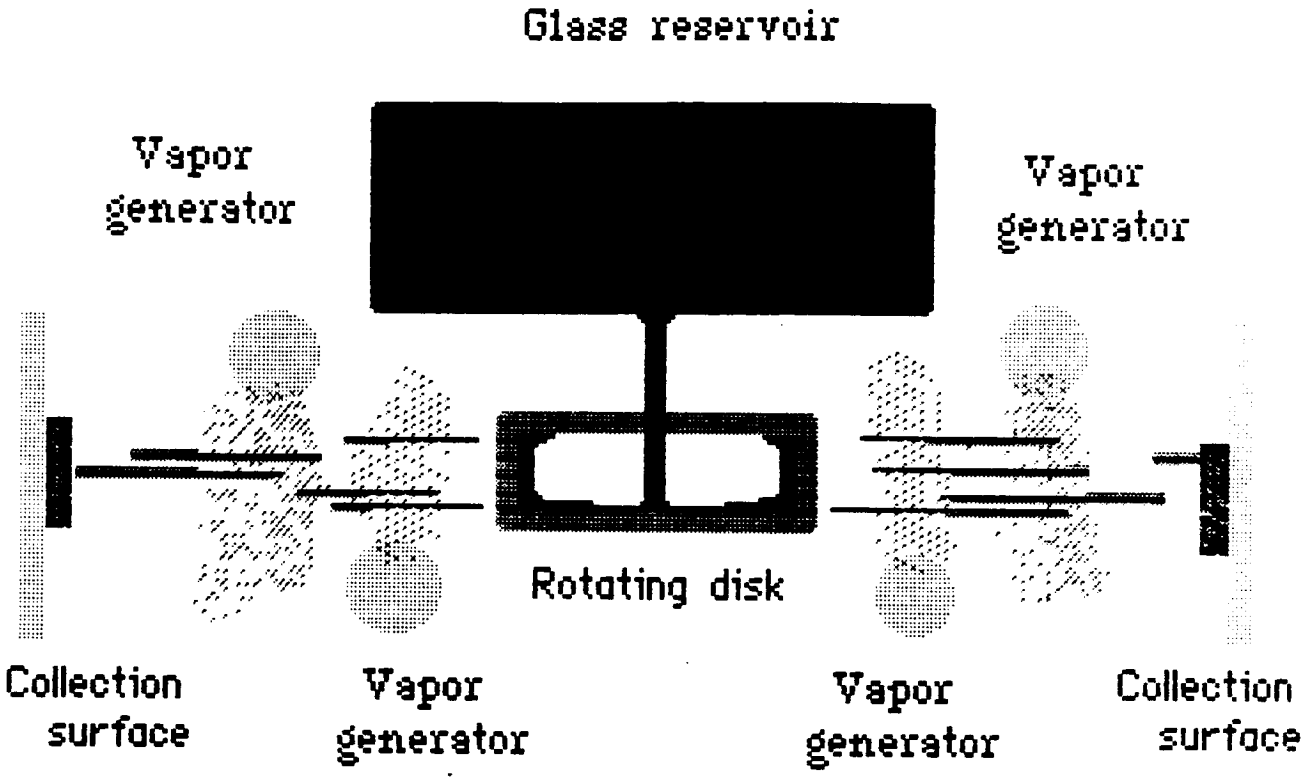

Figure 1. Disk fiberization.

Preparation for Laboratory Work

The rotating disk process is not suitable for laboratory use. Accordingly, a method called the "textile process," shown in Figure 2, was selected. The textile process relies on an glass reservoir with a nozzle (called a bushing) in its bottom. Glass flowing through the bushing is caught and wound onto a reel at high speed (about 3 meters / second). It can be metal coated while between the bushing and the reel.

The laboratory equipment is designed to pull about 30 kilometers of a 30E-6 meter diameter fiber from the reservoir, metal coat it, and wind it around a sample collecting reel in the form of cigarette sized samples. The entire operation should take about 3 hours. Samples will be subject to material properties tests.

The overall textile process system consists of three parts: a glass melting furnace,[k] capable of 1600° C and containing a platinum reservoir, a computer controlled[l] takeup reel,[m] capable of producing 6 test samples of about 6 cm length by 0.6 cm diameter, and a calcium vapor generator,[n] capable of vaporizing up to 100 grams of calcium over a six hour interval at about 850° C. All components are to operate in vacuum of 8E-5 torr.[p]

Clear bottle glass is to be used for equipment checkout and first approximation composite property determination. Apollo 16 regolith simulant (assembled from bulk chemicals) will be used after the system is seen to work well with bottle glass.[q]

Calcium is selected as the metal for glass coating because it can be made to sublimate at a fairly low temperature in vacuum[r] and could be extracted from lunar regolith.

Laboratory work

Of these three components, only the reel has been successfully and completely tested in vacuum.

The calcium vapor generator has been tested, and molecular flow of calcium in what appears to

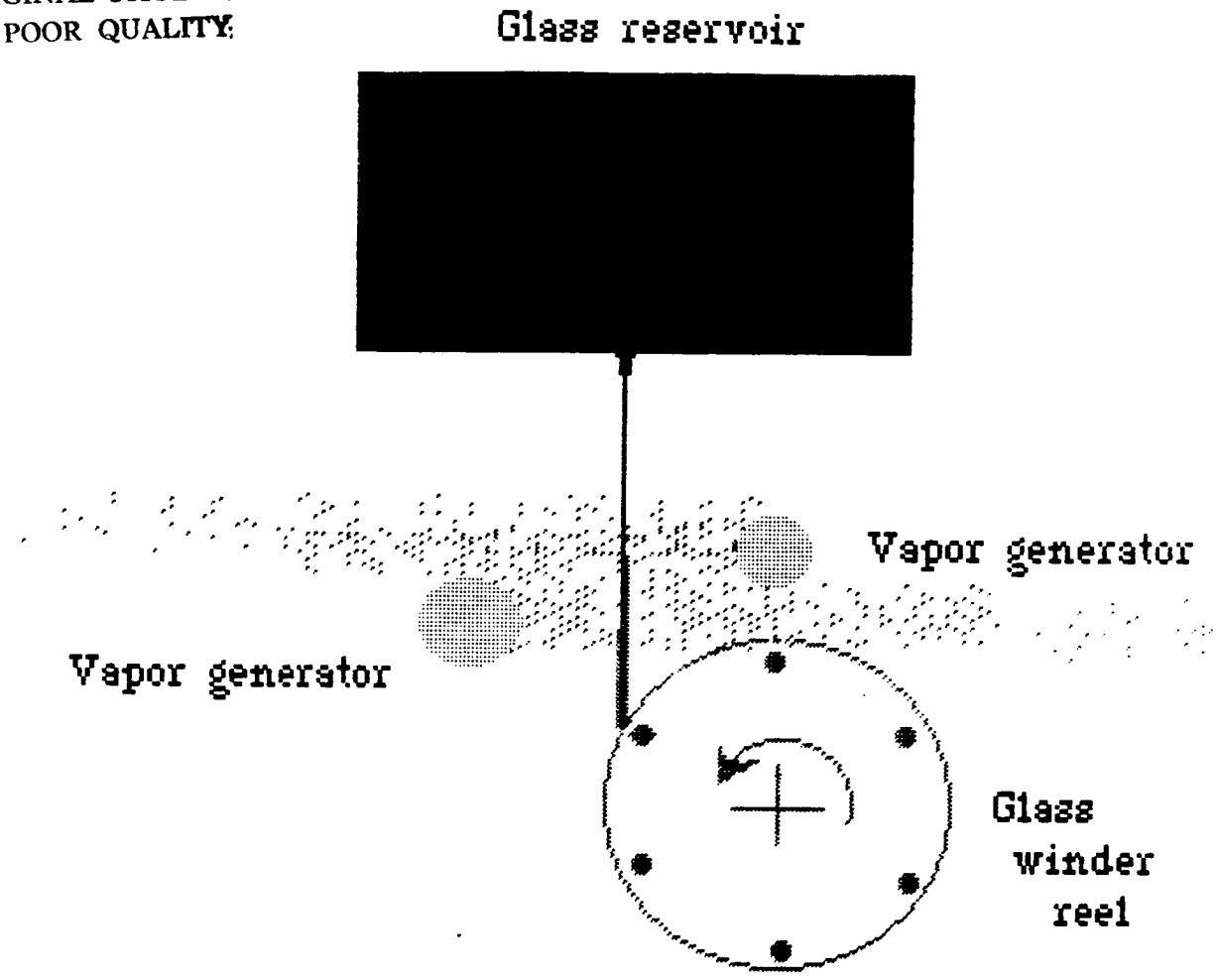

Figure 2. Textile Process

be adequate volume has been demonstrated. However, the generator itself was severely damaged during the test run, and repair proved uneconomical. The calcium vapor nozzle was apparently cool enough to permit condensation inside the orifice; when the orifice become plugged, vapor escaped through gaps around the endcaps in enough volume to damage heating coils and surrounding refractory.[v] It should be noted that this escape posed no hazard to any person, and that the vacuum chamber was not damaged in any way. A calcium vapor generator not susceptible to these failures has been conceptually designed.

The furnace reaches rated temperature (1200° C) in air and in vacuum. The glass melts properly in air. We have succeeded in drawing fibers from Apollo 16 regolith simulant.[s]

First, we learned that a crucible bottom of pure platinum becomes wetted by molten glass; this inhibits fiber formation. We reduced wetting to acceptable levels by alloying the platinum with a few percent gold.[t] We next found that our empirical formula for nozzle design[u] required adjustment for the small flow rates we wanted. Our data lead us to believe that a nearly stationary boundary layer of about 0.5 mm forms on platinum surfaces. This reduces effective bushing diameter by about 1 mm. Accordingly, we added 1 mm to our calculated bushing diameter in an attempt to increase flow to the desired amount. This change produced the desired flow for bottle glass.

After establishing that the furnace / reel combination could fiberize bottle glass, pulling rate was increased until 30E-6 meter diameter fibers were obtained. The reel was next moved from side to side (translated) by the translation motor under computer control.

This equipment was used to determine flow rate for bottle glass at several temperatures. From this, and a knowledge of bottle glass viscosity, it should be possible to determine the geometric constant D^4/L in our empirical flow formula for the crucible.

We next attempted to fiberize Apollo 16 simulant.[s] A frit of glassy fragments had been prepared at Clemson. The crucible was filled

with this frit and heated in air to 1250°C, at which point the melted simulant's viscosity permitted fiberization. We were able to produce fibers of 30E-6 meter diameter with a pulling rate of about 9 feet per second.

To our knowledge, this is the first time simulated lunar material has been fiberized using the textile process. While the fibers produced have not been formally tested, they seem somewhat stronger and more rigid than bottle glass. Produced on a large scale, they could be used with epoxy matrix to make standard fiberglass.

Fibers were pulled at three different temperatures to establish flow rate. From this it should be possible to deduce a viscosity vs. temperature relation for the lunar simulant.

Conclusion

To date, the project has taken up one semester of planning and nine weeks of laboratory work. The laboratory work will not be complete this summer; we intend to return to Clemson, think and plan some more, and complete the laboratory work in 1987.

Acknowledgements

Funding was from the Universities Space Research Association, under John Sevier, and the American Society of Engineering Educators (ASEE). The Clemson project student members who worked this summer are: Robert Dalton (ceramic engineer), William Dover (computer control), and Todd Nichols (geology and electromechanical devices). Additionally, abundant thanks are due to the following people at JSC, without whose help this project would have been impossible: Mike Duke, Head, Solar System Exploration Division, Bayliss McInnis, ASEE representative, James Townsend, Solar System Exploration Division, Jerry Winkler, Lockheed liaison, Al Lanier, petrological laboratory, and the Lockheed crew in Building 33 (vacuum chambers): Bill Keeton, Ron Buckley, Tom Bacot, John

Ceglinski, Buddy Moore, Stan Rasmussen, Bob Wirt, and Sherwin Wade.

Footnotes

[a] Ideal fiberglass should contain, by weight percent:
SiO_2: 60; AL_2O_3: 5; CaO/MgO: 35; FeO/TiO_2: 0.
Lunar regolith at the Apollo sites 11, 12, 14, 15, and 16 has average weight percents of:
SiO_2: 45.6; AL_2O_3: 17.8; CaO/MgO: 21.0;
FeO/TiO_2: 14.5 (from data in Rose).[5]
It is a bit long on SiO_2 and Al and Fe/Ti oxides.

[b] In fact the ultimate tensile strength of common bottle glass, made into fibers, is 200 kpsi, as compared to 224 kpsi for bridge wire steel. From Table 1-115, Bolz.[7]

[c] A beam supported at both ends and loaded by a weight at midspan is in compression above the neutral axis and in tension below the neutral axis. While more complicated loadings are usually encountered, typically some sections of any beam are in compression and others in tension. Ropes, in contrast, are in tension throughout, and bricks in compression throughout.

[d] A third method is to alter the ceramic material so that free surface energy is drastically increased, or so that cracks tend to branch when propagated. Both strategies increase the critical crack length, but neither can be made from "minimally processed material," and are accordingly outside the scope of this project.

[e] The main drawback of fiberglass is not its ultimate tensile strength, but rather its flexibility. Glass fibers are as strong as steel (those with perfect surfaces are considerably more so), but are also more flexible. Glass typically has a Young's Modulus (E) of 11 Mpsi, whereas steel has an E of about 30 Mpsi. The same load will produce about three

times the deformation for a glass as a steel structure, if the geometries are identical.

f Pressure at the lunar surface is 1E-14 torr. The vacuum chamber used this summer (Chamber P, Bldg. 33, NASA Johnson Space Center, Houston, TX) could provide a vacuum of 8E-5 torr with textile process equipment inside, but this vacuum is thought to be sufficient to permit vacuum welding of newly created free surfaces.

g From an application of Rankine's formula, estimating phi using Ritter's Rational Formula, as described in Eshbach,[4] pg. 528 ff. Ultimate compressive strength of 160E3 psi, and E of 10.4E6 psi assumed are for silica glass, as given in Table 1-120, Bolz.[7] An l/d ration of 20 is assumed.

h Table 1-124, Bolz.[7]

i Composition of Apollo 16 regolith by weight percent is: SiO_2: 44.9; AL_2O_3: 26.7; CaO/MgO: 21.6; FeO/TiO_2: 6.1.[5] Variations by weight percent are: SiO_2: 0.7; AL_2O_3: 2.9; CaO/MgO: 3.9; FeO/TiO_2: 2.4.[5,6]

j Lunar oxygen production processes break up selected metal oxides into oxygen and metal byproducts. If the selected metals are not desirable in glass (iron, titanium, and excess aluminum oxides, for example) regolith discarded from the process may be better suited to glass formation than raw regolith. Any metal byproducts will be useful as matrix.

k The furnace is custom designed. It is a hexagonal cylinder, 6" wide sides (outer dimensions), 1.5" thick outer walls, 4.5" top, 3.0" bottom, kaowool (alumina silicate) construction. An additional molybdenum foil infrared shield (from GTE Sylvania) is used in vacuum. Heating is by 6 bayonet glowbars, 12 inch height, 5 ohms nominal resistance (from I^2R). A PID controller is used to control temperature. Normal power consumption at 1200° C is about 2 kw.

[l] The computer is an NCR Mk. IV with 256K bytes of memory running LMI Forth under NCR DOS 2.1. The interface board is a Metrabyte PIO board, which uses an Intel parallel I/O chip to send step and direction information. The stepper motor control board was fabricated by group members.

[m] The reel is rotated by a dc motor, and moved transversely by a stepper motor. It has been tested at 408 rpm, corresponding to a 3.4 meter / second pulling rate.

[n] The calcium generator was custom designed. It consisted of a containment vessel and a furnace. The containment vessel consisted of a pipe with endcaps and a 3.8 cm long, .63 cm inner diameter nozzle. The furnace was wrapped around the pipe and consisted of ceramic and Canthol, with molybdenum radiation shielding. The furnace was controlled by a PID controller, and was rated at 1 kw.

[p] Lunar regolith simulant is metastably crystalline below about 1200° C. It has been fiberized at Clemson at about 1500° C. Bottle glass can be fiberized at about 1100° C, and its behavior is well understood.

[q] Ball Aerospace, of Denver, Colorado, adapted our dc electric motor for vacuum use by baking out volatiles and relubricating with low vapor pressure grease.

[r] Calcium has a vapor pressure of 1 torr at about 840° C, and 10 torr at about 950° C[7].

[s] The gold was applied in a thin surface layer by sputtering, and alloyed with the crucible platinum by heating in air at 1200° C for an hour.

[t] The regolith simulant had the following composition (weight percent):
SiO_2: 45; Al_2O_3: 27; CaO: 16; MgO: 6.48; FeO: 5.47; TiO_2: trace; MnO_2: 0.18; K_2O: 0.11; Na_2O: 0.11.

[u] flow = K*(D⁴*h) / (l*Viscosity). flow:: volume of glass per unit time passing through bushing; K:: dimensional constant; D:: bushing diameter; h: height of glass in reservoir (head); l:: length of bushing. Note that flow is proportional to the **fourth** power of bushing diameter.

[v] The damage consisted of Canthol fusion, alloying between Canthol and calcium vapor, reactions between calcium and ceramic, and welding of the endcaps to the pipe. Use of other heating methods and a different container geometry should eliminate the causes of this failure.

References

1 United States. National Commission on Space.
Pioneering the space frontier, pg. 86.
Bantam Books, 1986.
ISBN 0-553-34314-9.

2 J. E. Gordon.
Structures.
Plenum Press, 1978.
ISBN 0-306-40025-1.

3 W. Brandt Goldsworthy.
Composites Fibers and Matrices from Lunar Regolith.
The High Frontier Newsletter XI(5):1-3,5; September / October 1985.
Available from Space Studies Institute, 285 Rosedale Road, P.O. Box 82, Princeton, NJ 08540.

4 Ovid W. Eshbach, Bott Souders, ed.
Handbook of Engineering Fundamentals, 3rd Ed.
ISBN 0-471-24553-4.

5 H. J. Rose et. al.
Compositional data for twenty two Apollo 16 samples.
In **Proceedings of the Fourth Lunar Science Conference, March 5-8, 1973, Supplement 4, Geochimica et Cosmochimica Acta, Volume 2**, pp. 1149-1158.

6 Lunar Sample Preliminary Examination Team (LPSET).
Preliminary examination of lunar samples from Apollo 16.
Science (17):23-34, 1973.

7 Ray E. Bolz, George L. Tuve, ed.
Handbook of Tables of Applied Engineering Science, 2nd Ed.
CRC Press, 1973.
ISBN 0-87819-252-2.

1986

NASA/ASEE SUMMER FACULTY RESEARCH FELLOWSHIP PROGRAM

Johnson Space Center

University of Houston

An Evaluation of Turbo Prolog with an Emphasis on Its Application to the Development of Expert Systems

Prepared by:	Richard B. Loftin, Ph.D.
Academic Rank:	Associate Professor
University and Department:	University of Houston-Downtown Department of Natural Sciences
NASA/JSC	
Directorate:	Mission Support
Division:	Mission Planning and Development
Branch:	Technical Development and Applications
JSC Colleague:	Robert T. Savely
Date:	August 8, 1986
Contract*:	NGT-44-005-803 (University of Houston)

AN EVALUATION OF TURBO PROLOG WITH AN EMPHASIS ON ITS APPLICATION TO THE DEVELOPMENT OF EXPERT SYSTEMS

Richard B. Loftin, Ph.D.
Associate Professor of Physics
Department of Natural Sciences
University of Houston-Downtown
One Main Street
Houston, TX 77002

Turbo Prolog is a recently-available, compiled version of the programming language Prolog (Programming in Logic), originally developed at the University of Marseilles in the period from 1972 to 1974. Turbo Prolog is designed to provide not only a Prolog compiler, but also a program development environment for the IBM Personal Computer family.

An evaluation of Turbo Prolog was made, comparing its features to other versions of Prolog and to the community of languages commonly used in artificial intelligence (AI) research and development. Three programs were employed to determine the execution speed of Turbo Prolog applied to various problems: (1) a program which computes the factorial of a given integer was used to test the execution speed of Turbo Prolog with a purely computational problem, (2) the "Towers of Hanoi" was used to evaluate the speed of Turbo Prolog in executing a simple but intensely-recursive problem, and (3) the NASA benchmark planning problem (the "monkey and bananas" problem) was used to test the speed of Turbo Prolog with a problem used by NASA in its own evaluation tests[1].

The results of this evaluation demonstrated that Turbo Prolog can perform much better than many commonly-employed AI languages for numerically- intensive problems and can equal the speed of development languages such as OPS5+ and CLIPS, running on the IBM PC family of computers, with the NASA benchmark program. Applications for which Turbo Prolog is best suited include those which (1) lend themselves naturally to backward-chaining approaches (*e.g.*, theorem proving), (2) require extensive use of mathematics, (3) contain few rules, (4) seek to make use of the windowing/color graphics capabilities of the IBM PC, and/or (5) require linkage to programs in other languages (*e.g.*, C, Pascal, FORTRAN, or Assembler) to form a complete executable image.

[1]G.D. Riley, "Timing Tests of Expert System Building Tools" and "Availability of an Expert System Tool", NASA Memos FM7(86-51) and FM7(86-117).

NASA Colleague: Robert T. Savely FM72 X4751

AN EVALUATION OF TURBO PROLOG WITH AN EMPHASIS ON ITS APPLICATION TO THE DEVELOPMENT OF EXPERT SYSTEMS

Richard B. Loftin, Ph.D.
Associate Professor of Physics
Department of Natural Sciences
University of Houston-Downtown
One Main Street
Houston, TX 77002

Introduction

Two of the tasks of the Artificial Intelligence (AI) Section of the Technology Development and Applications Branch, Mission Support Directorate, Johnson Space Center, are (1) the evaluation and development of AI software for building expert systems and (2) the evaluation of AI languages. A recently-available product (May, 1986), Turbo Prolog[1] offers both a new version of an AI language and a programming environment for building expert systems. The goals of the project described in this report were (1) the evaluation of Turbo Prolog as an AI language and (2) the production of benchmark programs, written in Turbo Prolog, which permit Turbo Prolog's execution speed to be directly compared with that of alternatives already evaluated by the AI Section[2].

In order to achieve the first goal, time was devoted to a study of Turbo Prolog in the context of other versions of Prolog and the development of simple programs using this language. Two simple tests of Turbo Prolog's execution speed were made using the computation of factorials and the Towers of Hanoi. The final benchmark program was of the standard type used by the AI Section in evaluating the speed of a number of expert system development tools[3]. The problem is one of proceeding to a prescribed goal by means of subgoals which must be achieved first. Initial conditions are supplied and approximately thirty rules specify the manner in which the subgoals and the final goal may be satisfied. This benchmark has been written and implemented in a variety

of languages on a variety of computers. By comparing the speed with which this benchmark program executes when written in Turbo Prolog with the same benchmark in different programming languages running on the same computer, a measure of Turbo Prolog's efficacy as a language for the development of expert systems can be had.

This report begins by discussing the history of Prolog and continues by presenting the major features of Turbo Prolog, emphasizing those which set it apart from other versions of the language. Finally, the benchmark timing results are presented and come conclusions are drawn regarding the use of Turbo Prolog as a tool in the development of expert systems.

A Brief History of Prolog

The origins of Prolog (Programming in Logic) can be traced back to the 1965 publication of the Resolution Principle by J. A. Robinson[4]. During the early 1970's a number of workers attempted to implement languages that embodied logic[5,6,7,8,9,10]. Kowalski's development of predicate calculus in 1972[11] added a powerful tool to the kits of those seeking to produce languages that were oriented toward theorem proving. It was the collaborative efforts of R. A. Kowalski and Alain Colmerauer during the year Kowalski spent at the University of Marseilles that led to the development of Prolog's specifications[12] in 1972. Colmerauer and his coworkers at Marseilles quickly began to implement these specifications and produced the first interpreters in 1973[13,14]. With the detailed publication of Prolog's specifications in and of its implementation in 1975[15], other university groups began to use the "Marseilles" Prolog and began to develop their own Prolog versions[16,17,18,19,20]. It was the publication of Programming in Prolog by Clocksin and Mellish in 1981[21] that brought some order to the proliferation of dialects of Prolog. By 1984, with the appearance of the second edition of Clocksin and Mellish[22], most users of Prolog were accustomed to a common syntax and grammar for the language.

The announcement by Japan in 1982[23] that Prolog would be the

language for their "fifth-generation" project catapulted Prolog, until that time a predominantly European institution, into international prominence. Until recently most U.S. AI practitioners have eschewed the use of Prolog in favor of Lisp, in large measure due the the availability of powerful development environments for Lisp machines. The advent of Turbo Prolog may well serve to introduce Prolog into the "mainstream" of computing in the U.S. It provides a powerful and inexpensive (<$100) development environment for Prolog utilizing an extremely popular personal computer family--the IBM PC/XT/AT).

Features of Turbo Prolog

Naturally, the feature that sets Turbo Prolog (and, for that matter) all Prologs apart from other AI languages is its backward-chaining nature. Most commonly used expert system development tools are implemented with forward-chaining, although some, like KEE and ART, can employ backward-chaingin also. At first glance Turbo Prolog seems to have embraced the syntax and functionality of the "standard" set by Clocksin and Mellish[22]. Syntactically, this is more "almost" correct. Important differences exist, however, which are pitfalls for the experienced Prolog programmer. One essential difference (from which flows many "subdifferences") is the typed nature of the Turbo Prolog compiler. In this instance Turbo Prolog resembles FORTRAN or Pascal--each domain's type must be declared, either in the "domain" section or in the declaration of a predicate. This single feature sets Turbo Prolog apart from other versions of Prolog and from most other AI languages in general. It is both a weakness and a strength. There is no doubt that much of the speed and error checking power of the compiler is due to domain typing. Experienced AI programmers are not accustomed to a requirement that domains be typed. It is common to have functors, for example, whose arguments may change from integer to real as a result of a clause. In Turbo Prolog this means that each possible argument type must be declared at the time the program is written. Additional "deltas" with other Prolog versions also exist. For example, "=" is not the unification operator of Clocksin and Mellish, rather it is more like the "is" operator; commas do not act as operators; the programmer cannot define his own infix operators; the result of an arithmetic operation depends on

the type(s) of the arguments; operators cannot be passed as functors; and missing are the standard predicates arg, functor, clause, univ, and op. Turbo Prolog unfortunately lacks a virtual database support and database predicates are not executable.

Figure 1 shows the structure of a Turbo Prolog program. The elements that are enclosed in brackets are optional. The program section is used if this program is to linked to others (written in Prolog, C, FORTRAN, Pascal, or Assembler) to form an executable whole. The directives section is used to issue orders to the compiler (for example, invoking the trace facility or declaring the amount of memory to be allocated to the code). The domains section is used to declare the types of all predicate arguments (it may be omitted if there are no compound predicates and the type declaration can be included in the predicate section). Global domains are used for those predicates that will be

PROLOG PROGRAM STRUCTURE

[PROGRAM]

[DIRECTIVES]

DOMAINS

[GLOBAL DOMAINS]

[DATABASE]

PREDICATES

[GLOBAL PREDICATES]

CLAUSES

[GOAL]

FIGURE 1: The Structure of a Turbo Prolog Program

accessed by other programs linked to the present one and the database section is used to identify those predicates that will be changed by "assert" during program execution. The predicate section contains a list of all predicates and their arguments and the global predicate section serves the same function as the global domains section. Clauses are listed in the clause section. Goals may be declared in the program itself. If the goal section is missing, Turbo Prolog prompts the user for a goal in the dialogue window.

In "giving" up some of the familiar features of other Prologs, the user of Turbo Prolog does gain a great deal. Unlike most AI languages, Turbo Prolog contains a complete set of arithmetic and trigonometric operators. In addition, there are about thirty "new" standard predicates that allow the programmer to access the full range of power of the IBM PC family. For example, Turbo Prolog contains a complete set of graphics commands for the PC, including windowing and the ability to mix text and graphics in the same window. Sound and color are both supported as well as input/output via files, devices, or ports. Turbo Prolog allows the programmer to link a prolog program to other programs written in C, FORTRAN, Pascal, or Assembler. The programmer (as well as the user of a developed application) has full access to DOS, BIOS, and the built-in Turbo editor. Perhaps the "nicest" thing provided by Turbo Prolog is a powerful development environment, based on the PC, that is extraordinarily inexpensive compared with those used by most AI programmers. The development environment provides four windows (the user controls the size and foreground/background color of each window): editor, dialogue, trace, and message. A banner menu is provided allowing the user to select editor, run (compiles and runs), compile (allows the user to compile to an object or executable file), options (selects whether the compilation is to an object or executable file), setup (allows the user to configure the windows, define directories, and perform other useful "housekeeping" tasks) and quit (which returns the user to DOS). The editor is a "full-window" editor and uses the commands of Wordstar. The compiler, like that of Turbo Pascal, stops when an error in encountered, returns to the programmer to the editor, and places the cursor at the location of the error. The powerful trace facility allows the user to examine every call and return for the entire program or for selected

clauses. All-in-all, Turbo Prolog is a pleasant way to quickly develop executable code.

Benchmarks

Three benchmarks were chosen to measure the speed of execution of a Turbo Prolog program in performing three very different tasks. To test Turbo Prolog's execution speed with arithmetic operations, a simple program was used to compute the factorial of an integer (Appendix A contains the source code for this program). The program was run on an IBM PC and an IBM PC/AT to compute the factorial of 170 (the result of this computation is near the capacity of the PC). The time required for this computation is shown in Table 1. The Towers of Hanoi problem provides another benchmark program which is intensively recursive and makes large demands on the stack (Appendix B contains the source code for this program). The times required for the execution of this program with different numbers of disks are also included in Table 1.

The final benchmark was chosen to permit the speed of Turbo Prolog to be directly compared to that of other expert system tools in the execution of a rule-based expert system. The problem tackled was a variation of the well-known "monkey and bananas" problem[24]. This particular variation was developed by the AI Section as a means of comparing a large number of expert system development tools[2,3]. The general problem is prototypical of a number of planning problems in which many subgoals must be identified and reached in order for the "main" goal to be achieved.

The monkey and bananas program, as implemented in Turbo Prolog (the source code for the program is contained in Appendix C) consists of 34 "rules" in the form of clauses or subclauses. A total of 22 predicates were used. Table 2 contains the time required for execution of this program on both the IBM PC and IBM PC/AT. The table also contains the accumulated timing tests obtained by the AI Section through the end of July, 1986. It should be noted that there is some ambiguity in determining the execution speed of a Turbo Prolog program. After compilation is complete, but before execution begins, Turbo Prolog

TABLE 1: Execution Times for Two Benchmarks Using Turbo Prolog (See Appendices for Source Code)

Benchmark	Execution Times (s)	
	IBM PC	IBM PC/AT
Factorial of 170	0.27	0.10
Towers of Hanoi		
3 Disks	<0.005	----
10 Disks	0.27	0.10
12 Disks	1.20	0.43
15 Disks	9.55	3.40
16 Disks	----	6.86

checks the program's clauses against the given goal(s). Those clauses which will be called in order to reach the given goal(s) are selected through this "preprocessing". Only after this is accomplished is the goal actually executed. This means that the internal time function can only be accessed after the preprocessing is complete. Since the user is normally concerned with the total "run" time, which includes both preprocessing and execution, it is this run time which is reported. A footnote gives the measured execution times for the program running on both machines tested.

Conclusions

Turbo Prolog may be, in the view of at least one evaluator[25], not so much another version of Prolog, as a new language in itself. Turbo Prolog has proven to be exceptionally easy to begin to use and Borland has "encased" it in an superb development environment. The syntax of the language and its standard predicates depart significantly from the Prolog "standard"; this may pose a barrier to the experienced Prolog programmer,

Table 2: Timing Tests of Expert System Tools for the NASA "Monkey and Bananas" Benchmark*

TOOL(VERSION)	MACHINE	TIME(S)
ART(V2.0)	SYMBOLICS	1.2
ART(V2.0)	TI EXPLORER	2.4
ART(V2.0 BETA)	LMI	3.0
ART**	SYMBOLICS	7.6
ART(V BETA 3)	VAX	17
CLIPS(V3.0)	SUN	1.2
CLIPS(V3.0)	VAX	2.5
CLIPS(V3.0)	HP9000	4.0
CLIPS(V3.0)	IBM PC/AT	7.0
CLIPS(V3.0)	IBM PC	21.1
ExperOPS5(V1.04)	MACINTOSH	55
KEE(V2.1.66)**	SYMBOLICS	17.8
KEE(V2.2.66)	SYMBOLICS	165
OPS5(VAX V2.0)	VAX	1.3
OPS5(FORGYVPS2)	SYMBOLICS	1.7
OPS5+(V2.0003)	IBM PC/AT	5.2
OPS5+(V2.0002)	MACINTOSH	14
OPS5+(V2.0002)	IBM PC	19
OPS83	VAX	0.46
OPS83	IBM PC/AT	1.1
OPS83	IBM PC	3.3
TURBO PROLOG	IBM PC/AT	6.73***
TURBO PROLOG	IBM PC	20.43***

*SOURCES (EXCEPT TURBO PROLOG): NASA MEMOS FM7(86-51) AND FM7(86-117)

**IMPLEMENTED USING BACKWARD-CHAINING RULES

***"RUN TIME", EXECUTION TIMES are 0.21S AND 0.65 FOR PC/AT AND PC

but others (especially fans of Turbo Pascal) will appreciate the "unique" features of Turbo Prolog. Those predicates which are missing from Turbo Prolog are either seldom used or their function can be achieved in other ways. The superb programming environment (convenient editor, powerful trace facility, compiler, built-in mathematical functions, and access to IBM PC features such as graphics, windows, color, sound, and I/O through ports or files) coupled with its inexpensive cost makes Turbo Prolog an attractive tool for those who have not tackled an AI language before. For those developing expert systems, Turbo Prolog may prove to be well-suited for fast prototyping of "small" rule bases or for those applications that lend themselves to backward-chaining approaches (for example, theorem proving). Surprisingly, Turbo Prolog executes the NASA benchmark as fast as popular expert system development tools like OPS5+ or NASA's own CLIPS.

Appendices

The appendices mentioned in the body of this paper are not included with the published report due to their length. Copies of these appendices may be obtained directly from the author or from his NASA/JSC colleague, Robert T. Savely (NASA/Johnson Space Center, Mail Code FM72, Houston, TX 77058).

REFERENCES

1. Turbo Prolog is a product of Borland International, Inc., 4585 Scotts Valley Drive, Scotts Valley, CA 95066.

2. Gary D. Riley, "Timing Tests of Expert System Building Tools," NASA/ Johnson Space Center, Memo FM7(86-51); Robert T. Savely, "Availability of an Expert System Tool," NASA/Johnson Space Center, Memo FM7 (86-117).

3. Gary D. Riley, "Benchmarking Expert System Tools," in Proceedings of Robex '86 (The Second Annual Workshop on Robotics and Expert Systems), held at NASA/Johnson Space Center, 4-6 June 1986, p. 61.

4. J. A. Robinson, "A Machine-Oriented Logic Based on the Resolution Principle," J. ACM 12(1), 23(1965).

5. G. Sussman and D. V. McDermott, "MICRO-PLANNER Reference Manual," AI Memo 203, AI Laboratory, MIT, 1970.

6. R. M. Burstall, J. S. Collins, and R. J. Popplestone, Programming in POP-2, Edinburgh: Edinburgh University Press, 1971.

7. C. Hewitt, "Description and Theoretical Analysis (using schemata) of PLANNER, a Language for Proving Theorems and Manipulating Models in a Robot," Report No. TR-258, AI Laboratory, MIT, 1972.

8. D. J. M. Davies, "POPLER: A POP-2 Planner," Rep. No. MIP-89, School of AI, University of Edinburgh, 1972.

9. G. Sussman and D. V. McDermott, "CONNIVER Reference Manual," Memo 259, AI Laboratory, MIT, 1972.

10. D. Davies, et. al., POPLER 1.5 Reference Manual, Edinburgh: University of Edinburgh, 1973.

11. R. A. Kowalski, "The Predicate Calculus as a Programming Language," in Proceedings of the International Symposium and Summer School on Mathematical Foundations of Computer Science, held at Jabłonna, Poland, 1972.

12. A. Colmerauer, H. Kanoui, P. Roussel, and R. Pasero, "Un Système de Communication Homme-Machine en Français", Rapport preliminaire, Groupe d'Intelligence Artificielle, Université d'Aix-Marseille, 1972.

13. G. Battani and H. Meloni, "Interpréteur du langage de programmation PROLOG," Group d'Intelligence Artificielle, Université d'Aix-Marseille, 1973.

14. A. Colmerauer, H. Kanoui, P. Roussel, and R. Pasero, "Un système de Communication Homme-Machine en Français," Rapport de Rechereche sur le contrat CRI no 72-18 de février 72 a juin 73, Groue d'Intelligence Artificielle, Université d'Aix-Marseille, 1973.

15. P. Roussel, PROLOG, Manuel de Référence et d'Utilisation, Université d'Aix-Marseille: Groupe d'Intelligence Artificielle, 1975.

16. D. H. D. Warren, "Implementing Prolog--Compiling Predicate Logic Programs," DAI Report Nos. 39 and 40, Edinburgh, 1977.

17. D. H. D. Warren, L. M. Pereira, and F. C. N. Pereira, "Prolog--the Language and Its Implementation Compared with Lisp," presented at the ACM Symposium on Artificial Intelligence and Programming Languages, Rochester, New York, SIGART Newsletter No. 64, SIGPLAN Notices 12(8), 109 (1977).

18. J. Bendl, P. Köves, and P. Szeredi, "The MPROLOG System," in Tärnlund 1980, 201 (1980).

19. F. G. McCabe, Micro PROLOG Programmer's Reference Manual, London: Logic Programming Associates Ltd., 1981.

20. F. Kluźniak and S. Szpakowicz, Prolog, Warsaw: Wydawnictwa Naukowo-Techniczne, 1983.

21. W. F. Clocksin and C. S. Mellish, Programming in Prolog, Berlin: Springer-Verlag, 1981.

22. W. F. Clocksin and C. S. Mellish, Programming in Prolog, Second Edition, Berlin: Springer-Verlag, 1984.

23. "Outline of Research and Development Plans for Fifth Generation Computer Systems," Institute for New Generation Computer Technology (ICOT), Tokyo, May, 1982.

24. L. Brownston, R. Farrell, E. Kant, and N. Martin, Programming Expert Systems in OPS5, Reading, MA: Addison-Wesley Publishing Co., 1985.

25. D. Rubin, "Turbo PROLOG: A PROLOG Compiler for the PC Programmer," AI Expert, Premier Issue, 87 (1986).

1986

NASA/ASEE SUMMER FACULTY RESEARCH FELLOWSHIP PROGRAM

JOHNSON SPACE CENTER

UNIVERSITY OF HOUSTON

TRANSVERSE DIFFUSION OF ELECTRONS IN A MAGNETOPLASMA

Prepared by:	Bernard McIntyre
Academic Rank:	Associate Professor
University & Department:	University of Houston
	Department of Electronics
NASA/JSC	
Directorate:	Space and Life Sciences
Division:	Solar System Exploration
Branch:	Space Sciences
JSC Colleague:	Andrei Konradi
Date:	August 8, 1986
Contract #:	NGT 44-005-803

N87-25894

ABSTRACT

Plasma density and temperature profiles were measured for plasma electrons which were generated by a plasma source and ionization from a 1 kev electron beam. Electron plasma parameters were measured with a cylindrical Langmuir probe which was moved perpendicular to the axis of the beam and field.

Electron densities decreased exponentially from the beam center and the decay constant varied with magnetic field in accordance with the Bohm theory of cross field diffusion. This enhanced diffusion effect due to instabilities generated by the electron beam is orders of magnitude larger than that due to particle collisions.

INTRODUCTION

When a large magnetic field is applied to a group of electrons the electron motion along the field is not effected but the motion trasnsverse to the field is constrained to circular motion about the magnetic field lines. This constraint limits the transverse conductivity of a plasma. The electrons and ions both orbit about the field lines, but the ion radii are much larger because of their larger mass. The ions in a plasma then are not as easily magnetized as the electrons and their transverse conductivity is less effected by the magnetic field.

The usual way in which electrons diffuse across the field lines is through collisions. As the electrons orbit about the field they eventually collide with other particles and undergo a random walk type of trajectory. This is not a very efficient process because of the relatively large mean free paths for the electrons. A much more efficient way to

enhance the transverse diffusion of electrons is to have them interact with plasma waves. Bohm [1] showed that plasma instabilities can have high frequency plasma oscillations associated with them which interact strongly with the plasma electrons. This interaction enhances the transverse electron diffusion by orders of magnitude over that due to collisions alone. Bohm also postulated that the form of the diffusion coeficient due to plasma oscillations (called the Bohm diffusion coeficient) should vary with magnetic field as 1/B. The collision dominated diffusion coefficient on the other hand varies as $1/B^2$, and so, in principle, the two diffusion mechanisms can be differentiated by varying the magnetic field.

The approach taken in this project was to inject an electron beam into a plasma parallel to a magnetic field. The electron beam tends to interact with the plasma and generate plasma oscillations which in turn enhance the transverse diffusion. According to Szuszczewicz [2] , the

plasma density should decrease exponentially from the beam center and the decay constant should vary as the inverse square root of the diffusion coefficient. By measuring the plasma density transverse to the beam for two different values of magnetic field, the field variation of the diffusion coefficient can be found. For Bohm diffusion the exponential decay constant varies directly as the square root of the field while for collision dominated diffusion it varies with the first power of field.

EXPERIMENTAL CONFIGURATION

A 3′ by 8′ vacuum chamber was configured with an electron gun on one end and a plasma source on the other. Both were aligned to produce beams centered on the axis of the chamber. The plasma source utilized argon gas and resulted in a chamber pressure of 0.2 millitorr. A hot

filament in the source emited electrons which were accelerated and ionized the argon atoms. Equal numbers of electrons and ions were extracted through an exit grid so as to produce a plasma density in the chamber the order of 10^7 /cc. The electron gun was operated at 1 kev energy and 3-5 ma of current, well below the threshold for initiating any beam plasma discharge. A set of magnetic coils provided an axial magnetic field of 19 and 38 gauss. A cylindrical Langmuir probe was moved in one half inch intervals across the beam region. The function of the probe was to measure the plasma electron density and temperature. The electron density measurements were ploted on semilog graph paper and are shown in figure 1.

DISCUSSION

As seen from figure 1, the density profile can be used to identify the center region of the electron beam. The

ionization produced by the electron beam falls off exponentially from the center region and far from the beam, the background plasma density falls off nearly linearly to the chamber walls. For both values of the magnetic field used the background plasma density from the plasma source was nearly equal. The electron density data shows that as the field increased to 38 gauss the electron current to the probe was decreased. The ion current to the probe was the same for both magnetic field values so this decrease in electron density is a real effect due to the magnetic field constraining electron collection. The data also illustrates the effect of a larger magnetic field in compressing the electron beam diameter. Although the raw probe data is not shown here, the probe characteristic curves indicated that electron current exhibited strong saturation effects far from the central beam region, while near the beam region they did not. The likely explaination for this behavior is that strong plasma oscillations in the central region result

in Bohm diffusion and a large transverse conductivity to the probe. Outside this region the plasma oscillations are absent or of a low amplitude and the transverse conductivity to the probe is dominated by collisions and is much smaller and the electron current saturates.The slope of the density data in figure 1 increases by a factor of 1.5 as the magnetic field doubled. This implies that the slope varies as the square root of the field, the diffusion coefficient varies as the inverse of the field and Bohm diffusion dominates the transverse motion of the electrons.

REFERENCES

1. Bohm, D.,E.H.S.Burhop, H.S.W.Massey and R.M.Williams,Characteristics of Electrical Discharges in Magnetic Fields, edited by Guthrie and Wakerling, McGraw-Hill, N.Y.,1949

2. Szuszczewicz, E.P., D.N.Walker, and J.C.Holmes "Plasma Diffusion in a Space Simulation Beam Plasma Discharge",Geophysics Research Letters, 6,201,1979

FIGURE CAPTION

FIGURE 1: Semilog plot of electron plasma density vs relative position of the Langmuir probe for two values of magnetic field.

FIGURE 1

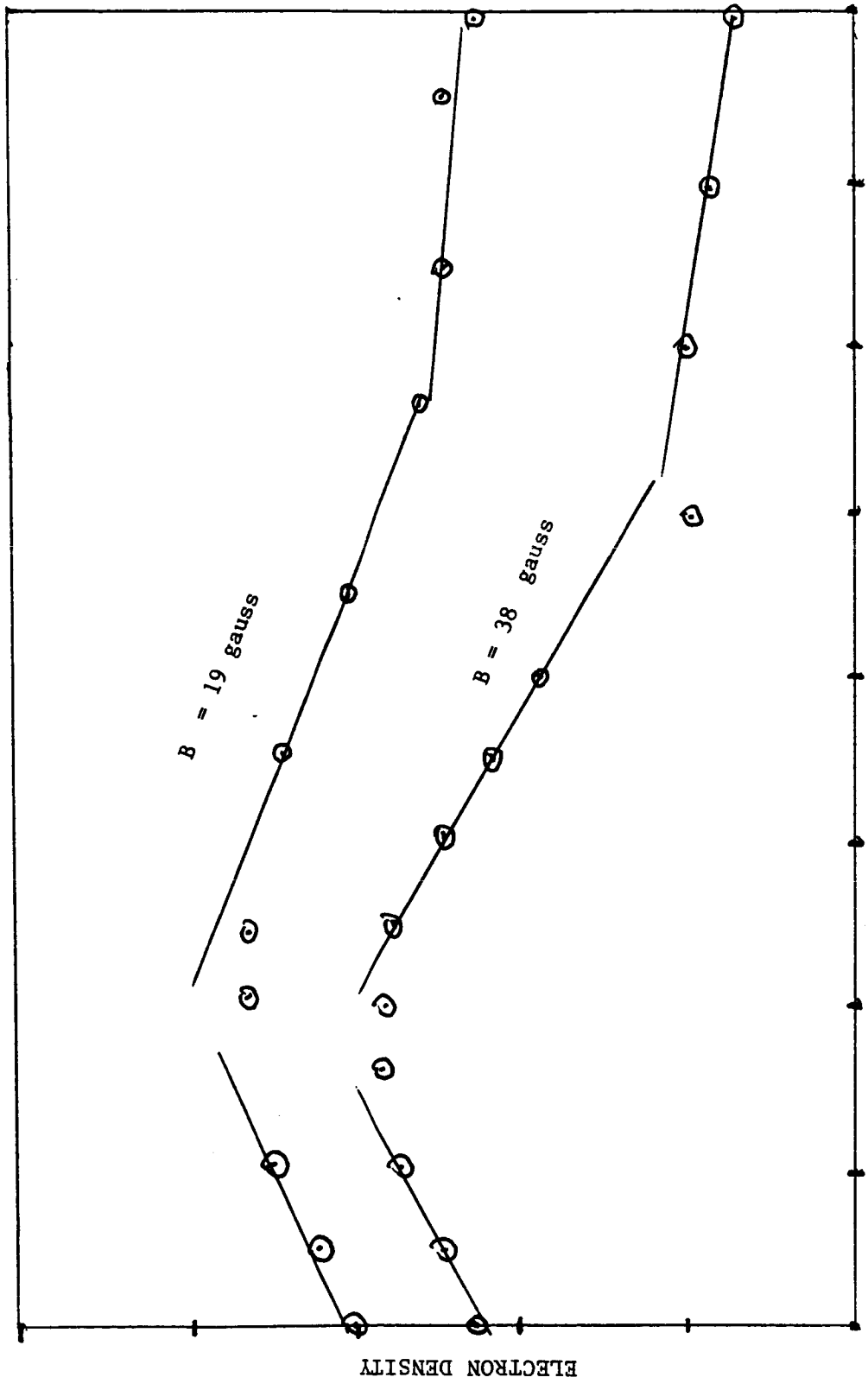

1986

NASA/ASEE Summer Faculty Research Fellowhip Program
Johnson Space Center
and
University of Houston

"HIGH TEMPERATURE ELECTROLYZER/FUEL CELL POWER CYCLE: PRELIMINARY DESIGN CONSIDERATIONS"

Prepared by:	Jeffrey H. Morehouse
Academic Rank:	Associate Professor
University & Department:	University of South Carolina Mechanical Engineering Department
NASA/JSC	
Directorate:	Engineering
Division:	Propulsion and Power
Branch:	Power
JSC Colleague:	Thomas L. Davies
Date:	August 8, 1986
Contract #:	NGT-44-005-803

HIGH TEMPERATURE ELECTROLYZER/FUEL CELL POWER CYCLE: PRELIMINARY DESIGN CONSIDERATIONS

Jeffrey H. Morehouse
Associate Professor
Mechanical Engineering Department
University of South Carolina
Columbia, SC 29208

A model of a high temperature electrolyzer/fuel cell, hydrogen/oxygen, thermally regenerative power cycle is developed and used to simulate system performance for varying system parameters. Initial estimates of system efficiency, weight, and volume are provided for a one KWe module assuming specific electrolyzer and fuel cell characteristics, both current and future. Specific interest is placed on examining the system responses to changes in device voltage versus current density operating curves, and the associated optimum operating ranges.

The performance of a solar-powered, space-based system in low earth orbit is examined in terms of the light-dark periods requiring storage. The storage design tradeoffs between thermal energy, electrical energy, and hydrogen/oxygen mass storage are examined. The current technology module is based on the 1000°C solid oxide electrolyzer cell and the alkaline fuel cell. The "Future Technology" system examines benefits involved with developing a 1800K electrolyzer operating with an advanced fuel cell.

NASA Colleague: Thomas L. Davies EP5 X3133

TABLE OF CONTENTS

INTRODUCTION

The renewed interest in space-based activities, both NASA-related and "Star Wars" related, has led to the examination of numerous types of power systems which might be appropriate for space applications [Refs. 1,2]. The energy source for these power systems is envisioned as being either nuclear or solar energy. Both sources supply thermally-driven dynamic systems, with solar able to use photovoltaic systems to directly produce electricity.

The possibility of thermally-driving a fuel cell power system is attractive from several engineering aspects, as it combines some of the better features of both photovoltaic (PV) and dynamic systems. Like the PV system, a fuel cell power cycle can produce electricity without the rotating motor-generator mechanical components. Moreover, the fuel cell power cycle is capable of higher efficiencies than PV systems; much closer to the higher dynamic system thermal efficiencies. As the fuel cell cycle is thermally-driven, it can operate during a complete light-dark orbit using stored thermal energy, similar to the dynamic system operating concept. A hydrogen-oxygen fuel cell is proposed because of high efficiency and because using water as the working fluid with space missions has several inherent advantages, including crew compatibility (non-toxic, life supporting) and possible use as a reaction fuel.

HIGH TEMPERATURE ELECTROLYZER/FUEL CELL CYCLE CONCEPT

The development of the basic relations for the high temperature electrolysis/fuel cell system is based on the water dissociation energy reaction:

$$H_2 + 1/2O_2 \rightleftharpoons H_2O \qquad (1)$$

The dissociation energy or energy of reaction (ΔH_f) is a mild function of reaction temperature, as seen in Figure 1. For an isothermal reaction, this ΔH_f can be thought of as "ideally" consisting of two parts or types of energy input (or output, depending on the direction of reaction):

$$\Delta H_f = \Delta G_f + T^\circ \Delta S_f \qquad (2)$$

where,

ΔG_f is the Gibb's free energy, the available work (ideal work)

$T^\circ \Delta S_f$ is the isothermal heat transfer (ideal heat transfer)

As is seen in Figure 1, the ideal heat and work in the water reaction are strong functions of the reaction temperature. This property of the water reaction is what permits operation of a thermally regenerative fuel cell cycle. At high temperatures, a small amount of work is available from the hydrogen-oxygen association reaction.

The High Temperature Electrolyzer/Fuel Cell (HTE) system consists of an electrolyzer operating at high temperature, T_H, a regenerative heat exchanger, and a fuel cell operating at low temperature, T_C. The electrolyzer is run

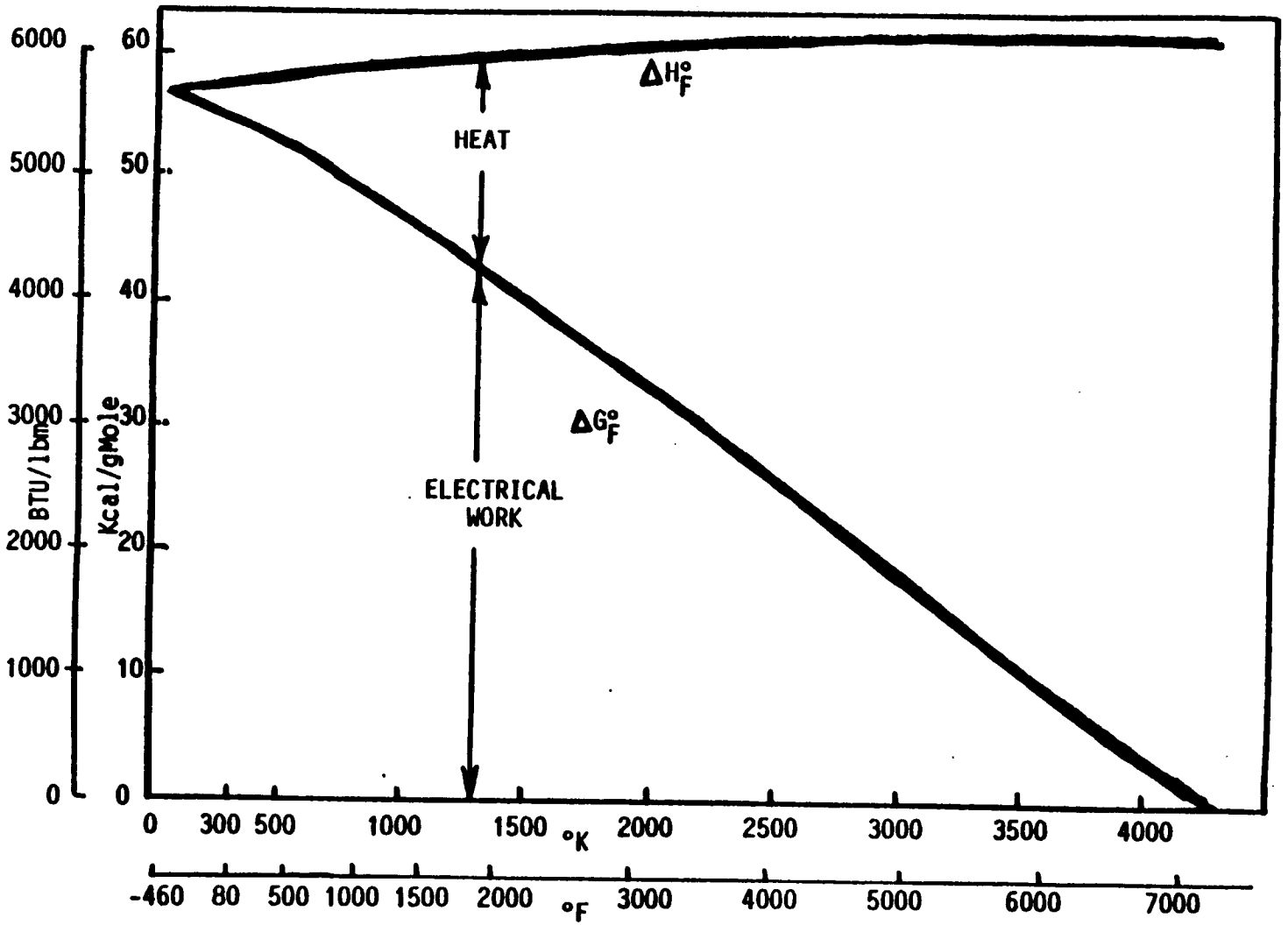

Figure 1. DISSOCIATION ENERGY (ΔH_F°) AND GIBB'S FREE (ΔG_F°) ENERGY AS A FUNCTION OF TEMPERATURE FOR WATER

from the electrical output of the fuel cell, plus a high temperature heat input. The cycle net work output consists of the fuel cell's electrical work which exceeds the electrolyzer requirements; this net work is graphically illustrated as the difference between ΔG's at two temperatures on Figure 1. The basic HTE heat engine schematic is shown in Figure 2 with heat input at high temperature where water is electrolyzed into hydrogen and oxygen, a regenerative heat exchange between the water and hydrogen-oxygen, and a fuel cell producing electrical energy while rejecting heat.

HTE CYCLE INVESTIGATIONS

The HTE power cycle was described thermodynamically as early as 1959 [Refs. 3,4,5]. These early analyses dealt with the cycle conceptually and defined ideal cycle efficiency and its relation to Carnot efficiency. While work on high temperature electrolyzers has continued to be of interest, the primary thrust has been directed towards producing hydrogen as a fuel [Refs. 6,7]. However, the energy situation in the 70's did stimulate interest in solar energy and thus, in thermally regenerative electrochemical systems [Ref. 8]. Those studies which did examine HTE cycles concluded that these cycles were not of practical interest since no high temperature electrolyzer existed [Refs. 8,9]. More recently, it has been suggested that the high temperature electrolyzers under development may be appropriate for the HTE cycle [Refs. 10, 11].

The present approach to development of high temperature electrolyzers and fuel cells involves the use of a solid oxide electrolyte (SOE). In the USA, the Department of Energy sponsors much of the solid oxide fuel cell development work [Refs. 12-15], while the German emphasis is on a SOE nicknamed "Hot

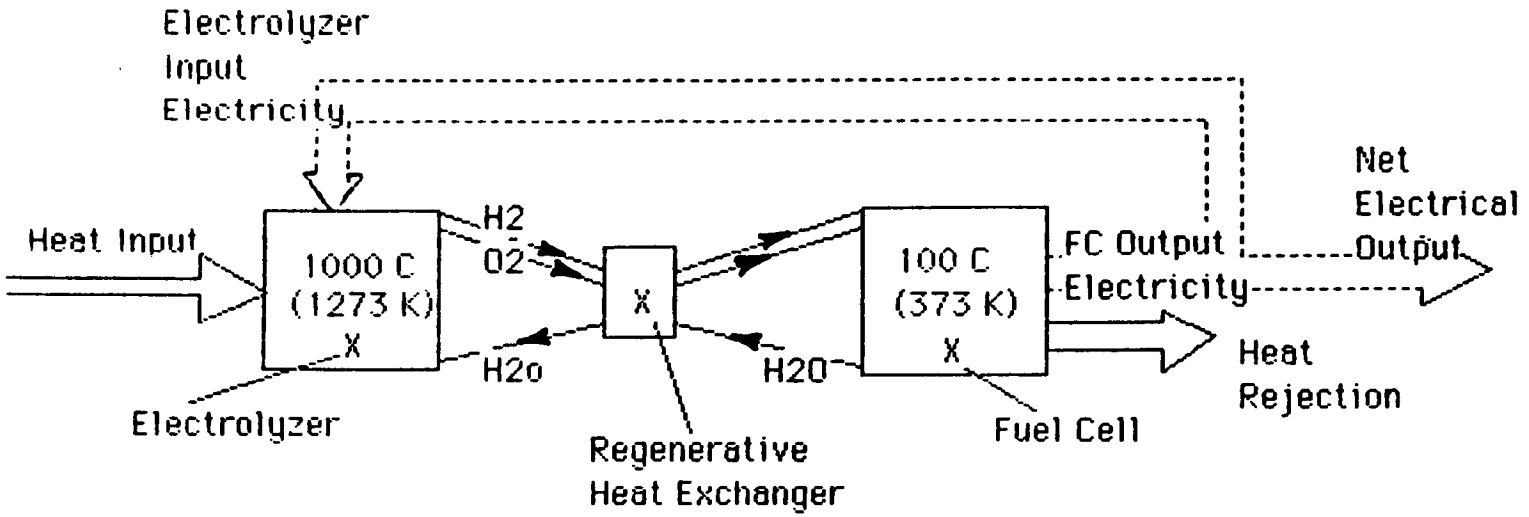

Figure 2. SCHEMATIC OF THERMALLY-DRIVEN REGENERATIVE FUEL CELL HEAT ENGINE

Elly" [Refs. 16,17]. The solid oxide cell being developed has a 30-micron thick solid electrolyte consisting of a Yttria-stablized Zirconia. Currently, the cell stacks are being tested in the 1300°K range. Single cells have been tested for hundreds of hours without degradation and with near-theoretical open-circuit voltage.

DESCRIPTION OF WORK

The objective of this work is to examine the high temperature electrolyzer/fuel cell power cycle for preliminary design and sizing considerations. The examination includes looking at both individual devices and the overall system characteristics and performance.

Scope of Work

A model of the HTE cycle is developed and used to simulate system performance for varying system parameters. Initial estimates of system efficiency, weight, and volume are provided for a 1 KWe module assuming specific electrolyzer and fuel cell characteristics, both current and future. Specific interest is placed on examining the system responses to changes in device voltage versus current density operating curves, and the associated optimum operating ranges. "Current Technology" is based on the 1000°C solid oxide electrolyzer cell and the alkaline fuel cell. The "Future Technology" system examines benefits involved with developing a 1800K electrolyzer operating with an advanced fuel cell.

The performance of a solar-powered, space-based system in low earth orbit is examined in terms of the light-dark periods requiring storage. The storage design tradeoffs between thermal energy, electrical energy, and hydrogen/oxygen mass storage are examined.

A computer program was developed to simulate the HTE cycle. The basic equations and definitions used with the cycle and each device have been previously described [Refs. 10, 11]. Figure 3 illustrates the logic used in the program to simulate the HTE cycle.

Figure 3.

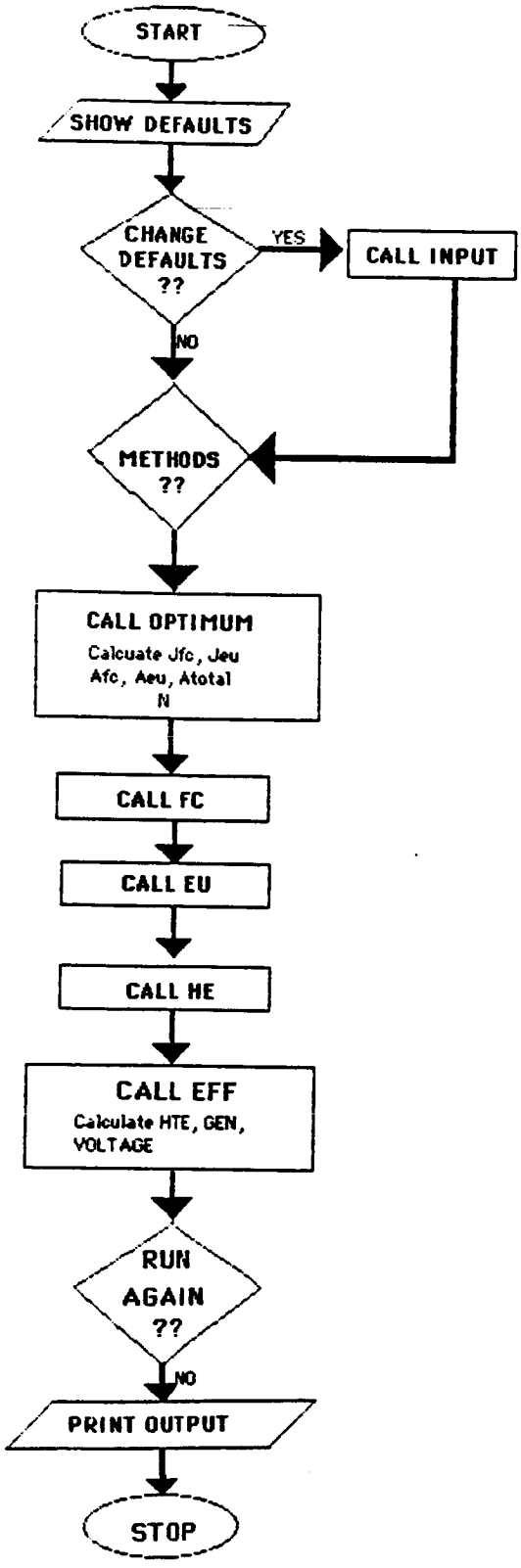
START
SHOW DEFAULTS
CHANGE DEFAULTS ??
YES
CALL INPUT
NO
METHODS ??
CALL OPTIMUM
Calcuate Jfc, Jeu
Afc, Aeu, Atotal
N
CALL FC
CALL EU
CALL HE
CALL EFF
Calculate HTE, GEN, VOLTAGE
RUN AGAIN ??
NO
PRINT OUTPUT
STOP

Current and Future Technology

The description of the fuel cell and electrolyzer devices was in terms of performance and physical measurements. For the computer model, the device cell performance was indicated by the polarization curve (voltage versus current density), plus the cell current efficiency. The physical measurements (volume, mass) of the devices were examined on a unit cell-area basis.

1. Polarization Curves

The polarization curves of cell voltage versus current density are presented in Figure 4 for both the current and future technology fuel cells and electrolyzers. The current technology fuel cell (alkaline) polarization curve was taken from an alkaline cell developed for NASA [Ref. 18]. The future fuel cell is a projection of what an acid (SPE-type) cell would exhibit with greatly reduced electrode-electrolyte resistance and concentration effects. These polarization relations (linearized) are (with V in volts, J in ma/cm^2):

$$\text{Future FC:} \quad V = 1.16 - 0.000667J$$

$$\text{Current FC:} \quad V = 1.14 - 0.0045J \quad (0 < J \leq 20)$$

$$V = 1.05 - 0.00275J \quad (20 < J \leq 40)$$

$$V = 0.995 - 0.0006J \quad (40 < J)$$

The current technology electrolyzer cell polarization curve was taken from data on the solid oxide electrolyte (SOE) under development [Ref. 19]. The projected technology 1500K and 1800K SOE cell curves are based on similar internal resistances and equivalent approach to ideal open circuit voltage.

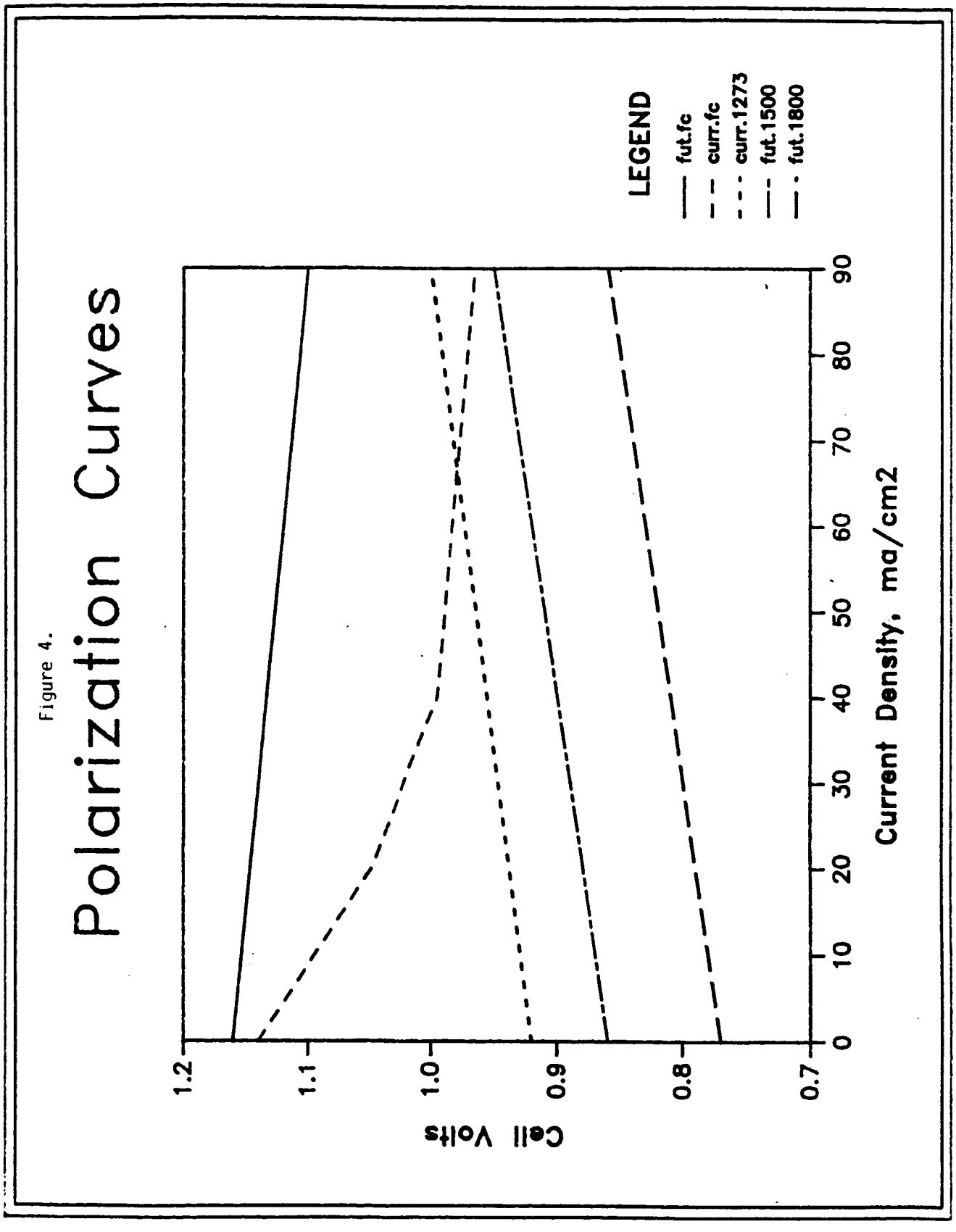
Polarization Curves
LEGEND
fut.fc
curr.fc
curr.1273
fut.1500
fut.1800
Cell Volts
1.2
1.1
1.0
0.9
0.8
0.7
0
10
20
30
40
50
60
70
80
90
Current Density, ma/cm2

Figure 4.

The equations for these electrolyzer cells are:

Current SOE (1273K): $V = 0.92 + 0.000889J$

Future SOE (1500K): $V = 0.86 + 0.001J$

Future SOE (1800K): $V = 0.77 + 0.001J$

2. Physical Measurements

The values for the current and future technology fuel cell and electrolyzer volume and mass per unit cell-area presented in Table 1. The values for the current technology fuel cell and electrolyzer are taken from developmental work on the NASA Space Station project [Ref. 20]. The future technology values are for SPE-type fuel cells and SOE electrolyzer cells.

TABLE 1 . MASS AND VOLUME VALUES

CURRENT TECHNOLOGY	MASS (kg/m2 of cell area)	VOLUME (m3/m2 of cell area)
o Fuel Cell		
-Alkaline	8.1	0.014
-Acid	2	0.01
o Electrolyzer		
-Alkaline	16.6	0.02
-Solid Oxide (1000 C)	26.2	0.013
FUTURE TECHNOLOGY		
o Fuel Cell	2	0.01
o Electrolyzer		
-Solid Oxide (1500 K)	6.5	0.01
-Solid Oxide (1800 K)	6.5	0.01

STORAGE OPTIONS

In solar powered systems, energy storage is necessary for operation during sunless periods. For a solar system in a 270 nautical mile high equatorial orbit, the 95 minute orbital period would consist of 59 minutes of sun (TS) and 36 minutes of dark (TD). Thus, the HTE cycle has to collect enough energy during the sun period both to operate the system and to charge the storage system.

Three storage options are examined for their effect on overall system efficiency and design:

1) Thermal storage - collected high temperature thermal energy is stored before it is input to the HTE cycle;
2) Chemical storage - H2 and O2 are stored within the HTE cycle; and
3) Electrical storage - electrical energy output from the HTE cycle is stored prior to delivery.

These three options are shown schematically as located in the overall system in Figure 5.

For purposes of comparing these three storage options, the following assumptions are made concerning the HTE cycle and overall system conditions:

- Output - 25 kWe continuously delivered to the load during sun and dark periods.
- Input - 1354 w/m^2 solar flux with a 70 percent collection efficiency provides the collected thermal energy input.
- HTE cycle - Electrolyzer at 1273K and the fuel cell at 373K, with actual cycle efficiency of 33 percent (= 1/2 of ideal efficiency).

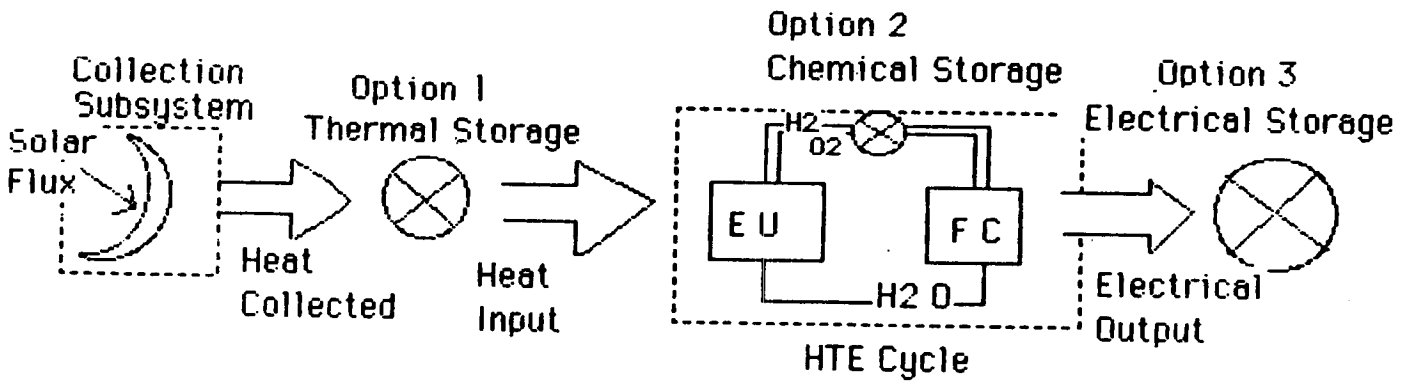
Collection
Subsystem
Solar
Flux
Heat
Collected
Option 1
Thermal Storage
Heat
Input
Option 2
Chemical Storage
H2
02
E U
F C
H2 O
HTE Cycle
Option 3
Electrical Storage
Electrical
Output

Figure 5.

System Efficiencies

The overall system efficiency is based on the ratio of the electrical energy delivered to the solar energy input:

$$\eta_{os} = \frac{\text{Electrical Energy Delivered}}{\text{Solar Energy Intercepted}}$$

The overall system is assumed to consist of three subsystems and their associated efficiencies: collection, HTE cycle, and storage subsystems. The overall system efficiency can be expressed in terms of the three subsystem efficiencies as:

$$\eta_{os} = \eta_{coll} \cdot \eta_{stor} \cdot \eta_{cyc}$$

Since for all storage options the collection subsystem is unchanged, it is convenient to write

$$\eta_{sys} = \eta_{stor} \cdot \eta_{cyc} = \frac{\text{Electrical Energy Delivered}}{\text{Thermal Energy Collected}}$$

where, $\eta_{stor} = \frac{\text{Energy From Storage}}{\text{Energy Input to Storage}}$

$$\eta_{cyc} = \frac{\text{Electrical Output}}{\text{Thermal Input}}$$

The power delivered (Pdel) is required both during sun and dark (TS+TD), while the solar energy collected must be done during sun (TS). So,

$$\eta_{sys} = \frac{\text{Energy Delivered}}{\text{Energy Collected}} = \frac{Pdel \cdot (TS + TD)}{Pcol \cdot TS}$$

where Pcol is the rate of energy collection.

It is also seen that the thermal energy collected can be thought of as

being used in two ways:

$$\text{Energy Collected} = \text{Energy used directly} + \text{Energy stored}$$

The energy used directly will provide power during the sun period and will only involve the HTE cycle:

$$P_{del} \cdot TS = \eta_{cyc} \cdot (\text{Energy Used Directly}).$$

The energy stored will provide power during the dark period and will involve both storage and HTE cycle subsystems:

$$P_{del} \cdot TD = \eta_{stor}\eta_{cyc} \cdot (\text{Energy Stored})$$

So, substituting yields:

$$P_{col} \cdot TS = \frac{P_{del} \cdot TS}{\eta_{cyc}} + \frac{P_{del} \cdot TD}{\eta_{stor}\eta_{cyc}}$$

and $$\frac{P_{col}}{P_{del}} = \frac{1}{TS}\left(\frac{TS}{\eta_{cyc}} + \frac{TD}{\eta_{stor}\eta_{cyc}}\right)$$

which can be substituted back into the η_{sys} equation to give the general expression to be used for the storage-system efficiency relationship:

$$\eta_{sys} = \eta_{\frac{cyc \cdot (TS+TD)}{TS + \frac{TD}{\eta_{stor}}}} \qquad (3)$$

In the sections below, each of the three storage options is examined for efficiency and subsystem sizing effects.

1. Thermal Storage

The thermal storage option consists of placing the thermal storage between the collection and HTE cycle subsystems, as shown in Figure 6. During sun periods, the HTE cycle is driven directly from the energy collected to produce 25 kWe. During dark periods, the HTE cycle is driven from storage to produce 25 kWe. Thus, the HTE cycle should be sized to produce 25 kWe.

The system efficiency from Eq. 3, with thermal storage being 90 percent efficient, is 31.7 percent. This gives an overall system efficiency of 22.2 percent with a required collector area of 133.9 m^2.

While operating at 1300K, the thermal storage unit must be sized to accept 50.5 kWHR of thermal energy input at a rate of 51.4 kW. The unit must also discharge 45.5 kWHR of thermal energy at 75.8 kW.

2. Electrical Storage

The electrical storage configuration is shown in Figure 7, with the storage located between the HTE cycle and the electrical load. The HTE cycle operates only during the sun period, and must supply both the load and the energy to charge the electrical storage during this period. The energy which must be delivered by the HTE cycle is given by:

$$\text{HTE Energy Delivered} = \text{Pdel} \cdot \text{TS} + \frac{\text{Pdel} \cdot \text{TD}}{\eta_{\text{stor}}}$$

And since this energy must be delivered during sun, TS, then the HTE cycle must be sized to produce power at:

$$\text{HTE Power} = \frac{\text{HTE Energy Delivered}}{\text{TS}} = \text{Pdel}\left(1 + \frac{\text{TD}}{\text{TS} \cdot \eta_{\text{stor}}}\right)$$

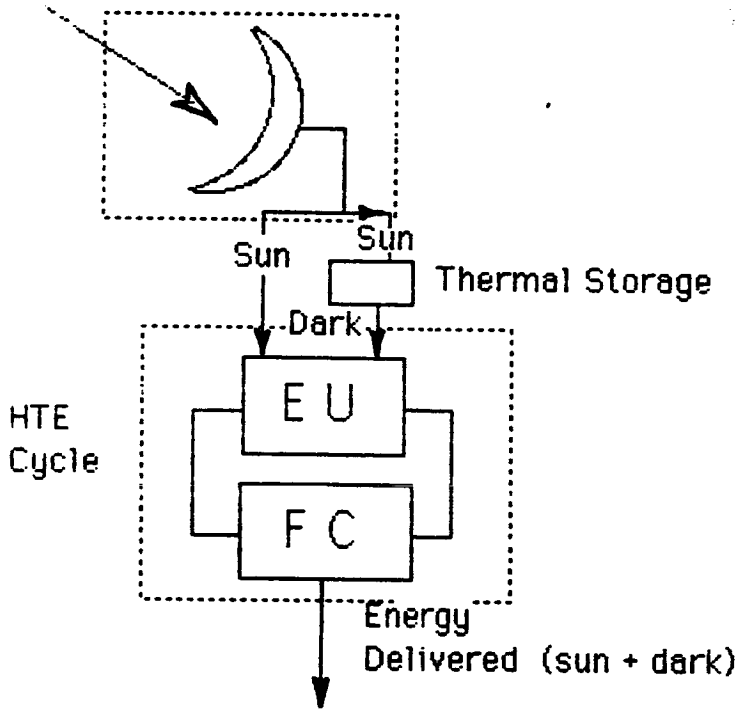
Sun
Sun
Thermal Storage
Dark
HTE
Cycle
E U
F C
Energy
Delivered (sun + dark)

Figure 6.

ELECTRICAL STORAGE OPTION

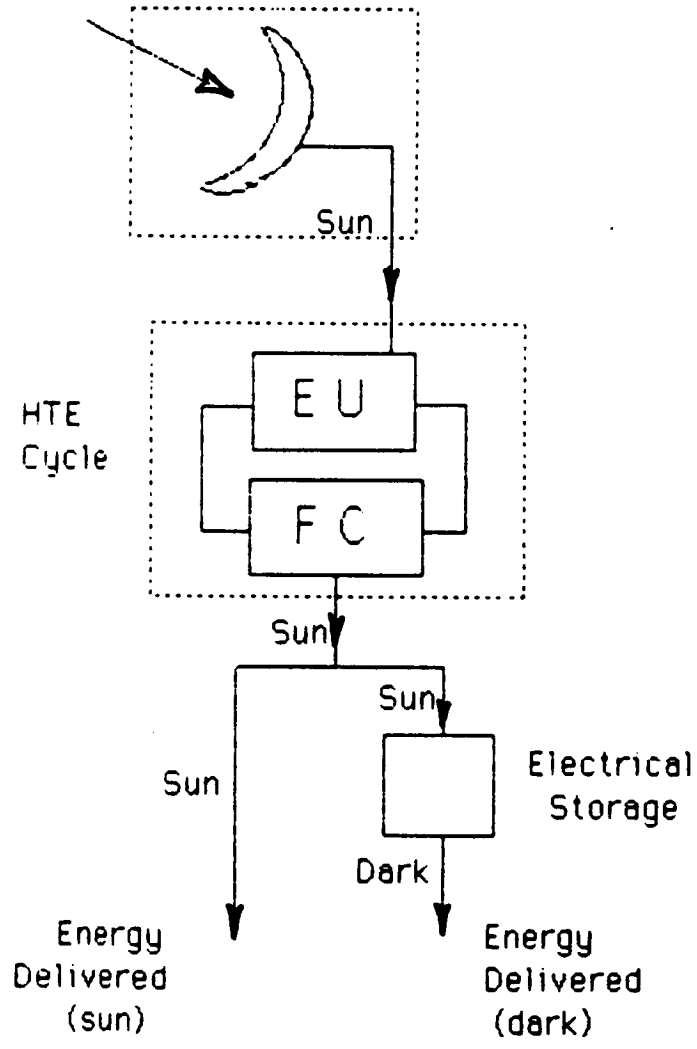

Figure 7.

Thus, even with 100 percent efficient electrical storage, the HTE cycle would have to be sized to produce 40.3 kWe.

Assuming 80 percent electrical energy storage efficiency, the HTE cycle is sized at 44.1 kWe, while the system efficiency (from Eq. 3) is 30.1 percent. The overall system efficiency is 21.1 percent and the needed collector area is $140.9 m^2$.

The input to the electrical storage system at 80 percent storage efficiency is 18.8 kWHR in order to provide the required 25 kWe dark period output. Since storage charging is done during the sun period, the rate of charging is 19.1 kWe.

3. Chemical Storage

The chemical storage concept involves operating the HTE cycle during the sun period to produce enough excess H_2 and O_2 to run the fuel cell during the dark period. Figure 8 presents the H_2 and O_2 storage configuration which illustrates the sun and dark period mass flow paths. The electrolyzer must produce at a rate (TD+TS)/TS greater than when operating continuously, so the HTE cycle devices must be sized at 1.61 times larger than the 25 kWe continuously operating cycle. Thus, a 40.3 kWe sized HTE cycle is required.

Assuming a fuel cell voltage efficiency of 95 percent, 4.6 kg of H_2O (or 0.5 kg Hz and 4.1 kg of O_2) must be stored. Thus, volume storage for 250 g moles of H_2, 125 g moles of O_2 and 4.6 liters of liquid water will be needed.

The storage efficiency for chemical storage is associated with the mechanical work done to store the H_2 and O_2. It is assumed that the storage work is done in isothermally compressing the H_2 and O_2 from 1 atmosphere to

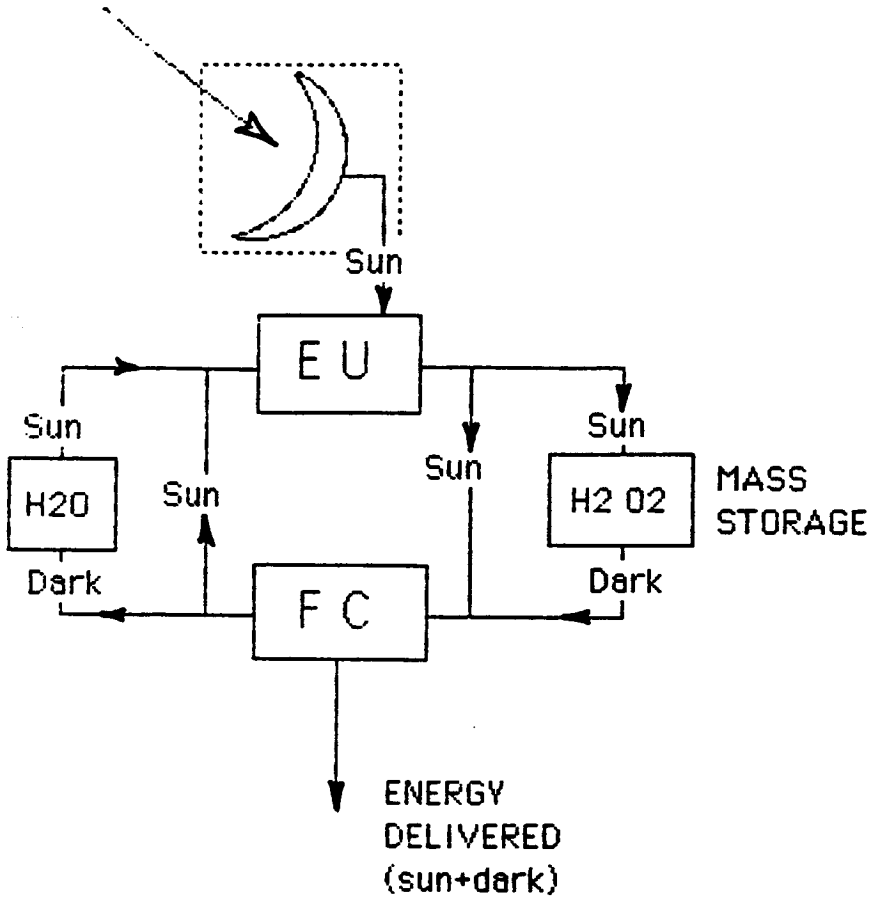
Sun
E U
Sun
Sun
Sun
H20
Sun
H2 02
MASS
STORAGE
Dark
Dark
F C
ENERGY
DELIVERED
(sun+dark)

Figure 8.

C-3

the storage pressure (Pstor):

$$Wstor = \frac{3}{2} R \cdot T \cdot \ln Pstor$$

A definition of storage efficiency, similar to previous options, must be derived from HTE cycle considerations, since this chemical option storage is integral to the cycle itself. The cyclic efficiency with chemical storage will be less than the "normal cycle" efficiency due to the work done to pressurize the electrolysis products for storage. Thus, the "integral storage cycle" efficiency ($\eta_{cyc\ stor}$) can be defined:

$$\eta_{cyc\ stor} = \frac{\text{Net work output per orbit}}{\text{Thermal input per orbit}}$$

$$= \frac{Pdel \cdot (TD + TS) - Nstor \cdot Wstor}{\frac{Pdel \cdot (TD+TS)}{\eta_{cyc}}}$$

where Nstor is the number of moles of water stored.

Noting that $\eta_{cyc\ stor}$ combines the previous definition of η_{cyc} and η_{stor}:

$$\eta_{cyc\ stor} = \eta_{cyc}\,\eta_{stor} = \eta_{cyc} \cdot \left(1 - \frac{Nstor \cdot Wstor}{Pdel \cdot (TD+TS)} \right)$$

So we now have a "standard" definition for this chemical storage efficiency:

$$\eta_{stor} = 1 - \frac{Nstor \cdot 3/2 \cdot RT \cdot \ln Pstor}{Pdel \cdot (TD + TS)}$$

Since Nstor = 250 g moles for the present situation:

$$\eta_{stor} = 1 - 0.00816 \ln Pstor,$$

Assuming a storage pressure of 20 atmospheres gives a 97.6 percent storage

efficiency, and the resulting combined cycle-storage system efficiency is 32.2 percent. This in turn leads to an overall system efficiency of 22.5 percent, requiring a collector area of 131.9m^2.

Summary of Storage Options

All three storage options possess individual attributes, such as reliability, weight, volume, etc., which are not addressed here. The actual selection of a storage option would have to take these and many more factors into consideration before an engineering selection could be made. It should also be noted that the time profile of the electrical load to be met will directly influence option performance via the storage required for a given profile.

However, with the conditions stated for the system options described, a summary comparison of the three options is presented in Table 2. The system efficiencies and resultant collector areas are seen to be very similar for the options, but the HTE cycle size which must be installed is much less for the thermal storage option. Thus, thermal storage was chosen as the option to be used with the system parametric studies below.

TABLE 2. STORAGE OPTION COMPARISON

	THERMAL ENERGY	CHEMICAL ENERGY	ELECTRICAL ENERGY
STORAGE EFFICIENCY(%)	90	97.6	80
HTE CYCLE SIZE (KWe2)	25	40.3	44.1
OVERALL SYSTEM EFFCIENCY (%)	22.2	22.5	21.1
COLLECTOR AREA (m2)	133.9	131.9	140.9

PARAMETRIC ANALYSES

The parametric analyses are structured to provide results for two separate purposes: the determination of optimium operating conditions, and the investigation of system sensitivities to parametric variations around the optimum conditions. The optimizations and sensitivities are done for both current and future technology devices, with different combinations of the devices used to examine the effect of developing a particular device.

Important Parametric Variables

In addition to defining the technology values and establishing the system configuration, it is necessary to identify the major variables important to system operation. These variables can be identified by looking at the cycle efficiency equation,

$$\eta_{cyc} = \frac{Wf - We}{Qhot} = \frac{\eta_{fc} \cdot \Delta Gf - \Delta Ge/\eta_e}{\Delta He - (\Delta Ge/\eta_e) + Qhx}$$

and by substituting using many relations which are defined and described in the subsection below:

$$\eta_{cyc} = \frac{Vf \cdot \eta_{cf} \cdot n \cdot F - Ve \cdot n \cdot F/\eta_{ce}}{\Delta He - Ve \cdot n \cdot F/\eta_{ce} + (1 - \varepsilon hx)(h_{Th} - h_{Tc})}$$

It is seen that two major variable types influence the cycle efficiency: device voltage (Vf, Ve) and device current efficiency (η_{cf}, η_{ce}). These variables are the one expected to be of importance, and both voltage and current efficiency are known to be functions of the device operating current density. As is shown below, the optimizations and sensitivities were performed against these identified important variables.

Optimization Scheme

The generalized function to be optimized is assumed to be related to the fuel cell and electroylzer areas in the additive manner:

$$BT = BF \cdot AF + BE \cdot AE \ , \qquad (4)$$

where BT represents the total system parameter (mass, volume, area, cost, etc.), BF and BE represent parametric values (or functions) on a unit area basis, and AF and AE represent the fuel cell and electrolyzer cell areas, respectively.

The optimization of the generalized function is performed assuming that the system is operating with a given net power (Pnet) and with given fuel cell and electrolyzer operating curves (V versus J). The areas to be used depend on the current density, and resulting device efficiency, desired for the overall system. Thus, the three variables chosen as independent are:

$\dot{N}$ - The molal fuel flow rate which determines the overall current developed and used

JF - The fuel cell current density: $JF = \frac{If}{AF}$

JE - The electrolyzer current density: $JE = \frac{Ie}{AE}$

Now writing the generalized function, Eq. 4, in terms of the three variables,

$$BT = \frac{BF \cdot If}{JF} + \frac{BE \cdot Ie}{JE}$$

where $If = Io \cdot \eta cf$ and $Ie = \frac{Io}{\eta ce}$

with $Io = n \cdot F \cdot \dot{N}$, n = #electrons per reaction

F = Faraday's constant

and cf and ce are the current efficiences for the fuel cell and electrolyzer, respectively. So, the area function becomes,

$$BT = \frac{BF \cdot n \cdot F \cdot \eta cf \cdot \dot{N}}{Jf} + \frac{BE \cdot n \cdot F \cdot \dot{N}}{\eta ce \cdot Je} = f(JF, JE, \dot{N})$$

and defining $C1 = n \cdot F \cdot \eta cf$ and $C2 = \frac{n \cdot F}{\eta ce}$

$$\text{then, } BT = \frac{BF \cdot C1 \cdot \dot{N}}{JF} + \frac{BE \cdot C2 \cdot \dot{N}}{JE} \qquad (5)$$

where it is assumed current efficiency (ηcf, ηce) is a constant for the conditions given.

A constraining relation can be defined for the given net power level,

$$Pnet = Pf - Pe$$
$$= If \cdot Vf - Ie \cdot Ve$$

where the Vf and Ve are the operating voltages for the fuel cell and electrolyzer, both of which are functions of their respective current densities. Substituting for the currents as before:

$$Pnet = n \cdot F \cdot \eta cf \cdot \dot{N} \cdot Vf - \frac{n \cdot F \cdot \dot{N} \cdot Ve}{\eta ce}$$
$$= C1 \cdot \dot{N} \cdot Vf - C2 \cdot \dot{N} \cdot Ve$$

So, the constraint relation can be written:

$$(JF, JE, \dot{N}) = Pnet - C1 \cdot \dot{N} \cdot Vf + C2 \cdot \dot{N} \cdot Ve = 0 \qquad (6)$$

where $Vf = f(JF)$ and $Ve = f(JE)$.

Extremum by Lagrangan Multiplier

The extremum of the BT function, Eq. 5, may now be found subject to the constraint, Eq. 8, by using the Lagrangan multiplier approach. This approach yields four equations and four unknowns (JF, JE, $\dot{N}$, λ) with three equations arising from the external condition,

$$\frac{\partial F}{\partial Xi} - \lambda \frac{\partial \phi}{\partial Xi} = 0 \qquad i = 1, 2, 3 \qquad Xi = (JF, JE, \dot{N}) \tag{7}$$

and the constraint equation itself,

$$\phi = 0 .$$

Substituting into the three extremal condition equations, Eq. 9, yields:

$$\frac{BF}{JF^2} - \lambda \frac{\partial Vf}{\partial JF} = 0$$

$$\frac{BE}{JE^2} + \lambda \frac{\partial Ve}{\partial JE} = 0$$

$$\frac{Bf \cdot C1}{JF} + \frac{BE \cdot C2}{JE} - \lambda(-C1 \cdot Vf + C2 \cdot Ve) = 0$$

and the constraint equation, Eq. 6, provides the fourth equation for the four unknowns:

$$Pnet - (C1 \cdot Vf + C2 \cdot Ve) \cdot \dot{N} = 0$$

Thus, the mathematical problem is to solve four non-linear equations for the four variables. Note that the Vf and Ve functions must be inserted into these equations before solving. Also note that if the BF and BE terms are

functions of area, the areas would have to be converted to N and J functions as outlined earlier.

Unconstrained Optimization Approach

It should also be noted that the optimization problem could be solved as an unconstrained problem by combining the generalized function and the constraint equation by eliminating a variable through substitution. This leaves the following expression in two variables to be optimized:

$$BT(JF, JE) = \frac{Pnet}{C1 \cdot VF - C2 \cdot VE}\left(\frac{BF \cdot C1}{JF} + \frac{BE \cdot C2}{JE}\right)$$

where VF, VE, BF and BE are known explicit functions in JF and JE.

Specific Solutions: Linear Polarization Curves

Both the non-linear equation approach and the unconstrained optimization approach were used by application of an algorithm described in [ref. 21]. However, for the case where the voltage-current density polarization curves can be described by linear relations of the form:

$$Vf = Vfo - a \cdot JF$$

$$Ve = Veo + b \cdot JE,$$

then the Lagrangian method yields the exact solution:

$$JF = \frac{C1 \cdot Vfo - C2 \cdot Veo}{2 \cdot C1 \cdot a + 2 \cdot C1 \cdot (a \cdot b \cdot BE/BF)^{1/2}}$$

$$JE = \frac{C1 \cdot Vfo - C2 \cdot Veo}{2 \cdot C1 \cdot (a \cdot b \cdot BF/BE)^{1/2} + 2 \cdot C2 \cdot b}$$

with $\dot{N}$ given by substitution back into Eq. 8. This approach using linear

polarization curves was utilized in this investigation in order to accommodate the large number of parametric variations investigated.

Example Results

The optimization of the HTE cycle to minimize mass, volume, and/or cell area was performed using the exact linearized procedure. The HTE cycles examined were grouped into three areas:

- Current Technology - cycle composed of current fuel cell (alkaline) and a current solid oxide cell electrolyzer operating at 1000°C;
- Near Term Technology - three cycles composed of:
  a. Current fuel cell and solid oxide electrolyzer at 1500°K,
  b. Advanced fuel cell (SPE-type) and current solid oxide electrolyzer at 1000°C,
  c. Advanced fuel cell and solid oxide electrolyzer at 1500°K; and
- Future Technology - cycle composed of future fuel cell and solid oxide electrolyzer operating at 1800°K.

The characteristics of these devices are described in Table 1 and Figure 4. The results discussed below were generated assuming a 1 kWe cycle output.

The generalized system parameter, BT, was optimized for a range of fuel cell to electrolyzer parametric ratios (BF/BE) for the three basic technology cases. The results of these optimizations is presented graphically in Figure

9. Also shown in Figure 9 is the effect of device current efficiency on the value of BT. Note that the current efficiency variation causes a large variation in the system parameter, especially for the current technology case.

More detail illustrating this system sensitivity to current density efficiency is presented in Figure 10. The minimum total cell area for the HTE cycle is shown as a function of the fuel cell current efficiency and the electrolyzer current efficiency for a current technology system.

In the analysis of 'off-optimum' operating conditions, the 'brute force' method described earlier was used to generate a range of operating conditions. Figure 11 presents an example of this approach using current technology devices. The variation around the minimium total area can be seen, as well as the individual fuel cell and electrolyzer areas. Figure 12 presents another aspect of data from these same 'brute force' simulation runs. It is seen that the electrolyzer operating point is relatively constant, no mattery at what condition the fuel cell is operating.

Figure 9.

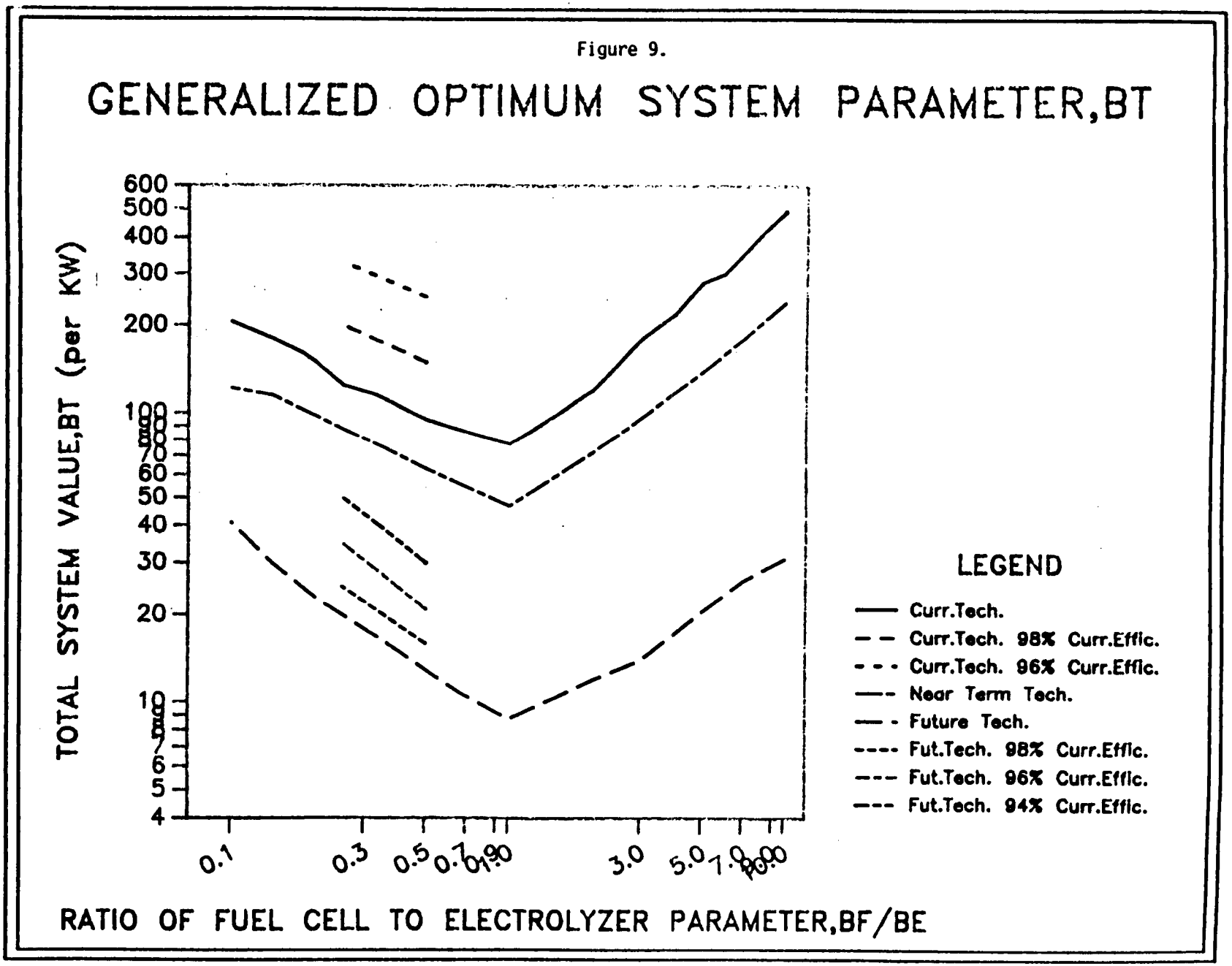
GENERALIZED OPTIMUM SYSTEM PARAMETER,BT
TOTAL SYSTEM VALUE,BT (per KW)
600
500
400
300
200
100
60
50
40
30
20
10
6
5
4
0.1
0.3
0.5
0.7
1.0
3.0
5.0
10.0
RATIO OF FUEL CELL TO ELECTROLYZER PARAMETER,BF/BE
LEGEND
Curr.Tech.
Curr.Tech. 98% Curr.Effic.
Curr.Tech. 96% Curr.Effic.
Near Term Tech.
Future Tech.
Fut.Tech. 98% Curr.Effic.
Fut.Tech. 96% Curr.Effic.
Fut.Tech. 94% Curr.Effic.

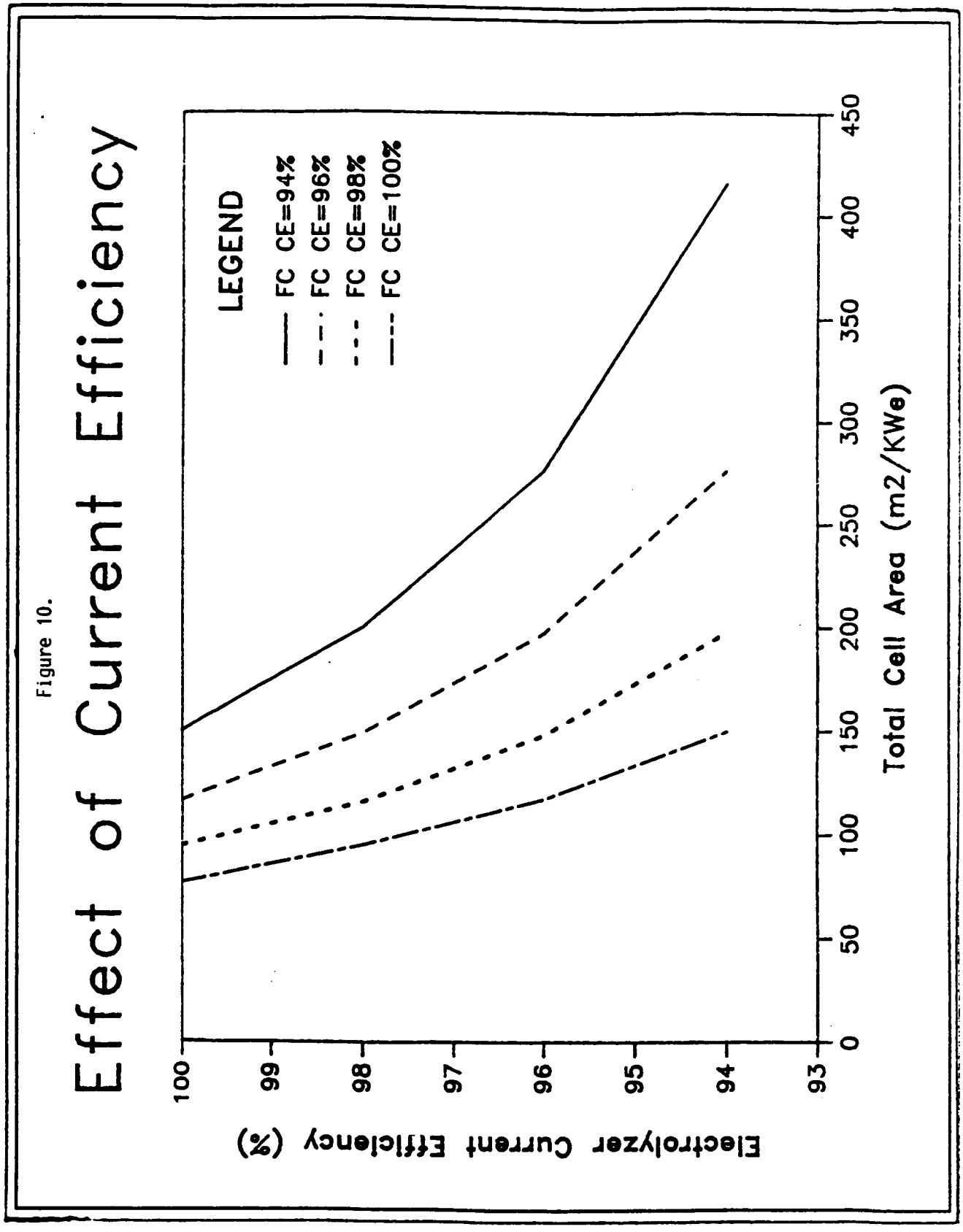
Effect of Current Efficiency
LEGEND
FC CE=94%
FC CE=96%
FC CE=98%
FC CE=100%
Electrolyzer Current Efficiency (%)
100
99
98
97
96
95
94
93
0
50
100
150
200
250
300
350
400
450
Total Cell Area (m2/KWe)

Figure 10.

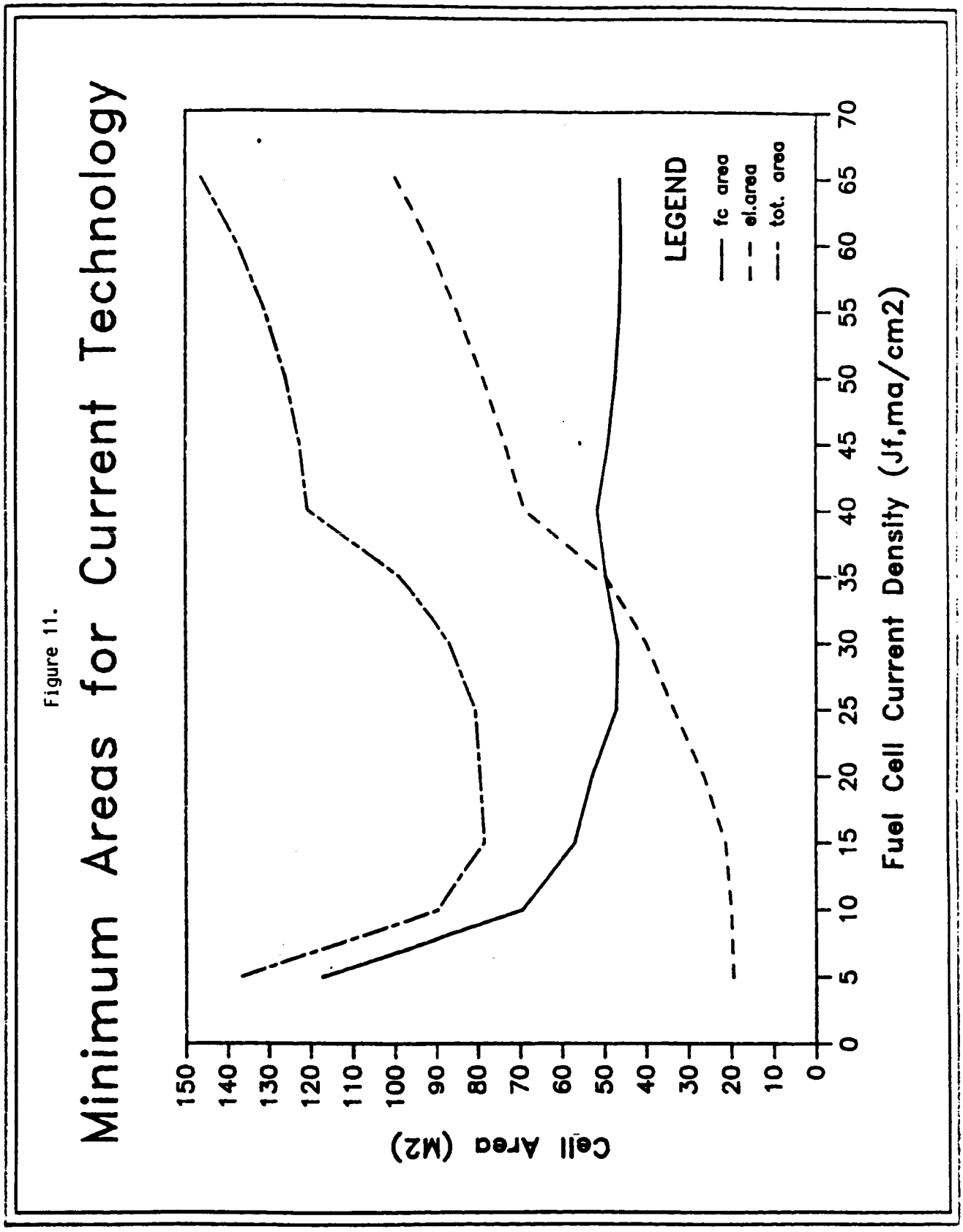
Minimum Areas for Current Technology
Cell Area (M2)
Fuel Cell Current Density (Jf,ma/cm2)
LEGEND
fc area
el.area
tot. area
150
140
130
120
110
100
90
80
70
60
50
40
30
20
10
0
0
5
10
15
20
25
30
35
40
45
50
55
60
65
70

Figure 11.

Figure 12.

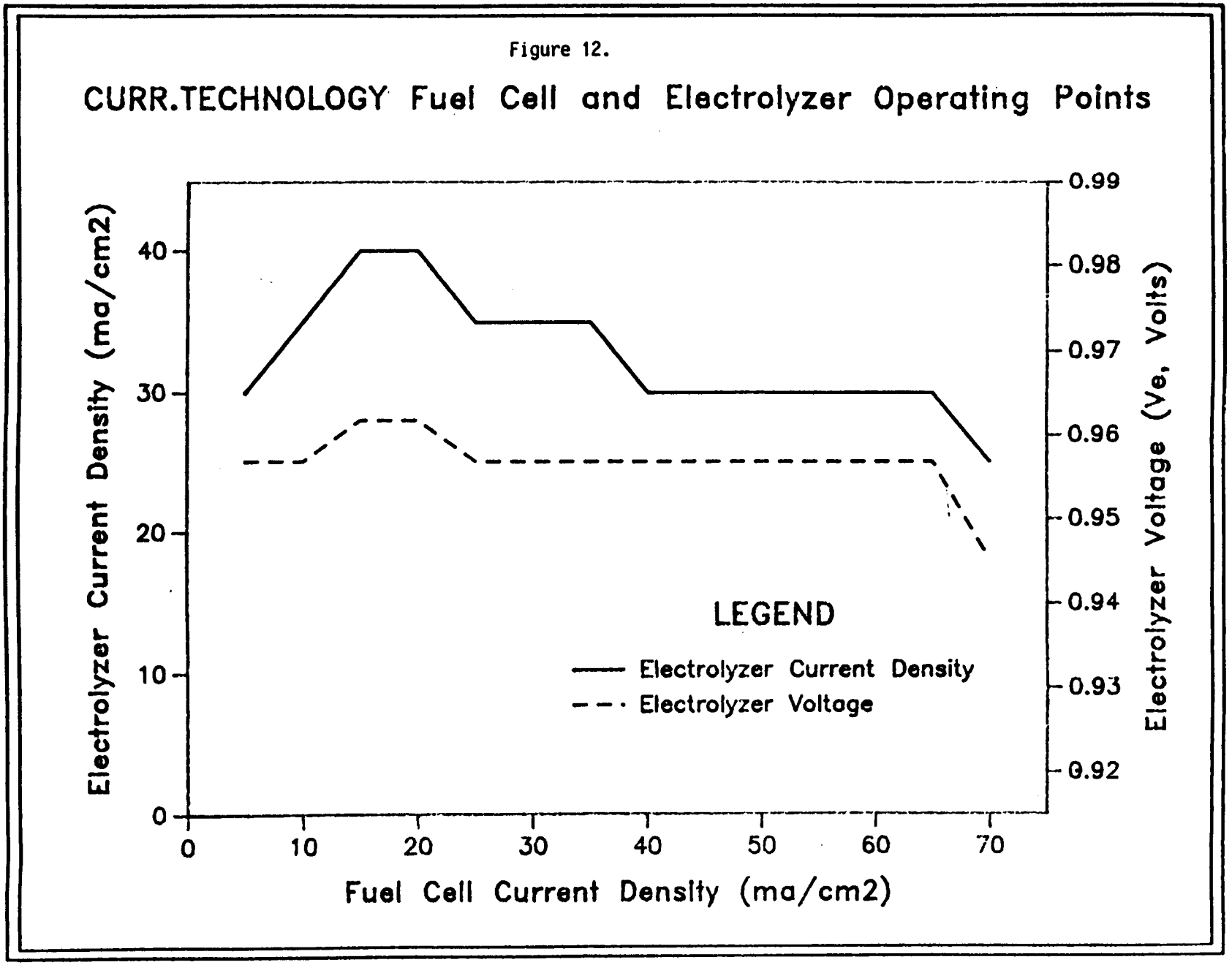
CURR.TECHNOLOGY Fuel Cell and Electrolyzer Operating Points
Electrolyzer Current Density (ma/cm2)
Electrolyzer Voltage (Ve, Volts)
Fuel Cell Current Density (ma/cm2)
0
10
20
30
40
50
60
70
0.92
0.93
0.94
0.95
0.96
0.97
0.98
0.99
LEGEND
Electrolyzer Current Density
Electrolyzer Voltage

Table 3.

SUMMARY OF SYSTEM DESIGN PARAMETERS

	1 KWe MODULE				
	CYCLE EFFIC.[1] (%)	TOTAL CELL AREA [2] (m2)	TOTAL VOLUME (m3)	TOTAL MASS (kg)	GROSS POWER (KW)
CURRENT TECH. (98% curr.effic.)	26.8	116.2	1.85	1606.5	11.8/10.8
NEAR-TERM TECH. (98% curr.effic.)					
a)Curr.FC/1500K EU	30.8	66.9	0.85	506.7	8.6/7.6
b)Fut.FC/Curr. EU	31.5	31.7	0.37	482	11.0/10.0
c)Fut.FC/1500K EU	35.8	19.8	0.2	89.2	8.3/7.3
FUTURE TECH. (99% Curr.Effic.)	43.4	9.6	0.1	43.3	5.8/4.8

[1] 95% Heat Exchanger Effectiveness
[2] Optimized Parameter

Figure 13.

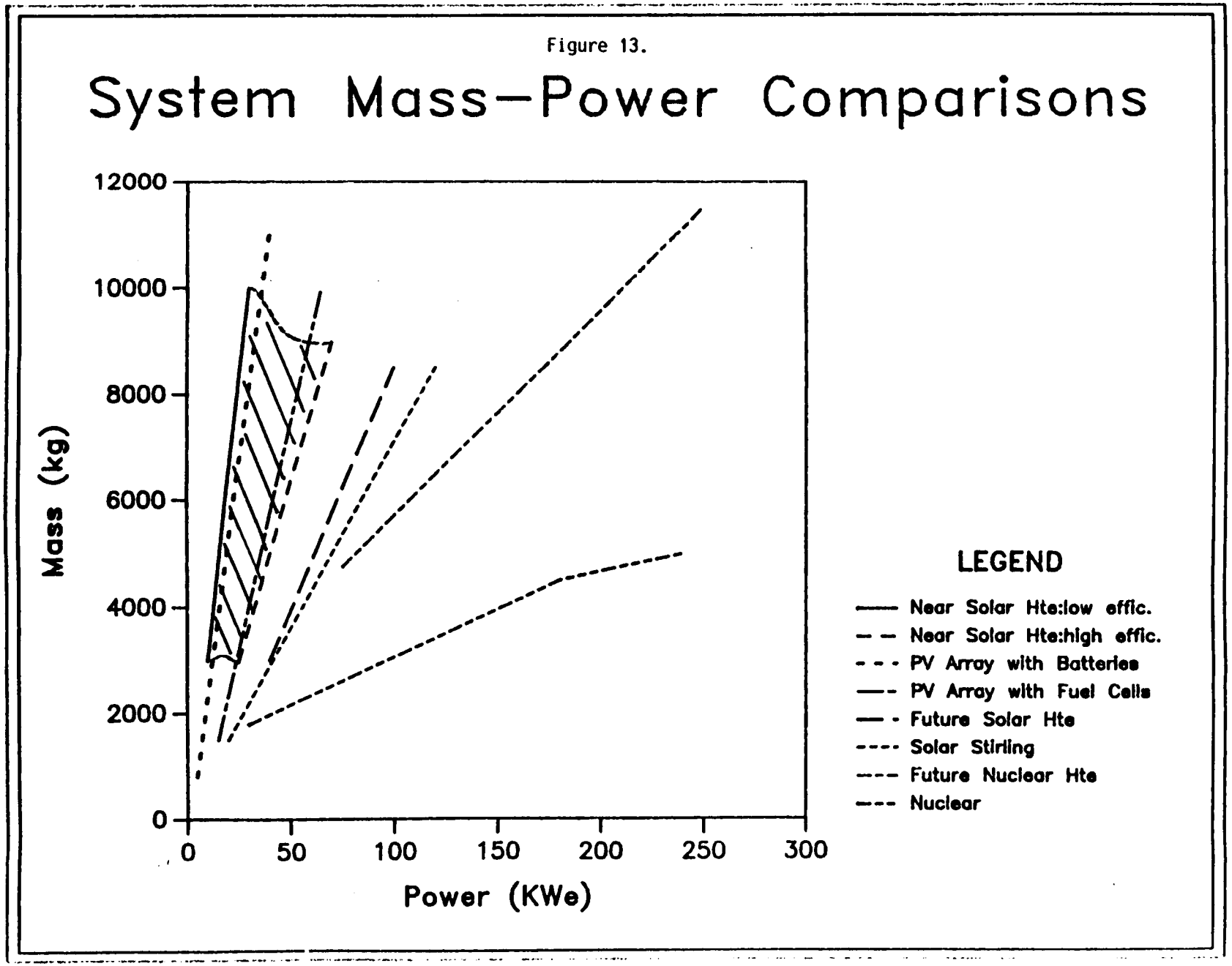
System Mass–Power Comparisons
12000
10000
8000
6000
4000
2000
0
Mass (kg)
0
50
100
150
200
250
300
Power (KWe)
LEGEND
Near Solar Hte:low effic.
Near Solar Hte:high effic.
PV Array with Batteries
PV Array with Fuel Cells
Future Solar Hte
Solar Stirling
Future Nuclear Hte
Nuclear

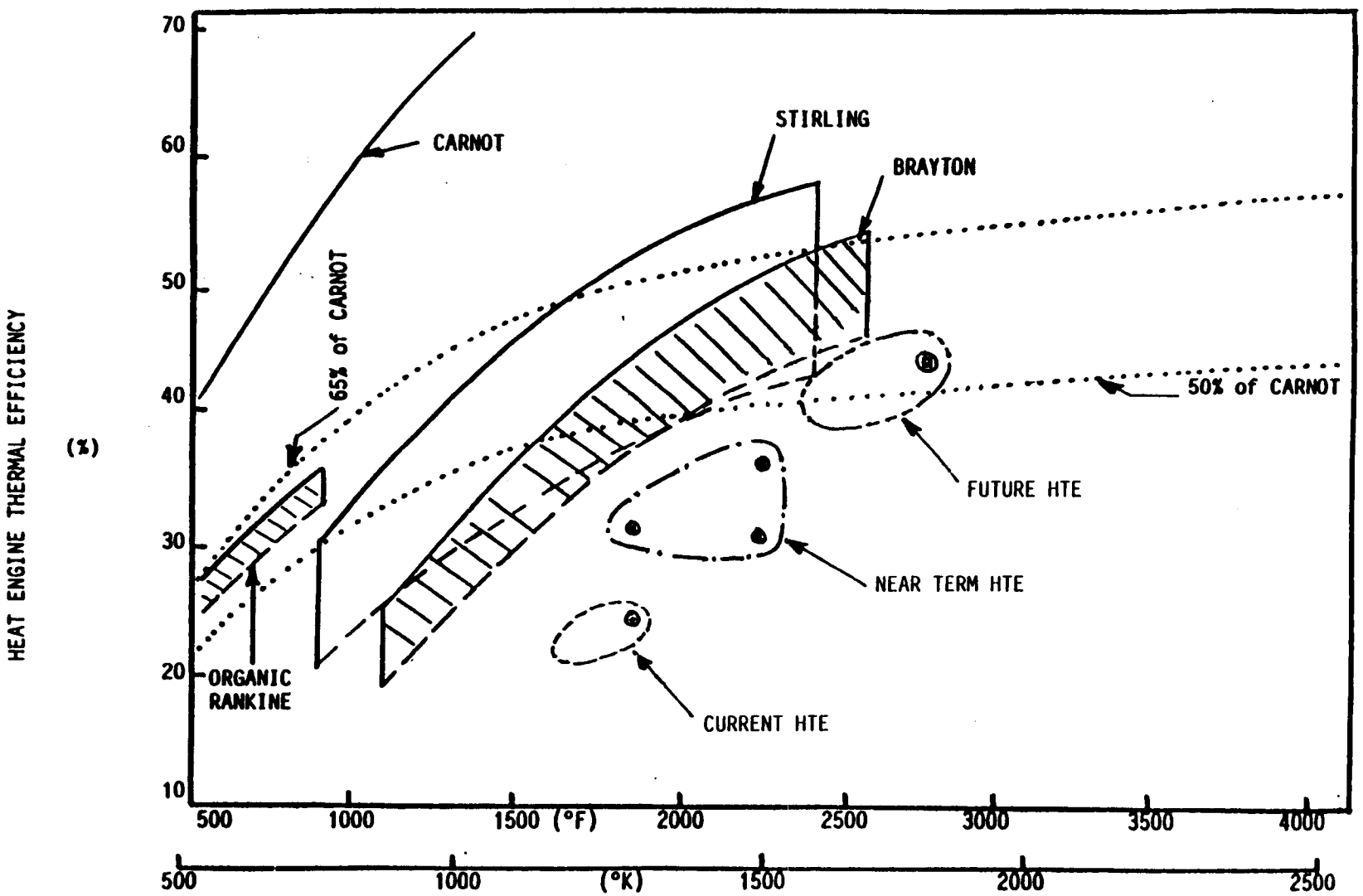

Figure 14 . THERMODYNAMIC CYCLE COMPARISONS FOR VARIOUS OPERATING TEMPERATURES

SUMMARY

The HTE cycle was examined using simulations which identified optimum system operating conditions under various parametric situations (i.e., minimum cell area, volume, mass, etc.). These optimum conditions were found for systems composed of fuel cell and electrolyzer technology representing current, near term, and future developmental efforts. A summary of general HTE cycle design parameters, fuel cell and electrolyzer devices only, is presented in Table 3 and is based on an area minimization.

The Table 3 data represents a 1 kWe module, and it can be seen that while current technology HTE cycles could be constructed with reasonable efficiencies, the mass, volume, and cell areas needed are extremely large. Near term developments would lead to significant mass, area, and volume reductions, while future technology developments will also provide significant increases in cycle efficiency and device sizing requirements (gross power).

Comparison to Other Cycles

The data presented in Table 3 allows a comparison between the HTE cycle and other power cycles. A comparison of overall system mass-to-power ratios is presented in Figure 13. The graph itself is adapted from [Ref. 2], with the entire system mass being included for each system type, including the HTE cycles with solar collectors and radiators [Ref. 9]. The current technolgy HTE curve is almost coincident with the left axis, but near term technology HTE's are in the cross-hatched area along with PV systems. Future technolgy HTE's are shown as similar to the best solar dynamic, and even approaching

nuclear dynamic systems.

Another comparison can be made in terms of efficiency and operating temperature. In Figure 14, various dynamic systems are represented, with the HTE cycles presented by time of technology development. It should be noted that while the HTE cycle appears to be 'under' the curves of the Brayton and Stirling cycles, it can be thought of as being to the 'side' of them, meaning the HTE operates at higher temperature. This type of interpretation is possible when it is realized that the HTE cycle does not have reciprocating or revolving mechanical parts which operate at these high temperatures.

Further Developments

Fuel cells and the electrolyzer exist to build a HTE today. However, it would be large, heavy and costly. The cycle efficiency is reasonable, but it was found that the current technology cycle is very sensitive to device current efficiency. Two and three percent current efficiency losses correspond to doubling and tripling the cell areas needed. Thus, a current technology HTE cycle would represent a formidable engineering challenge.

In the near term, the fuel cell and/or the electrolyzer can be improved. The solid oxide electrolyzer existing today might be able to be modified to work at 1500°K, but it would probably take a major developmental effort to gain the fuel cell improvements described in Figure 4 and Table 1. It appears reasonable that a near term HTE, as represented on Figures 13 and 14, could be demonstrated with two to five years of development. Such a HTE system would exhibit comparable mass and efficiency to current PV and solar dynamic systems.

The future HTE systems are envisioned as operating at 1800°K electrolyzer heat input, with an advanced SPE-type fuel cell at 100°C (373°K). Both the electrolyzer and fuel cell will require major developmental efforts to achieve the desired performance. However, a HTE power cycle operating at these conditions will be as-good-as or better than other envisioned solar cycles, while still retaining its 'no moving parts' attraction.

REFERENCES

1. "Conceptual Design and Evaluation of Selected Space Station Concepts," JSC-19521, NASA/Johnson Space Center, 1983.

2. Buden, et al; 19th IECEC Proceedings, Vol. I, p. 89. San Francisco, CA, 1984.

3. Liebhafsky, H. A., "The Fuel Cell and the Carnot Cycle," Journal of the Electrochemical Society, Vol. 106, pp. 1068-1071, 1959.

4. de Bethune, A. J., "Fuel Cell Thermodynamics," Journal of the Electrochemical Society, Vol. 107, pp. 937-939, 1960.

5. Abraham, B. M. and Schreiner, F., "General Principles Underlying Chemical Cycles Which Thermally Decompose Water into the Elements," Industrial and Engineering Chemistry, Fundamentals, Vol. 13, No. 4, pp. 305-310, 1974.

6. Veziroglu, T. N. and Kakac, S., "Solar Hydrogen Energy System and Solar Hydrogen Production Methods," International Symposium-Workshop on Solar Energy, Cairo, Egypt, pp. 275-296, June 1978.

7. Liepa, M. A. and Borhan, A., "High Temerature Steam Electrolyses: Technical and Economic Evaluation of Alternative Process Designs", International Journal of Hydrogen Energy, Vol. II, No. 7, pp. 435-442, 1986.

8. Chum, H. L. and Osteryoung, R. A., "Review of Thermally Regenerative Electrochemical Systems", SERI/TR-332-416, Solar Energy Research Institute, Golden, CO, August 1980.

9. "Space Station Electrical Power System Configuration Impact Assessment," JSC-19994 Power System Branch, NASA/Johnson Space Center, August 1984.

10. Morehouse, J. H., "Thermally Regenerative Hydrogen/Oxygen Fuel Cell Power Cycles", Final Report NASA/ASEE Summer Faculty Program, NASA/JSC; Houston, TX, August 1985.

11. Morehouse, J. H., "Thermally Regenerative Hydrogen/Oxygen Fuel Cell Power Cycles", Solar Engineering - 1986: Proceedings of the ASME Solar Energy Conference, Anaheim, CA, pp. 113-119, April, 1986.

12. Isenberg, A. O., "Cell Performance and Life Characteristics of Solid Oxide Electrolyte Fuel Cells," Proceedings of the Conference on High Temperature Solid Oxide Electrolytes Brookhaven National Lab; Vol. I, pp. 5-15, October 1983.

13. Masalick, N. J., et. al., "Hydrogen Production Employing High-Temperature Solid Oxide Cells," Proceedings of the 19th IECEC, San Francisco, CA, pp. 1415-1420, 1984.

14. Powell, J. R. and Fillo, J. "Advanced Synfuel Production with Fusion," Proceedings of the 14th IECEC, Boston, MA, pp. 1549-1552, 1979.

15. Fee, D. C., et. al., "Solid-Oxide Fuel Cell Performance," 2nd Solid Oxide Fuel Cell Workshop, Brookhaven National Lab, August 1983.

16. Doenitz, W., et. al., "High Temperature Electrolysis of Water Vapor - Status and Perspectives of the German Research and Development Activities," Proceedings of the Conference on High Temperature Solid Oxide Electrolytes, BrookHaven Nat. Lab (BNL51728), pp. 67-80, 1983.

17. Dietrich, G. and Shaffer, W. "Advances in the Development of Thin-Film Cells for High Temperature Electrolysis, International Journal of Hydrogen Energy, Vol. 9, No. 9, pp. 747-752, 1984.

18. Personal Communication - Power Branch, NASA/JSC, Houston, Texas, August 1986.

19. Personal Communication - Venture Technology Group, Westinghouse R&D Center, Pittsburg, PA, July 1986.

20. "Regenerative Fuel Cells: Space Station Design Definition", Life Systems, Inc. Technical Status Report, TR-862-6A, November 1985.

21. Dennis, J. E. and Schnabel, R. B., "Numerical Methods for Unconstrained Optimization and Nonlinear Equations", ISBN 0-13-627216-9, Prentice-Hall, 1983.

1986

NASA/ASEE SUMMER FACULTY FELLOWSHIP PROGRAM

Johnson Space Center

University of Houston

Evaluation of an Automated Karyotyping System for Chromosome Aberration Analysis

Prepared by:	Howard M. Prichard, Ph.D.
Academic Rank:	Associate Professor
University and Department:	The University of Texas School of Public Health Occupational Health
NASA/JSC	
Directorate:	Space and Life Sciences Directorate
Division:	Medical Sciences
Branch:	
JSC Colleague:	Gerald Taylor, Ph.D.
Date:	December, 1986
Contract #:	NGT-44-005-803 University of Houston

ABSTRACT

Chromosome aberration analysis is a promising complement to conventional radiation dosimetry, particularly in the complex radiation fields encountered in the space environment. Manual aberration analysis is time and labor intensive, and requires subjective evaluations by trained personnel. In-flight chromosome studies would therefore require either the transmission of images to ground facilities or automated scoring routines that would not require a major committment of flight personnel. In either case, the quality of the digitized image and the amount of data storage required is of great importance.

In this project, the capabilities of a recently developed automated karyotyping system were evaluated both to determine current capabilities and limitations and to suggest areas where future development should be emphasized. Cells exposed to radiomimetic chemicals and to photon and particulate radiation were evaluated by manual inspection and by automated karyotyping. It was demonstrated that the evaluated programs were appropriate for image digitization, storage, and transmission. However, automated and and semi-automated scoring techniques must be advanced significantly if in-flight chromosome aberration analysis is to be practical. A degree of artificial intelligence may be necessary to realize this goal.

NASA Colleague: Gerald Taylor, Ph.D., S.D. 3

INTRODUCTION

While short LEO (Low Earth Orbit) missions have not produced crew radiation exposures at levels of concern, other projected missions involve the possibility of high, even life-threatening exposures. Lunar and deep space missions beyond the earth's magnetosphere involve the risk of solar flare radiation, and some earth orbits involve appreciable time in the Van Allen radiation belts. Even extended low earth orbit missions such as those envisioned for Space Station personnel involve some accumulated exposure to Inner Van Allen Belt radiations, due primarily to repeated passage through the South Atlantic Anomaly. Space radiation environments are generally complex and qualitatively different from terrestrial radiation fields that have produced the bulk of our knowledge on the biologic effects of radiation. While there is at present a great deal of interest in the biological effects of the high energy heavy nuclei found in the galactic cosmic ray flux, it appears at present that protons in the range of (approximately) 10 to 1000 MeV are the limiting form of radiation for most comptemplated deep space and Low Earth Orbit (LEO) missions. In terms of flux, energy deposition, and presumed biological effect, protons are the single most important component of galactic cosmic rays, solar flare radiation, and Inner Van Allen belt radiation (Haffner, 1967). While such exposures are of only moderate concern for the welfare of Space Station crew, it is important for future programs to determine as much as possible about the biological effects of space radiations administered in the environment of a spacecraft.

The Space Station represents an invaluable resource for the conduct of these types of radiobiological experiments. Potentially confounding effects such as weightlessness are the default condition, and access to the energetic protons of he inner Van Allen Belt can be achieved with little energy expenditure. Small experimental packages could be subjected to repeated passages through the belt if "piggybacked" on transfer vehicles operating between LEO and GEO. A relatively small delta vee could subject a dedicated probe to a pre-programmed exposure to belt protons prior to retrieval. The effects of various types of shielding and differential responses between physical dosimeters and biological systems under flight conditions could be studied much more readily from the station than from a facility on the ground. Of particular interest are the responses of human cells, such as lymphocytes, exposed deliberately in vitro or incidently in vivo . Chromosome aberration analysis is one of the principle techniques used to quantitate the response of such systems.

Chromosome aberration studies have long been used to determine the extent of radiation exposure in cases in which conventional dosimetry systems were either not in place or not appropriate for the mode of irradiation (e.g. Collins 1980, Brewen 1982, Evans 1979, Lloyd 1979). At present, the most labor-intensive and potentially subjective aspect of the procedure is the manual evaluation of chromosome spreads. A trained cytological technician must examine each spread and make what are in many cases subjective decisions as to whether or not an observed feature represents a true anomaly.

Many cells must be examined to obtain reliable statistics on a single sub-lethal radiation exposure, the exact number being dependent on the dose and the degree of precision required, among other things. (A one Gray (100 rad) dose produces an expected yield of dicentric and acentric aberrations on the order of 1 per 20 cells, while the "spontaneous" background rate is about one per hundred cells (Lloyd 1980).) While the Space Station is a very good place to perform relevant experiments, it would be a misuse of resources to dedicate one or more crew members to extensive manual cytological examinations if a reasonable alternative were available. One alternative is to digitize microscopic images of cell preparations for transmission and reconstruction on the ground, where conventional cytological analysis could be pursued. A related option is to use appropriate software to process digitized images in flight. The latter option is particularly attractive for situations in which data links to the ground are at a premium, as might be the case in a deep space mission. Both alternatives require that the digitized be of adequate quality for analysis and that data storage and transmission requirements not be excessive.

MATERIALS AND METHODS

Slide Preparation

Slides of human lymphocytes arrested at metaphase after various radiation and chemical treatments had been prepared previously (Prichard, 1986). Blood samples had been subjected to one of three radiation treatments: 1). Control - no radiation, 2). Gamma - 0.662

MeV gamma rays from a Cs-137 irradiator, and 3). Proton - 40 MeV protons from the University of Texas Health Science Center at Houston Cyclotron Facility. Venous blood had been drawn into a heparinized 15 ml vacutainer tube, which was then shaken and placed into a 35 to 37 degree transfer case until treatment and/or culture. Aliquots were given the appropriate radiation treatment and returned to the sample case. Another aliquot was cultured for a predetermined interval, irradiated, then returned to the incubator. One half ml of treated whole blood was placed in a culture tube along with 4.5 ml of modified RPMI culture medium and stimulated with the mitogen PHA. The culture tubes were placed in a 37 C incubator for the desired incubation period (72 hours or 48 hours, depending on circumstances). One hour before harvest, Colcemide (final conc. = 0.1 ug/ml) was added to arrest dividing cells at metaphase. The medium was spun down to separate the cellular mass from the supernatent plasma and all but the lower half centimeter of plasma was pipetted off and replaced by hypotonic KCl. The solution was, mixed and allowed to stand for 30 minutes, after which three ml of fixative solution was added, the solution mixed, and spun down. After three successive washes, slides were prepared by allowing several drops of the fixative containing suspended cells to fall ca. one meter onto a clean slide still wet from storage in 4 C distilled water. The slides were then air dried, stained with Giemsa, and coverslipped after a zero point disk had been placed in the center to facilitate mapping.

Metaphase Spread Selection

The previously prepared slides were mapped at low power with a Zonax micro-computer driven microscope and the locations of chromosome spreads were stored on a floppy disk to permit rapid examination under high power objectives. Spreads which under high power oil lenses seemed suitable for metaphase aberration analysis were logged by map number. A set of spreads were selected for automated and manual analysis.

Image Digitization

An analog image of the microscope field was generated by a videocamera mounted on the microscope. The program Chromexec, by Perceptive Systems, Inc, and associated hardware permitted a variety of contrast adjustment routines prior to digitization of the image. The digitized image consisted of a 256 x 256 array of 8 bit bytes. When cameras and monitors of appropriate quality were used, the visual quality of the image was judged by the author to be quite adequate for gross abnormality or karyotype analysis. This judgement was confirmed by a panel of experienced cytogeneticists assembled to review the quality of the image and other features of the system (Pathak, 1986). However, a four-fold reduction in pixel number produced obvious degradation of the image, thus confirming the appropriateness of the 256 x 256 array size. The time required to recall a mapped spread, adjust focus and gray levels, and to digitize, document, and store an image was found to be on the close

order of two minutes. Most of this time could be eliminated by the application of macros and program features not available on the tested version of the program.

Automated vs Manual Image Analysis

In manual scoring of metaphase spreads, the trained cytotechnician visually scans the microscopic images and identifies gross abnormalities such as rings, dicentrics, gaps, chromatid breaks, and chromosome breaks. In the sort of scoring traditionally done for radiation exposure assessment, finer distinctions requiring banding and full karyotyping are generally not performed. A trained cytologist can perform this sort of evaluation on a good spread in a minute or two. The automated karyotyping feature of the Chromexec program produces a full karyotype of a digitized spread in about four minutes, provided that few of the chromosomes touch or overlap. While the program produces a display that is much easier to score than an unsorted spread, and makes possible a much more refined class of analyses, the current version of the program consumes considerably more time than a manual scoring. Furthermore, the advantage of the manual scorer becomes greater as the spread gets "messier", i.e., more touches and overlaps.

CONCLUSIONS AND RECOMMENDATIONS

The advantage in speed currently held by manual scoring can be reduced on one or both of two fronts. In the first case, it is recognized that the contest is unfair, in that the manual scorer is

not required to separate and sort chromosomes, but rather to detect anomalies. If this were the goal of the scoring program, the competition would be more direct. Pattern recognition routines such as those under development in other fields would be one approach to this effort. The other strategy would be to take full advantage of the karyotyping abilities of the existing program and develop dosimetric techniques based on the more sophisticated chromosome analysis procedures. This approach would be especially attractive if it could be shown that reliable dosimetry could be performed by intensive study of a small number of cells, rather than by the superficial investigation of a large number of cells, as is the current practice.

In any event, it has been shown that even with the current state of the art, it is possible to digitize, store, and transmit cytogenetically useful images. Even if no further advances are made in the area of automated scoring, it is seen that the unique radiobiological environment represented by the Space Station could be exploited by sending digitized images to the ground for analysis.

REFERENCES

Bettega 1981 - "Chromosome Aberrations Induced by Protons up to 31 MeV in Cultured Human Cells", D. Bettega, S. Dubini, A. M. F. Conti, T. Pelucchi, and L. T. Lombardi, Radiat. Environ. Biophys. 19, 91-100, 1981

Brewen 1982 - "Chromosome Aberrations in Mammals as Genetic Parameters in Determining Mutagenic Potential and Assessing Genetic Risk." Progress in Mutation Research, Vol. 3, ed. by K. C. Bora, G. R. Douglas, and E. R. Nestman, Elsevier Biomedical Press, Amsterdam, Oxford, New York.

Collins 1980 - "A Case of Child Abuse by Radiation Exposure", V. P. Collins and M. E. Gaulden, in The Medical Basis for Radiation Accident Preparedness, ed by K. F. Hubner and S. A. Fry., Elsevier North Holland Inc. 1980.

Evans 1979 - "Radiation Induced Chromosome Aberrations in Nuclear Dockyard Workers", H. J. Evans, K. E. Buckton, G. E. Hamilton, and A. Carothers. Nature 277, 531-534, 1979

Haffner 1967 - "Radiation and Shielding in Space", James W. Haffner, Academic Press, New York, 1967

Lloyd 1979 - "Radiation Exposure and Chromosome Damage", D. C. Lloyd, Occupational Health, Nov. 1979, pp 504-509.

Lloyd 1980 - "The Incidence of Unstable Chromosome Aberrations in Peripheral Blood Lymphocytes from Unirradiated and Occupationally Exposed People", D. C. Lloyd, R. J. Purrott, and E. J. Reeder, Mutation Research 72, 523-532, 1980.

Pathak 1986 - Sen Pathak, Ph.D., M.D. Anderson Hospital and Tumor Institute, personal communication, 1986.

Prichard 1986 - "Cytogenetic Analyses of Peripheral Lymphocytes Subjected to Simulated Solar Flare Radiation", H. M. Prichard, NASA Contractor Report 17931, July, 1986, pp 23-1 23-9.

1986

NASA/ASEE SUMMER FACULTY RESEARCH FELLOWSHIP PROGRAM

Johnson Space Center

University of Houston

Genetic Toxicity Studies of Organic Chemicals Found as Contaminants in Spacecraft Cabin Atmospheres

Prepared by:	Joseph Torres Jr., Ph.D.
Academic Rank:	Assistant Professor
University & Department:	Southeastern Louisiana University Department of Biological Sciences Hammond, Louisiana 70402
NASA/JSC	
Directorate:	Space and Life Sciences
Division:	Medical Sciences
Branch:	Biomedical Laboratories
JSC Colleague:	Martin E. Coleman, Ph.D.
Date:	August 8, 1986
Contract Number:	NGT-44-005-803 (University of Houston)

GENETIC TOXICITY STUDIES OF ORGANIC CHEMICALS FOUND AS CONTAMINANTS IN SPACECRAFT CABIN ATMOSPHERES

Joseph Torres Jr., Ph.D.
Assistant Professor
Department of Biological Sciences
Southeastern Louisiana University

ABSTRACT

Astronauts can be exposed during spaceflight to organic chemical contaminants in the spacecraft cabin atmosphere. Toxic exposures may cause lesions in the cellular DNA which are subsequently expressed as sister-chromatid exchanges (SCE). Analysis of SCE is a sensitive short-term assay technique to detect and quantitate exposures to DNA-damaging (mutagenic) substances. The increase in SCE incidence over baseline (control) levels is generally proportional to the concentration of the mutagen and to the duration of exposure.

The BHK-21 baby hamster kidney cell line was the in vitro test system used for this study. Test organics were added to the culture media for 18 hours, in concentrations ranging from one to 20 parts per million (ppm). Acetaldehyde and carbon disulfide were chosen for this study since they have occurred as atmospheric contaminants in many of the STS flights, and have been reported to have toxic and mutagenic effects in various test systems. Glutaraldehyde was chosen because few data are available on the mutagenicity of this common fixative, which is carried on STS flights for use in biological experiments. Acetaldehyde was a very strong inducer of SCE at concentrations of 2 ppm and above. Glutaraldehyde and carbon disulfide failed to induce SCE.

INTRODUCTION

Control of potentially toxic exposures to organic chemical contaminants in spacecraft cabin atmospheres is a vital concern to astronauts, who are exposed during spaceflight to a recirculating atmosphere containing trace amounts of numerous organic chemicals.

Analysis of sister-chromatid exchanges (SCE) is a sensitive short-term assay technique to detect and quantitate exposures to mutagenic substances (Perry & Evans, 1975; Latt & Schreck, 1980). The increase in SCE over baseline (control) levels is generally proportional to the concentration of the mutagen and to the duration of exposure. BHK-21, an established baby hamster kidney cell line, was chosen as the in vitro test system. BHK-21 cells are readily maintained in culture, are well-known in the biological literature, and are highly sensitive to toxic or mutagenic substances present in their growth media. BHK-21 cells are also capable of metabolically activating promutagens into mutagenically active compounds.

Acetaldehyde and carbon disufide were selected from a list of more than 70 volatile organics detected during STS flights since they have occurred as contaminants in about half of the STS flights, and have been reported to have toxic or mutagenic effects in various test systems. Glutaraldehyde was chosen because relatively few data are available on the mutagenicity of this common biological fixative, which is carried on STS flights for use in biological experiments. This study proposed to test the genotoxic effects of acetaldehyde, glutaraldehyde,

and carbon disulfide -- i.e., their ability to alter or damage cellular DNA or chromosomes. Discovery of significant genetic toxicity of any of these compounds would be an important factor in determining the appropriate spacecraft maximum allowable concentration (SMAC) limit.

MATERIALS AND METHODS

BHK-21 baby hamster kidney cells were obtained from the Biochemistry Department of the M.D. Anderson Hospital, Houtson, Texas. Cells were cultured in RPMI-1640 medium supplemented with 10% fetal calf serum (FCS) and maintained in a 37°C incubator in a humidified atmosphere of 5% carbon dioxide and 95% air.

Cell population doubling times were calculated from cell counts done on a Coulter model Zf electronic particle counter.

The following SCE studies were carried out: (1) Negative controls, to determine the baseline SCE levels and the optimum exposure period for the test chemicals, (2) Positive controls, using 10 to 500 micromolar concentrations of cyclophosphamide, a known mutagen which requires metabolic activation in order to produce SCE, and (3) Tests with acetaldehyde, glutaraldehyde, and carbon disulfide, in 1 to 20 parts per million (ppm) concentrations, to test for induction of SCE.

SCE staining was done by the standard "fluorescence-plus-Giemsa" techniques currently used to resolve SCE for light microscopy (Kato, 1974; Perry & Wolff, 1974). Cells were exposed to bromodeoxyuridine (BrdU) for two cell cycles (approximately 18 hours for BHK-21 cells), followed by metaphase arrest of the mitotic cells with colcemid. Exposure to BrdU

for two S-phases results in metaphase chromosomes in which one sister chromatid contains DNA with BrdU bifilarly substituted for thymidine, the other chromatid unifilarly substituted. This condition is the basis for differential staining techniques in which one chromatid is lightly stained (unifilar BrdU) and the other darkly stained (bifilar BrdU).

BHK-21 cells were exposed in darkness (in aluminum foil-wrapped flasks) for 18 hours to either BrdU (5 ug/ml) alone (controls) or to BrdU plus either 1 ppm, 2 ppm, 5 ppm, 10 ppm, or 20 ppm of one of the test organics. Colcemid (0.1 ug/ml) was added for the final two hours. The cells were harvested by mitotic shake-off and centrifuged (5 minutes at 200 x g); then washed once in phosphate-buffered saline (PBS) and re-centrifuged. The cells were incubated in hypotonic solution (20% FCS) for 15 minutes at 37°C. The cells were finally centrifuged, resuspended in about 0.5 ml of hypotonic solution, and fixed with a 3:1 mixture of methanol:acetic acid (4°C). Chromosome spreads were prepared by dropping the cell suspension onto cleaned, wet microscope slides. The slides were air-dried and then stained with Hoechst 33258 (5 ug/ml in pH 6.8 phosphate buffer) for 20 minutes. They were then exposed for 1 hour to ultraviolet light (the germicidal UV lamp in the tissue culture hood), incubated in a 62°C water bath for 2 hours, and stained with 3% Giemsa in pH 6.8 buffer for 25 minutes. Slide preparations were air-dried and coverslipped.

SCE were scored by counting the number of times the polarity of light- vs. dark-staining segments was reversed, each marking a symmetrical interchange of material between sister chromatids. The number of SCE in 30 well-differentiated spreads was counted, averaged, and expressed as

the number of SCE per cell. Statistical significance was determined using a t-test ($p < .05$, with 58 degrees of freedom).

RESULTS

Control BHK-21 cells grew rapidly in culture, with population doubling times of 9 to 10 hours. Exposure to BrdU for 18 hours gave the best proportion of completely-differentiated SCE spreads, and this exposure time was used throughout the study. BHK-21 metaphase spreads contained complements of 44 chromosomes (metacentric, submetacentric, and telocentric, with a single large metacentric X chromosome), consistent with published karyotypes of the BHK-21 cell line.

Exposure of BHK-21 cells to cyclophosphamide (Table 1; Fig. 1) showed a very strong exponential dose-response to CP, with 10 uM and higher concentrations inducing significant numbers of SCE. CP was used as a positive control to confirm the ability of the BHK-21 cells to metabolically activate a known mutagen.

Exposure of BHK-21 cells to acetaldehyde (Table 2; Fig. 2) also showed a strong exponential dose-response. Concentrations of 2 ppm (17.7 uM) acetaldehyde and above induced significant numbers of SCE. Cells exposed to 20 ppm (177 uM) acetaldehyde had too many SCE to accurately count (about 65 SCE per cell).

BHK-21 cells exposed to 1 to 10 ppm glutaraldehyde (14.5 to 145 uM) did not show increased SCE rates (Table 3). Neither did cells exposed to 1 to 20 ppm carbon disufide (16.6 to 166 uM) (Table 4). However, BHK-21 cells exposed to 20 ppm glutaraldehyde (290 uM) were severely inhibited in cell division.

TABLE 1: SISTER-CHROMATID EXCHANGES IN BHK-21 CELLS EXPOSED TO CYCLOPHOSPHAMIDE FOR 18 HOURS IN VITRO

Cyclophosphamide concentration (uM)	SCE per cell (mean ± s.d.)	t-test versus Control	
		t-value	significance
0 (Control)	4.47 ± 2.01		
10	5.93 ± 2.19	2.69	n.s.
50	7.16 ± 2.10	4.97	$p < .01$
100	8.07 ± 2.05	6.86	$p < .0001$
250	13.97 ± 4.68	10.21	$p < .0001$
500	20.93 ± 5.01	16.19	$p < .0001$

TABLE 2: SISTER-CHROMATID EXCHANGES IN BHK-21 CELLS EXPOSED TO ACETALDEHYDE FOR 18 HOURS IN VITRO

Acetaldehyde concentration ppm (uM)	SCE per cell (mean ± s.d.)	t-test versus Control	
		t-value	significance
0 (Control)	7.16 ± 2.36		
1 (17.77)	6.73 ± 1.91	0.776	n.s.
2 (35.54)	9.90 ± 3.33	3.667	$p < .0005$
5 (88.85)	14.87 ± 4.29	8.625	$p < .0001$
10 (177.7)	26.06 ± 7.68	12.877	$p < .0001$

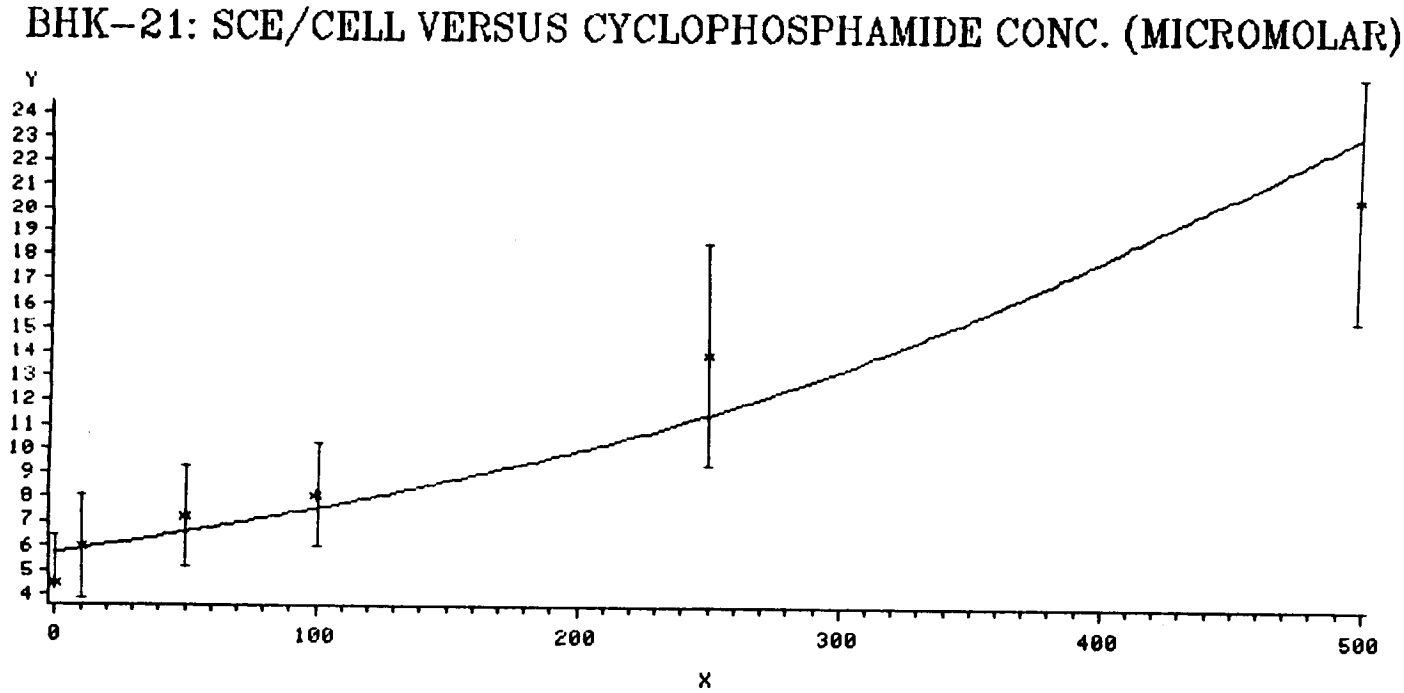

Figure 1: BHK-21: SCE induction by cyclophosphamide, 18 hours in vitro. SCE/cell versus concentration (micromolar).

Exponential regression: $Y = A * e^{BX}$ with A = 5.707, B = 0.003, and correlation coefficient, r = 0.960.

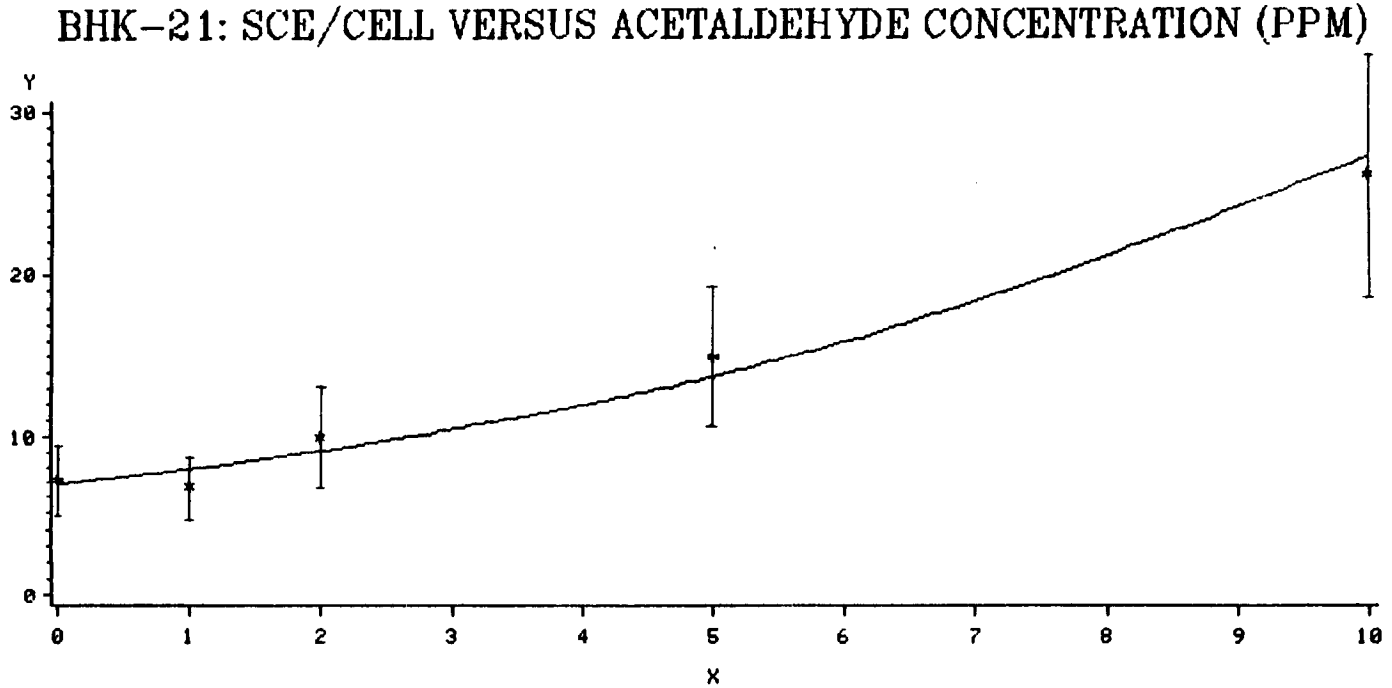

Figure 2: BHK-21: SCE induction by acetaldehyde, 18 hours in vitro. SCE/cell versus concentration (ppm).

Exponential regression: $Y = A * e^{BX}$ with A = 6.932, B = 0.137, and correlation coefficient, r = 0.983.

TABLE 3: SISTER-CHROMATID EXCHANGES IN BHK-21 CELLS EXPOSED TO GLUTARALDEHYDE FOR 18 HOURS IN VITRO

Glutaraldehyde concentration ppm (uM)	SCE per cell (mean ± s.d.)	t-test versus Control	
		t-value	significance
0 (Control)	5.30 ± 1.78		
1 (14.5)	5.70 ± 1.29	0.998	n.s.
2 (29.0)	6.06 ± 2.00	1.554	n.s.
5 (72.5)	5.20 ± 2.00	0.204	n.s.
10 (145.0)	5.90 ± 2.11	1.190	n.s.

TABLE 4: SISTER-CHROMATID EXCHANGES IN BHK-21 CELLS EXPOSED TO CARBON DISULFIDE FOR 18 HOURS IN VITRO

Carbon Disulfide concentration ppm (uM)	SCE per cell (mean ± s.d.)	t-test versus Control	
		t-value	significance
0 (Control)	6.57 ± 1.65		
1 (16.59)	6.13 ± 2.01	0.928	n.s.
2 (33.17)	6.20 ± 1.99	0.785	n.s.
5 (82.94)	6.03 ± 1.84	1.199	n.s.
10 (165.9)	6.10 ± 2.29	0.910	n.s.
20 (331.7)	6.13 ± 1.83	0.980	n.s.

DISCUSSION

BHK-21 cells are a rapidly-growing, easily maintained permanent cell line, and are sensitive to the effects of genotoxic agents in their growth medium. BHK-21 cells are able to metabolically activate indirect mutagens such as cyclophosphamide, presumably through the activity of mixed-function oxidase (MFO) enzymes. The exponential dose-response of BHK-21 cells to cyclophosphamide, with a minimum effective concentration of 10 uM, is apparently equal to the dose-response of several hepatoma cell lines, which are known known to possess MFO enzymes (Abe et al., 1983). Cyclophosphamide is a powerful anticancer agent, which acts by alkylating DNA.

Acetaldehyde is a direct-acting mutagen which has been identified as a cross-linker of DNA (Ristow & Obe, 1978). It is an inducer of SCE in relatively low concentrations — about 40 micromolar for human lymphocytes and fibroblasts in culture (Veghelyi & Ostovics, 1978) and about 35 micromolar for BHK-21 cells. Acetaldehyde was a much stronger inducer of SCE than cyclophosphamide (Fig. 3); this effect may be attributable in part to the direct-acting mechanism of acetaldehyde in producing SCE. The mutagenic potential of acetaldehyde should be considered in conjunction with its toxic and irritating properties in setting exposure limits (current SMAC 30 ppm). However, acetaldehyde should not present toxicity problems in spacecraft cabin atmospheres, since the source of acetaldehyde is attributed to offgassing from plastic materials in the cabin, and measured acetaldehyde concentrations

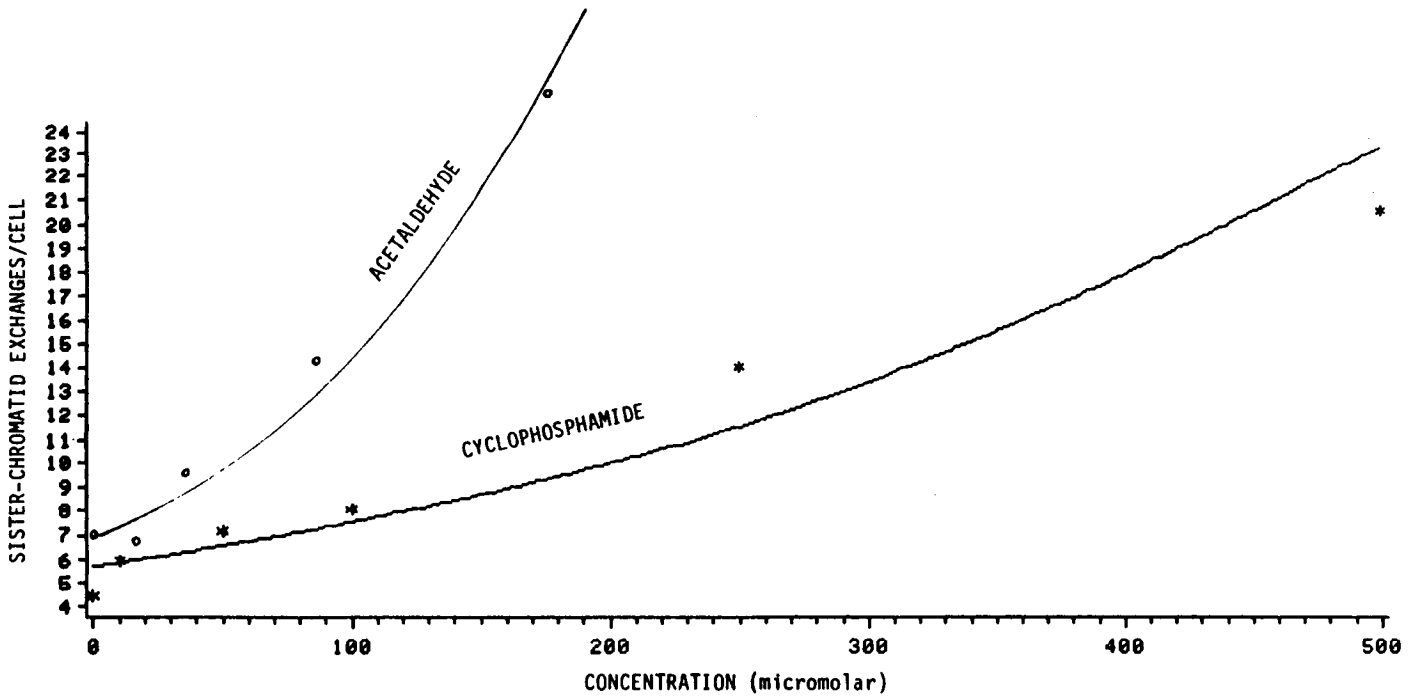

Figure 3: BHK-21: Comparison of SCE induction by acetaldehyde and cyclophosphamide, 18 hours in vitro. SCE/cell versus concentration (micromolar).

have been low (maximum 0.31 ppm, average approximately 0.15 ppm).

Glutaraldehyde is a common fixative which is carried on STS flights for use in biological experiments. It is a highly irritating compound, with low SMAC limits (0.098 ppm), but was negative for induction of SCE in BHK-21 cells exposed for 18 hours to from 1 to 20 ppm glutaraldehyde. Likewise, it was found to be negative for SCE induction in Chinese hamster ovary (CHO) cells in 0.6 to 2.5 uM concentrations, with and without S-9 mix (rat liver microsomal enzymes added to provide metabolic activation) by Slesinski et al. (1983). They found that 5 uM glutaraldehyde produced excessive mitotic inhibition to carry out the SCE test. BHK-21 cells were much less sensitive to the antimitotic effects of glutaraldehyde than were CHO cells; concentrations of 20 ppm (290 uM) halted mitosis and prevented spreading of the chromosomes. Glutaraldehyde is a strong cross-linking agent of proteins and most likely interacts with proteins in the cell membrane and cytoplasm, making interactions with DNA unlikely (Slesinski et al., 1983).

Carbon disulfide has been found in minute concentrations in spacecraft cabin atmospheres (about 0.001 ppm when present) apparently from offgassing from plastic materials in the cabin. It is a potent neurotoxin, with SMAC limits of 0.96 ppm. Carbon disulfide failed to induce SCE in BHK-21 cells following 18-hour exposures to 1 to 20 ppm concentrations (16 to 331 uM).

CONCLUSIONS

The BHK-21 baby hamster kidney cell line is a useful model system for in vitro genetic toxicology research. BHK-21 cells are capable of metabolically activating indirect mutagens such as cyclophosphamide.

Neither glutaraldehyde nor carbon disulfide induced sister-chromatid exchanges during 18-hour exposures to 1 to 20 ppm concentrations of these chemicals. No modification of SMAC limits for glutaraldehyde or carbon disulfide are suggested by these preliminary results.

Acetaldehyde strongly induced sister-chromatid exchanges in BHK-21 cells, in concentrations as low as 2 ppm (35 uM). These findings are consistent with similar SCE studies in the literature which confirm that acetaldehyde is a strong inducer of SCE even at relatively low concentrations. The SMAC limits for acetaldehyde should be considered for toxicological review in light of the significant mutagenic potential of this compound.

REFERENCES

Abe, S., Nemoto, N. & Sasaki, M. (1983). Sister-chromatid exchange induction by indirect mutagens/carcinogens, aryl hydrocarbon hydroxylase activity, and benzo(a)pyrene metabolism in cultured human hepatoma cells. Mutation Research, 109, 83-90.

Kato, H. (1974). Spontaneous sister chromatid exchange detected by a BUdR-labelling method. Nature, 251, 70-72.

Latt, S.A. & Schreck, R.R. (1980). Sister chromatid exchange analysis. Annual Review of Human Genetics, 32, 297-313.

Perry, P. & Evans, H.J. (1975). Cytological detection of mutagen-carcinogen exposure by sister chromatid exchanges. Nature, 258, 121-125.

Perry, P. & Wolff, S. (1974). New Giemsa method for differential staining of sister chromatids. Nature, 251, 156-158.

Ristow, H. & Obe, G. (1978). Acetaldehyde induces cross-links in DNA and causes sister-chromatid exchanges in human cells. Mutation Research, 58, 115-119.

Slesinski, R.S., Hengler, W.C., Guzzie, P.J. & Wagner, K.J. (1983). Mutagenicity evaluation of glutaraldehyde in a battery of in vitro bacterial and mammalian test systems. Food and Chemical Toxicology, 5, 621-629.

Veghelyi, P.V. & Ostovics, M. (1978). The alcohol syndromes: The intrarecombigenic effect of acetaldehyde. Experientia, 34, 195-196.

1986

NASA SUMMER FACULTY FELLOWSHIP PROGRAM

Johnson Space Center

University of Houston

Affirmative Action As Organization Development At the Johnson Space Center

Prepared by:	Mfanya Donald L. Tryman, Ph.D.
Academic Rank:	Associate Professor
University & Department:	Prairie View A & M University Benjamin Banneker Honors College
NASA/JSC	
Program Office:	Equal Opportunity Programs Office
JSC Colleague:	Joseph D. Atkinson, DPA
Date:	July 25, 1986
Contract #:	NGT 44-005-803 (University of Houston)

AFFIRMATIVE ACTION AS ORGANIZATION DEVELOPMENT AT THE JOHNSON SPACE CENTER

(ABSTRACT)

This project investigated the role of affirmative actions as an interventionist Organization Development (OD) strategy for insuring equal opportunities at the NASA/Johnson Space Center. In doing so, an eclectic and holistic model is developed for the recruiting and hiring of minorities and females over the next five years. The strategy, approach, and assumptions for the model are quite different than those for JSC's five year plan.

The study concludes that Organization Development utilizing affirmative action is a valid means to bring about organizational change and renewal processes, and that an eclectic model of affirmative action is most suitable and rational in obtaining this end.

AFFIRMING EQUAL OPPORTUNITY:

A Futuristic Plan

Affirming, or reaffirming, equal opportunity among racial, ethnic and minority groups at NASA is obviouly a clearcut goal. This has not been simply rhetorical statements used as a means to mollify minorities and females. Or, for that matter, to give the appearance of being in compliance with Federal law. It is clear that the NASA-JSC has made progress (through uneven) in the area of affirmative action and equal opportunity. The policy statement for the last five year plan reads as follows:

> The National Aeronautics and Space Administration (NASA) Johnson Space Center (JSC) is dedicated to achieving its technical mission with a fully integrated work force. JSC's policy is to provide equal employment opportunity for all persons regardless of race, color, religion, sex, age, national origin, or handicap...
>
> JSC will provide sufficient resources to administer an effective Affirmative Action Program, including making center facilities accessible to handicapped individuals. All JSC employees, managgers and supervisors at all levels are expected to support affirmative actions to insure that the objectives of equal employment become a reality.[1]

It is not unreasonable to expect that NASA will have a similar policy statement for the next five years, inclusive of FY87 to FY91. It is important to mention that under the 1964 Civil Rights Act, and as recently as May of 1986, the U.S. Supreme Court indicated that on-the-job racial preferences in hiring and promoting are still constitutional in order to remedy the effects of past discrimination. Hence, the policy statement should note that there will be equal promotional as well as equal employment opportunity.

It should be noted that a broad-based view of affirmative action must examine conceptual, social, economic and organizational components of affirmative action, each of which are worthy of brief discussion here.

Conceptual

Affirmative action is designed to provide minorities, females and the handicapped with the same preferential treatment (ceteris paribus) that white males traditionally and historically have enjoyed. It should not be felt that affirmative action as a legal component can remedy in a short time institutionalized racial discrimination that dates back to, and was part of, the U.S. Constitution that was ratified in 1789.

Social

It is at the societal level where racial discrimination is the most pervasive and deeply rooted. Social values are developed early in life at the familial level and reinforced by peer groups, public schools, co-workers, friends, and, inter alia, institutions of higher education. Social values influence our cultural values, which often results in ethnocentrism and stereotypical attitudes and behavior. It is from attitudinal predispositions that one begins to divide races, sexes and ethnic groups into hierarchical social classes based upon positions and roles of the group in question.

Racial and gender discrimination tend to be individual as well as institutional, and while individuals may assert that they harbor no ill feelings or prejudicial attitudes toward minorities and females, it is the institutions or collective entities noted above that are less innocuous. These institutions educate and train whole generations of people in, subliminally and overtly, in the development of racial attitudes and discriminatory practices.

Economic

Affirmative action assists in closing the economic gap between minorities and non-minorities, on the one hand, and males and females on the other hand. One of the most glaring inequalities in America has been economic in nature, due to past and the on-going effects of present discrimination. Statistics tend to indicate that the income gap between the Black and white family in America is increasing rather than decreasing. In the seventies Black family income had reached 62% of that for its white counterpart. In 1982, Black family income had dropped to 55% of that for white families.[2]

Affirmative action programs that seek to be effective must be aggressive not only in hiring minorities and females in institutional settings, but in promoting them as well. It is clear that as one goes up the organizational ladder, the pyramidal structure tends to have less and less minorities and females as the apex is approached. Affirmative action has been less successful in this respect, even at NASA-JSC.

Organizational

Effective affirmative action programs result in better racial and human relations between various groups of people as well as understanding of cultural relativism. Such an integrative

approach can result in better informal human relations as well. Affirmative action is, contrary to its critics, a democratic principle designed, in part, to insure more equal representation in the workplace. Ideally, ethnic, racial and gender representation in the workforce and organizational settings should be comparable to the more general representation of these groups as a whole in society. While this cannot always be done, there are alternative ways and means of setting affirmative action hiring goals, which will be addressed later in this study. The use of T-Groups, outside consultants, other Organization Development (OD) strategies, and the role of the Equal Opportunity Programs Office must continue to be catalysts of change in organizational settings.

The JSC Five-Year Plan

Strategy

The Johnson Space Center strategy for the next five years is: 1) to continue with proven approaches through a) college recruiting, and b) the co-op program; 2) to begin focusing more attention on the Asian /Pacfic Islander group by a) determining where they are, and b) conducting targeted recruiting activities; and 3) to closely monitor plans and

accomplishments for all groups by a) close coordination between the EO office and Personnel office, and b) regular feedback to management and employees.[3]

Approach

This strategy will be pursued through the following approach:

1) recruitment of the "highest quality" (my quotations) candidates will be number one priority,

2) continuing progress in all minority/female areas (groups),

3) a special emphasis upon non-minority females and Asian/Pacific Islanders, and

4) an annual increase of approximately 20 minority/female positions.[4]

Assumptions

The following asumptions, both implicit and explicit, are built into the JSC five year plan:

1) minority scientists and engineers will be hired in their field if NASA does not hire them,

2) census and other data are correct and accurate in reporting data regarding the status of minorities,

3) minority scientists and engineers are not underemployed even when hired in their respective fields,

4) racial discrimination is not a factor in minorities and women finding

jobs in their fields,

5) a constant workforce strength, and

6) a 5.5% turnover for non-minority males and a 4.5% turnover for minorities and females.

The strategy, approach, and assumptions discussed here relate primarily to the recruitment of minorities and females in the areas of science and engineering. Science and engineering are easily the largest occupational categories at NASA Johnson Space Center. Table I reflects the breakdown of various scientific and engineering representation models based upon the work force in the population at-large, compared with data developed by the Assistant Administrator for the Office of Equal Opportunity Programs at NASA headquarters in Washington, D.C. These data reveal statistics broken down by race, ethnicity, and gender.

As of January 1986, minorities and females made up 18.5% of the scientists and engineers at JSC. Non-minority females make up the largest category with 148 (7.5%) employees. Black males, along with Hispanic males, constitute the second largest numbers with 76 and 75 workers respectively (3.8% each). Other than non-minority females, Black female scientists and engineers make up 21 (1.1%), Hispanic females

TABLE I

JSC SCIENTIFIC & ENGINEERING WORK FORCE
A COMPARISON OF VARIOUS REPRESENTATION MODELS

MODEL	NM		BLACK		HISPANIC		A/PI.		AM. IND.	
	M	F	M	F	M	F	M	F	M	F
ON-BOARD STRENGTH AS OF 1-28-86	81.5%	7.5%	3.8%	1.1%	3.8%	.5%	.9%	.4%	.5%	.1%
	1611	148	76	21	75	10	18	8	9	1
CENSUS	82.4%	7.6%	2.4%	.6%	2.0%	.3%	4.0%	.4%	.2%	.0%
	1629	149	47	12	40	5	79	9	4	0
ΔON-BOARD	+18	+1	-29	-9	-35	-5	+61	+1	-5	-1
COLLEGE GRADS. (80-81 YEAR)	73.5%	15.9%	2.6%	1.0%	1.6%	.3%	3.8%	.9%	.2%	.05%
	1493	314	51	20	32	6	75	18	4	1
ΔON-BOARD	-118	+166	-25	-1	-43	-4	+57	+10	-5	0
60 COLLEGE/40 CEN.	77.1%	12.6%	2.5%	.8%	1.8%	.3%	3.9%	.7%	.2%	.03%
	1524	249	51	16	36	6	77	14	4	1
ΔON-BOARD	-87	+101	-25	-5	-39	-4	+59	+6	-5	0
HARRIETT JENKINS	70%	14%	4%	1.5%	4%	1.1%	4%	.8%	.5%	.1%
	1384	277	79	30	79	22	79	16	10	2
ΔON-BOARD	-227	+129	+3	+9	+4	+11	+61	+8	+1	+1

SOURCE: JOHNSON SPACE CENTER 1986

10 (.5%), Asian/Pacific Islanders 8 (.4%), and American Indian females 1 (.1%). Proportionately speaking to the S&E total workforce at JSC, minority women tend to be the most underrepresented. In fact, based upon JSC's data, minority women constitute a total of only 2.1% of the workforce compared to 7.5% non-minority females. As a whole, women in the aggregate make-up 9.6% of the scientists and engineers.

The JSC fares better in some of the minority and female categories than the other representative models and worse in other categories vis a' vis these models. However, the workforce groups at JSC appears to be comparable or at a higher percent for most of the models. The exception tends to be with non-minority females and Asian/Pacific Islanders. It is these two groups, of course, that have been targeted for the next five year plan.

The initial proposal put forth by Harriet G. Jenkins (Assistant Administrator) seems to allow for the fact that minority females are grossly underrepresented at the JSC vis a' vis other groups. This model allows for anywhere from one to 11 new hires over the next five years for the various categories of minority females and 129 new hires for non-minority females.

Table II reflects JSC's counter-proposal to Jenkins' initial plan. One thing that is immediately clear is that JSC's

TABLE II

COUNTER JSC MINORITY AND

FEMALE RECRUITMENT PLAN

Group	Current-1986	Five Year Projection		
Number				
NMM	81.5%	76.4%	-	100
NMF	7.5%	10.7%	+	64
BM	3.8%	3.9%	+	1
BF	1.1%	1.2%	+	3
HM	3.8%	3.9%	+	2
HF	.5%	.6%	+	4
A/PI M	.9%	2.0%	+	22
A/PI F	.4%	.6%	+	4
NAM	.5%	.5%	+	1
NAF	.1%	.1%	+	1

Source: Personnel Department, Johnson Space Center, 1985

counter-proposal would reduce the non-minority male workforce by only 5.1% whereas Jenkins' plan would reduce this group of workers by more than twice this percent (11.5%). All

minority groups and specifically minority females would not fare as well under JSC's counter-proposal. Obviously, non-minority males and females would make the biggest gains under this proposal. Ironically, Asian/Pacific Islander males would have been hurt the most under the initial JSC counter-proposal.

Table III reveals data from Tables I and II above as well as Jenkins' second proposal, followed by JSC's recommended proposal. Jenkins' second proposal reduces her original number of non-minority females from an increase of 124 (14% of the workforce) to 68 (11% of the workforce) with almost all other categories maintaining roughly the same percents, except for non-minority males which would experience a 4.5% increase. The final recommended proposal that NASA-JSC has settled on is a partial compromise between Jenkins' second proposal and the JSC's counter-proposal. This is applicable to the non-minorities, Blacks and Hispanic males in particular, and to a lesser extent with American Indians, though this latter category is almost statistically insignificant because of the low number and percent that they constitute of the total workforce.

TABLE III

S&E'S
5 YEAR PLANS

Plan	Nonminority		Black		Hispanic		A/PI		Am. Ind.	
	M	F	M	F	M	F	M	F	M	F
Harriett's First Proposal (would require 62% M/F new hires)	70.0% -227	14.0% +129	4.0% +3	1.5% +9	4.0% +4	1.1% +11	4.0% +61	.8% +8	.5% +1	.1% +1
JSC Counter Proposal (would require 35% M/F new hires)	76.4% -100	10.7% +64	3.9% +1	1.2% +3	3.9% +2	.6% +2	2.0% +22	.6% +4	.5% +1	.1% +1
Harriett's Second Proposal (would require 42% M/F new hires)	74.5% -138	11.0% +68	4.3% +9	1.4% +7	4.0% +4	.8% +6	2.5% +31	.9% +10	.5% +1	.1% +1
JSC Recommended Proposal (would require 36.8% M/F new hires)	75.8% -112	11.0% +68	4.0% +3	1.4% +7	4.0% +4	.6% +2	2.0% +22	.6% +4	.5% +1	.1% +1

SOURCE: JOHNSON SPACE CENTER 1986

Under the JSC recommended proposal, non-minority males and females are the biggest beneficiaries. This proposal increases the percent of non-minority males 5.8% over the Assistant Administrator's first proposal, through the percent of women hired will actually be 3% less. It is interesting to note that, although JSC has emhasized recuiting Asian/Pacific Islander's over the next five years, the JSC recommended proposal will cut the total number hired from 69 in Jenkin's first proposal to 26, a reduction of 43 new recruits. This is a reduction of almost two-thirds (62.5%). At the same time, while the five year plan will double the number of Asian/Pacific Islanders, this is not the case with the other targeted group, non-minority females. Their number will decrease from the 129 proposed in Jenkin's proposal to 68 in the JSC proposal, a reduction of 61 non-minority females since the numbers and percent for the other minority groups will remain generally the same. It appears that the increase in the numbers and percent for non-minority males will be at the expense of non-minority females and Asian/Pacific Islanders--the targeted groups.

Table IV reflects the annual EO hiring goals for scientists and engineers over a 5 year period and over a 10 year period. Depending upon the plan and workforce model

used, this would mean hiring anywhere from 28% to 62% minorities and females over a five year period and from 22% to 38% over a ten year period.

TABLE IV

ANNUAL EO HIRING GOALS FOR

SCIENTISTS AND ENGINEERS

5 Year Approach

Census Plan	College Grad Plan	60/40 Plan	Harriet Jenkins Plan
28%	60%	47%	62%

10 Year Approach

22%	38%	31%	31%

Source: Johnson Space Center 1986

Obviously, the plan that is most favorable toward minorities and females is Jenkins' plan and the college graduation plan. These plans project the most optimistic approach regarding equal opportunity and affirmative action. The least favorable approach regarding minorities and females is the census plan, which has projections that would more than cut in half affirmative action hiring over the next five years

relative to Jenkins' plan, and project less than two-thirds the number hired over a ten year period, compared to Jenkins' plan.

Weaknesses of the Five Year Plan

The five year plan suffers from a number of weaknesses which could be remedied through the development of an alternative plan that would be more eclectic and holistic in nature. Before turning to such a plan, though, it is prudent to examine the weaknesses of the five year plan at the JSC.

Perhaps unwittingly, an unintended consequence of the five year plan recommended by the JSC is that it will create greater disparities in numbers and percents between non-minority males/females and Asian/Pacific Islanders, on the one hand, and Blacks, Hispanics and American Indians, on the other hand. By doing this, "affirmative action" will be bridging the gap between the dominant group (non-minority males) and minority female groups while at the same time developing larger inequities between non-minority females and minority and minority female groups. The primary goal of affirmative action is to allow those groups that historically

have been victims of discrimination to "catch-up" with white males, who traditionally have enjoyed preferential treatment.

The rationale for this pattern of recruitment and hiring, of course, lies in the argument that minority and minority female groups are not producing scientists and engineers in the population at-large. There are, however, several problems associated with this rationale. One, it must be assumed that census figures are correct since they are used to make projections. Two, such a rationale does not take into account the intensity and length of time of discrimination against minorities and minority-female groups. And three, while various representative models are drawn upon in order to make projections for the various minority groups, the recommended plan ultimately involves arbitrary figures.

Each of these points deserve cursory review. Utilization of census figures, or data arrived at using census figures, have come under sharp attack in the past. Critics argue that the methodological approach used to arrive at total minority populations most often undercount the group in question. Cultural as well as social reasons often come into play which census-takers ignore in making estimates. Hence, the use of these data for making projections tend to be unreliable

because of statistical and reporting errors based upon fallacies and inaccurate assumptions.

The second point, regarding intensity and length of time of discrimination, is not addressed in terms of a concrete formula. That is to say, there is no rational compensatory mechanism which addresses or allows for the effects of past discrimination in the plan. This same problem applies to the third point regarding an arbitrary figure. While the use of the various representative model have some value for establishing ballpark figures, there is a need for providing a formula or model using a holistic and more comprehensive approach.

Another weakness of the five year plan is that it attempts to recruit minorities and females based upon statistical data (even assuming the data is correct) which does not account for institutional barriers which may limit the number of minorities and females entering into, and graduating from, schools of science and engineering. Prima facie as well as invidious and more subtle forms of discrimination occur not only in the job sector, but in higher education as well. Colleges and universities with science and engineering programs and majors, like other entities in higher education,

have not been exempt from discriminatory practices. As noted in Chapter II, part of the 1964 Civil Rights Act was designed to specifically address discrimination in institutions of higher learning. Since affirmative action involves, in part, a compensatory component, it would seem that a five year plan would need to address the institutionalization of discrimination and the negative impact thereof.

How will the more pervasive forms of racial and gender discrimination be addressed involving women who are females, on the one hand, and minorities on the other hand in the five year plan? Asian/Pacific Islander women and Hispanic women, for instance, are two categories of people who face dual discrimination as minorities and as women. What recruitment formula would best reflect their social status and representation in the population? Dual discrimination represents a more vexing problem that should be addressed in affirmative action plans in a manner that reflects their "double-negative" status in the profession as well as society as a whole. Black females, historically the most severely discriminated against double minority, will make only a miniscule gain in the five year plan. Their representation in the JSC workforce would rise from a mere 1.1% in 1986 to 1.4% in 1991. This situation is similar for other females at

the JSC.

The approach of the JSC affirmative action plan is one which states that it will seek the "highest quality" candidates as the number one priority over the next five years. However, the phrase "highest quality" is left undefined and subject to interpretation. While it has been stated by JSC that the EO goals are flexible, it is not clear how flexible these goals are. If equal opportunity means, at the JSC, that when there are two equally qualified candidates, one a non-minority male and the other a minority male, the latter will get the job, then such thinking would be in line with the traditional approach and conceptual underpinnings of affirmative action. In juxtaposition to this scenario, if a non-minority female (targeted group) and a minority female (facing dual discrimination) with equal credentials apply for a single slot, which candidate should get the position? Again, it seems that such instances beg for a more definitive formula for recruiting and hiring when a more complex recruiting situation exists.

Affirming Equal Opportunity:

An Eclectic Model

Strategy

The strategy of the five year plan is well designed except for emphasizing Asian/Pacific Islanders. An alternative viable strategy would address concentrating and emphasizing all minority and female groups in recruitment and hiring as opposed to selectively recruiting in sub-areas of these categories.

Approach

The approach for this model would emphasize: 1) quality as determined by candidates graduating at or near the top of their class, 2) targeting those minority and female groups that historically as well as currently are impacted by discrimination, 3) putting forth a special effort to recruit and hire candidates who encounter dual discrimination, and 4) constructing an objective and rational model for determining the number and percent of minorities and females to be hired, involving a compensatory variable that is congruent with the letter and spirit of affirmative action.

Assumptions

The holistic (eclectic) model developed here, in contradistinction to the five year plan, would inculcate the following premises:

1) a higher percent of minorities and women should be hired than the actual percent graduating from schools of science and engineering,

2) a holistic approach is a more representative and equitable means of addressing the "misrepresentation" of minorities and women,

3) a compensatory variable/percent is a valid means of addressing the historical and institutional discrimination against minorities and women,

4) a holistic model is more compatible and consistent with OD, and

5) developing a statistical mean based upon a diversity of statistics and sources is a more valid means for establishing hiring goals.

Limitations of the Model

1) The model is developed for NASA-JSC, though it may be applicable to other centers.

2) The data for the variables differ in years, which may affect the mean.

3) Sources for the data differ, which could affect the mean.

4) The model provides examples for Blacks and women engineers only, but would utilize the same formula for the other

minority and minority female goups.

Rationale for the Model

The formula or equation for the model constitutes the following variables: 1) population at-large, 2) college graduates, 3) NASA employees, 4) compensatory adjustment, and 5) percent of minority-female S&E's employed. These variables combine representative numbers in the population at-large and NASA-JSC with the actual numbers graduating from college and those employed in science and engineering. This approach is more consistent with affirmative action plans, which usually attempt to design programs which reflect the representation in the community--in this case the national population and Federal government. This approach for the model attempts to achieve parity with representative figures in the social structure and professionals in government. Affirmative action is turned on its head when attempts are made to use indigenous institutional data for on-board minority and female projections as the sine qua non for recruiting and hiring.

Variables

Population at-large (PAL). The percent of the minority or female group as represented in the general population (e.g.,

Blacks make-up 12% of the U.S. population).

College graduates (CG). The percent of the minority or female group that graduates from colleges and universities in a given year in science and engineering.

NASA employees (NASA). The percent of minority and female scientists and engineers currently on-board at NASA-JSC.

S&E's in workforce (S&E's). The percent of minorities and females in science and engineering in the active labor force.

Compensatory adjustment (CA). This variable constitutes a combination of historical, social, institutional and workforce-related structural factors. Historical as meaning a way to compensate for past discrimination. Social as used here relating to societal values that contribute to and influence the continuing pervasiveness of discrimination. Institutional relates, in the context used here, to organizational cultures that influence discriminatory attitudes. Structural relates to employment factors in the labor force that discriminate against minorities and females. The compensatory adjustment would weigh one percent for minorities and females and two for minority females.

The proposed model of recruitment and hiring for Blacks, than, would consist of the following data:

FIGURE I

BLACK REPRESENTATION MODEL

Year	Variable	(%)
1980	PAL	11.0%
1981	CG	3.6% = 21.9% - 4 = 5.5% +1 = 16.5%
1982	S&E's	2.4% (Mean) (CA)
1986	NASA	4.9%

The model consists of simply taking the four variable percents of PAL, CG, NASA and S&E's and totaling them (21.9), divided by the total number of variables (4) in order to arrive at the mean (5.5%). The mean is added to the compensatory adjustment (CA) variable of plus 1.0% in order to arrive at the final affirmative action recruitment and hiring goal of 6.5% over the next five years for Blacks.

Similarly, the proposed model for females over five years would use the same formula (model) but with the following numbers.

FIGURE II

FEMALES REPRESENTATION MODEL

Year	Variable	
1980	PAL	51.0%
1981	CG	27.3% = 114.3 - 4 = 28.6% + 1.0% = 29.6%
1982	S/E'S	26.4% (Mean) (CA)
1986	NASA	9.6%

It should be kept in mind here that the figure of 29.6% is inclusive of both non-minority females as well as minority females, and the sum total represents females in all of the representative racial and ethnic groups at NASA. Contrary to the JSC plan, the above model projects a recruitment and hiring rate of more than twice the percent of the former plan--29.6% compared to 13.7%. The particular models computed for the female minorities would, as noted earlier, include a CA of plus 2.0 percent.

SUMMARY AND CONCLUSION

In summary, the purpose of this study has been to lay out the JSC policy of equal opportuntiy, discuss a broad-based view

of affirmative action which includes the conceptual, social, economic and organizational underpinnings, examine the JSC five year affirmative action plan, inclusive of the strategy, approach, assumptions, goal projections and weaknesses of the five year plan, and to offer an alternative five year plan.

The alternative five year plan can be viewed as both eclectic and holistic. The strategy, approach, and assumptions for this model are quite different. As with any field of research, normative values of the investigator have a bearing on research findings. Hence, as with the JSC five year plan, the strategy, approach and assumptions of the "interventionist" come into play. However, it may be argued that the OD interventionist brings a more neutral and objective approach for investigating structural and functional aspects of an organization. This is one of the main advantages of OD. The proposed model, as with any model or theoretical treatise, has limitations, and these have been delineated as well. Nevertheless, it has been argued that an eclectic model which takes into account the "best of all worlds" is a more fruitful and prudent avenue for setting affirmative action goals. Of utmost significance, the holistic model takes into account social and institutional factors that impact upon the level and degree of

discrimination. Given the long history and rising tide of racial and sexual discrimination in America, the model proposed here is a modest and reasonable alternative to the JSC plan.

The following conclusions can be reached as a result of this study:

1) OD is a legitimate means of using affirmative action to bring about organizational change and renewal, 2) JSC has come quite a ways in the recruitment and hiring of minorities and women from FY70 to FY85, 3) a higher percent of minorities and females can and should be hired at JSC than that percent actually graduating from colleges and universities, 4) the political environment has made it harder to sustain effective affirmative action programs and easier torationalize doing away with such programs, 5) affirmative action is still a viable tool for integrating the workforce in the public as well as private sector, 6) while there are certain negative perceptions of affirmative action, the posiotive and advantageous factors outweigh the negative and disadvantageous variables, and 7) there are more structured methods of arriving at affirmative action goals which are less capricious and less arbitrary.

NOTES

1. Joseph D. Atkinson, Jr., Multi-Year Affirmative Action Plan FY82 Through 86, Equal Opportunity Programs Office: NASA-Lyndon B. Johnson Space Center, p. 1.

2. Denys Vaughn-Cooke, "The Economic Status of Black America - Is There A Recovery?," in The State of Black America, 1984, New York: National Urban League, Inc., 1984, p. 6.

3. This is part of the Johnson Space Center's proposed modifications affirmative action goals and timetables as of May, 1986. No pages given.

4. Ibid. No page number given.

BIBLIOGRAPHY

AA/Director, "Work Force Representation Objectives," Memorandum to NASA Headquarters: Attention U/Harriett Jenkins, May 14, 1986.

Antieau, Chester J., Federal Civil Rights Acts, Rochester: The Lawyers Co-operative Publishing Co., 1971.

Argyis, Chris, Personality and Organization, New York: Harper and Row, 1957.

Argyris, Chris, "The Organization: What Makes It Healthy?" in Organization Theories, edited by William P. Sexton, Columbus: Charles E. Merrill Publishing Co., 1970.

Argyris, Chris, The Applicability of Organizational Sociology, Cambridge: Harvard University Press, 1972.

Atkinson, Joseph D., Jr., "The State of the Art and Science of Managing Equal Opportunity and Affirmative Action at NASA Johnson Space Center: A Public Policy Issue," Unpublished Paper, June 1, 1979.

Atkinson, Joseph D. Jr., "FY85 Accomplishment Report of Affirmative Action for Minorities and Women, Equal Opportunity Programs Office: NASA-Johnson Space Center.

Atkinson, Joseph D. Jr., "Equal Opportunity Programs Office FY'85 Annual Report," Equal Opportunity Programs Office: NASA-Johnson Space Center, Fiscal Year 1985 Annual Report.

Atkinson, Joseph D., Jr., Multi-Year Affirmative Action Plan FY82 Through FY86, Equal Opportunity Programs Office: NASA-Lyndon B. Johnson Space Center.

Bowe, F., Handicapping America: Barriers to Disabled People, New York: Harper and Row, 1978.

Cartwright, Dorwin, "Achieving Change in People," in Organization Theories, edited by William P. Sexton, Columbus: Charles E. Merrill Publishing Co., 1970.

Davis, Louis E. "Organization Design and Effectiveness," Human Relations, Vol. 30, March, 1977, pp. 261-73.

Eddy, William B., "Beyond Behavioralism? Organization Development in Public Management," Public Personnel Review, July, 1970, pp. 166-74.

Eddy, William B., "Organization Development and Change," in Current Issues in Public Administration, second edition, by Frederick S. Lane, New York: St. Martins Press, 1982.

Etzioni, Amitai, Modern Organizations, Englewood Cliffs: Prentice-Hall, 1964.

French, William L., and Cecil H. Bell, Jr., Organization Development, Englewood Cliffs: Prentice-Hall, Inc., 1973.

Gaborro, J., "Diagnosing Organization - Environment Fit: Implications for Organizational Development," Education and Urban Education, Vol. 6, No. 2, February, 1974, pp. 153-175.

Glazer, Nathan, Affirmative Discrimination, New York: Basic Books, Inc., 1978.

Golembiewski, Robert T., Men, Management and Morality, New York: McGraw-Hill, 1967.

Harvey, James, "Civil Rights, Blacks and the Reagan Administration," in Institutional Racism and Black America, edited by Mfanya Donald Tryman, Lexington: Ginn Press, 1985.

Harvey, James C., "The Stotts Decision and Its Legal Consequences for Human Resources Management," Paper Presented at the American Society for Public Administration Meeting, April 14, 1986.

Hefner, James A., "The Economics of the Black Family," Paper Presented at the Afro-American Family Lecture Series, Jackson, February 7, 1985.

Huse, Edgar F., Organization Development and Change, second edition, St. Paul: West Publishing Co., 1980.

Jones, Edward W., Jr., "Black Managers: The Dream Deferred," Harvard Business Review, May-June, 1986, pp. 84-93.

Knowles, L., and K. Prewitt, Institutional Racism in America, Englewood Cliffs: Prentice-Hall, Inc., 1969.

Lawrence, Paul, and Jay Lorsch, Organization and Environment: Managing Differentiation and Integration, Boston: Harvard University Graduate School of Business Administration, 1967.

Lorsch, J., and J. Morse, Organizations and Their Members: A Contingency Approach, New York: Harper and Row, 1974.

Orfield, Gary, The Reconstruction of Southern Education: The Schools and the 1964 Civil Rights Act, New York: Wiley, 1969.

Presthus, Robert, The Organizational Society, revised edition, New York: St Martin's Press, 1978.

Reed, Rodney J., "Affirmative Action in Higher Education: Is It Necessary?," The Journal of Negro Education, Vol. 52, Summer, 1983, pp. 331-339.

Report of a Special Task Force to the Secretary of Health, Education and Welfare, Work In America, Cambridge: The MIT Press, 1973.

Rogers, Carl, "On Becoming a Person," Boston: Houghton Mifflin Co., 1961.

Rubin, James H., "O'Connor Stance on Affirmative Action Surprising," The Houston Post, May 25, 1986, p. 28A.

Taylor, Frederick W., "The Finest Type of Ordinary Management,"in Organization Theories, edited by William P. Sexton, Columbus: Charles E. Merrill Publishing Co. 1970.

Tryman, Donald L., "Colonialism and 'Reverse Discrimination': A Political Systems Approach," The Western Journal of Black Studies, Vol. 2, No. 1, Spring, 1978, pp. 10-17.

Tryman, Mfanya Donald, "Reversing Affirmative Action: A Theoretical Construct," Journal of Negro Education, Vol. 55, No. 2, Spring, 1986, p. 185-199.

Vaughn-Cooke, Denys, "The Economic Status of Black America - Is There A Recovery?," in The State of Black America, 1984, edited by James D. Williams, New York: National Urban League, Inc., 1984.

Weber, Max, The Theory of Social and Economic Organization, New York: Oxford University Press, 1947.

Weed, Roger O., and Timothy F. Field, "The Differences and Similarities Between Public and Private Sector Vocational Rehabilitation: A Literature Review," Journal of Rehabilitation, Vol. 51, No. 2, April - June, 1985, pp. 19-23.

1986

NASA/ASEE SUMMER FACULTY RESEARCH FELLOWSHIP PROGRAM

Johnson Space Center

University of Houston

Analysis of the Continuous Stellar Tracking Attitude Reference (CSTAR) Attitude Rate Processor

Prepared by:	J. Uhde-Lacovara
Academic Rank:	Assistant Professor
University and Department:	Stevens Institute of Technology Department of Electrical Engineering
NASA/JSC	
Directorate:	Engineering
Division:	Avionics Systems Division
Branch:	Control Subsystems
JSC Colleague:	Charles Price
Date:	August 15, 1986
Contract #:	NGT44-005-803

ANALYSIS OF THE CONTINUOUS STELLAR TRACKING ATTITUDE REFERENCE (CSTAR) ATTITUDE RATE PROCESSOR

J. Uhde-Lacovara
Assistant Professor
Department of Electrical Engineering
Stevens Institute of Technology
Hoboken, N.J. 07030

The Continuous Stellar Tracking Attitude Reference (CSTAR) system is an in-house project for Space Station to provide high accuracy, drift free attitude and angular rate information for the GN&C system. The outputs of the solid state star trackers are processed to provide attitude information; rate data is then derived from the attitude. Rate derivation is based on discrete time polynomial approximation techniques. This gives simple algorithms which allow for interpolation by other users. Attitude rate is modeled as a constant with low amplitude, low frequency sinusoids superimposed.

The rate processor is parameterized to account for the effects of random errors, sample rate, data processing rate and perturbation frequency. The baseline system may be characterized as follows: the three sigma attitude accuracy is 0.01 degrees, the three sigma rate accuracy is 0.0001 degrees per second, the sample rate is 100 Hertz,the sampled signal is bandlimited to 0.5 Hertz, and the data processsing rate is 10 Hertz. The above system requires a differentiator of length 127. This will track rate perturbations of frequencies less than 0.01 Hertz with low systematic errors.

INTRODUCTION

The Orbiter uses rate gyroscopes and accelerometers as sensing devices to provide data for position and attitude control. These instruments need to be periodically updated by inertial reference information from star trackers, because their accuracy drifts with time. An alternative to this traditional system is being developed for Space Station as an in-house project of the Avionics System Division at Johnson Space Center. This project is called CSTAR for Continuous Stellar Tracking Attitude Reference. Drift free, high accuracy attitude information is supplied by using solid state star trackers to continuously track stars.

The CSTAR system requires multiple fields-of-view (f.o.v.) to provide three-axis information with minimal possibility of obscuration. The three sigma accuracy requirements for attitude and attitude rate on Space Station are presently set at 0.01 degrees and 0.0001 degrees per second respectively. This data is to be provided at a rate of 10 Hertz. The current, two f.o.v. breadboard CSTAR system is capable of meeting the three sigma attitude accuracy requirement at the 10 Hertz rate. The breadboard CSTAR uses a modifed charge injection device (CID) television camera. Attitude rate is to be derived from the attitude information to provide backup for the rate gyroscopes. The attitude rate processor at the sensor level is to meet the accuracy and sampling rate requirements in a reasonable frequency range. It is not intended to be a sophisticated, adaptive type processor which meets the very specific needs of individual users. Examples of these types of processors may be found in the references [1,2].

THEORY

An attitude rate processor must perform the operation of differentiation on the attitude data. This may be treated as a numerical analysis problem in the discrete time domain where the samples are equally spaced. Shannon's sampling theorem is of prime importance [3,4]. The system will not be able to accurately reproduce or process any data which has frequency components greater than one half of the sampling frequency. The steady state transfer function of a differentiator is given by

$$H(e^{j\omega T}) = j\omega \text{ , where T is the sample period [5].}$$

This means that the magnitude response is proportional to frequency with a phase shift of ninety degrees for frequencies from zero to 1/2T Hertz; this response repeats periodically.

Discrete time differentiation is amenable to polynomial approximation techniques where the coefficients are derived from the data points [6]. The signal component of the attitude data is assumed to be a ramp with one or more sinusoids superimposed on it. The ramp slope is proportional to the dc component of the rate; the sinusoids are assumed to be of relatively low frequency. The ramp portion of the signal can be correctly differentiated by an approximation of order one or greater. A sinusoid cannot be represented by a finite sum of polynomials. No matter how high the order of the approximation, it will not exactly reproduce the derivative of a sinusoid.

Lagrange approximation techniques yield a curve fit in which the order of the approximation is equal to the number of data points used

for the fit [7]. An example of this type of fit is given by the Stirling approximation for the derivative [8]. A sixth order approximation yields the following transfer function:

$$H(z) = (z^{3} - 9 z^{2} + 45 z - 45 z^{-1} + 9 z^{-2} - z^{-3})/60$$

This transfer function may be made causal by multiplying by z^{-3}. A plot of the magnitude response of the Stirling differentiator and the ideal differentiator is shown in Figure 1. The frequency in Hertz is given by N/(1024T) where N is the frequency value on the plot. The Stirling differentiator closely approximates the ideal response in the lower frequency range; higher frequencies are attenuated. This should not be of concern, because the sample rate can always be chosen so that the frequencies of interest are not significantly attenuated. From a noise standpoint, the attenuation of higher frequencies may be desirable.

In practice, numerical differentiation is a more difficult operation than numerical integration [9,10]. The data to be differentiated are made up of a signal component and a noise component. The noise is assumed to be zero mean, uncorrelated, white Gaussian noise. This assumption is confirmed by analysis of the experimental data obtained from the CSTAR breadboard system. When this random noise is differentiated, the derived rate can have a very large noise component added to it. The Stirling differentiator shown in Figure 1 does not sufficiently attenuate the random noise to meet the rate accuracy requirements. A least squares type of approximation is more appropriate for this application [11].

In a least squares curve fit, the order of the approximation, m, is equal to or less than the number of data points to be fit, L. The length of the digital filter which realizes the approximation is L. In this application, the spacing between the data points is uniform and is equal to the sample period, T. The point at which the approximation is made is also a variable. For example, it may be placed in the middle of the data points or at the end. Errors in the approximation are due to both the random errors in the original signal, and the systematic errors introduced by the approximation itself. The above parameters affect how the random errors are reduced, and how large the systematic errors are. Random errors are decreased by the following:

1). Increasing the filter length, L.

2). Increasing the sample period, T.

3). Using a lower order approximation, m.

4). Smoothing to the center.

The systematic errors are reduced by the following:

1). Decreasing the filter length for a given sample period.

2). Decreasing the sample period for a given length.

3). Using a higher order approximation.

4). Smoothing to the center.

It can be seen from the above statements that, except for smoothing to the center, the selection of parameters to reduce random errors is in direct conflict with the need to choose parameters to decrease the systematic errors. Although smoothing to the center is desirable, it is not possible in a causal system without introducing time delay.

The variance reduction factor (VRF) for the approximation of the derivative is given by the following:

$$VRF = K/(T^2 L^3) \quad \text{for large values of L.}$$

K is a constant which depends on the order of the approximation and the point at which the data is smoothed. If L is not large, the exact expression will give a VRF which is smaller than the one obtained from the above equation. The systematic errors will be considered in relation to the steady state frequency response of the digital filter which implements the differentiator. This type of treatment lends itself to the analysis of signals which are other than sinusoids. A Fourier decomposition of an arbitrary function will yield its sinusoidal components. Superposition can be used to obtain the systematic error for the function.

The derivation of the coefficients in terms of the data points for a second order least squares curve fit, smoothed to the center follows: The function evaluated at the jth point from the center point is

$$f(j) = p_0 + p_1 j + p_2 j^2$$

Differentiating this gives

$$d[f(j)]/dj = p_1 + 2p_2 j$$

The coefficients may be calculated from the following set of simultaneous equations:

$$p_0 \sum_{k=-N}^{N} 1 + p_1 \sum_{k=-N}^{N} k + p_2 \sum_{k=-N}^{N} k^2 = \sum_{k=-N}^{N} x_{K-k}$$

$$p_0 \sum_{k=-N}^{N} k + p_1 \sum_{k=-N}^{N} k^2 + p_2 \sum_{k=-N}^{N} k^3 = \sum_{k=-N}^{N} k\, x_{k-k}$$

$$p_0 \sum_{k=-N}^{N} k^2 + p_1 \sum_{k=-N}^{N} k^3 + p_2 \sum_{k=-N}^{N} k^4 = \sum_{k=-N}^{N} k^2 x_{K-k}$$

where (2N + 1) = L; N is an integer. Let $S_m(N) = \sum_{k=0}^{N} k^m$, the

simultaneous equations reduce to

$$\begin{bmatrix} L & 0 & 2S_2(N) \\ 0 & 2S_2(N) & 0 \\ 2S_2(N) & 0 & 2S_4(N) \end{bmatrix} \begin{bmatrix} p_0 \\ p_1 \\ p_2 \end{bmatrix}$$

$$= \begin{bmatrix} 1 & 1 & \cdots & 1 & 1 & 1 & \cdots & 1 & 1 \\ N & N-1 & \cdots & 1 & 0 & 1 & \cdots & -(N-1) & -N \\ N^2 & (N-1)^2 & \cdots & 1 & 0 & 1 & \cdots & (N-1)^2 & N^2 \end{bmatrix} \begin{bmatrix} x_{k+N} \\ \vdots \\ x_k \\ \vdots \\ x_{k-N} \end{bmatrix}$$

Expressions for S_m are given by

$$S_1 = N(N + 1)/2$$

$$S_2 = N(N + 1)(2N + 1)/6$$

$$S_3 = L^2(L + 1)^2/4$$

$$S_4 = L(L + 1)(2L + 1)(3L^2 + 3L + 1)/30$$

The simultaneous equations give simple solutions for the polynomial coefficients in terms of the data points. The approximation of the derivative at the endpoint is obtained by setting j = N. The same transfer function is obtained if the simultaneous equations are set up to smooth to the endpoint directly. Such an evaluation involves the inversion of a 3x3 matrix, which is not necessary in the above derivation. It is also useful to have all of the coefficients availible so that users may obtain rate estimates for times which are not sample points.

The sampling rate and the rate at which the data points are processed need not be the same [12]. Time decimation requires that the

sampled signal is bandlimited to prevent aliasing at the processing rate. Bandlimiting the original signal will eliminate some of the high frequency components. This reduces the standard deviation of the random noise. A shorter length filter is then required to achieve the same overall variance reduction. The systematic errors may thereby be improved.

RESULTS

It is desirable to look at variance reduction in a normalized fashion. All of the calculations and graphs are done in terms of the ratio of the rate standard deviation, σ_R , to the position standard deviation, σ_A . The ratio will be denoted by R for convenience. For the Space Station requirements specified, R = 0.01. Figure 2 shows the differentiator length as a function of the sample period for a second order approximation smoothed to the endpoint with L determined by the equation below.

$$L = [192/(R^2T^2)]^{1/2}$$

A differentiator of length 577 is required for a sample rate of 10 Hertz and R = 0.01. For a sample rate of 1 Hertz and R = 0.25, the differentiator length required is reduced to 15.

The magnitude response of a second order, length 15 differentiator smoothed to the endpoint is presented in Figure 3, along with the ideal response. The frequency in Hertz is given by N/(1024T) where N is the frequency value on the plot. The magnitude response agrees well with the ideal at very low frequencies; frequencies above this range are

over emphasized in comparison to the ideal response. High frequencies are attenuated; this is consistent with the desire to reduce the variance of the Gaussian noise. A sine wave with amplitude of one and frequency of 1/5400 Hertz (this is roughly the rate at which the Space Station will orbit the Earth) was differentiated by the above filter. A plot of the differentiated sine wave, both ideal and filtered, is given in Figure 4. The agreement between the ideal and the filtered waveforms is excellent with only the first 14 samples showing any major deviation.

The systematic error for a given differentiator was related to the difference between the magnitude response of the ideal transfer function and that of the filter. This treatment ignores the phase response which makes it inexact. At low frequencies, the phase shift of the filter from ninety degrees is very small. This justifies the use of only the magnitude response at low frequencies. At high frequencies, the phase shift is large and adds significantly to the systematic error. The magnitude error at these frequencies is also very large, and operation at these frequencies should be avoided on that basis alone. Plots of the systematic error versus frequency for second order differentiators smoothed to the end point are given in Figures 5 and 6. In each case, the sampling rate and the processing rate are the same: 10 Hertz and 1 Hertz respectively.

If the data is sampled at one rate, and then processed at another rate, the sampled signal must be bandlimited so that there is no aliasing at the lower rate. Bandlimiting also produces the desirable

effect of reducing the standard deviation of the Gaussian noise. Fifth order digital Butterworth filters with prewarping are used for bandlimiting [13,14]. Table 1 gives the standard deviation, after bandlimiting, of a set of 10,000 normally distributed randoms numbers with original standard deviation of 1. Reducing the standard deviation of the random noise via bandlimiting reduces the length of the differentiator needed to meet a certain set of specifications. This, in turn, improves the systematic errors.

Several schemes for sampling and processing at differents rates are presented in Table 2. The systematic errors for each of these processing schemes are given in Figures 7 through 10. In all of the graphs, T represents the sample period, and τ represents the period at which the data is processed. Figures 11 through 16 present a comparison of the systematic errors of the appropriate schemes for various processing rates and values of R.

CONCLUSIONS

The above analysis shows that it is difficult to achieve differentiators which have the desired data bandwidth, reduce random errors, and accuratly process signals with other than very low frequency components. The length 577 differentiator which meets the current Space Station requirements for accuracy and bandwidth will have systematic errors comparable to the random errors for frequencies greater than 0.001 Hertz; this is assuming a sine wave of amplitude one. For bandlimiting R = 0.01. If R is increased to 0.1 in scheme D,

the usable frequency range edges up to about 0.01 Hertz. This decrease in the value of R could represent a relaxation of the Space Station requirements and/or the improvement of the CSTAR attitude processor accuracy. Bandlimiting below 0.5 Hertz should provide greater variance reduction, and, therefore, shorter length differentiators with lower systematic errors.

The digital filters needed for bandlimiting and differentiation can be implemented in a straight forward manner with currently available processors. Using Texas Instruments' TMS320 family, the number of machine cylces per iteration of the filter is about equal to the length of the differentiator (a nonrecursive filter), and twice the order of the Butterworth lowpass filter (a recursive structure). Some overhead must be added for inputting and outputting data, setting up registers, etc. The TMS32025C has a cycle time of 100 nanoseconds with very low power consumption. Other processors should give comparable results.

REFERENCES

1. Haykin, S., Adaptive Filter Theory, Prentice-Hall, Englewood Cliffs, N.J., 1986

2. Giordano, A., HSU, F., Least Squares Estimation with Applications to Digital Signal Processing, Wiley, N.Y., 1985

3. Oppenheim, A., Wilsky, A., Young, I., Signals and Systems, Prentice-Hall, Englewood Cliffs, N.J., 1983

4. Cadzow, J., Van Landingham, H., Signals, Systems, and Transforms, Prentice-Hall, Englewood Cliffs, N.J., 1985

5. Rabiner, L., Gold, B., Theory and Applications of Digital Signal Processing, Prentice-Hall, Englewood Cliffs, N.J., 1975

6. Williams, C., Designing Digital Filters, Prentice-Hall, Englewood Cliffs, N.J., 1986

7. Blackman, R., Linear Data-Smoothing and Prediction in Theory and Practice, Addison-Wesley, Reading, Ma., 1965

8. Antoniou, A., Digital Filter Analysis and Design, McGraw-Hill, N.Y., 1979

9. Hamming, R., Numerical Methods for Scientists and Engineers, McGraw-Hill, N.Y., 1965

10. Ralston, A., A First Course in Numerical Analysis, McGraw-Hill, N.Y., 1965

11. Morrison, N., Introduction to Sequential Smoothing and Prediction, McGraw-Hill, N.Y., 1969

12. Hamming, R., Digital Filters, Second Edition, Prentice-Hall, Englewood Cliffs, N.J., 1983

13. Stanley, W., Stanley, G., Dougherty, R., Digital Signal Processing, Second Edition, Reston, Reston, Va., 1984

14. Poularikas, A., Seely, S., Signals and Systems, PWS Engineering, Boston, 1985

TABLE 1

REDUCTION OF THE STANDARD DEVIATION WITH BANDLIMITING

$\omega_c T/2\pi$	SIGMA
1×10^{-3}	3.46×10^{-2}
2×10^{-3}	5.66×10^{-2}
5×10^{-3}	1.01×10^{-1}
1×10^{-2}	1.43×10^{-1}
2×10^{-2}	2.00×10^{-1}
5×10^{-2}	3.14×10^{-1}
1×10^{-1}	4.45×10^{-1}
2×10^{-1}	6.27×10^{-1}

TABLE 2

SCHEMES FOR BANDLIMITING AT DIFFERENT SAMPLING AND PROCESSING RATES

SCHEME	CUTOFF FREQUENCY	SAMPLING RATE	PROCESSING RATE
A	5 HERTZ	100 HERTZ	10 HERTZ
B	0.5 HERTZ	100 HERTZ	1 HERTZ
C	0.5 HERTZ	10 HERTZ	1 HERTZ
D	0.5 HERTZ	100 HERTZ	10 HERTZ

FIGURE 1

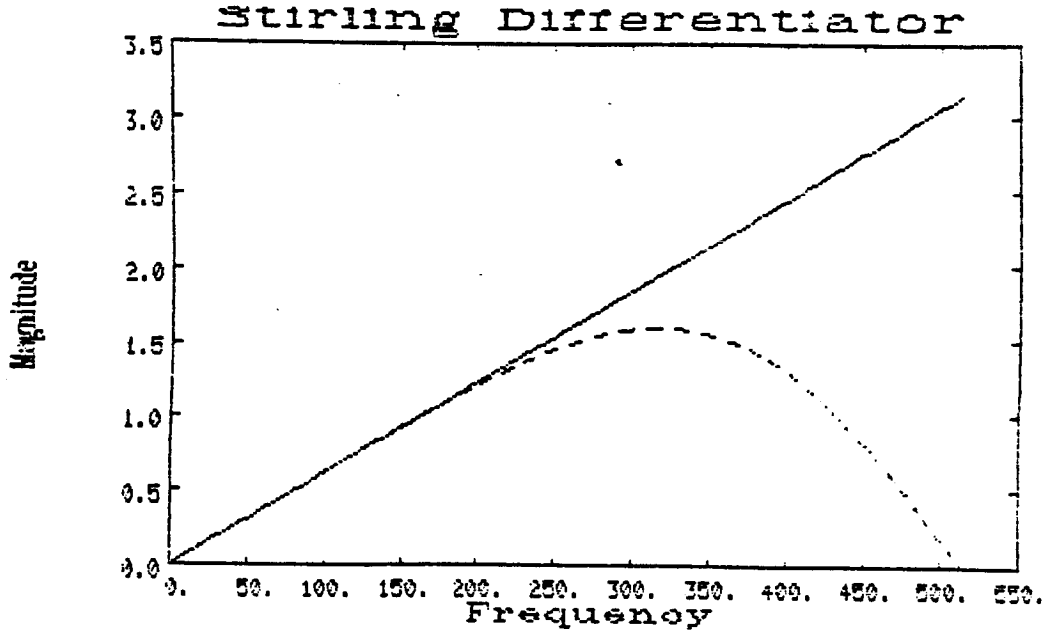
Stirling Differentiator
Magnitude
3.5
3.0
2.5
2.0
1.5
1.0
0.5
0.0
0.
50.
100.
150.
200.
250.
300.
350.
400.
450.
500.
550.
Frequency

FIGURE 2
SECOND ORDER APPROXIMATION

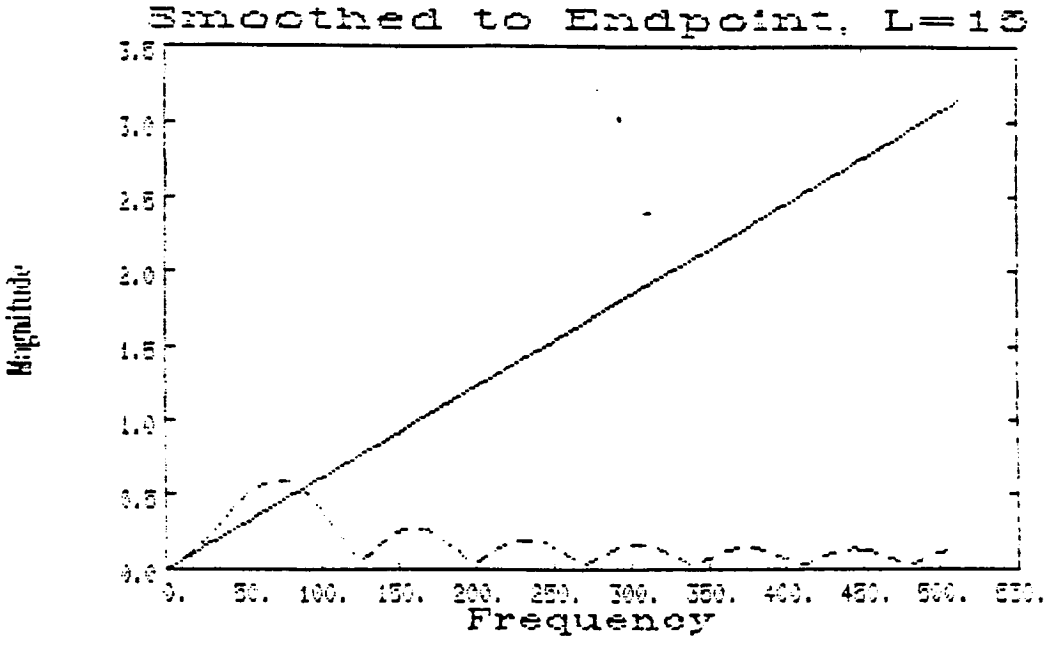

FIGURE 3
SECOND ORDER APPROXIMATION, L=15
SMOOTHED TO THE ENDPOINT

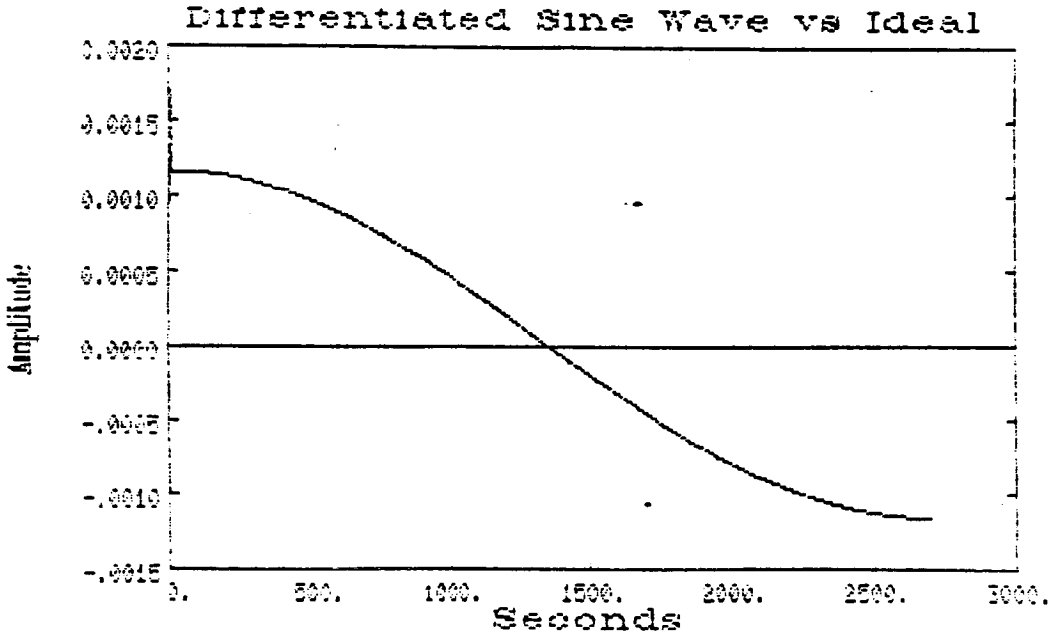

FIGURE 4
SMOOTHED TO THE ENDPOINT

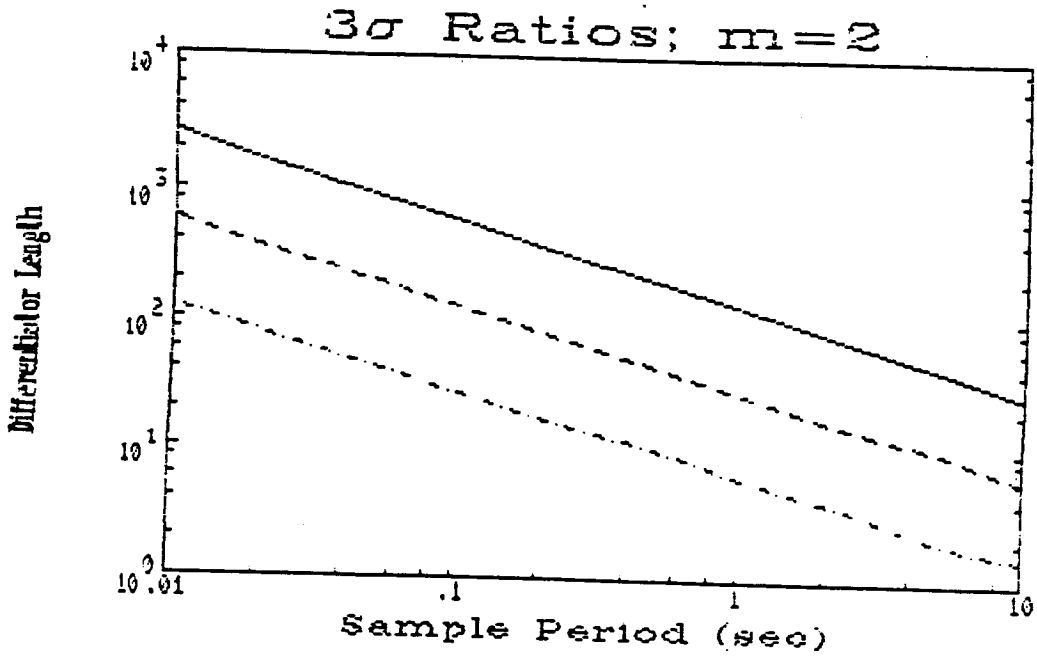

Legend

Linetype	R
Solid	0.01
Dashed	0.10
Dotdash	1.00

FIGURE 5

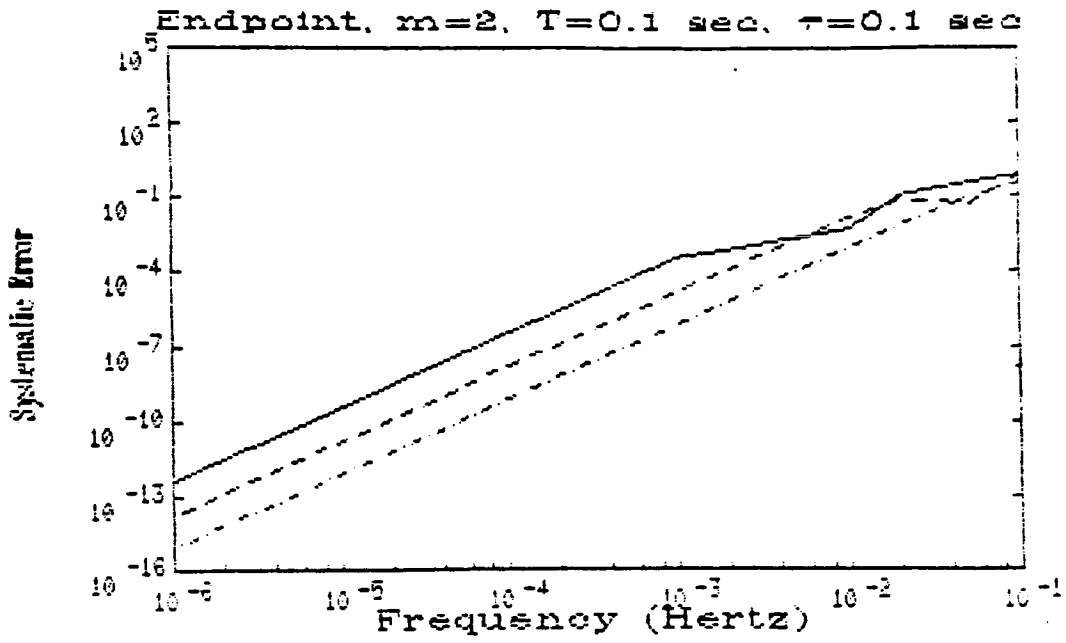

Legend

Linetype	R
Solid	0.01
Dashed	0.10
Dotdash	1.00

FIGURE 6

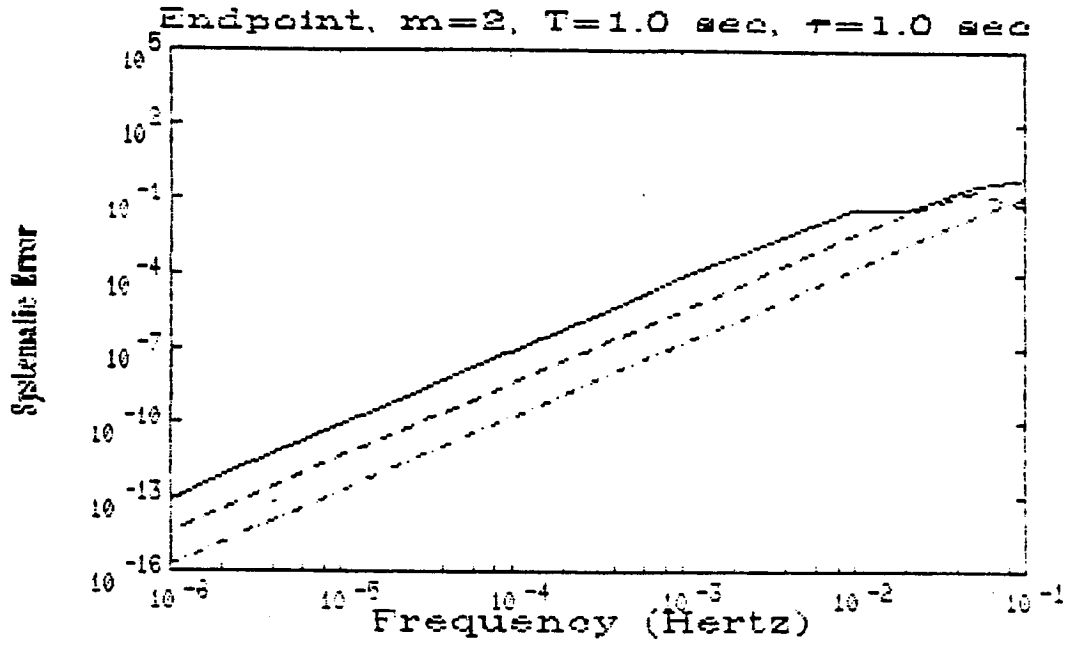

Legend

Linetype	R
Solid	0.01
Dashed	0.10
Dotdash	1.00

FIGURE 7
SCHEME A

ORIGINAL PAGE IS
OF POOR QUALITY

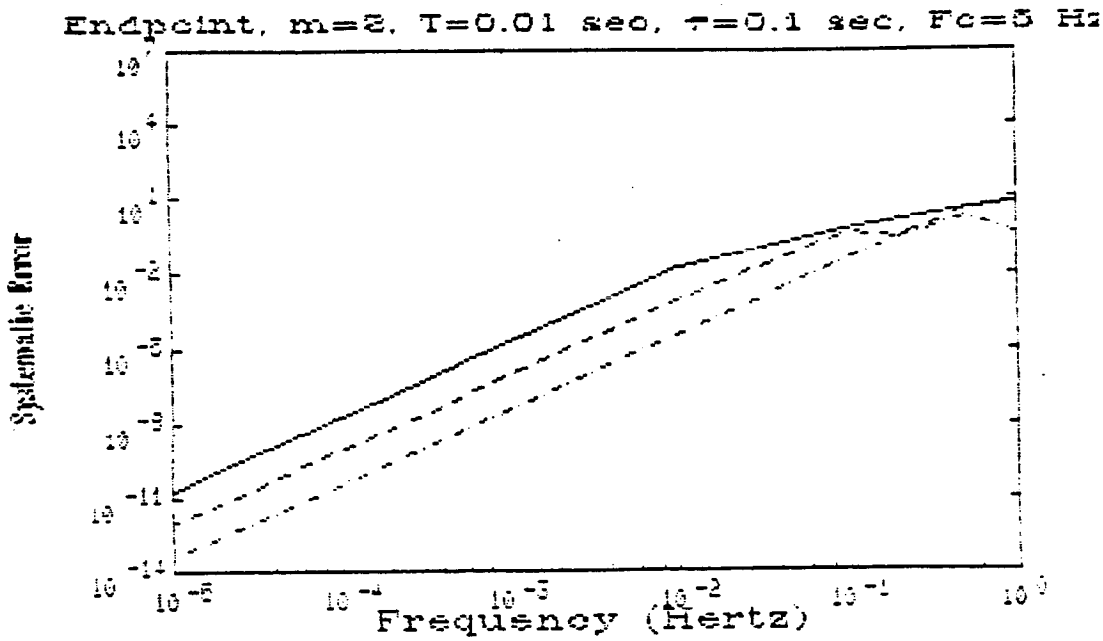

Legend

Linetype	R
Solid	0.01
Dashed	0.10
Dotdash	1.00

FIGURE 8
SCHEME B

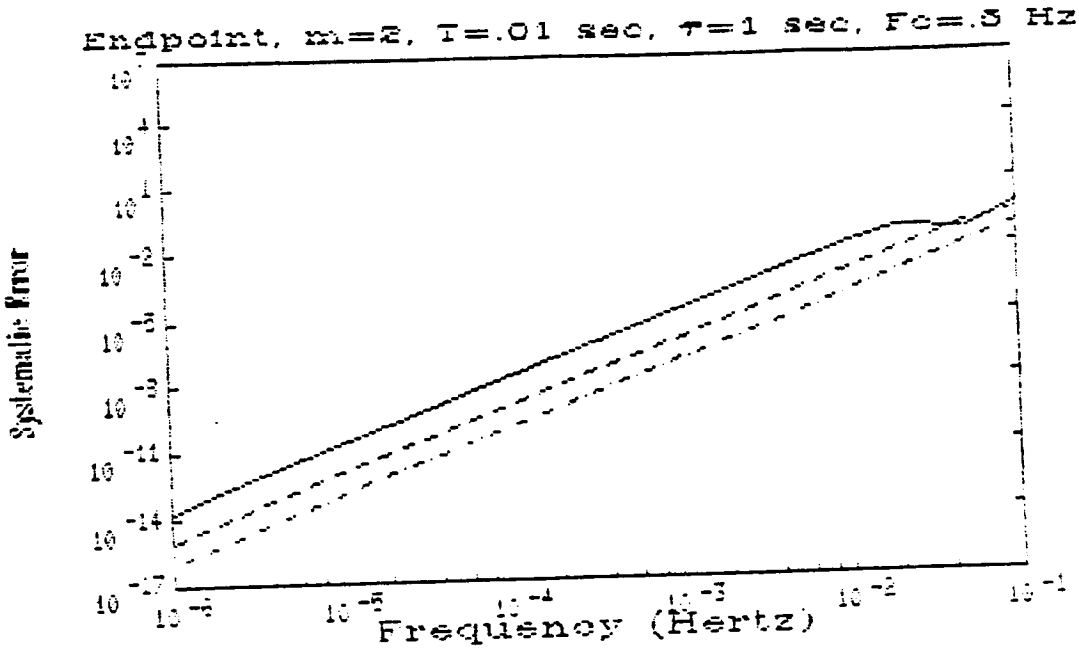

Legend

Linetype	R
Solid	0.01
Dashed	0.10
Dotdash	1.00

ORIGINAL PAGE IS
OF POOR QUALITY

FIGURE 9
SCHEME C

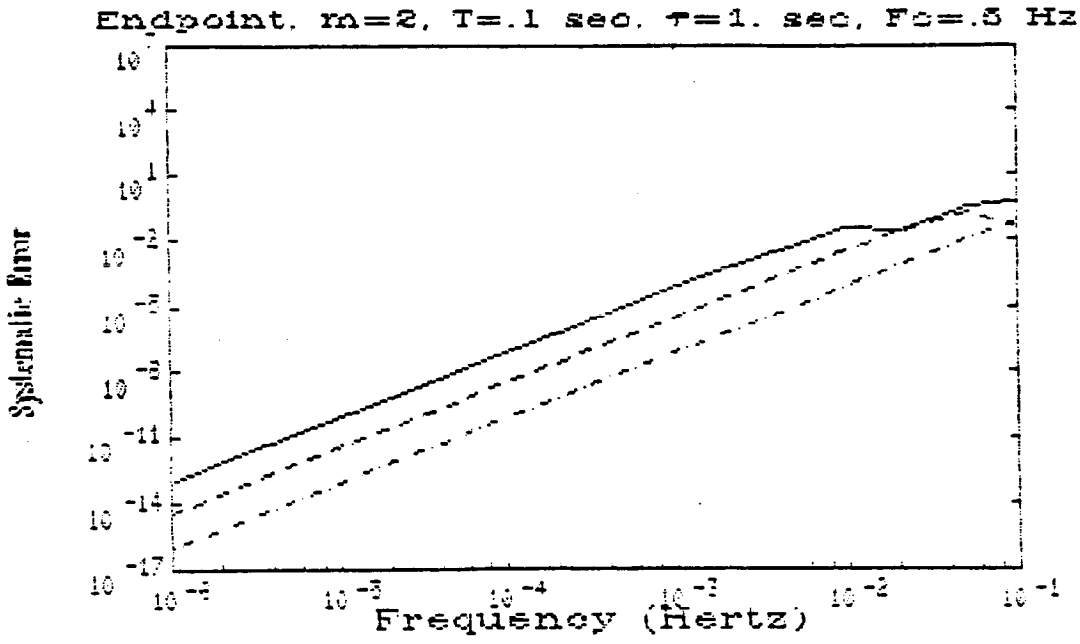

Legend

Linetype	R
Solid	0.01
Dashed	0.10
Dotdash	1.00

FIGURE 10
SCHEME D

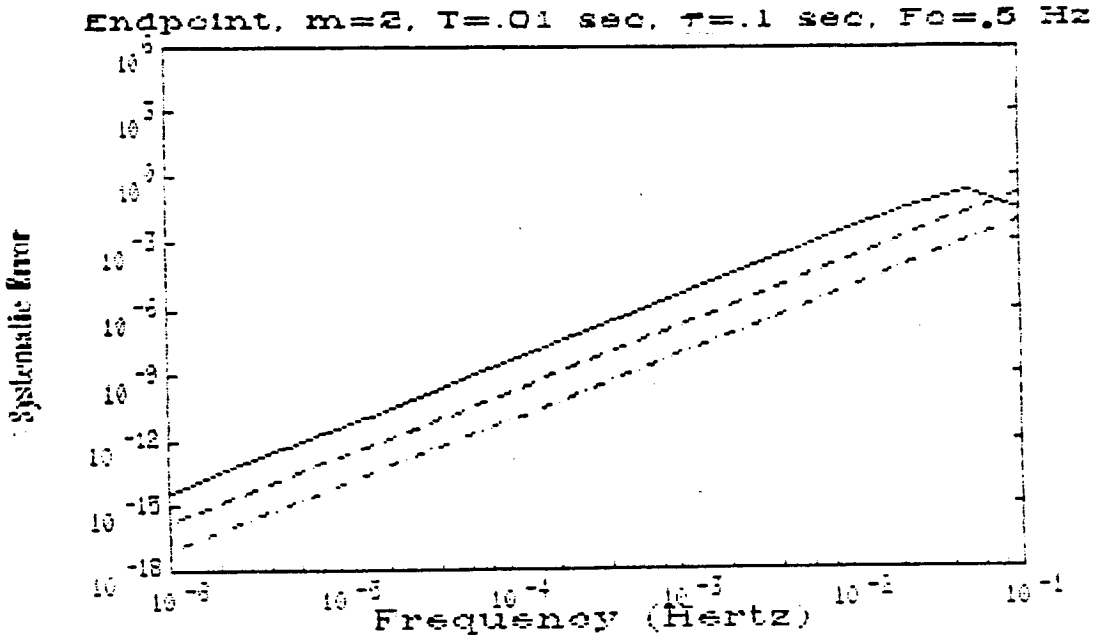

Legend

Linetype	R
Solid	0.01
Dashed	0.10
Dotdash	1.00

FIGURE 11
10 HERTZ PROCESSING, R = 0.01

ORIGINAL PAGE IS
OF POOR QUALITY

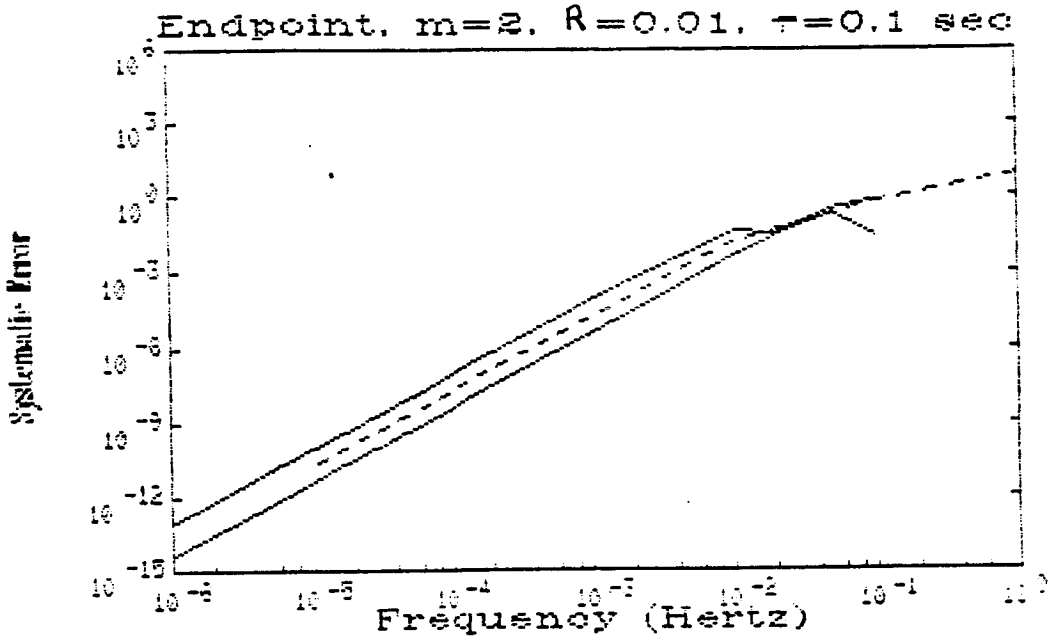

Linetype	Legend Processing Scheme
Solid	No Bandlimiting
Dashed	A
Dotdash	D

FIGURE 12
10 HERTZ PROCESSING, R = 0.10

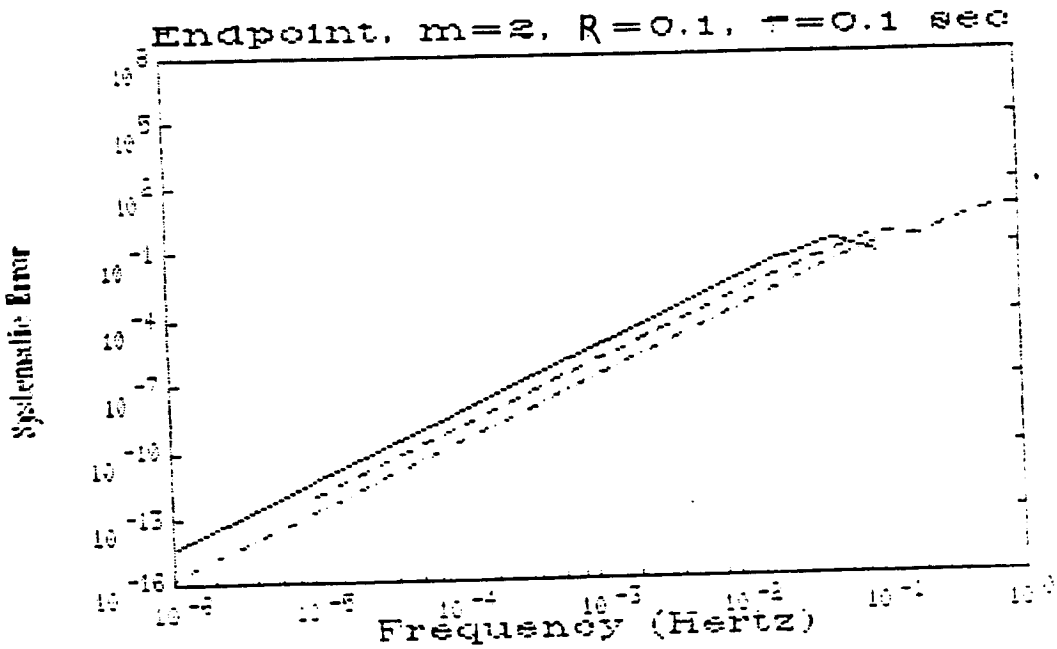

Legend

Linetype	Processing Scheme
Solid	No Bandlimiting
Dashed	A
Dotdash	D

FIGURE 13
10 HERTZ PROCESSING, R = 1.00

ORIGINAL PAGE IS
OF POOR QUALITY

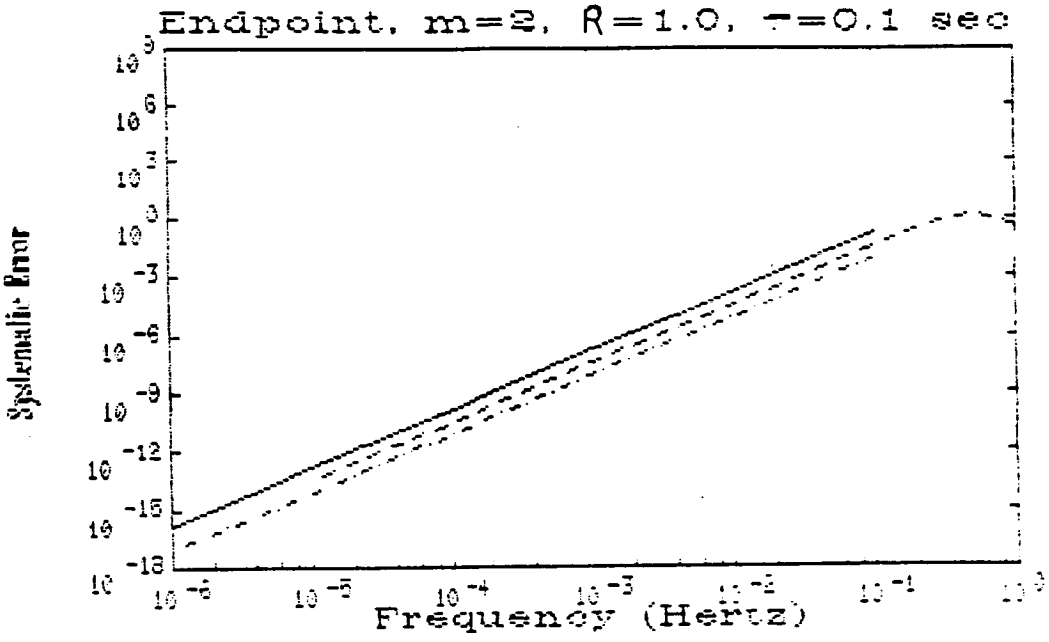

Linetype	Legend Processing Scheme
Solid	No Bandlimiting
Dashed	A
Dotdash	D

FIGURE 14
1 HERTZ PROCESSING, R = 0.01

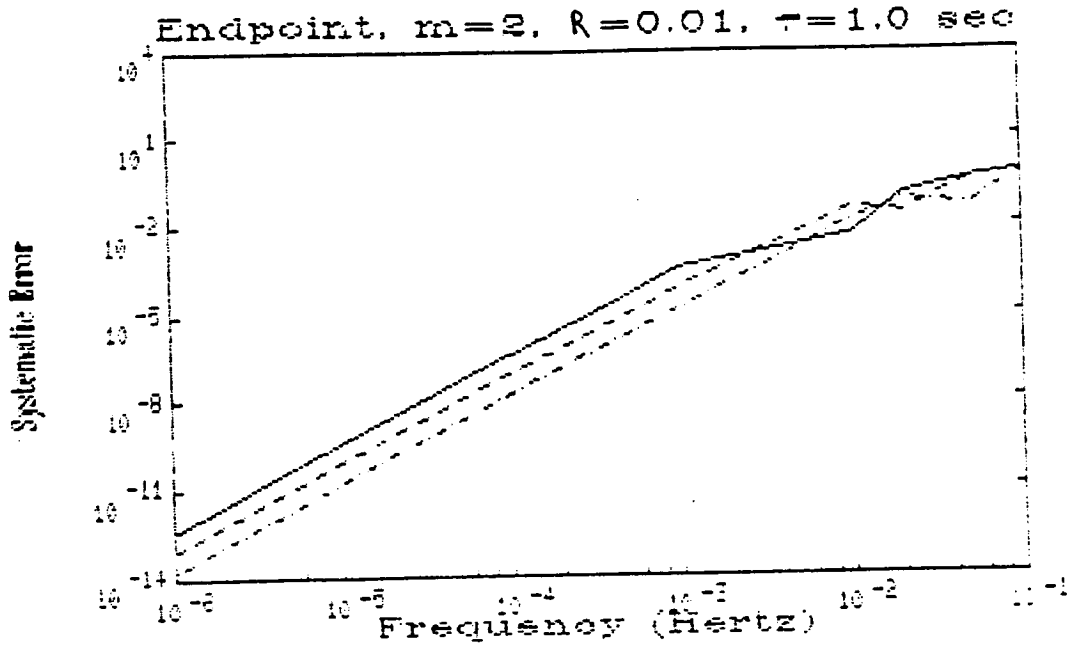

Legend	
Linetype	Processing Scheme
Solid	No Bandlimiting
Dashed	C
Dotdash	B

FIGURE 15
1 HERTZ PROCESSING, R = 0.10

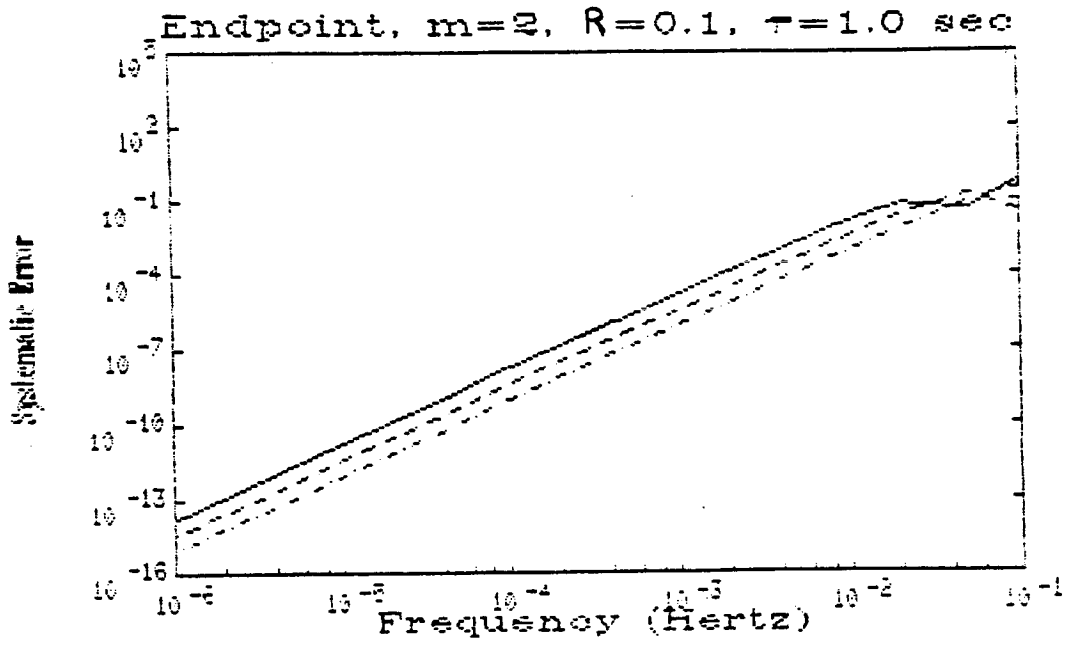

Linetype	Legend Processing Scheme
	No Bandlimiting
Solid	A
Dashed	C
Dotdash	B

FIGURE 16
1 HERTZ PROCESSING, R = 1.00

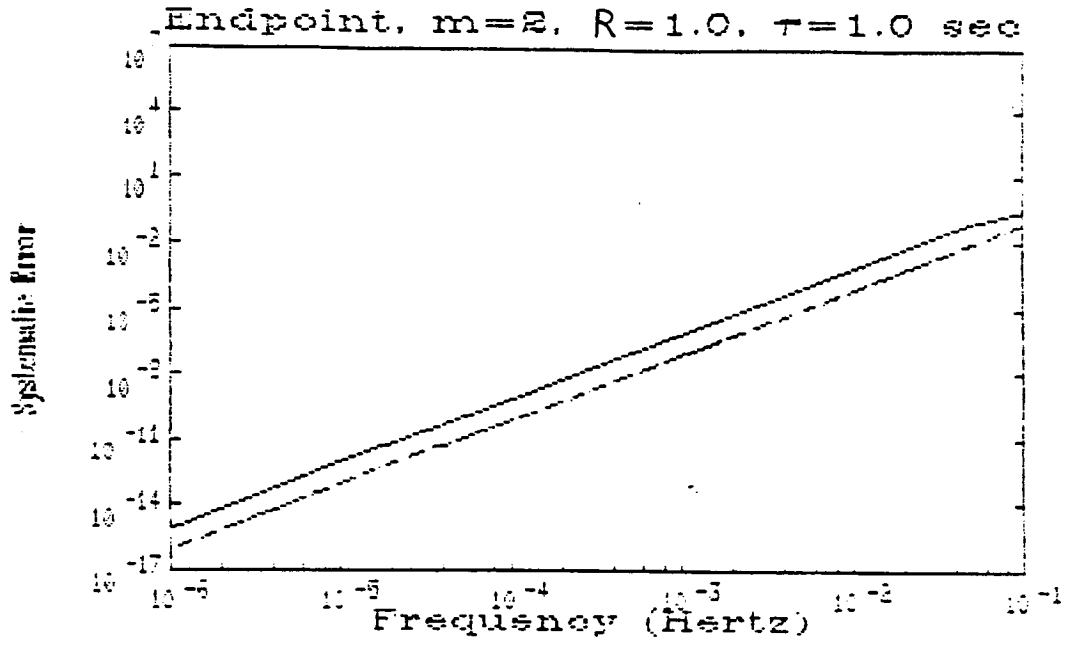

Linetype	Legend Processing Scheme
Solid	No Bandlimiting
Dashed	C
Dotdash	B

1986

NASA/ASEE SUMMER FACULTY RESEARCH FELLOWSHIP PROGRAM

Johnson Space Center

University of Houston

Bone Density Measurements in Limb-Immobilized Beagles

Prepared by:	Ira Wolinsky, Ph.D.
Academic Rank:	Associate Professor
University & Department:	University of Houston - University Park Dept. of Human Development

NASA/JSC	
Directorate:	Space and Life Sciences
Division:	Medical Sciences
Branch:	Space Biomedical Research Inst. (SD5)
JSC Colleague:	Victor Schneider, M.D.
Date:	August 8, 1986
Contract #:	NGT-44-005-803 (Univ. of Houston)

BONE DENSITY IN LIMB-IMMOBILIZED BEAGLES AN ANIMAL MODEL FOR BONE LOSS IN WEIGHTLESSNESS

Ira Wolinsky, Ph.D.
Associate Professor
Department of Human Development
University of Houston
Houston, Texas 77004

Prolonged weightlessness is man in space flight results in a slow progressive demineralization of bone accompanied by an increased calcium output in the urine resulting in negative calcium balances. This possibly irreversible bone loss may constitute a serious limiting factor to long duration manned space flight. In order to seek and test preventative measures an appropriate ground-based animal model simulating weightlessness is necessary. Use of the mature Beagle in limb immobilization has been documented as an excellent model for orthopedic research since this animal most closely simulates the phenomenom of bone loss with regards to growth, remodelling, structure, chemistry and mineralization. The purpose of this project is to develop a research protocol for the study of bone loss in Beagles during and after (recovery) cast immobilization of a hindleg; research will then be initiated.

NASA Colleague: Victor Schneider, M.D. SD5 X 5281

INTRODUCTION

Loss of bone mineral in astronauts is a predictable major consequence of spaceflight (1). Mechanical unloading during weightlessness is the most obvious factor which may play a role in this phenomena since bone is dynamically responsive to the function demand placed on it (2). Two derangements of calcium metabolism occur during spaceflight: negative calcium balance and loss of bone mass. During 84 days spaceflight mineral content from astronauts' os calcis declined 4-5%, or about a loss of 100 mg calcium lost (3). There is some question whether this bone mineral loss is reversible post flight (4). Unchecked losses of body calcium and bone mass, coupled with normally-occurring age-related osteopenia, may eventually result in bone fracture, kidney stones or ectopic calcium deposition thereby compromising the health of crewmembers and mission success.

There is a need for a ground-based animal model for the study of the effect(s) of simulated weightlessness on bone loss. Several models have been proposed and evaluated by this laboratory (5). Experimentally induced immobilization bone loss in the beagle dog affords the best experimental model from the viewpoint of similarity of this specie's skeleton to that of man both in its static architecture and dynamic response(s) to environmental stresses.

This project will monitor the degree and rate of bone loss with limb hypodynamia and more importantly the degree and rate of possible bone recovery following reambulation.

OBJECTIVES

1) To immobilize right hindleg of mature beagles in order to simulate hypogravity or weightlessness for varying periods of time.

2) To measure regional and total bone loss over time in the immobilized limb, using dual-photon absorptiometry.

3) To measure time course and extent of possible bone recovery in the remobilized dog limb.

4) To monitor bone loss and possible recovery using histological and morphometrical techniques.

METHODS AND MATERIALS

The use of mature beagles in orthopedic research has several advantages over other animal models viz: the skeleton of adult man and the beagle are nearly identical in composition and manner of remodelling; well documented normative values for numerous physiological systems, including

bone histomorphometric data, are available; there are proven experimental models available for studies on specific types of bone loss; the time required for intervention studies is shorter than in man because of beagles' shorter life span and faster rate of bone turnover; beagles are available from commercial, inbred, controlled colonies (6-11).

Six 15-month old, young adult, male Beagles from a commercial closed inbred colony (Laboratory Research Enterprises, Kalamazoo, Mich.) will be used for this study. At this age the dogs are fully mature and all bone physes have closed. The dogs will be purchased free of endo- and ectoparasites and fully immunized, including rabies. They will have been partially muted and socialized. Each dog will have been marked by a distinctive ear tatoo and medical and genetic histories available from the supplier. They will be shipped by air freight and upon arrival be housed individually in the University of Houston laboratory animal facility in dog runs and examined by the staff veterinarian. The dog runs are temperature and humidity controlled and a 12 hr. light-dark cycle will be maintained. Each dog will be weighed shortly after arrival and at periodic intervals throughout the course of the experiment. They will be fed standard laboratory dog chow (Purina Canine Maintenance Diet) and top water ad libitum. The University of Houston animal facilities are fully accredited by A.A.A.L.A.C. and meet all N.I.H. standards.

The right hindleg of each animal will be immobilized in a nylon net pouch attached to a commercial dog jacket (Alice King Chatham Medical Arts, Los Angeles). The pouch will be closed by a zipper and adjusted by laces so that the lower hindleg containing the tibia is flexed back along the upper foreleg containing the femur. The result will be to shorten the leg so it cannot be used for ambulation. Bone density measurements (DP3 Dual Photon Spine Scanner, Lunar Radiation Corp., Madison, Wisc.) will be taken prior to immobilization and every 4 weeks thereafter. Trabecular bone of the distal femur and proximal tibia will be compared with shaft cortical regions. When bone loss is detected, at various times after immobilization, the hindleg will be remobilized by removing the constraining pouch and the dog allowed to ambulate freely on all four limbs. Bone density measurements will be taken periodically during the remobilization It period. It is anticipated that the extent of bone loss and the extent and speed of possible reversal after remobilization will be directly related to the duration of constraint and to the duration of remobilization, resp. While it is difficult to predict, bone loss in our young adult dogs may be seen as early as four weeks of constraint followed by possible bone loss reversal at about 8-10 weeks after mobilization (12,13). During bone density measurements the constraining pouch will be removed and the animals will be tranquilized with xylazine (Ropum) in order to insure the animal remains still during the procedures. At the end of the experiment animals will be sacrificed by an overdose of Nembutol. Bones of the control and experimental limbs will be used for histological and morphometry analyses including cross-sectional and medullary areas, measurements of resorption and oppositional rates (11).

ANTICIPATED OUTCOMES

Once a phenomenon is understood, at least in part, it can be manipulated, the aim of experimental therapeutics. Completion of these experiments will provide normative, base-line data on the extent and rate of bone loss during limb immobilization (employed as an analog of weightlessness) and, more critically, whether full bone recovery may be expected after remobilization. Our results will enable future studies on techniques for preventing bone loss in immobilization and promoting subsequent recovery. These techniques may include the effect of exercise, dietary calcium and/or phosphorus substances and the use of specific prophylactic drugs.

BIBLIOGRAPHY

1. Dietlein, L.F., Skylab: a beginning, In: Johnston, R.S., Dietlein, L.F. (eds.), Biomedical Results from Skylab, NASA, SP-377, Washington D.C., 1977, pp. 408-418.

2. Woo, S. L.-Y., Kuei, S.C., Amiel, D., Gomez, M.A., Hayes, W.C., White, F.C.,Akeson, Witt, W.H., The effect of prolonged physical training on the properties of long bone: a study of Wolff's law. J. Bone Joint Surg. 63A:780-787(1981).

3. Rambaut, P.C., Johnston, R.S., Prolonged weightlessness and calcium loss in man. Acta Astronautica 6:1113-1122(1979).

4. Tilton, F.E., Degioanni, J.J., Schneider, V.S., Long-term follow-up of Skylab bone demineralization. Aviat. Space Environ. Med. 51:1209-1213(1980).

5. Wolinsky, I., Schneider, V.S., LeBlanc, A.D., Animal models in ground-based weightlessness studies (unpublished).

6. Anderson, A.C., Good, L.S. (eds.), The Beagle as an Experimental Dog, Iowa State Univ. Press, Ames, Iowa, 1970.

7. Jaworski, Z.F.G., Kimmel, D.B., Jee, W.S.S., Cell kinetics underlying skeletal growth and bone tissue turnover. In: Recker, R.R. (ed.), Bone Histomorphometry: Techniques and Interpretation, CRC Press, Inc., Boca Raton, Fla., 1983, pp. 225-239.

8. National Research Council, Mammaliam Models for Research on Aging, Natl. Acad. Press, Washington, D.C., 1981.

9. Beddoe, A.H., A quantitative study of trabecular bone in man, rhesus monkey, beagle and miniature pig. Calc. Tiss. Intl. 25:273-281(1981).

10. Martin, R.K., Albright, J.P., Jee, W.S.S., Taylor, G.N., Clarke, W.R., Bone loss in the beagle tibia: influence of age, weight, and sex. Calc Tiss. Intl. 33:233-238(1981).

11. Uhthoff, H.K., Sekaly, G., Jaworski, Z.F.G., Effect of long-term nontraumatic immobilization on metaphyseal spongiosa in young adult and old beagle dogs. Clin. Orthop. Rel. Res. 192: 278-283 (1985).

12. Uhthoff, H.K., Jaworski, Z.F.G., Liskova-Kiar, M., Age-specific activity of bone envelopes in experimental disuse osteoporosis and its reversal. Orthop.Trans. 3:206(1979).

13. Jaworski, ZF.G., Liskova-Kiar, M., Uhthoff, H.K., Effect of long-term immobilization on the pattern of bone loss in older dogs. J. Bone Joint Surg. 62B:104-110(1980).

1. Report No.	2. Government Accession No.	3. Recipient's Catalog No.
NASA CR 171984		

4. Title and Subtitle	5. Report Date
NASA/ASEE Summer Faculty Fellowship--1986 Volume 2	June 1987
	6. Performing Organization Code
7. Author(s)	8. Performing Organization Report No.
Editors: Bayliss McInnis and Stanley Goldstein	
	10. Work Unit No.
9. Performing Organization Name and Address	
The University of Houston--University Park and Texas A&M University	11. Contract or Grant No. NGT-44-005-803
	13. Type of Report and Period Covered Contractor Report
12. Sponsoring Agency Name and Address	
National Aeronautics and Space Administration Washington, D.C. 20546	14. Sponsoring Agency Code

15. Supplementary Notes

16. Abstract

The Johnson Space Center (JSC) NASA/ASEE Summer Faculty Fellowship Program was conducted by the University of Houston--University Park and the Johnson Space Center. The ten week program was operated under the auspices of the American Society for Engineering Education (ASEE). The program at JSC, as well as the programs at other NASA Centers, was funded by the Office of University Affairs, NASA Headquarters, Washington, D.C. The basic objectives of the programs, which began in 1965 at JSC and in 1964 nationally, are (a) to further the professional knowledge of qualified engineering and science faculty members; (b) to stimulate an exchange of ideas between participants and NASA; (c) to enrich and refresh the research and teaching activities of participants' institutions; and (d) to contribute to the research objectives of the NASA Centers.

Each faculty fellow spent ten weeks at JSC engaged in a research project commensurate with his interests and background and worked in collaboration with a NASA/JSC colleague. This document is a compilation of the final reports on the research projects done by the faculty fellows during the summer of 1986. Volume 1 contains sections 1 through 14, and volume 2 contains sections 15 through 30.

17. Key Words (Suggested by Author(s))	18. Distribution Statement
	Unclassified - Unlimited

19. Security Classif. (of this report)	20. Security Classif. (of this page)	21. No. of pages	22. Price*
Unclassified	Unclassified	303	NTIS

*For sale by the National Technical Information Service, Springfield, Virginia 22161